IMPROVING

PERI-OPERATIVE STAGING

IN COLORECTAL CANCER

Christopher James Hunter

Thesis submitted for the degree of Doctor of Philosophy

2014

Department of Surgery and Cancer

Clinical Medicine Research

Imperial College London

Declaration of Originality

I declare that this thesis and the work that it describes is entirely my own. Any assistance received in preparing this thesis has been acknowledged and any sources appropriately referenced.

Copyright Declaration

The copyright of this thesis rests with the author and is made available under a Creative Commons Attribution Non-Commercial No Derivatives licence. Researchers are free to copy, distribute or transmit the thesis on the condition that they attribute it, that they do not use it for commercial purposes and that they do not alter, transform or build upon it. For any reuse or redistribution, researchers must make clear to others the licence terms of this work.

Acknowledgements

I am deeply grateful to a number of people without whom I would not have been able to complete this research project.

My supervisors, Gina Brown, Muti Abulafi and Paris Tekkis, have provided me with invaluable advice on the design of this research through to its write up.

Louis Temple and Abed Arnaout have patiently provided histopathological assessment for specimens involved in this study.

Jan Harris, Kim Chamberlain, and Sheena Woodward have helped me greatly with patient recruitment.

Suzanne St-Rose (Royal Marsden statistics department) and Tom Fanshawe (University of Oxford statistics department) have provided me with invaluable statistical support both during the design and write up of this project.

The Bowel Disease Research Foundation provided a grant to help fund the MRI scans, consumables and transportation costs relating to the Colon MRI study. Croydon University Hospital provided two bursaries to support both the colon MRI and the Specimen MRI studies.

Abstract

The last few decades have seen a dramatic increase in the treatment options for colorectal cancer.

These include adjuvant and neoadjuvant chemotherapy and radiotherapy, extended resections, local excision, and deferral of surgery amongst others. These developments are increasing the need for accurate staging of colorectal cancer through imaging; many treatment decisions are now taken before histopathology is available, optimal outcomes are achieved if the first surgical procedure is the definitive procedure, and histopathology results which have determined the need for adjuvant therapy are now frequently affected by neoadjuvant treatment. Assessment of imaging has predominantly judged its accuracy by comparing it to histopathology as a "gold standard". However, this approach may underestimate the accuracy of imaging due to inaccuracies in histopathological assessment. It may also fail to focus on the adverse risk features which are most reliably identified on imaging.

This thesis investigates the role of MRI in improving perioperative staging of both colon and rectal cancer. In a retrospective study of rectal cancer patients undergoing pre-treatment PET/CT and CT, I demonstrated that patients with high-risk features on rectal MRI have an odds ratio of 6 for synchronous metastatic disease compared to those with low-risk features. This suggests that, at least in rectal cancer, MRI is not only accurate when compared to histological staging, but can independently risk stratify patients with systemic disease. The next aim of this thesis was to determine whether it is possible to extend the benefits of local cancer staging with MRI seen in rectal cancer patients to patients with colon cancer.

I, therefore, went on to develop a number of MRI sequences in healthy volunteers which allowed good visualisation of the colon. I then applied these to a cohort of colon cancer patients in an attempt to obtain more accurate local staging using 1.5T MRI and 3T than is currently achieved with CT. Overall, I was not able to demonstrate that MRI was significantly more accurate than CT in the local staging of colon cancer, but I was able to obtain a similar accuracy in T staging with 3T MRI (56-

76%) to that achieved with CT (66-72%). In the best multiplanar 3T MRI scans, T-staging accuracy was greater than CT (67-79%).

In the final part of this thesis, I investigated whether ex-vivo specimen MRI could improve that accuracy of histological staging by helping to select tumour blocks. I hypothesised that part of the "inaccuracy" demonstrated by imaging staging was due to sampling error in the selection of sections for histopathology, and that performing a high-resolution ex-vivo MRI of the specimen might reduce this error by helping to select tumour blocks. I was unable to demonstrate any benefit from this technique.

Table of Contents

Title page 1
Declaration of Originality 2
Copyright Declaration 2
Acknowledgements 2
Abstract 4
Table of Contents 6
Index of Figures 11
Index of Tables 13
List of Abbreviations 17

1 Introduction 20

1.1 My role in this chapter 21

1.2 Incidence of colorectal cancer 21

1.3 Aetiology and risk factors 22
1.3.1 Age 22
1.3.2 Adenomatous polyps 22
1.3.3 Inflammatory bowel disease 22
1.3.4 Genetic risk factors 23
1.3.5 Environmental risk factors 26

1.4 Pathogenesis 28
1.4.1 Adenoma-carcinoma sequence 29
1.4.2 Molecular pathways 29
1.4.3 Principle genes involved in colorectal cancer 31
1.4.4 Molecular classification of colorectal cancer 33

1.5 Spread of colorectal cancer 34
1.5.1 Direct invasion 34
1.5.2 Lymphatic spread 35
1.5.3 Haematogenous spread 35
1.5.4 Transcoelomic spread 35

1.6 Sites of metastasis in colorectal cancer 36
1.6.1 Liver metastases 36
1.6.2 Lung metastases 37
1.6.3 Ovarian metastases 38
1.6.4 Peritoneal metastases 38
1.6.5 Other sites 39

1.7 Anatomy of the colon and rectum 39
1.7.1 Layers of the colonic and rectal wall 39
1.7.2 Peritoneal coverings of the colon and rectum 40
1.7.3 Fascial coverings of the colon and rectum 40
1.7.4 Blood supply of the colon and rectum 41
1.7.5 Lymphatic drainage of the colon and rectum 43
1.7.6 Anatomical relations of the colon and rectum 46

1.7.7 Anatomical definition of the rectum 48

1.8 Treatment of colorectal cancer 48
1.8.1 Colorectal cancer surgery 48
1.8.2 Radiotherapy 57
1.8.3 Chemotherapy 61

1.9 Histopathological assessment of colorectal cancer 65
1.9.1 Dukes stage 65
1.9.2 TNM stage 66
1.9.3 Venous invasion 71
1.9.4 Lymphatic invasion 72
1.9.5 Depth of extramural spread 72
1.9.6 Circumferential resection margin 73
1.9.7 Histological grade 73
1.9.8 Histological type 74
1.9.9 Perineural invasion 74
1.9.10 Tumour deposits 74
1.9.11 Tumour regression grade 75
1.9.12 Tumour budding 76
1.9.13 TME grading 77
1.9.14 Histopathological technique 77
1.9.15 Limitations in histopathological assessment 77
1.9.16 Lymph node number **Error! Bookmark not defined.**

1.10 Radiological staging of colorectal cancer 78
1.10.1 Computed Tomography (CT) 79
1.10.2 Magnetic Resonance Imaging (MRI) – Primary rectal cancer 85
1.10.3 MRI – restaging after chemoradiotherapy 96
1.10.4 MRI – predicting and assessing response to neoadjuvant chemoradiotherapy 98
1.10.5 MRI – local staging of colon cancer 100
1.10.6 MRI – assessment of systemic disease in colorectal cancer 100
1.10.7 ^{18}F-Fleurodeoxyglucose Positron Emission Tomography (FDG-PET) 101
1.10.8 FDG-PET/Computed Tomography (FDG-PET/CT) 104
1.10.9 MRI with diffusion weighted imaging **Error! Bookmark not defined.**
1.10.10 Ultrasound (US) 105

1.11 Summary 112

1.12 Hypotheses and aims 113
1.12.1 Hypotheses 113
1.12.2 Aims 113

2 Investigation of whether high risk features on rectal cancer MRI are associated with an increased incidence of metastatic disease 115

2.1 My role in this chapter 116

2.2 Introduction and rationale 116

2.3 Materials and Methods 122
2.3.1 Subjects 122

2.3.2 Procedures 123
2.3.3 Evaluation 124
2.3.4 Statistical analysis 126

2.4 Results 128
2.4.1 Patients 128
2.4.2 Identification of distant metastases in high and low risk groups 129
2.4.3 Univariate analysis 131
2.4.4 Multivariate analysis 133
2.4.5 Model testing 134

2.5 Discussion 137

3 Optimising MRI protocols for imaging colon cancer 144

3.1 My role in this chapter 145

3.2 Introduction and rationale 145

3.3 Materials and Methods 148
3.3.1 Subjects 148
3.3.2 Procedures 148

3.4 Results 151
3.4.1 MRI Sequences 151
3.4.2 Two dimensional and three dimensional acquisition 156
3.4.3 Patient positioning 158
3.4.4 Small bowel distension 159
3.4.5 Respiratory triggering 160

3.5 Summary 162

4 Comparison of the diagnostic accuracy of MRI with CT in staging colonic cancer 164

4.1 My role in this chapter 165

4.2 Introduction and rationale 165

4.3 Materials and Methods 167
4.3.1 Subjects 167
4.3.2 Procedures 169
4.3.3 Evaluation 175
4.3.4 Statistical analysis 177

4.4 Results 180
4.4.1 Recruitment 180
4.4.2 Patient demographics 183
4.4.3 Outcome measures 186

4.5 Discussion 206

5 Diagnostic accuracy of MRI and CT in subgroups 213

5.1 My role in this chapter 214

5.2 Introduction and rationale 214
5.2.1 1.5T MRI 214
5.2.2 3T MRI 215

5.3 Materials and Methods 216
5.3.1 Subjects 216
5.3.2 Procedures 216
5.3.3 Evaluation 216
5.3.4 Statistical analysis 217

5.4 Results 218
5.4.1 Tumour location 218
5.4.2 Scan quality 222
5.4.3 Number of imaged planes 227
5.4.4 Discussion 232

6 Randomised comparison of conventional histological processing of colorectal cancers with MRI guided specimen dissection for histology 237

6.1 My role in this chapter 238

6.2 Introduction and rationale 238

6.3 Materials and Methods 242
6.3.1 Subjects 242
6.3.2 Randomisation 243
6.3.3 Procedures 243
6.3.4 MRI technique 243
6.3.5 Specimen MRI assessment 244
6.3.6 MRI-Specimen correlation 244
6.3.7 Tumour block selection 247
6.3.8 Evaluation 249
6.3.9 Statistical analysis 250

6.4 Results 252
6.4.1 Recruitment 252
6.4.2 Demographics 253
6.4.3 Specimen characteristics 259
6.4.4 Primary outcome measure 261
6.4.5 Secondary outcome measures 262

6.5 Discussion 265

7 General discussion 270

7.1 Summary 271

7.2 Further work 271

7.3 Conclusion 273

8 References **275**

9 Appendix – Publications arising from this work **300**

Index of Figures

Figure 1.1: CT image acquisition 80

Figure 1.2: Positron detection in positron emission tomography 102

Figure 1.3: Ultrasound imaging 107

Figure 2.1: Incidence of metastatic disease in high and low risk rectal cancer 129

Figure 2.2: ROC curves for logistic regression and clinical models 136

Figure 3.1: Balanced steady-state gradient echo sequence 152

Figure 3.2: Fast spin echo sequence 153

Figure 3.3: Single-shot fast spin echo sequence 154

Figure 3.4: T1 weighted spoiled gradient echo sequence 155

Figure 3.5: T1 weighted spoiled gradient echo images pre (left) and post (right) contrast 156

Figure 3.6: 3D (left) and 2D (right) balanced steady state gradient echo sequences 157

Figure 3.7: 3D (left) and 2D (right) fast spin echo sequence 157

Figure 3.8: Balanced steady-state gradient echo images obtained in the supine (left) and prone (right) positions 158

Figure 3.9: Balanced steady-state gradient echo images with no oral prep (top left), 1L of water (top left), 1L of Klean-prep (bottom left) and 1L of E-Z-CAT (bottom right) 160

Figure 3.10: Navigator echo 161

Figure 4.1: Colon MRI study flow diagram 169

Figure 4.2: Patient recruitment flow diagram 182

Figure 4.5: Imaging delay to surgery 187

Figure 6.1: Specimen MRI and histological section correlation 245

Figure 6.2: Correlation of off axis specimen MRI and histological section 246

Figure 6.3: Specimen MRI trial flow diagram 249

Index of Tables

Table 1.1: Lymph node stations 45

Table 1.2: TNM staging system 5th to 7th editions 69

Table 1.3: TNM stage groupings for 5th to 7th editions 70

Table 1.4: Tumour regression grading systems 76

Table 2.1: Entry criteria on imaging for trials of additional neoadjuvant chemotherapy 119

Table 2.2: MRI definition of "low risk" and "high risk" rectal cancer patients 121

Table 2.3: Demographic details 128

Table 2.4: Univariate analysis of MRI risk factors for synchronous metastases; separate variables 132

Table 2.5: Univariate analysis of MRI risk factors for synchronous metastases; dichotomous variables 133

Table 2.6: Multivariate analysis of MRI risk factors for synchronous metastases 134

Table 3.1: MRI sequence names and acronyms 150

Table 4.1: MRI sequence parameters 174

Table 4.2: Patient recruitment 180

Table 4.3: Reasons for withdrawal from trial 181

Table 4.4: Patient demographic details 184

Table 4.5: Overall staging on CT and 1.5T MRI 188

Table 4.6: Overall staging on CT and 3T MRI 188

Table 4.7: Comparison of scan accuracy in identifying T3/4 disease 189

Table 4.8: T3 or greater disease 191

Table 4.9: Test bias: proportion positive for T3+ disease on pathology and radiology, ... 193

Table 4.10: Inter-observer agreement for reporting T3+ disease 193

Table 4.11: Stage-for-stage T-stage accuracy, ... 194

Table 4.12: N1 or greater disease 196

Table 4.13: Test bias in reporting N1 or greater disease compared to pathology 197

Table 4.14: Inter-observer agreement for reporting N1 or greater disease 197

Table 4.15: Extra mural vascular invasion 200

Table 4.16: Test bias in reporting EMVI compared to pathology 201

Table 4.17: Inter-observer agreement for reporting EMVI positivity 201

Table 4.18: T3c or greater disease 203

Table 4.19: Test bias in reporting T3c or greater disease compared to pathology 205

Table 4.20: Inter-observer agreement for reporting T3c or greater disease 205

Table 5.1: Tumour location 218

Table 5.2: Imaging accuracy for T3 or greater disease, radiologist 1, according to tumour location 219

Table 5.3: Imaging accuracy for T3 or greater disease, radiologist 2, according to tumour location 219

Table 5.4: Imaging accuracy for N1 or greater disease, radiologist 1, according to tumour location 220

Table 5.5: Imaging accuracy for N1 or greater disease, radiologist 2, according to tumour location 220

Table 5.6: Imaging accuracy for EMVI, radiologist 1, according to tumour location 221

Table 5.7: Imaging accuracy for EMVI, radiologist 2, according to tumour location 221

Table 5.8: Imaging accuracy for T3c or greater disease, radiologist 1, according to tumour location 222

Table 5.9: Imaging accuracy for T3c or greater disease, radiologist 2, according to tumour location 222

Table 5.10: 1.5T MRI and 3T MRI scan quality – number of scans 223

Table 5.11: 1.5T MRI accuracy in identifying T3 or greater disease, according to scan quality 223

Table 5.12: 3T MRI accuracy in identifying T3 or greater disease, according to scan quality 224

Table 5.13: 1.5T MRI accuracy in identifying N1 or greater disease, according to scan quality 224

Table 5.14: 3T MRI accuracy in identifying N1 or greater disease, according to scan quality 225

Table 5.15: 1.5T MRI accuracy in identifying EMVI, according to scan quality 225

Table 5.16: 3T MRI accuracy in identifying EMVI, according to scan quality 226

Table 5.17: 1.5T MRI accuracy in identifying T3c or greater disease, according to scan quality 226

Table 5.18: 3T MRI accuracy in identifying T3c or greater disease, according to scan quality 227

Table 5.19: 1.5T MRI and 3T MRI number of imaged planes..... 227

Table 5.20: 1.5T MRI accuracy in identifying T3 or greater disease, according to number of imaged planes 228

Table 5.21: 3T MRI accuracy in identifying T3 or greater disease, according to number of imaged planes 229

Table 5.22: 1.5T MRI accuracy in identifying N1 or greater disease, according to number of imaged planes 229

Table 5.23: 3T MRI accuracy in identifying N1 or greater disease, according to number of imaged planes 230

Table 5.24: 1.5T MRI accuracy in identifying EMVI, according to number of imaged planes 230

Table 5.25: 3T MRI accuracy in identifying EMVI, according to number of imaged planes 231

Table 5.26: 1.5T MRI accuracy in identifying T3c or greater disease, according to number of imaged planes 231

Table 5.27: 3T MRI accuracy in identifying T3c or greater disease, according to number of imaged plane 232

Table 6.1: Reasons patients not recruited to specimen MRI trial 252

Table 6.2: Reasons for withdrawal from specimen MRI trial 253

Table 6.3: Demographic details 255

Table 6.4: Pre-operative treatment 258

Table 6.5: Specimen characteristics 260

Table 6.6: Primary end point (AJCC stage) 261

Table 6.7: Secondary end points 263

Table 6.8: Secondary end points (binary outcomes) 264

List of Abbreviations

Abbreviation	Meaning
2D	Two dimensional
3D	Three dimensional
5-FU	Fluorouracil
ACPGBI	Association of Coloproctology of Great Britain and Northern Ireland
ADC	Apparent diffusion coefficient
AIC	Akaike information criterion
AJCC	American Joint Committee on Cancer
ANOVA	Analysis of variance
APR	Abdominoperineal resection
APC	Adenomatous polyposis coli
AUC	Area under the curve
BFFE	Balanced fast field echo
BSGE	Balanced steady-state gradient echo
BTFE	Balance turbo field echo
CIMP	CpG-island methylation phenotype
CIN	Chromosomal instability
CME	Complete mesocolic excision
COLOR trial	Colon carcinoma laparoscopic or open resection trial
CRM	Circumferential resection margin
CSS	Cancer specific survival
CT	Computed tomography
CXB	Contact X-ray brachytherapy
DFS	Disease free survival
DNA	Deoxyribonucleic acid
DWI	Diffusion weighted imaging
EAUS	Endo-anal ultrasound
EBRT	External beam radiotherapy
EGFR	Epidermal Growth Factor Receptor
ELAPE	Extralevator abdominoperineal excision
EMD	Extramural depth (of tumour invasion)
EMR	Endoscopic mucosal resection
EMVI	Extra mural vascular invasion
EUS	Endoscopic or endorectal ultrasound
FAP	Familial adenomatous polyposis
FBP	Filtered back projection
FDG	18F-fluorodeoxyglucose
FDG-PET	18F-fluorodeoxyglucose positron emission tomography
FDG-PET/CT	18F-fluorodeoxyglucose positron emission tomography/computed tomography
FFE	Fast field echo
FLASH	Fast low angle shot
FOLFOX	Flourouracil, leucovorin and oxaliplatin
FOXTROT	Fluoropyrimidine, oxaliplatin & targeted receptor pre-operative therapy for colon cancer
FRGE	Fully rewound gradient echo

FSE	Fast spin echo
FSGR	Fast spoiled gradient recall echo
GE	Gradient echo
GI	Gastrointestinal
GRAPPA	Generalised auto calibrating partially parallel acquisitions
GWA	Genome wide association
HASTE	Half-Fourier acquisition with single-shot turbo spin echo
HNPCC	Hereditary non-polyposis colon cancer
IMRT	Intensity modulated radiotherapy
ITC	Isolated tumour cells
KRAS	Kirsten rat sarcoma viral oncogene homolog
LOH	Loss of heterozygosity
LV5FU	Fluorouracil and leucovorin
MAP	MYH associated polyposis
MAPK	Mitogen activated protein kinase
MDCT	Multi-detector computed tomography
MDT	Multi-disciplinary team
MERCURY	Magnetic resonance imaging and rectal cancer European equivalence
MLH1	MutL homolog 1
MMR	Mismatch repair
MRC	Magnetic resonance colonography
MRE	Magnetic resonance enterography
MRI	Magnetic resonance imaging
MSH2	MutS homolog 2
MSI	Microsatellite instability
MYH or MUTYH	mutY Homolog (E.coli) gene
NOSE	Natural orifice specimen extraction
NOTES	Natural orifice transluminal endoscopic surgery
NPRM	Non-peritonealised resection margin (CRM)
OS	Overall survival
OSEM	Ordered subset expectation maximization
pCR	Pathological complete response
PEG	Poly ethylene glycol
PFS	Progression free survival
PNI	Perineural invasion
RARE	Rapid acquisition with relaxation enhancement
RFS	Recurrence free survival
RF	Radiofrequency
ROC	Receiver operator curve
ROPE	Respiratory ordered phase encoding
SENSE	Sensitivity encoding
SGE	Spoiled gradient echo
SNR	Signal to noise ratio
SPACE	Sampling perfection with application optimized contrasts using different flip angle evolution
SPIO	Super paramagnetic iron oxide
SS-FSE	Single-shot fast spin echo

SS-TSE	Single-shot turbo spin echo
STARD	Standards for the reporting of diagnostic accuracy
SUV	Standardised uptake value
TAMIS	Transanal minimally invasive surgery
TD	Tumour deposits
TE	Time to echo
TEMS	Transanal endoscopic microsurgery
TGFBR2	TGF-β type 2 receptor gene
TGF-β	Transforming growth factor beta
THRIVE	T1 high resolution interpolated volume excitation
TME	Total mesorectal excision
TNM	Tumour node metastases staging system
TNM5	Tumour node metastases staging system, 5th edition
TNM6	Tumour node metastases staging system, 6th edition
TNM7	Tumour node metastases staging system, 7th edition
TP53	Tumour protein 53
TR	Time to relaxation
TRG	Tumour regression grade
True-FISP	True fast imaging with steady-state precession
TSE	Turbo spin echo
UK	United Kingdom
US	Ultrasound
VIBE	Volume interpolated body examination
VISTA	Volume isotropic turbo spin echo acquisition
VMAT	Volume modulated arc radiotherapy
WHO	World Health Organisation
Wnt	Wingless-related integration site
yp	Prefix to denote post neoadjuvant pathology assessment in TNM

CHAPTER 1

Introduction

The ideal staging modality for colorectal cancer would be available at the time of diagnosis, repeatable following treatment, non-invasive, and highly accurate for staging local and distant disease, and would include no risk to the patient in the form of ionising radiation. Unfortunately, no such staging modality is available, and so a multi-modality strategy is currently adopted. This incorporates both pre-operative imaging and post-operative histology. The overarching aim of this research project is to improve the accuracy of this perioperative staging.

1.1 My role in this chapter

With the support of my supervisor, I performed the literature search for this chapter, reviewed the literature and wrote this chapter. I was first author for two book chapters and one review article which relate to this introduction (Hunter et al., 2016, Hunter and Brown, 2015, Hunter and Brown, 2013).

1.2 Incidence of colorectal cancer

Colorectal cancer is a major health problem. Worldwide, there were nearly 1.4 million new cases of colorectal cancer diagnosed in 2012 (Ferlay et al., 2012). The global incidence of colorectal cancer is increasing, with a projected annual worldwide incidence of 2.4 million by 2035. In the United Kingdom (UK), there are around 36,000 new cases per annum and around 14,000 deaths per year (Westlake, 2009). This makes colorectal cancer the second most common cause of cancer death in the UK, and colorectal cancer represents a lifetime risk of around 5% for the UK population.

1.3 Aetiology and risk factors

1.3.1 Age

Incidence of colorectal cancer increases sharply with age, with 90% of cancer cases occurring in those over aged 50 years. The incidence rate is more than 50 fold in those aged 60 to 79 years compared to those aged less than 40 years (Haggar and Boushey, 2009). However, certain inherited conditions predispose to colorectal cancer at an early age, and those diagnosed with colorectal cancer at a younger age tend to present with more advanced disease and have a higher 5 year recurrence rate (Steele et al., 2014).

1.3.2 Adenomatous polyps

Adenomatous polyps are associated with an increased risk of developing colorectal cancer, and the risk is increased in the presence of large and multiple polyps. Individuals with large (>1cm) adenomas have a standardized incidence ratio of 3.6 for developing colorectal cancer, and this increases to 6.6 if multiple adenomas are present (Atkin et al., 1992). Endoscopic removal of colorectal polyps reduces the risk of colorectal cancer. There is approximately a 53% reduction in mortality from colorectal cancer in patients undergoing surveillance with colonoscopic polypectomy (Zauber et al., 2012).

1.3.3 Inflammatory bowel disease

Ulcerative colitis and Crohn's disease are both associated with an increased risk of colorectal cancer. The risk is dependent on the extent of colonic inflammation and duration of disease. There is little or no increased risk in proctitis, but those with pancolitis have a cumulative incidence of colorectal cancer of 2% at 10 years, 8% at 20 years and 18% at 30 years (Eaden et al., 2001). Colorectal cancer is more likely to develop if there is ongoing active inflammation in the colon (Rutter et al., 2004).

Active treatment to prevent persistent colonic inflammation and regular colonoscopic surveillance to identify and treat dysplasia may reduce the risk of colorectal cancer.

1.3.4 Genetic risk factors

Colorectal cancer is common, with a lifetime risk of around 5% in the UK. The majority of these cancers will occur in individuals with no genetic predisposition, so called sporadic cancers. Due to the common nature of this cancer, a large number of people will therefore have first degree relatives who have developed bowel cancer. However, as the number of affected relatives increases so does the risk of developing colorectal cancer. At the high risk end of this spectrum a number of conditions have been identified which confer a very high risk of developing colorectal cancer.

Familial adenomatous polyposis

Familial adenomatous polyposis (FAP) is an autosomal dominant disorder caused by mutation in the tumour-suppressor adenomatous polyposis coli (APC) gene on the long arm of chromosome 5. It causes affected individuals to develop hundreds of colonic adenomas at a young age, and confers a near 100% risk of developing colorectal cancer by age 40 (Markowitz and Bertagnolli, 2009). FAP is also associated with a number of extra-colonic manifestations, including adenomas and carcinomas of the duodenum, stomach, small intestine, biliary tract, thyroid and adrenal as well as epidermoid cysts and desmoid tumours. FAP is diagnosed clinically by the identification of over 100 colonic adenomas. A mutation in the APC gene can then be identified in around 80% of affected individuals, and family members can then be offered genetic testing to see whether they have inherited the family mutation. Patients with confirmed FAP should be offered prophylactic colectomy or restorative proctocolectomy and screening for extra-colonic manifestations.

MYH-associated polyposis

MYH-associated polyposis (MAP) has substantial clinical overlap with FAP, with half of affected individuals developing over 100 colonic adenomas. However, the degree of polyposis is more

variable, with some affected individuals developing only a few polyps. MAP also confers a very high risk of developing colorectal cancer, with 80%of affected individuals developing colorectal cancer by age 70 (Goodenberger and Lindor, 2011). MAP is also associated with extra-colonic manifestations, including duodenal polyps, gastric polyps and desmoid tumours, but these are less common than in FAP. MAP is caused by biallelic mutations of the mutY Homolog (E.coli) (MYH or MUTYH) gene on the short arm of chromosome 1. It therefore demonstrates autosomal recessive inheritance, and around 1% to 2% of the population are carriers of MYH mutations.

Hereditary non-polyposis colorectal cancer

Individuals with a very strong family history of colorectal cancer, in the absence of the large numbers of adenomas seen in the polyposis syndrome, have been described as having hereditary non-polyposis colorectal cancer (HNPCC). To be classified as such, patients should either fulfil the Amsterdam criteria II or have an identified mismatch repair (MMR) mutation. The Amsterdam criteria II are defined as (Vasen et al., 1999):

At least three relatives with colorectal, endometrial, small bowel, ureteric, or renal pelvis cancer, one of whom should be a first-degree relative of the other two.

- At least two successive generations should be affected
- At least one colorectal cancer should be diagnosed before the age of 50
- Familial adenomatous polyposis should be excluded
- Tumours should be verified by pathological examination

Men with HNPCC have a 47% risk of developing colorectal cancer by age 70, and women a 33% risk of developing colorectal cancer and a 14% risk of developing endometrial cancer by 70 (Alarcon et al., 2007). They are also much more likely to develop colorectal cancer at a young age, with the average age of diagnosis being 45. They are therefore 148 times more likely to have developed colorectal cancer by the age of 40 than the general population (Voskuil et al., 1997). Patients fulfilling the

Amsterdam II criteria without MMR deficiency have more recently been described as having familial colorectal cancer type X (Goodenberger and Lindor, 2011).

Lynch syndrome

Approximately 50% of individuals with HNPCC will have an identifiable germline mutation in mismatch repair (MMR) genes. MMR genes are tumour-suppressor genes which are responsible for repairing base-base mismatches and small insertions or deletions in DNA. In Lynch syndrome, one of the inherited alleles is faulty. For tumour formation, the other allele becomes damaged, leaving the cell with no functioning copy. DNA mismatches therefore accumulate within the cell, leading to mutations in many other genes and ultimately tumour formation. Cancers occur most commonly in the colon, but also occur with increased frequency in the endometrium, stomach, ovary and urothelium compared to the general population. As only one faulty autosomal gene is required to inherit Lynch syndrome, it is autosomal dominantly inherited.

Microsatellite DNA consists of repetitive sequences of 1 to 6 bases. Microsatellite DNA is found throughout the human genome, and makes up about 3% of human DNA. Microsatellites are most common in introns, but also occur in coding regions of many genes which regulate cell growth or promote apoptosis. These repetitive sequences are more prone to replication errors than other parts of the genome, and so accumulate mutations in MMR defective cells. This leads to microsatellite instability (MSI) in Lynch syndrome cancers, with highly variable microsatellites.

Other hereditary colorectal cancer

A number of other syndromes are associated with an increased risk of developing colorectal cancer, included Peutz-Jeghers syndrome, juvenile polyposis and Cowden disease. Patients with a strong family history of colorectal cancer but without one of the previously defined syndromes may also be at increased risk of developing colorectal cancer. Patients with one first degree relative, who developed colorectal cancer before the age of 45 years, or with two first degree relatives with colorectal cancer, have a 3 to 6 fold increase risk in developing colorectal cancer compared to the

general population and may benefit from endoscopic surveillance. Many of these families are likely to have clustering of a number of alleles which individually confirm only a small increased risk of colorectal cancer, but when grouped together may be associated with a significant increased risk. This is in keeping with the L shaped distribution of allelic effects, where a small number of variants have a large effect on phenotype (such as APC, MYH and MMR genes), but a large number of variants will have an individually small effect. Genome wide association (GWA) studies have recently identified 10 common genetic variants linked to colorectal cancer, and these may offer opportunities for targeted surveillance or new avenues of therapeutic research in the future (Tenesa and Dunlop, 2009).

1.3.5 Environmental risk factors

There is a wide variation in colorectal cancer incidence rates between countries, with higher incidence rates in more developed regions and lower incidence rates in less developed regions. The lowest incidence is in Western Africa (4.5 per 100,000 in men and 3.8 per 100,000 in women), and the highest incidence in Australia and New Zealand (44.8 per 100,000 in men and 32.2 per 100,000 in women) (Ferlay et al., 2012). In migrant populations, the incidence in migrants and their descendants has tended to reach that of their adopted country, within one or two generations.(Ponz de Leon and Roncucci, 2000). These data suggest that dietary or environmental factors may be important in the aetiology of colorectal cancer, although these incidence rates may be subject to a high degree of ascertainment bias (there may be under reporting in developing countries).

Diet

These data supporting an environmental aetiology in colorectal cancer have led to a number of studies looking at the association between diet and colorectal cancer. In animal studies, diets containing more than 40% of their calories as fat are associated with a higher incidence of colorectal cancers than those with a low fat content (Ponz de Leon and Roncucci, 2000). However, a

subsequent meta-analysis found no evidence to support the association between animal fat and animal protein dietary intake and colorectal cancer in humans (Alexander et al., 2009).

Several studies have examined more specifically the association between dietary red and processed meat intake and colorectal cancer. A large cohort study of almost 150,000 followed over 20 years found that high dietary intake of red and processed meat was associated with an increased risk of developing colorectal cancer, particularly when sustained over 10 years, but that a high intake of poultry and fish was associated with a lower colorectal cancer risk (Chao et al., 2005). However, the evidence for this has again been inconsistent and a meta-analysis in 2011 concluded that the available epidemiologic data was not sufficient to support an independent and unequivocal positive association between red meat intake and colorectal cancer (Alexander et al., 2011).

High alcohol intake is associated with an increased risk of developing colorectal cancer, with a relative risk of 1.41 for developing colorectal cancer in those consuming 45g/day of alcohol compared to non-drinkers (Cho et al., 2004). These findings have been relatively consistent across a number of cohort studies, and between colorectal cancer site (Moskal et al., 2007). There is a j-shaped dose-response, with low levels of alcohol intake possibly offering some protection against colorectal cancer compared to complete abstinence.

Several studies have also looked at dietary components which might exert a protective effect against colorectal cancer. The American Institute for Cancer Research suggests that high dietary fibre intake, garlic, calcium and milk probably protect against colorectal cancer, and that there was limited evidence that non-starchy vegetables, fruits, folate, selenium , fish and vitamin D protect against colorectal cancer (World Cancer Research Fund / American Institute for Cancer Research, 2007)

Physical activity

Higher overall levels of physical activity are associated with a lower risk of developing colon cancer (Robsahm et al., 2013). There is evidence of a dose response-effect, with increased frequency and intensity of physical activity associated with reduced risk of developing colorectal cancer (Haggar

and Boushey, 2009). The biological mechanism for this action is not fully elucidated, but may be related to increased metabolic efficiency, reduced insulin resistance or increased gut motility.

Obesity

There is a positive relationship between body mass index (BMI) and cancer risk for both colon cancer and rectal cancer. A recent meta-analysis suggested a relative risk of 1.59 for developing cancer in the distal colon for obese patients compared to those with a normal BMI, and a relative risk of 1.23 for developing rectal cancer (Robsahm et al., 2013).

Tobacco

Tobacco smoking is associated with an increased risk of developing colorectal cancer. Although this effect is much smaller than that seen in some other cancers, such as lung cancer, it is still significant with an relative risk of 1.36 for ex-smokers and 1.96 for current smokers (Zhao et al., 2010). There is a stronger association between tobacco smoking and cancer risk in rectal cancer than in colon cancer. Individuals exposed to tobacco smoke are also significantly more likely to develop colorectal cancer at a younger age (Peppone et al., 2008).

1.4 Pathogenesis

Cell replication and division in the human body is a tightly regulated process. For colorectal epithelial cells to escape this tight regulation and replicate in an uncontrolled manor, invade adjacent tissues and then metastasize to different sites requires a large number of mutations. Although these mutations occur randomly within individual cells in a neoplastic lesion, the defects accumulate in a non-random fashion because they confer important survival advantages (Goel and Boland, 2010). At least three distinct pathways are now recognised by which different types of colorectal cancer acquire the required genetic changes to become invasive malignancies.

1.4.1 Adenoma-carcinoma sequence

In the 1951, Jackman and Mayo published a paper suggesting that there may be a link between colorectal adenomas and carcinomas, based on similarities in their location within the large bowel, age and sex distribution, and high incidence of colorectal cancer in patients with Familial Adenomatous Polyposis (Jackman and Mayo, 1951). Although initially disputed, the identification of varying degrees of dysplasia arising within polyps, adenomas demonstrating the very earliest stages of invasion, and frank carcinomas with residual adenomatous regions at the edge led to a general consensus that most carcinomas of the large bowel develop in adenomas (Day and Morson, 1978).

Vogelstein et al subsequently studied genetic alterations in different stages of colorectal neoplasia, from early adenomas to advanced carcinomas. He observed that ras-gene mutations occurred frequently in advanced adenomas and carcinomas, but infrequently in early adenomas, and that chromosome 17p sequences were usually lost in carcinomas but not in adenomas (Vogelstein et al., 1988). Progressive acquisition of mutations causing the loss of tumour suppressor genes and the activation of oncogenes was therefore felt to mark the progression of the adenoma-carcinoma sequence.

1.4.2 Molecular pathways

Chromosomal Instability Pathway (CIN)

This is now recognised as the Chromosomal Instability (CIN) Pathway. Mutation of the adenomatous polyposis coli (APC) tumour suppressor gene on the long arm of chromosome 5 occurs early, which results in chromosomal instability and loss of heterozygosity (LOH) due to the loss of segments of chromosomes (Kudo et al., 2008). Consequent mutations include the activation of the KRAS oncogene early in the pathway, and mutations in the p53 and other tumour suppressor genes occur later. Tumours occurring via the CIN pathway are seen in sporadic adenomas and Familial Adenomatous Polyposis (FAP), and account for around 57% of colorectal cancers (Kudo et al., 2008).

Microsatellite Instability Pathway

Lynch syndrome (page 25) tumours exhibit different histological features to sporadic and FAP (page 23) tumours. Lynch syndrome cancers are more commonly right sided, and more commonly poorly differentiated or mucinous. This led to the suggestion that there may be an alternative molecular pathway responsible for the formation of these tumours, and this has subsequently been described as the Microsatellite Instability Pathway. In this pathway, a defect in mismatch repair (MMR) genes leads genomic instability through the accumulation of base errors. These are particularly evident in microsatellite regions of the genome. These are regions of the genome with long sequences of mononucleotide or dinucleotide repeats. Loss of mismatch repair ability leads to changes in the size of these microsatellite regions of the genome, termed microsatellite instability, which can be used to identify these tumours. In Lynch syndrome, germ line mutation of one allele of an MMR gene (commonly MLH1 or MSH2) is coupled with a somatic inactivation of the functioning parental allele. Biallelic silencing of an MMR gene can also lead to mismatch repair in approximately 15% of patients with sporadic colorectal cancer (Markowitz and Bertagnolli, 2009).

CpG-island methylation phenotype (CIMP)

In addition to chromosomal instability and microsatellite instability, a third mechanism of gene inactivation is now recognised in colorectal cancer. In these tumours, methylation of CpG dinucleotides aberrantly occurs in CpG rich "CpG islands" in the promoter regions of genes rather than in the areas of repetitive DNA outside exons where it is seen in the normal genome. This can result in the epigenetic silencing of genes (Issa, 2004). In sporadic MSI high cancers, methylation of the promoter region of MLH1 leads to a mismatch repair defect and microsatellite instability. This is thought to be the pathway responsible for the formation of colorectal cancer through serrated adenomas, and is seen predominantly in right sided cancers in older women.

1.4.3 Principle genes involved in colorectal cancer

Although there are at least three distinct pathways now recognised which allow the accumulation of genetic changes to form colorectal cancers, there is substantial overlap between these pathways in the tumour suppressor genes which are deactivated and the oncogenes which are activated.

Adenomatous Polyposis Coli (ACP) gene

The APC gene is a tumour suppressor gene located on the long arm of chromosome 5. It has a number of functions, including cell adhesion and migration, spindle formation and chromosome migration. Mutation of APC is found in 80% of colorectal adenomas and carcinomas, and is one of the earliest mutations in colon cancer progression (Goss and Groden, 2000). APC normally suppresses the Wnt signalling pathway which controls cell proliferation and differentiation in the intestine, by allowing destruction of the beta-catenin protein (Aoki and Taketo, 2007). Inactivation of this mechanism is thought to be a key early step in the formation of most colorectal carcinomas.

Tumour Protein p53 (TP53) gene

The TP53 gene is a tumour suppressor gene located on the short arm of chromosome 17. Tumour Protein p53, the protein coded by the TP53 gene, is important in the regulation of the cell cycle and induction of apoptosis in cells and is activated in response to a number of cell stresses. In colorectal neoplasms, loss of both TP53 gene alleles usually occurs near the transition from benign to malignant growth (Baker et al., 1990).

Transforming Growth Factor Beta (TGF-β) type II receptor gene

The TGF-β signalling pathway is involved in a number of cellular processes, including cell cycle arrest and apoptosis. The TGF-β type II receptor gene (TGFBR2) is a tumour suppressor gene located on the short arm of chromosome 3. The TGFBR2 gene is inactivated in 90% of colorectal cancers arising through the MSI pathway, and correlates closely with the progression of adenomas to cancers (Grady et al., 1998).

KRAS

Ras proteins are a family of related proteins involved in the intra-cellular signalling of cell growth and survival, the mitogen-activated protein kinase (MAPK) cascade. There are three Ras genes in humans; HRAS, KRAS, and NRAS. Of these, KRAS is a common oncogene in colorectal cancer with mutation occurring in 37% of colorectal cancers. Mutation of KRAS leads to promotion of cell replication. In isolation, this may lead to a hyperplastic polyp or serrated adenoma, but in combination with APC mutation may progress to colorectal cancer (Vogelstein and Kinzler, 2004). Two new therapeutic agents, cetuximab and panitumumab, are Epidermal Growth Factor Receptor (EGFR) inhibitors. These work by inhibiting activation of the KRAS intra-cellular signalling pathway through EGFR. Cetuximab and panitumumab are therefore ineffective for tumours with KRAS mutations. This has increased the clinical importance of testing tumours for KRAS mutation.

BRAF

Raf kinases are also intracellular signalling proteins and form the next step in the MAPK cascade, activated by RAS. Inappropriate activation of Raf can therefore also lead to promotion of cell replication. There are three Raf kinase proteins in humans, A-Raf, B-Raf and C-Raf. The gene which codes for B-Raf is called BRAF. This is a proto-oncogene in colorectal cancer and mutation is found in 18% of colorectal cancers (Davies et al., 2002). Mutation in both KRAS and BRAF would confer no survival advantage to cell lines as they both activate the same intra-cellular signalling pathway, and therefore mutations in these two oncogenes tend to be mutually exclusive. BRAF mutations occur more commonly in CIMP pathway colorectal cancers, and therefore tend to be seen more in right sided tumours arising in serrated adenomas. BRAF mutation also makes treatment with cetuximab or panitumumab ineffective as B-Raf is further down the same intracellular signalling pathway as KRAS, and so tumours are routinely tested for BRAF and KRAS mutations before commencing treatment with cetuximab.

1.4.4 Molecular classification of colorectal cancer

These different molecular pathways have been used to identify 5 distinct groups of colorectal cancers which exhibit distinct pathological features (Jass, 2007):

- Group 1 (sporadic MSI-H) tumours are MSI high, CIMP high, and chromosomally stable. They normally have methylation of MLH1 and demonstrate BRAF gene mutation. These tumours are predominantly right sided, affect women more than men, are often mucinous and arise in serrated adenomas. They account for approximately 12% of colorectal cancers.
- Group 2 tumours are MSI stable or MSI low, CIMP high, and chromosomally stable. They may demonstrate BRAF, KRAS, APC or TP53 gene mutation. These tumours are also predominantly right sided and occur more commonly in women, are often mucinous and arise in serrated adenomas. They account for approximately 8% of colorectal cancers.
- Group 3 tumours are MSI stable or MSI low, CIMP low, and chromosomally unstable. They usually demonstrate KRAS and TP53 mutation and may have APC mutation. They are predominantly left sided and affect men more than women. They may arise in serrated adenomas or adenomas and are less commonly mucinous. They account for around 20% of colorectal cancers.
- Group 4 tumours are MSI stable, CIMP negative and chromosomally unstable. The usually demonstrate APC, TP53 and KRAS mutation. They are predominantly left sided and occur more commonly in men, are less commonly mucinous and arise in adenomas. These tumours include sporadic, FAP associated and MUTYH polyposis associated tumours and account for around 57% of colorectal cancer.

- Group 5 (Lynch syndrome) tumours are MSI high, CIMP negative and chromosomally stable. They often exhibit APC and KRAS mutations, are predominantly right sided and occur more commonly in men than women. They also arise in adenomas and are less commonly mucinous. They account for around 3% of colorectal cancers.

This classification of colorectal cancer pathogenesis into distinct subgroups links recent molecular insight to some of the pathologically subtypes which have been recognised for some time. Although there is overlap between the subgroups, and indeed development of invasive colorectal cancer probably requires disruption of most if not all of the cellular signalling pathways, recognition of these subgroups may help research into the aetiology of colorectal cancer, chemoprevention, prognostication and targeted therapeutics.

1.5 Spread of colorectal cancer

Colorectal cancer may spread from its primary site through direct invasion of adjacent tissues, lymphatic spread, haematogenous spread and transcoelomic spread.

1.5.1 Direct invasion

Direct invasion is the process by which colorectal cancers grow into adjacent tissues. The vast majority of colorectal cancers start as adenomas, benign neoplasms arising from the colorectal mucosa. For these neoplasms to become carcinomas, they must first invade through the muscularis mucosa into the submucosa (Haboubi and Scott, 2000). At this stage, they become malignant neoplasms with the potential for distant metastasis.

Colorectal cancers may then continue to invade through the layers of the bowel wall, into the pericolic and perirectal fat, through the serosal layer where present, and into adjacent organs.

1.5.2 Lymphatic spread

Lymph node metastases are found in approximately 30% of resected colorectal cancer specimens on standard histological assessment , although a further 20% to 30% of patients may have micrometastases or isolated tumour cells if lymph nodes are examined by step sectioning and immunohistochemistry (Bembenek et al., 2005). Colorectal cancers usually metastasize first to para-colic or para-rectal lymph nodes, and then spread in a step wise fashion along draining lymphatics towards the para-aortic lymph nodes. However, lymph node metastases may skip a lymph node tier in approximately 20% of cases (Merrie et al., 2001).

1.5.3 Haematogenous spread

The process of haematogenous spread starts with intravasation of colorectal cancer cells, helped by angiogenesis within the primary tumour. However, this process alone is not enough to allow haematogenous spread of colorectal cancer cells. They must then adhere to the endothelium and extravasate into a suitable site to form metastatic deposits. This is a complex process and requires a large number of additional mutations for colorectal cancer cells form viable metastatic deposits.

The primary venous drainage of the colon and rectum is via the portal venous system to the liver, and it is therefore unsurprising that the liver is the most common site of distant metastases in colorectal cancer. As well as being the most common site of visceral metastases in colorectal cancer, the liver is the only site of visceral metastases in 30-40% of cases. The lower third of the rectum has dual venous drainage via the portal and systemic circulation, and it is probably for this reason metastasis to the lung is more common in rectal cancer.

1.5.4 Transcoelomic spread

The final mechanism of metastasis encountered in colorectal cancer is spread tumour cells across the peritoneal cavity. This usually occurs when tumour has invaded through the peritoneum (T4 disease), which may be apparent on pre-operative imaging, macroscopically at the time of operation,

or on histopathological assessment postoperatively. Occasionally, this form of spread may result from peritoneal spillage of tumour cells at the time of surgical resection.

Peritoneal deposits have a predilection for certain sites within the abdominal cavity; these include the superior and inferior ileocaecal recesses, the recto-vesical pouch (Pouch of Douglas), the under surface of the diaphragm and the transverse mesocolon (DeMeo et al., 1995, Coakley and Hricak, 1999, Meyers et al., 1987).

1.6 Sites of metastasis in colorectal cancer

1.6.1 Liver metastases

As mentioned previously, the liver is the most common site for visceral colorectal metastases. Over the period from 1984 to 2005, 5 year overall survival for patients undergoing resection of hepatic metastases improved from 23% to 46%, despite patients undergoing operations with more severe disease (Andres et al., 2008).

Improved survival following treatment for colorectal liver metastases has been attributed to a number of different factors. These include; improved techniques for anatomical resection (Geoghegan and Scheele, 1999, Jaeck et al., 1997, Fong et al., 1997), increased use of intraoperative ultrasound (Foroutani et al., 2000, Cervone et al., 2000), reduction in perioperative morbidity and mortality (Choti et al., 2002), second resections for recurrent hepatic metastases (Nordlinger and Wind, 1994) and the use of chemotherapy (Clavien et al., 2002, Shankar et al., 2001, Adam et al., 2001, Giacchetti et al., 1999).

A number of different studies have identified risk factors which predict outcome after resection of liver metastases. One of the largest studies by Fong et al included over 1000 patients, and identified the following prognostic factors: size of metastasis >5cm, potential involvement of the resection margin, >1 liver metastasis, poor prognosis primary, synchronous primary tumour and liver

metastases (within 12 months), and extra hepatic metastatic disease. Overall 5 year survival was 60% with none of these risk factors, falling to <20% with 4 or more risk factors (Fong et al., 1999).

It is therefore very important to have accurate pre-operative imaging prior to treatment for liver metastases for careful patient selection. The aims of imaging for patients undergoing resection of liver metastases are:

- To accurately demonstrate anatomical distribution of liver metastases and segmental sparing
- To exclude widespread micro metastatic disease within the liver
- To exclude extra hepatic metastases
- To discriminate between benign and malignant liver lesions
- To stratify patients in terms of prognosis following metastasectomy.

When assessing patients pre-operatively for occult intra or extra hepatic malignancies, it is worth bearing in mind that the risk is strongly related to the number and distribution of hepatic metastases; both occult intra hepatic metastases and extra hepatic metastases are rare with solitary unilobar metastases, but much more common with multiple bilobar metastases (Strasberg et al., 2001).

1.6.2 Lung metastases

The lungs are the second most common site of metastasis in colorectal cancer. If resection can be safely undertaken, then excellent outcomes can be achieved, with five year survival of 55.4% to 71% (Rama et al., 2009, Borasio et al., 2011). Patient undergoing repeat thoracotomy for recurrent pulmonary metastases may also achieve good outcomes, but the presence of hilar or mediastinal lymph node involvement or extra-pulmonary metastases are associate with poor survival rate (Ogata et al., 2005). As with liver metastases, it is therefore important to identify lesions early, when curative resection may still be achieved, and to exclude poor prognosis features such as extra-pulmonary metastases and hilar or mediastinal lymph node involvement.

Lung metastases usually present initially as small nodules, which are often <5mm in diameter. Multi-detector CT allows early detection and is superior to any other modality in the detection of these small lesions (Reinhardt et al., 2006). Although this does result in the identification of more benign lesions, a baseline CT and serial examinations allow indeterminate lesions to be interpreted more confidently during follow up.

1.6.3 Ovarian metastases

Ovarian metastases occur in 6-8% of women, making the ovaries the third most common site of visceral metastases in women. Radiologically, colorectal ovarian metastases may be easily mistaken for primary mucinous adenocarcinoma of the ovary (Cho and Gold, 1985). It is therefore important that the reporting radiologist is aware of any current or previous diagnosis of colorectal cancer when interpreting radiological imaging. Colorectal ovarian metastases may appear as large oval or lobulated, cystic or solid ovarian masses (Kuhlman et al., 1989, Kim et al., 1996).

1.6.4 Peritoneal metastases

Peritoneal metastases occur through spread of tumour cells across the peritoneal cavity. They therefore usually occur in the presence of T4 disease where the serosa has been breached by tumour cells.

The pattern of peritoneal spread is related to tumour grade, with poorly differentiated tumours tending to produce diffuse seeding, whereas well differentiated tumours are more likely to produce solitary deposits. Peritoneal metastases are the most common cause of ureteric obstruction due to colorectal cancer, and should be considered when unexplained ureteric obstruction is identified in patients with a history of colorectal cancer.

Although peritoneal metastases are usually managed palliatively, very carefully selected cases may have a good outcome if treated surgically (Glehen et al., 2004, Sugarbaker et al., 1996), and so patients should be discussed in a multidisciplinary setting if peritoneal disease is identified.

1.6.5 Other sites

A less common site of distant metastases in colorectal cancer is the brain (2%) (Mongan et al., 2009). Other sites of colorectal metastases are rare, and include: the spleen, kidneys, pancreas, adrenals, breast, thyroid and skin. However, it appears that unusual sites of metastasis are becoming more common with the increased use of systemic agents. There also appears to be a relationship to the number of systemic therapies received (Sundermeyer et al., 2005).

1.7 Anatomy of the colon and rectum

1.7.1 Layers of the colonic and rectal wall

The large intestine comprises an inner mucosal layer, a submucosal layer, a muscularis layer and an outer layer of adventitia.

The innermost mucosal layer can be further divided into three tissue layers. The epithelium lines the inner surfaces of the bowel. It is made up from enterocytes, which are responsible for the absorptive functions of the large intestine, and goblet cells which secrete mucous to help lubricate the passage of solid faeces. Underlying this epithelium is a loose connective tissue layer called the lamina propria, separated from the submucosa by a thin layer of muscle cells called the muscularis mucosa.

The submucosa is made up of collagenous tissue and provides strength to the wall of the large intestine. Within the submucosa run blood vessels and a neuronal network called Meissner's plexus.

Outside the submucosa lies the muscularis propria. This consists of a further neuronal network, Auerbach's plexus and an inner circular muscle layer. The outer longitudinal muscle layer of the bowel is reduced to 3 bands in the large intestine, named the taenia coli, except for the appendix and the rectum where they merge to form a continuous layer.

The adventitia is a layer of loose connective tissue surrounding the colorectum, through which the bowel receives it's vascular and nervous supply. This contains a varying amount of fat. In places the colorectum is covered by a serosal layer or visceral peritoneum, although this is absent where the mesorectum and mesocolon join the large bowel, below the peritoneal reflexion in the rectum and over part of the surface of the colorectum where they are retroperitoneal. Where present, the serosa is continuous with the adventitia and is lined by squamous epithelium (Burkitt et al., 1993).

1.7.2 Peritoneal coverings of the colon and rectum

The portions of the large intestine which lie within the peritoneal cavity are covered by a serosa (visceral peritoneum). This consists of a layer of squamous epithelium (mesothelium). The transverse colon and sigmoid colon lie freely within the peritoneal cavity on a long mesentery and have a serosal layer over their whole surface except for the area where the mesentery attaches. The ascending and descending colon are largely retroperitoneal, and have a serosal layer covering their anterior surface only. The rectum also has a serosal covering over its anterior surface above the peritoneal reflection, but below this level is surrounded completely by mesorectum. The clinical significance of the visceral peritoneum is that if tumour cells have breached this layer, they then lie freely within the peritoneal cavity and have the capacity for transcoelomic spread (page 35). This is recognised in the T staging of colorectal cancers, and such tumours are categorised as T4 tumours (page 65).

1.7.3 Fascial coverings of the colon and rectum

The peritoneum is easy to visualize, as it forms a shiny layer which lines the peritoneal cavity and covers the peritoneal surface the intra-abdominal viscera and mesentery. However, there are other fascial layers surrounding the colorectum which are similarly important, and less easy to visualise as they are only evident on dissection.

In the seventh week of foetal life, the colon lies in the midline supported dorsally by the medial mesocolon. This mesocolon has a peritoneum on both sides. During embryological intestinal rotation, the ascending colon comes to lie on the right side of the abdomen with the descending colon on the left. At this stage, the peritoneum covering the dorsal aspect of the ascending and descending mesocolon fuse with the parietal peritoneum and become the fusion fascia of Toldt (Mike and Kano, 2014). This layer is clinically significant because it encloses the mesocolon, and dissection within this plane allows the complete mesocolic excision which may be associated with a lower incidence of locoregional recurrence following colon cancer resection (Sondenaa et al., 2014). This is equivalent to, although anatomically separate from, the mesorectal fascia. Sharp dissection of rectal cancers in this plane (Total Mesorectal Excision) has been demonstrated to reduce local recurrence in rectal cancer resection (Heald, 1988).

1.7.4 Blood supply of the colon and rectum

The arterial blood supply of the colon and rectum forms the anatomical basis for the resection of colorectal cancers. This is primarily because the lymphatic drainage (page 43) of the colon and rectum follows the arterial blood supply. In order to perform a colonic or rectal resection which removes as many potentially involved lymph nodes as possible, a proximal (high) tie is performed on the artery supplying the area of large bowel containing the cancer. An appreciation of the arterial vascular supply to the colon and rectum is therefore crucial in order to appreciate not only which artery should form the high tie for a given tumour, but also how proximally the artery can be ligated without rendering the bowel, and potentially the anastomosis between the remaining segments of bowel, ischaemic.

The caecum and ascending colon are supplied by the ileocolic artery and right colic artery. The ileocolic artery is the terminal branch of the superior mesenteric artery. The right colic artery arises as a common trunk from the middle colic artery in 50% of cases, and has a separate origin (from the superior mesenteric artery) in 40% (Rosenblum et al., 1997). Tumours of the caecum and ascending

colon are therefore usually resected by performing a high tie on the ileocolic or superior mesenteric artery at the level of the inferior border of the duodenum. Above this level, too many arterial branches to the small bowel would be ligated, potentially rendering the small bowel ischaemic. The right colic artery may be ligated at its origin from the middle colic artery or in common with the ileocolic artery if its origin is from the superior mesenteric artery below the level of the inferior border of the third part of the duodenum.

The transverse colon is supplied by the middle colic artery, which is also usually a branch of the superior mesenteric artery. However, multiple anatomic variants have been described including origins from the coeliac, common hepatic and splenic arteries (Rosenblum et al., 1997). Tumours of the transverse colon are therefore resected by performing high tie on the middle colic artery.

The descending colon and sigmoid colon are supplied by the left colic and sigmoid arteries respectively. These are branches of the inferior mesenteric artery, and as the inferior mesenteric artery doesn't supply any organs other than the large bowel, tumours in all of these areas can be resected by performing a high tie at the origin of the inferior mesenteric artery. Some surgeons will ligate the ascending left colic at its origin from the inferior mesenteric artery when resecting the descending colon to preserve the superior rectal artery blood supply to the rectum.

The predominant blood supply to the rectum is via the superior rectal artery, which is a terminal branch of the inferior mesenteric artery. The lower third of the rectum, which is embryologically distinct from the rest of the large bowel being ectodermic in origin, also derives blood supply from the internal iliac arteries. Classically this is described as being via the paired middle rectal arteries and inferior rectal arteries. The middle rectal arteries originate from the anterior division of the internal iliac arteries. The inferior rectal arteries originate from the internal pudendal arteries, themselves a branch of the anterior division of the internal iliac arteries (Moore, 2011). However, some cadaveric studies have questioned the consistency and importance of the middle rectal arteries, suggesting that they may be absent forty to eighty-eight percent of subjects and frequently

unilateral (Jones et al., 1999) (Ayoub, 1978). Oncologically adequate resection of the rectum is performed utilising a high tie on the inferior mesenteric artery close to its origin from the aorta.

The venous drainage of the colon and rectum is broadly similar to the arterial supply, with middle, right and ileocolic veins draining into the superior mesenteric vein and the superior rectal, sigmoid and left colic veins draining into the inferior mesenteric vein. However, as these form part of the portal circulation, the inferior mesenteric vein joins the splenic vein before draining with the superior mesenteric vein into the portal vein.

Venous drainage from the lower third of the rectum is also similar to the arterial supply, and so drains into the systemic circulation via the internal iliac veins. This is clinically important as tumour cells which spread via this route enter the systemic circulation rather than the portal venous system and are therefore more likely to spread to the lungs and less likely to spread to the liver.

1.7.5 Lymphatic drainage of the colon and rectum

The lymphatic drainage of the large bowel is of clinical significance as the regional lymph nodes are the most common location of metastatic spread in colorectal cancer (page 35). The lymphatic drainage of the colon and rectum essentially follows the arterial supply, and is contained within the same mesocolic and mesorectal envelope.

The Japanese Society for Cancer of the Colon and Rectum categorizes and numbers the lymph node stations draining the colon and rectum according to the closest named artery and proximity to the bowel. Epicolic, paracolic and pararectal nodes (up to the level of Sudeck's point) are categorized as station 1 nodes. Over ninety-nine percent of positive pericolic and perirectal lymph nodes will lie within 10cm proximal or distal to the tumour (Toyota et al., 1995). Intermediate nodes lie along the branches of the superior and inferior mesenteric arteries, and are categorised as station 2 nodes. Main nodes lie at the origin of the named colic arteries and along the inferior mesenteric artery

proximal to the left colic artery (Dennosuke, 1983). The numbers of these nodal stations are given in Table 1.1.

Colorectal cancer can also metastasize to lymph nodes outside the mesorectal or mesocolic envelope. This is perhaps unsurprisingly most common in the low rectum. As previously discussed, the lower third of the rectum is of embryological ectodermic origin, and derives some of its blood supply from the internal iliac arteries. Some of the lymphatic drainage of the rectum therefore also drains laterally to the internal iliac arteries, with lymph node metastases to lateral lymph nodes occurring in 8.8% of rectal cancers (Morikawa et al., 1994). The incidence of lateral spread in rectal cancer increases in more distal tumours, occurring in 12.3% of lower third rectal tumours compared to 2.6% of upper third tumours (Morikawa et al., 1994).

Colonic tumours can also metastasize to lymph nodes other than those accompanying the primary arterial supply, although this occurs less commonly. Hepatic flexure tumours may metastasize to lymph nodes over the pancreatic head in 5% of patients, and tumours of the hepatic flexure or transverse colon may metastasize to lymph nodes along the gastroepiploic arcade in 4%. Tumours of the transverse colon and splenic flexure may also metastasize to lymph nodes along the inferior border of the tail of the pancreas (Hohenberger et al., 2009).

		Epicolic, paracolic and pararectal nodes	Intermediate nodes	Main nodes	Superior mesenteric nodes	Paraaortic nodes
Superior mesenteric artery branches	Ileocolic	201	202	203	214	
	Right colic	211	212	213		
	Middle colic	221	222	223		
Inferior mesenteric artery branches	Left colic	231	232	253 (Inferior mesenteric nodes)		216
	Sigmoid colic	241	242			
	Superior rectal	251	252			

Table 1.1: Lymph node stations

1.7.6 Anatomical relations of the colon and rectum

Caecum

The caecum is usually located in the right iliac fossa. Typically the anterior and lateral surfaces are covered in peritoneum and may be in contact with although not usually attached to the small bowel, omentum or anterior abdominal wall. The posterior surface is usually retroperitoneal and lies over the iliacus and psoas muscles, and the femoral nerve. The appendix arises from the caecal pole and sometimes lies posterior to the caecum. In some individuals, the caecum is mobile, with a peritoneal covering over all its surfaces. In this case it may lie within the pelvis and be related to the right ovary and fallopian tube, or the sigmoid colon. In other individuals the caecum may be located more caudally in the position usually occupied by the ascending colon.

Ascending colon

The ascending colon is a continuation of the caecum, located in the right side of the abdomen above the level of the ileocaecal valve. The ascending colon is also covered by peritoneum on its anterior and lateral surfaces and these may also be in contact with small bowel, omentum, or the anterior abdominal wall. The posterior surface is retroperitoneal and overlies the iliacus and quadratus lumborum muscles, the right kidney, and iliohypogastric and ilioinguinal nerves. Medially the ascending colon is related to the right ureter and right gonadal vessels.

Hepatic flexure

The hepatic flexure is located in the right upper quadrant of the abdomen. Caudally, it may be in contact with although not usually attached to the liver and the gallbladder. Posteriorly, the hepatic flexure may overlie the right kidney. Medially, the hepatic flexure maybe related to the second part of the duodenum.

Transverse colon

The transverse colon is hangs quite freely from its mesentery and is largely covered in peritoneum. Its position is therefore quite variable, both between individuals within the same individual in different postures. Anteriorly it is usually related to the greater omentum and anterior abdominal wall. Posteriorly the transverse colon may be related to second part of the duodenum, the head of the pancreas, and to small bowel loops. Superiorly, the transverse colon may be related to the liver, gallbladder, stomach and spleen.

Splenic flexure

The splenic flexure is located in the left upper quadrant of the abdomen. Superiorly, the splenic flexure is related to the inferior border of the spleen, and may be very closely related in some individuals. The posterior aspect of the splenic flexure may overlie the left kidney or the tail of the pancreas.

Descending colon

The descending colon is located in the left side of the abdomen. Its anterolateral aspects are usually covered by peritoneum and its posterior aspect is retroperitoneal. The anterior surface may be in contact with but is not usually attached to small bowel loops, the omentum or the anterior abdominal wall. Posteriorly, the descending colon is related to the left kidney, the left ureter, the left gonadal vessels, the iliacus and psoas muscles, and the femoral nerve.

Sigmoid colon

The sigmoid colon is usually fairly free on its mesentery, with most of its surface covered by peritoneum. It is therefore often quite mobile, and its location may very significantly between and within individuals. The root of the sigmoid mesentery overlies the left ureter, left gonadal vessels and the left internal iliac artery. The sigmoid may be in contact with rectum, the uterus, both

ovaries and fallopian tubes, the bladder, small bowel loops, and occasionally the caecum. The sigmoid colon overlies the sacrum and sacral plexus.

Rectum

The rectum is located in the pelvis and is retroperitoneal except for the anterior surface of the upper third of the rectum. It has a number of close relations. Posterolaterally lie the sympathetic and pelvic splanchnic nerves, the sacral and coccygeal nerves, piriformis and levator ani muscles, the sacrum and the coccyx. Laterally lie the pelvic sidewall and pelvic veins. Anteriorly in the female lie the pouch of Douglas, small bowel, the vagina, the uterus and the urinary bladder. Anteriorly in the male lie the rectovesical pouch, small bowel, bladder, vas deferens, seminal vesicles and prostate.

1.7.7 Anatomical definition of the rectum

There is currently no international consensus on the distinction of rectal and colon cancer. The anatomical definition of the transition between the colon and rectum is either the point where the mesocolon ends, or the level of the third sacral vertebra. North American papers usually define the rectum as the large bowel within 12cm of the anal verge on rigid sigmoidoscopy, whereas UK texts usually define the rectum as the large bowel arising within 15cm of the anal verge. For the purposes of this research, the ACPGBI definition of rectal cancer is adopted (a cancer of the large bowel arising within 15cm of the anal verge on rigid sigmoidoscopy) (Association of Coloproctology of Great Britain and Ireland (ACPGBI), 2007).

1.8 Treatment of colorectal cancer

1.8.1 Colorectal cancer surgery

The mainstay of curative treatment for colorectal cancer is resection of the primary tumour along with the draining lymph nodes, and this remains the case almost two hundred years after Lisfranc

performed the first successful resection of a rectal cancer in 1826 via a perineal approach (Gordon and Cameron, 2000).

Standard resections

Standard colorectal cancer resections are dictated by the anatomical location of the tumour. The segment of colon or rectum containing the tumour is resected along with a margin of healthy bowel proximally and distally. The named artery or arteries supplying that colonic or rectal segment are ligated proximally, and the mesentery containing the lymphatic drainage for that segment of large bowel is removed with the specimen.

Tumours of the caecum and proximal ascending colon are surgically resected by performing a right hemicolectomy, removing the caecum and ascending colon and ligating the ileocolic artery proximally. Tumours of the transverse colon are treated with an extended right hemicolectomy, removing the caecum, ascending and transverse colon and additionally ligating the middle colic artery. Tumours of the descending colon are excised by performing a left hemicolectomy, removing the descending colon and ligating the ascending left colic artery. Tumours of the sigmoid colon and upper two thirds of the rectum are removed by performing an anterior resection, removing the sigmoid colon and part of the rectum and ligating the inferior mesenteric artery. The mesorectum is divided at the same level as the rectum, approximately 5cm distal to the distal edge of the tumour. In a high anterior resection, it is not necessary to continue the dissection below the peritoneal reflection. In a low anterior resection, the dissection is continued below the peritoneal reflection, but there is still sufficient length of rectum remaining to perform a stapled colorectal anastomosis. Tumours in the lower third of the rectum may be treated by an ultra-low anterior resection where the sphincter mechanism is not involved. The dissection is continued in the mesorectal plane to the pelvic floor, and the rectum is transected at the level of the pelvic floor. In an intersphincteric resection (ISR) or transanal abdominal transanal (TATA) resection, the mucosa is incised at the dentate line and dissection is continued through the internal sphincter to the intersphincteric plane,

then superiorly into the mesorectal plane. An anterior resection from an abdominal approach meets this dissection, and a hand sewn coloanal anastomosis is performed, removing the whole rectum (Kosinski et al., 2012). Distal clearance of 1cm is usually considered adequate for low rectal cancers. If preservation of the sphincter mechanism is not possible, tumours are resected by performing an abdominoperineal resection, removing the sigmoid, rectum, and anus and ligating the inferior mesenteric artery.

Clinical practice varies between surgical units and individual surgeons, with some favouring more limited segmental resections and some favouring more radical resections. More radical resections involve more proximal ligation of the supplying arteries, removal of a greater length of colorectum, and may involve additional lymphadenectomy.

Total Mesorectal Excision (TME)

Total Mesorectal Excision (TME) describes a surgical technique used to excise the rectum using sharp dissection to follow the anatomical plane around the mesorectal fascia, and remove the entire mesorectal envelope intact. The technique was described by Bill Heald in the early 1980's and is now the gold standard technique for resection of the rectum when performing an anterior resection or abdominoperineal resection (Heald et al., 1982). In a nineteen year period using this technique in over five hundred patients the Basingstoke group reported an overall local recurrence rate of 6%, with a local recurrence rate of 3% for R0 resections (Heald et al., 1998). Prior to the adoption of this technique anterior resection was usually performed with blunt dissection within the mesorectal plane and was associated with a recurrence rate of 12 to 40 percent (Heald et al., 1982).

High ligation

In 1908 Ernest Miles described the abdominoperineal approach to rectal cancer in an attempt to remove the upward lymphatic spread of rectal cancer which had been responsible for the near complete failure to cure rectal cancer by the perineal approach used up to that point, resulting in a huge improvement in the outcome of rectal cancer surgery and laying the foundations for the

anterior resections and abdominoperineal resections performed today. In his description of this procedure, he described division of the inferior mesenteric artery just distal to the ascending left colic branch ("low tie") (Miles, 1971). Subsequently, Moynihan described ligation of the inferior mesenteric artery more proximally, flush with the aorta, and suggested that this would remove even more proximal nodes. This has become known as a "high tie" on the inferior mesenteric artery, but the benefit of this approach has disputed. Pezim et al. compared survival outcomes in a large cohort of 1370 patients who had undergone rectal cancer resection with either a low tie or high tie on the inferior mesenteric artery. They reported no significant difference in overall survival in patients receiving a high tie or low tie, although interestingly their results did suggest a degree of under staging in the low tie group with worse survival in Dukes A and B patients but better survival in Dukes C patients compared to the high tie group (Pezim and Nicholls, 1984). Similar results were reported by Surtees et al. in a smaller group of 250 selected patients (Surtees et al., 1990). Conversely, a large study involving 2,409 patients operated on between 1951 and 1975 Slanetz et al. reported a significance benefit in cancer specific survival in the high tie compared to the low tie group. However, most of the difference was seen in local and staple line recurrence, with high local recurrence rates (30.7% in Dukes C cancers in the low tie group) (Slanetz and Grimson, 1997). These differences are therefore likely to represent variation in the degree of mesorectal excision in the pre-TME era. Hida et al. reviewed the available literature in 2013 and concluded that there was insufficient evidence to determine whether performing a high tie on the inferior mesenteric artery offered a survival benefit in conjunction with TME surgery and modern adjuvant therapy, but that it did offer a number of other advantages including more accurate staging (Hida and Okuno, 2013).

Complete Mesocolic Excision (CME)

Complete Mesocolic Excision (CME) for colon cancer is analogous to TME for colon cancer. It involves the sharp dissection of the visceral fascia covering the colon and mesentery from the retroperitoneal fascia, combined with the central ligation of the supplying artery and resection of an

adequate length of colon (Hohenberger et al., 2009). This results in a resection which is potentially oncologically superior, with resection of more mesocolon and an associated higher lymph node yield (West et al., 2010). To date, there is no evidence to demonstrate that this technique results in superior disease specific or overall survival.

Extended Pelvic Lymph Node Dissection

Since the late 1970's it has been common practice in Japan to perform an extended pelvic lymph node dissection for rectal cancers, particularly if there is any suspicion of the involvement of these lymph nodes on pre-operative imaging (Sugihara et al., 2006). This practice has not been widely adopted in Europe or Northern America, and the benefit of this practice remains controversial. Approximately 15% of patients undergoing extended pelvic lymph node dissection have positive lymph nodes in retrospective series (Kobayashi et al., 2009). However, there may be some selection of higher risk patients to undergo lateral pelvic lymph node dissection in these series and this proportion may be lower when considering all rectal cancer patients. These patients may potentially benefit from having involved lymph nodes removed, although Kobayashi et al failed to demonstrate a benefit in overall survival or local recurrence in a large cohort of 1,272 patients.

Extended pelvic lymph node dissection may also upstage some approximately 5% of patients who would be node negative with a standard TME resection but who have skip lymph node metastases (Liang et al., 2007), and these patients may benefit from adjuvant chemotherapy.

However, there is significant morbidity associated with this technique, principally due to bladder and erectile dysfunction due to pelvic nerve injury. One study which specifically investigated this issue reported that 100% of patients experienced bladder and erectile dysfunction following extended pelvic lymph node dissection without pelvic nerve preservation, and around 50% reporting erectile dysfunction even with pelvic-plexus preservation (Akasu et al., 2009).

To reliably assess the benefit of extended pelvic lymph node dissection, a very large randomised controlled trial would be required, and there is no such study underway at present. It is unlikely that

such a morbid technique will be widely adopted in Europe and Northern America without this level of evidence.

Extra Levator Abdominoperineal Excision (ELAPE)

The introduction of TME surgery has substantially reduced the local recurrence rate in rectal cancer. However, the margin positivity and local recurrence rates for low rectal tumours have remained high compared to mid and upper rectal tumours. In a large retrospective study of 1219 patients from the Dutch RT + TME trial, Nagtegaal et al. demonstrated that low rectal cancers (5cm or less from the anal verge) had a 26.5% CRM involvement rate compared to 12.6% for tumours >5cm from the anal verge, and that 30.4% of low rectal cancers treated by APR had a CRM involvement compared to 10.7% of those treated by anterior resection (Nagtegaal et al., 2005). Five year survival was also worse where the CRM was positive in the APR group compared to the anterior resection group (39.5% compared to 57.6%). This high rate of CRM involvement in low rectal tumours treated by conventional APR is probably due to the tapering of the mesorectum towards the anorectal junction, which naturally results in a narrowing of the specimen towards the sphincters if the mesorectal plane is followed to this level.

In 2007 Holm et al. described an extended abdominoperineal resection with gluteus maximus flap reconstruction of the pelvic floor for T3 and T4 low rectal cancers (Holm et al., 2007). This technique involves stopping the TME dissection at the top of the levator ani muscles and the upper border of the coccyx, then turning the patient prone and completing the perineal part of the operation outside the levator ani muscles, excising the coccyx to meet the abdominal dissection posteriorly, and dividing the levator ani muscles at their insertion. This results in a cylindrical specimen, without the waist at the top of the sphincters encountered in a conventional APR. This technique is in some ways similar to that originally described by Miles in 1908 (Miles, 1971). This technique has subsequently become known as an extra-levator abdominoperineal excision (ELAPE), and a variety of

methods have been used to close the perineal defect including gracilis and vertical rectus abdominis myocutaneous flaps, collagen meshes and primary closure (Butt et al., 2013).

Some small retrospective studies have reported reduced rates of inadvertent bowel perforation and positive CRM in ELAPE compared to conventional APR (Stelzner et al., 2011, Dalton et al., 2012), and a larger study based on the Swedish Rectal Cancer Registry suggests that there may be a benefit in low tumours where the CRM positivity rate was 7.3% compared to 15.5% with standard APE (Prytz et al., 2014). However, there is a higher associated rate of perineal wound complications using this technique (Prytz et al., 2014), and other authors have disputed whether ELAPE does in fact reduce the rate of margin involvement (Gash et al., 2014). Large scale prospective studies are therefore required to determine whether ELAPE is superior to standard APE.

Laparoscopic colorectal surgery

Since the first laparoscopic colorectal resection was performed in 1991, there has been a substantial move towards laparoscopic colorectal cancer with steadily increasing numbers of patients undergoing this form of surgery. There are now at least 15 randomised controlled trials which have compared open and laparoscopic colorectal surgery. These were recently summarised in a meta-analysis by Wang et al. including 6557 patients (Wang et al., 2014). This concluded that there is a significant benefit from laparoscopic colorectal surgery in short term outcomes including blood loss, length of hospital stay, time to first bowel movement and 30 day mortality. However, there was no difference in long term outcomes including overall 3 and 5 year survival and local recurrence rates. Laparoscopic colorectal cancer surgery should therefore be offered as an alternative to patients where local equipment and skills allow.

Local excision for rectal cancer

TME, with neoadjuvant radiotherapy and neoadjuvant or adjuvant chemotherapy where indicated, provides excellent local control of rectal cancer. However, there is a significant perioperative morbidity and mortality associated with this treatment. An analysis of the Dutch TME trial reported

faecal incontinence in 38.8% of patients (Wallner et al., 2008) and erectile dysfunction in 76% of men (Lange et al., 2009). Patients with low rectal tumours where it is not possible to preserve the sphincters will also be faced with a permanent stoma.

This has led to considerable interest in local excision of early rectal cancers. A variety of techniques have been described, including transanal excision, transanal endoscopic microsurgery (TEMS), transanal minimally invasive surgery (TAMIS) and endoscopic mucosal resection (EMR) amongst others. A number of single institution series have reported on local resection of rectal cancers, with quoted recurrence rates of 7% to 40% for T1 tumours and 25% to 62% for T2 tumours (Blackstock et al., 2010). These rates are significantly higher than those achieved with TME surgery in expert centres (5% to 8%), which also treat more locally advanced tumours. This is due to the fact that lymph node metastases in the mesorectum are not identified or treated by local excision.

Local excision has therefore been combined with radiotherapy or chemoradiotherapy in a number of studies in an attempt to treat any occult mesorectal lymph node metastases. In a recent systematic review Ung et al reported a median local recurrence rate of 10% (range 4.8% to 25%) for patients with T1 or T2 rectal cancer undergoing local excision combined with chemotherapy or chemoradiotherapy (Ung et al., 2014). Although this is higher than would be expected in a similarly selected group of patients undergoing TME surgery, most patients experiencing local recurrence were able to undergo successful salvage surgery.

Further research is needed in this area to clearly define the role of local excision in rectal cancer, but it may have a place in selected patients with small T1 or T2 tumours without lymph node metastases on preoperative imaging, patients with low rectal tumours unwilling to accept a permanent stoma and in elderly or infirm patients at high risk from TME surgery.

Natural Orifice Transluminal Endoscopic Surgery (NOTES) and Natural Orifice Specimen Extraction (NOSE)

Following on from the success of laparoscopic surgery, a number of authors have reported techniques to reduce or eliminate the number of laparoscopic port site and specimen extraction incisions. These involve either performing the whole operation through a natural orifice (trans-gastric, trans-vaginal, or trans-anal), which has been termed NOTES, or performing a hybrid procedure where the dissection is performed laparoscopically but the specimen is extracted through a natural orifice (sometimes described as NOSE) (Wexner and Edden, 2009). A number of authors have demonstrated that it is technically possible to perform a laparoscopic colectomy with specimen extraction via the transvaginal route in women (Torres et al., 2012, Karahasanoglu et al., 2011). Supporters of natural orifice surgery site the absence of abdominal scars and reduced post-operative pain as advantages of this technique, although safety and adequacy of oncological resection need further study.

Trans-anal TME

A recent development which combines some of the principles of NOTES surgery with equipment previously used for local resection of rectal tumours is trans-anal TME. In this technique, the rectum is closed with a purse string suture distal to the tumour, and then the rectum is divided below this level. TEMS or TAMIS equipment is then inserted per rectum, and used to perform a dissection in the mesorectal plane from “below-up”. This is usually combined with a laparoscopic trans-abdominal approach for the proximal dissection and ligation of the IMA. Atallah et al and de Lacy et al have reported small series which suggest that this approach may be safe, and allow easier dissection in the mesorectal plane, especially in obese males (Atallah et al., 2014, de Lacy et al., 2013). There is currently insufficient data to say yet whether this approach is oncologically superior or inferior to the purely transabdominal approach.

1.8.2 Radiotherapy

Local recurrence rates

There have been at least twenty-eight randomised trials comparing pre-operative or postoperative radiotherapy with surgery alone, which are well summarised in a meta-analysis published by the Colorectal Cancer Collaborative Group (Colorectal Cancer Collaborative Group, 2001). This demonstrated a highly significant trend towards greater efficacy of pre-operative radiotherapy with higher biologically effective doses. The large trials of pre-operative radiotherapy with a biologically effective dose of greater than 30Gy (Stockholm I & II, Swedish rectal cancer trail, UK MRC2 and Northwest England) all demonstrated a significant reduction in local recurrence rates with radiotherapy followed by surgery compared to surgery alone (Marsh et al., 1994, Cedermark et al., 1995, Stockholm Colorectal Cancer Study Group, 1996, Medical Research Council Rectal Cancer Working Party, 1996, Swedish Rectal Cancer Trial, 1997). Several large randomised trials of post-operative radiotherapy in rectal cancer, which all used an biologically effective dose of more than 30Gy, also demonstrated a significantly lower rate of local recurrence in patients receiving radiotherapy (Balslev et al., 1986, Fisher et al., 1988, Thomas and Lindblad, 1988). In a meta-analysis the overall risk of local recurrence following post-operative radiotherapy was 15.3% compared to 22.9% in those receiving surgery alone ($p<0.0001$), and the overall risk of local recurrence following pre-operative radiotherapy was 12.5% compared to 22.2% for surgery alone ($p<0.00002$) (Colorectal Cancer Collaborative Group, 2001).

Overall survival rates

Despite convincing evidence that adjuvant radiotherapy reduced the local recurrence rate of rectal cancer, individual trials did not convincingly demonstrate an overall survival rate for patient receiving adjuvant radiotherapy. In 2000 Camma et al. performed a meta-analysis of 14 randomised trials and demonstrated a significant overall survival benefit for patients receiving adjuvant radiotherapy with an odds ratio of 0.84 (Camma et al., 2000). This finding was supported by a larger

meta-analysis involving 28 trials performed by the Colorectal Cancer Collaborative Group in 2001 (Colorectal Cancer Collaborative Group, 2001).

Pre-operative or post-operative radiotherapy

Following on from these trials which demonstrated a clear benefit in terms of reduction in local recurrence following radiotherapy, a two large trials compared pre-operative with post-operative chemoradiotherapy in the German Rectal Cancer Study Group trial (Sauer et al., 2004), and pre-operative radiotherapy with selective postoperative chemoradiotherapy in the MRC CR07 trial (Sebag-Montefiore et al., 2009). These trials both demonstrated a significantly lower local recurrence rate (6% vs 13% in the German Rectal Cancer Study Group trial and 4.4% vs 10.6% in the MRC CR07 trail) for pre-operative radiotherapy compared to the post-operative radiotherapy groups. Acute toxic effects and long term toxic effects were also lower in the pre-operative radiotherapy group compared to the post-operative radiotherapy group (Sauer et al., 2004). These results are in keeping with the meta-analysis of previous radiotherapy compared to surgery alone trials which showed that the reduction in risk of local recurrence was significantly greater in the pre-operative radiotherapy group than the post-operative radiotherapy group in the trials where a biologically effective dose of >30Gy was used (risk reduction 57% vs 37%, p=0.01) (Colorectal Cancer Collaborative Group, 2001).

Radiotherapy and TME surgery

The introduction of TME surgery, discussed on page 50, has resulted in a dramatic reduction in the rate of local recurrence seen in rectal cancer. The majority of trials of radiotherapy compared to surgery alone started recruitment before TME surgery was widely practiced. This is reflected in the high rate of local recurrence seen with surgery alone in these trials of 21% to 36% (Stockholm Colorectal Cancer Study Group, 1996, Marsh et al., 1994), compared to the 6% reported by Heald et al with TME surgery (Heald et al., 1998). This has led some to question whether the benefits seen with radiotherapy in these trials are conferred to patients undergoing TME surgery.

The Dutch TME trial is a large, prospective multicentre randomised trial which aimed to address this issue. One thousand eight hundred and sixty one patients were randomised to preoperative short course radiotherapy and TME surgery or TME surgery alone. The quality of surgery was carefully monitored. The 10 year cumulative incidence of local recurrence was significantly lower at 5% in the radiotherapy and surgery group compared to 11% the surgery alone group (van Gijn et al., 2011). There was no overall survival benefit for the whole group with radiotherapy, but there was for a subgroup of patients with TNM stage III cancer and a negative CRM. As mentioned in the trial report, this study was conducted before accurate staging with MRI was widely available and so was associated with a higher rate of CRM positivity at 16% than would be expected with accurate MRI staging and MDT discussion (van Gijn et al., 2011). Subgroup analysis also demonstrated that although there was a significant reduction in local recurrence rates with radiotherapy for TNM stage I disease, the absolute risk reduction was low at 2.7% due to a low rate of local recurrence with TME surgery alone (3%).

Morbidity and mortality

Pre-operative radiotherapy is associated with an increased incidence of late faecal leakage and an increased frequency of bowel movements compared to patients undergoing surgery alone who do not have a permanent stoma (Wiltink et al., 2014). The incidence of urinary dysfunction is also increased, and male patients also report an increased frequency of erectile dysfunction following pre-operative radiotherapy compared to surgery alone (Prabhudesai et al., 2005).

In the Dutch TME study, although 10 year disease specific survival was significantly better in the radiotherapy group, this was cancelled out by an increased incidence of deaths from other causes, including radiotherapy complications (1% vs 0%) and secondary malignancy (14% vs 9%) (van Gijn et al., 2011). This raises the possibility that radiotherapy may be associated with more deaths from other causes whilst reducing cancer related deaths, and may in part explain the difficulty in

demonstrating an overall survival benefit for radiotherapy despite large reductions in the local recurrence rate in the pre-TME era.

Brachytherapy

Endorectal high dose rate brachytherapy has been used to deliver higher doses of radiotherapy to the tumour. In this procedure, radioactive sources are introduced via an endorectal applicator to allow close contact with the tumour. This has usually been used as a "boost" in addition to pre-operative external beam radiotherapy and chemotherapy. A randomised controlled trial of 248 patients reported a significantly lower CRM positivity rate and higher major pathological response rate with the addition of high dose rate brachytherapy to neoadjuvant chemoradiotherapy (Jakobsen et al., 2012). The current NICE guidelines recommend that although there is evidence that it is effective in reducing tumour size in combination with EBRT, there is no evidence that it provides additional benefit over EBRT (National Institute for Health and Clinical Excellence, 2014).

Contact radiotherapy

Low energy contact X-ray brachytherapy (CXB, also called the Papillion technique) involves delivering radiotherapy to the tumour by placing an X-ray tube into the rectum through the anus into close proximity with the tumour, and emitting low energy X-rays into the tumour. The penetration of these low energy X-rays is limited to a few millimetres, delivering high dose radiotherapy to the tumour but limiting exposure by adjacent organs.

This technique has variously been used as the sole treatment for small T1 tumours, following local excision of small T1 tumours, in combination with EBRT for T2-T3 tumours, and in combination EBRT followed by anterior resection to increase sphincter preservation rates for patients with low rectal cancers (Gerard et al., 2015). CXB alone or in combination with EBRT has been reported to induce clinical complete response in 26% to 73% of patients, and allow organ preservation without disease recurrence in 74% to 83% of these patients (Christoforidis et al., 2009, Ortholan et al., 2012).

Future developments

Intensity modulated radiotherapy (IMRT) and volume modulated arc radiotherapy (VMAT) are relatively new radiotherapy techniques which allow delivery of higher radiotherapy doses to the target tissue while reducing the dose to adjacent tissues. These can be combined with a CT scanner, and more recently an MRI scanner, to identify the target tissue accurately when planning the radiotherapy field. These technologies could potentially be used to reduce the incidence of radiotherapy related side effects and secondary cancers following treatment for rectal cancer, to increase the safe dose delivered to the tumour, or to perform radiotherapy in areas where injury to the small bowel has previously precluded it such as colon cancers.

1.8.3 Chemotherapy

Adjuvant chemotherapy in colorectal cancer

In 1990, the American National Institutes of Health recommended 12 months treatment with 5-FU (Fluorouracil) and levamisole for resected, node positive colon cancer (TNM stage III) (National Institues of Health (NIH), 1990). This was based on the results of three studies by Windle et al, the North Central Cancer Treatment Group and the Inter-group which showed significant survival benefit for patient treated with adjuvant 5-FU and levamisole compared to surgery alone, with overall 5 year survival of between 62% and 71% with chemotherapy compared to 55% without (Moertel et al., 1990, Laurie et al., 1989, Windle et al., 1987). Previous studies with single agents had failed to show any significant survival benefit in the adjuvant setting.

Subsequently the European MOSAIC trial has compared 5-FU plus leucovorin (LV5FU2) to fluorouracil plus leucovorin plus oxaliplatin (FOLFOX4) for 6 months in TNM stage II or III colon cancer. This demonstrated significantly better overall 6 year survival for FOLFOX4 compared to LV5FU2 in the whole group (78.5% compared to 76.0%) and in the stage III colon cancer subgroup

(72.9% compared to 68.7%) (Andre et al., 2009). This is the current standard for adjuvant treatment of stage III colon cancer following potentially curative resection for patients who are fit enough to receive it.

A further large study has compared oral capecitabine to fluorouracil plus leucovorin as adjuvant therapy for patients with resected stage III colon cancer, and demonstrated disease free survival to be at least equivalent with significantly fewer adverse events (Twelves et al., 2005). Capecitabine is therefore frequently used as an alternative to FOLFOX in the adjuvant setting for patients who do not wish to or who are not suitable to receive oxaliplatin based chemotherapy.

The majority of these studies have assessed the benefits of adjuvant chemotherapy in colon cancer rather than rectal cancer. In 2012, Petersen performed a meta-analysis of 21 trials, from which 9221 rectal cancer patients had adequate data for assessment of OS. This demonstrated a significant benefit in OS in patients receiving adjuvant 5-FU based chemotherapy, with a hazard ratio of 0.83 for OS and 0.75 for DFS (Petersen et al., 2012). Some controversy remains however, as these studies were largely performed in patients who had not received neoadjuvant chemoradiotherapy. EORTC 22921 investigated the benefit of adjuvant 5-FU and folinic acid chemotherapy in rectal cancer patients who had received neoadjuvant radiotherapy or chemoradiotherapy. There was no significant difference in 10-year DFS between the groups who had and had not received postoperative chemotherapy (Bosset et al., 2014).

Adjuvant chemotherapy for stage II colorectal cancer

The use of adjuvant chemotherapy for patients with TNM stage II colorectal cancer has been controversial, with a number of individual trials failing to show any significant benefit. In 2003 a pooled analysis from 3341 patients in seven randomised trials showed a consistent benefit for stage II and stage III disease, with a proportional reduction in the risk of recurrence and death, although the absolute reduction was less in stage II disease (Gill et al., 2003). The QUASAR trial showed a small but statistically significant benefit for patients with stage II colorectal cancer receiving

fluorouracil and folinic acid following resection compared to a controls not receiving chemotherapy, with an improvement in absolute survival of 3.6% (Gray et al., 2007b). The MOSAIC trial showed a trend towards improved disease free survival for patients receiving FOLFOX4 compared to 5-FU/LV for stage II patients with high risk features only. In a recent meta-analysis, Wu et al. demonstrated a significant improvement in overall and disease free survival for stage II colon and rectal cancer patients receiving adjuvant chemotherapy (Wu et al., 2012).

Neoadjuvant chemoradiotherapy in rectal cancer

A number of trials have compared the use of combination pre-operative chemoradiotherapy (fluorouracil or fluorouracil with folinic acid) with radiotherapy alone in the treatment of rectal cancer, including the European Organisation for the Research and Treatment of Cancer (EORTC) trial, the EORTC 22921 trial, the Federation Francophone de la Cancerologie Digestive (FFCD) trial and the Polish trial. A meta-analysis of these trials demonstrated a significant reduction in the rate of local recurrence in the chemoradiotherapy group (9.4%) compared to the radiotherapy alone group (16.5%) (Ceelen et al., 2009). However, some of these trials were performed in the pre-TME era and so the rate of local recurrence is relatively high. There was also a significantly higher rate of pathological complete response in the chemoradiotherapy group (11.8%) compared to the radiotherapy alone group (3.5%) (Ceelen et al., 2009)

The subsequent Trans-Tasman Radiation Oncology Group (TROG) trial 01.04 also demonstrated a trend towards reduced local recurrence rates for patients with MRI staged T3 tumours receiving chemoradiotherapy with 5-FU (4.4%) compared to those receiving radiotherapy alone (7.5%), although this difference was not statistically significant.

The NSABP R04 trial of 1608 patients compared 5-FU and it's oral equivalent, capecitabine, and found no differences in pathological CR rates or early local recurrence or disease free survival (Roh et al., 2011). Patients undergoing pre-operative chemoradiotherapy should probably therefore be offered treatment with 5-FU or capecitabine depending on patient preference. The addition of

oxaliplatin, bevacizumab, cetuximab, or irinotecan to 5-FU has not been demonstrated to confer any incremental benefit (Schrag, 2013).

Induction chemotherapy in rectal cancer

Current management of advanced rectal cancer involves chemoradiotherapy, followed by surgery, followed by systemic chemotherapy. This does not deliver effective systemic chemotherapy which may treat metastatic disease until at least 4 months from the start of treatment, despite the fact that most deaths from rectal cancer are from metastatic disease. There has therefore been growing interest in moving systemic forward in the treatment pathway by giving induction systemic chemotherapy before chemoradiotherapy.

In a phase 2 study of 105 patients who received 12 weeks of CAPOX chemotherapy, followed by chemoradiotherapy (capecitabine with 54 Gy), followed by TME and post-operative adjuvant capecitabine, Chua et al demonstrated a good pathological complete response rate of 20% and 3-year relapse-free survival of 74% (Chua et al., 2010). The EXPERT-C trial compared CAPOX with or without cetuximab for induction chemotherapy in high risk rectal cancer in 165 patients. The addition of cetuximab in this setting significantly improved radiological response rate and overall survival in this setting, although not pathological complete response (Dewdney et al., 2012)

Future developments

The FOXTROT trial is currently recruiting patient with colon cancer. The aim of this trial is to determine whether patients with high risk colon cancer who undergo neoadjuvant chemotherapy have a lower 2-year recurrence rate than patients receiving equivalent post-operative chemotherapy. A second arm of this trial will also compare whether adding panitumumab to neoadjuvant chemotherapy increases the tumour response rate.

The PROSPECT trial is also currently recruiting patients with locally advanced rectal cancer. This trial aims to see whether patients undergoing induction FOLFOX chemotherapy who have a good

response on restaging imaging can safely omit preoperative chemoradiotherapy with an equivalent outcome.

1.9 Histopathological assessment of colorectal cancer

Accurate histopathological assessment is important for a number of reasons. Firstly, accurate staging and assessment of histopathological risk factors allows the patient to be informed of the risk of recurrence of their cancer, should they wish to be so informed. Secondly, this information is important in determining whether the patient will benefit from post-operative chemotherapy. As discussed previously, post-operative chemotherapy is of benefit in colon cancer if lymph node metastases are present (Stage III disease)(Moertel et al., 1990, Moertel et al., 1995, Andre et al., 2004). It is of smaller benefit in the absence of lymph node metastases if other adverse features are present such as an involved resection margin, EMVI, perforation or serosal involvement (Gray et al., 2007a). There is significant morbidity and some mortality associated with chemotherapy, and so it is important that patients and clinicians are accurately informed about the potential benefits when making decisions about treatment.

1.9.1 Dukes stage

Staging colorectal cancer is the process of classifying how far cancer has spread. The first system widely used for classification was that described by Dukes. This system was based on the pathological and histological examination of the specimen following surgical resection of colorectal cancer. Dukes observed that patient's prognosis varied widely depending on whether the cancer had invaded through the bowel wall, and whether the cancer had spread to local lymph nodes. Five year survival was 81% if cancer was confined to the bowel wall, but this dropped to 64% with spread through the bowel wall and 27% if local lymph nodes were involved. Dukes and Bussey subsequently modified Dukes classification, subdividing stage C into C2 where the most apical lymph

node contained metastatic disease, and C1 where it did not, with a corrected 5 year survival of 40.0% for C1 disease and only 19.6% for C2 disease (Dukes and Bussey, 1958).

1.9.2 TNM stage

Subsequently, more detailed classification systems have been described for colorectal cancer. The American Joint Committee on Cancer (AJCC) Tumour, Node, and Metastases (TNM) system divides the spread of cancer into three areas. T-stage (T0 to T4) represents local invasion of the tumour into surrounding tissues, N-stage (N0 to N2) represents nodal lymph node metastases and M-stage (M0 or M1) represents metastases to distant sites. This staging system has been through a number of revisions, and is currently in its seventh edition (Edge and Compton, 2010). There has been some controversy surrounding the changes made in the between the 5th edition (TNM5, introduced in 1997), the 6th edition (TNM6, introduced in 2002) and the 7th edition (TNM7, introduced in 2010) which led to pathologists in the UK not adopting the 6th edition, which was felt to lack a good evidence base for the changes it introduced (Quirke et al., 2007). A summary of the basic TNM staging system for the 5th to 7th editions is shown in Table 1.2, with the AJCC stage groupings illustrated in Table 1.3.

Much of the controversy arises from the classification of mesocolorectal tumour deposits. These are small deposits of tumour, discontinuous with the main tumour mass, without residual normal structure such as a lymph node or blood vessel to indicate what they have arisen in. TNM5 introduced the 3mm rule, where any tumour deposit 3mm or greater in size should be considered a lymph node metastasis. A tumour nodule less than 3mm in size was considered discontinuous tumour extension and included in the T-stage. TNM6 withdrew the 3mm rule, and replaced with the contour rule. This states that smooth tumour deposits should be considered lymph node deposits and included in the N-stage assessment, whereas irregular deposits should be considered vascular invasion. TNM7 states that satellite peritumoral nodules may represent discontinuous spread, venous invasion with extravascular spread (V1/2), or a totally replaced lymph node (N1/2). Replaced

nodes should be counted separately as positive nodes in the N category, whereas discontinuous spread or venous invasion should be classified and counted as tumour deposits but also recorded as positive in the new N1c category.

Classification of isolated tumour cells and micrometastases has also varied between TNM editions. In TNM6, lymph nodes with tumour deposits < 0.2mm in diameter were classified as isolated tumour cells (ITC) and not classified as lymph node metastases (pN0), in contrast to TNM5 where they were counted as lymph node metastases. Lymph node deposits between 0.2mm and 2mm were classed as micrometastases and counted as positive lymph nodes (pN1). ITC are not considered lymph node metastases in TNM7.

The impact of these changes to the TNM staging system is significant. Kim et al. validated the 7th edition of the TNM staging system in a dataset of 2511 patients, and compared staging to the 6th edition. 10.2% of patients had a change in stage from TNM6 to TNM7, and this study suggested thatn TNM7 had a greater prognostic validity than TNM6 (Kim et al., 2011b). Changes to the nodal classification of patients are particularly important as they impact on the interpretation of clinical trials of adjuvant chemotherapy.

In addition to tumour, node and metastasis, TNM5 recognised tumour grade (G1-4) and histological type as independent prognostic factors. TNM6 additionally recognised radial margin involvement (R0-2) and venous invasion (V0-2). TNM7 also recognises lymphatic invasion (L), perineural invasion (PN), tumour deposits (TD), tumour regression grade (TRG), circumferential resection margin distance (CRM), microsatellite instability (MSI), and KRAS mutation as important prognostic features. MSI and KRAS have previously been discussed in sections 1.4.2 and 1.4.3 respectively. Other important prognostic features are discussed below.

		TNM 5 and 6 definition	TNM 7 change
Tumour [1]	T0	No evidence of primary tumour	
	Tis	Carcinoma in situ: intraepithelial or invasion of the lamina propria	
	T1	Tumour invades submucosa	
	T2	Tumour invades muscularis propria	
	T3	Tumour invades through muscularis propria into subserosa or into pericolorectal tissues	
	T4a	Tumour directly invades other organs or structures	Tumour perforates visceral peritoneum
	T4b	Tumour perforates visceral peritoneum	Tumour directly invades other organs or structures
Node [2]	N0	No regional lymph nodes contain tumour	
	N1	Between 1 and 3 regional lymph nodes contain tumour	
	N1a		Metastases in 1 regional lymph node
	N1b		Metastases in 2-3 regional lymph nodes
	N1c		Tumour deposits in the subserosa, or in non-peritonealised pericolic or perirectal soft tissue without regional lymph node metastases

	N2	4 or more regional lymph nodes contain tumour	
	N2a		Metastases in 4-6 regional lymph nodes
	N2b		Metastases in 7 or more regional lymph nodes
Metastases [3]	M0	No metastases to distant organs	
	M1	Metastases to distant organs (including non-regional nodal mets)	
	M1a		Metastasis confined to one organ
	M1b		Metastasis in more than one organ or the peritoneum

Table 1.2: TNM staging system 5th to 7th editions

1) In TNM5 T-stage includes mesocolorectal tumour nodules less than 3mm in diameter. In TNM6 T-stage includes mesocolorectal tumour nodules if they have an irregular outline. In TNM7 T-stage does not include mesocolorectal tumour nodules.
2) In TNM5 N-stage includes mesocolorectal tumour nodules 3mm or more in diameter. In TNM6 N-stage includes mesocolorectal tumour nodules if they have a smooth contour. In TNM7 N-stage includes peritumoural nodules if the pathologist considers them to be completely replaced nodes, otherwise these should be counted in the N1c category and as tumour deposits (TD)
3) M-stage includes lymph node metastases outside the normal lymphatic drainage for that segment of colorectum.

Stage grouping	TNM5	TNM6	TNM7
Stage 0	Tis N0 M0	Tis N0 M0	Tis N0 M0
Stage I	T1-2 N0 M0	T1-2 N0 M0	T1-2 N0 M0
Stage II	T3-4 N0 M0	T3-4 N0 M0	T3-4 N0 M0
Stage IIA	T3 N0 M0	T3 N0 M0	T3 N0 M0
Stage IIB	T4 N0 M0	T4 N0 M0	T4a N0 M0
Stage IIC			T4b N0 M0
Stage III	T1-4 N1-2 M0	T1-4 N1-2 M0	T1-4 N1-2 M0
Stage IIIA	T1-2 N1 M0	T1-2 N1 M0	T1-2 N1/N1c M0
			T1 N2a M0
Stage IIIB	T3-4 N1 M0	T3-4 N1 M0	T3-T4a N1/N1c M0
			T2-3 N2a M0
			T1-2 N2b M0
Stage IIIC	T1-4 N2 M0	T1-4 N2 M0	T4a N2a M0
			T3-4a N2b M0
			T4b N1-2 M0
Stage IV	T1-4 N0-2 M1	T1-4 N0-2 M1	T1-4 N0-2 M1
Stage IVA			T1-4 N0-2 M1a
Stage IVB			T1-4 N0-2 M1b

Table 1.3: TNM stage groupings for 5th to 7th editions

1.9.3 Venous invasion

A number of risk factors besides the TNM stage of colorectal cancer are known to be of prognostic importance. Dukes first reported the spread of rectal cancer into haemorrhoidal veins (Dukes and Bussey, 1941), and subsequently described the adverse influence of this pathological feature on 5 year survival (Dukes and Bussey, 1958). Venous invasion may be intramural or extramural, and may be identified macroscopically or only on microscopic examination.

Betge et al. investigated the prognostic significance of venous and lymphatic invasion 381 patients; they noted that both lymphatic and venous invasion had significantly worse progression free survival (PFS) and cancer specific survival (CSS). Extra mural venous invasion had an independent prognostic value which was equivalent to T-stage although inferior to lymph node status, with a hazard ratio of 2.29 for CSS (Betge et al., 2012). Betge et al. also noted in this study that identification of extra mural venous invasion was significantly associated with the number of tumour blocks taken, and that specimens in which more tumour blocks had been taken were more likely to have vascular invasion identified.

In early rectal cancers, microscopic intramural vascular invasion or submucosal vascular invasion in T1 tumours has also been demonstrated to be significantly associated with nodal metastases (Mou et al., 2013). This is important in the histopathological assessment of early rectal cancers which have been treated by local excision, as the risk of nodal metastases influences the decision on whether further treatment is needed.

TNM7 recommends that venous invasion is recorded as a site specific factor, and denoted as V0 if no venous invasion is present, V1 if microscopic venous invasion is present and V2 if macroscopic venous invasion is present (Edge et al., 2010).

1.9.4 Lymphatic invasion

Tumour may also invade along lymphatic channels, which again may be intramural or extramural. Butge et al. also investigated the prognostic significance of lymphatic invasion in the same study. Extramural lymphatic invasion was associated with significantly worse PFS and CSS with a hazard ratio of 1.61 and 1.52 respectively, although the prognostic impact of intramural lymphatic invasion was not significant. However, in this study the extramural lymphatic invasion did not remain prognostically significant when adjusted for lymph node involvement (Edge et al., 2010). Microscopic intramural lymphatic invasion or submucosal lymphatic invasion is predictive of lymph node involvement in T1 tumours, and this is a greater predictor of nodal involvement in this setting than submucosal vascular invasion (Mou et al., 2013). Again this is important in the histopathological assessment of locally resected tumours. TNM7 recommends that lymphatic invasion is recorded as a site specific factor for colorectal cancer (denoted L0 or L1).

1.9.5 Depth of extramural spread

The depth of extramural spread in T3 rectal cancers has also been shown to be of prognostic significance, and has led some to recommend subdividing T3 tumours. Willet noted that depth of extramural invasion was an important prognostic factor in T3N0 rectal cancer (Willett et al., 1999), and Merkel first recommended subdividing T3 tumours into 2 categories (Merkel et al., 2001). Merkel demonstrated that the distinction between T3 tumours with extramural spread of more than 5mm and T3 tumours with 5mm or less extramural spread was of greater prognostic significance than the distinction between T2 and T3 tumours with 5mm or less extramural spread. Bori noted that T3 tumours with more than 5mm of extramural spread were significantly more likely to be associated with lymph node metastases and venous invasion (Bori et al., 2009). Depth of extramural invasion has subsequently been divided four sub-categories for T3 tumours; T3a (1mm or less extramural spread), T3b (>1mm-5mm extramural spread), T3c (>5mm-15mm extramural spread) and T3d (>15mm extramural spread).

1.9.6 Circumferential resection margin

The circumferential resection margin (CRM) refers to the surgically cut non peritonealised radial margin, and is also called the non-peritonealised resection margin (NPRM). Involvement is associated with a very high risk local recurrence following resection of rectal cancer (Quirke et al., 1986), and colon cancer (Petersen et al., 2002). There has been some debate as to the distance from tumour to the margin which should be considered involved. Quirke in his paper recommended that tumour within 1mm of the margin should be considered involved, although others have suggested a cut-off of 2mm (Nagtegaal et al., 2002a), and Wibe noted that rates of local and distant recurrence increased exponentially as the distance of the tumour from the CRM decreased (Wibe et al., 2002). TNM7 recommends that any tumour within 1mm of any margin is considered involvement, and is recorded in the R category (R0 all margins >1mm, R1 microscopic involvement with a margin <1mm from the tumour, and R2 macroscopically involved margin with residual disease). It also recommends that the closest distance of the tumour from the CRM be recorded in millimetres (Edge et al., 2010).

1.9.7 Histological grade

The histological grade has also long been recognised as an important prognostic factor. Grinnell graded tumours from grade I (well differentiated) to grade III (poorly differentiated), based on loss of the glandular structure of the tumour, and noted 5 year survival was 76% in grade I cancers compared to 31% in grade 3 cancers (Grinnell, 1939). Grade has subsequently been demonstrated to be an independent predictor of outcome in multivariate analysis of large datasets (Freedman et al., 1984). TNM5 recommended reporting grade as follows; G1 – well differentiated, G2- Moderately differentiated, G3 –poorly differentiated and G4 – undifferentiated. However, there is significant inter-observer variability in the assessment of G1 and G2 tumours, and the WHO recommends dividing tumours into high-grade (G3-4) and low-grade (G1-2) (Maguire and Sheahan, 2014).

1.9.8 Histological type

The following histopathological types are recognised in TNM5-7; Adenocarcinoma in situ (high grade dysplasia), adenocarcinoma, mucinous carcinoma (greater than 50% mucinous), signet ring cell carcinoma (greater than 50% signet ring cell), squamous cell carcinoma, adenosquamous carcinoma, small cell carcinoma, and undifferentiated carcinoma. Carcinoid tumours, sarcomas and lymphomas may arise in the colorectum but are staged and treated separately. Small cell carcinomas, signet ring cell carcinomas and undifferentiated carcinomas have less favourable outcomes than other histological types (Fleming et al., 1997).

1.9.9 Perineural invasion

Perinerual invasion (PNI) describes invasion of tumour cells into the any of the three layers of the nerve sheath (Liebig et al., 2009). It has been demonstrated to be an independent marker of poor prognosis in colorectal cancer in multivariate analysis, with a 2.5-fold increase in disease recurrence at 5 years in PNI positive patients compared to PNI negative patients in T3N0 rectal cancer (Peng et al., 2011). In common with lymphovascular invasion, it is commonly missed on initial pathology reports. Peng reported that PNI was identified in 24.3% of cases on review compared to 7.5% of cases on initial report (Peng et al., 2011). TNM7 regcognises PNI and recommends that it is recorded as site specific factor (PN).

1.9.10 Tumour deposits

Tumour deposits are discrete foci of tumour in the pericolic and perirectal fat and mesentery adjacent to the primary tumour. They are associated with adverse outcomes in colorectal cancer, with a disease free survival (DFS) in stage II patients with tumour deposits comparable to stage III patients (Belt et al., 2010). As mentioned in section 1.9.2, they have caused some controversy in the TNM staging system, as changes to their classification between editions has resulted in changes in N classification, which potentially makes interpretation of trials of adjuvant chemotherapy difficult.

Step sectioning has demonstrated that tumour deposits can represent venous invasion, lymphatic invasion, perineural invasion and continuous tumour growth and that this cannot be distinguished by size or morphology (Wunsch et al., 2010). TNM7 recommends that they are recorded in the site specific TD, but has also added the new N category N1c and recommends that node negative tumours with tumour deposits should be designated N1c (Edge et al., 2010), which elevates these tumours to stage III in line with their poor prognosis.

1.9.11 Tumour regression grade

Many rectal cancer patients receive neoadjuvant chemoradiotherapy, as discussed in sections 1.8.2 and 1.8.3. A proportion of these patients undergo regression of their tumour prior to resection, where tumour is replaced by fibrosis, acellular mucin pools, or necrosis. The pathological staging of the tumour following this is denoted with the prefix "yp", and if there is no evidence of residual tumour or nodal metastases on pathological assessment these patients are staged as ypT0 ypN0. In this case, patients are described as having a pathological complete response (pCR). Patients with pCR had a better 5-year DFS compared to those who did not have a pathological complete response (83.3% and 65.6% respectively) in a pooled analysis of over three thousand patients (Maas et al., 2010).

Patients may also undergo a partial response to chemoradiotherapy or no response. They are staged according to the residual tumour with the TNM staging system and the "yp" prefix. Various grading systems have been described to assess the degree of response; the Mandard (Mandard et al., 1994), Dworak (Dworak et al., 1997) and TNM7 (Edge et al., 2010) are summarized in Table 1.4. A study assessing the reproducibility of regression scoring reported that the Mandard and Dworak scoring systems had fair inter-observer agreement with kappa values of 0.28 and 0.35 respectively (Chetty et al., 2012). Evidence to support the prognostic value of tumour regression grades other than the pCR group is less convincing (Maguire and Sheahan, 2014).

Mandard	Dworak	TNM 7
1: Complete regression - absence of residual cancer	0: No regression	TRG0: Complete response: no viable cancer cells
2: Fibrosis with scattered tumour cells	1: Predominantly tumour with significant fibrosis	TRG1: Moderate response: Single cells or small groups of cancer cells
3: An increase in the number of residual cancer cells, but predominantly fibrosis	2: Predominantly fibrosis with scattered tumour cells	TRG2: Minimal response: Residual cancer outgrown by fibrosis
4: Residual cancer outgrowing fibrosis	3: Only scattered tumour cells in fibrosis/acellular mucin	TRG3: Poor response: minimal or no tumour kill; extensive residual cancer
5: Absence of regressive changes	4: No viable tumour cells detectable	

Table 1.4: Tumour regression grading systems

1.9.12 Tumour budding

Tumour budding is defined as isolated cancer cells and clusters of less than five cancer cells ahead of the invasive front of the tumour (Ueno et al., 2002). These are thought to represent the first stage in cancer metastasis, as these cells have separated from the main tumour and can migrate through the extracellular matrix to invade lymphatics and blood vessels (De Smedt et al., 2015). Tumour budding is associated with a greater risk of lymph node metastases in T1 tumours (Kye et al., 2012), which makes it an important histopathological feature in the assessment of locally resected early rectal cancers. Tumour budding is also of independent prognostic significance in stage II rectal cancer, with a significantly worse five-year CSS (63% with tumour budding compared to 91% without) (Wang et al., 2009). However, a lack of consensus about the quantitative assessment of tumour budding has limited its introduction as a prognostic marker in colorectal cancer (De Smedt et al., 2015).

1.9.13 TME grading

The histopathology report should report the plane of surgery for rectal cancer resections. This is described as; mesorectal - when the entire mesorectum has been removed with the mesorectal fascia intact, intramesorectal – when there are defects in the mesorectal fascia and the mesorectum is torn but the muscularis propria is not exposed, and muscularis propria plane – when the muscularis propria is exposed (Nagtegaal et al., 2002b).

The plane of surgery achieved is strongly associated with the rate of local recurrence, with patients who have had a TME resection in the mesorectal plane significantly less likely to develop local recurrence at three years than those with a muscularis propria plane resection (Quirke et al., 2009). In an analysis of patients from the MRC CR07 trial, the three –year risk of local recurrence was 4% for the mesorectal plane, 7% for the intramesorectal plane and 13% for the muscularis propria plane.

1.9.14 Histopathological technique

The Royal College of Pathologist Dataset for Colorectal cancer (2nd edition) recommends that following visual inspection and inking, specimens are pinned out and fixed in formalin for a minimum of forty-eight hours. The tumour and adjacent tissue are then cut into transverse sections 3mm to 4mm apart, and four blocks of tumour are embedded together with any identified lymph nodes. These blocks should show the deepest penetration of the tumour through the bowel wall, any involvement of the serosa, any EMVI, the closest approximation to the non-peritonealised resection margin, involvement of any adjacent organs, and all lymph nodes. The selected blocks are embedded in paraffin and histological sections are taken from these blocks and stained for microscopic examination (Williams et al., 2007).

1.9.15 Limitations in histopathological assessment

Although histopathological assessment is usually considered the gold standard in terms of local and nodal staging of colorectal cancer, there is evidence that inadequate sampling can sometimes result

in under staging and missing other key prognostic features. It can be difficult to section the tumour into thin slices, particularly if fixation has not been adequate, and this may result in lymph nodes or important features being hidden within a thick slice. The number of tumour blocks taken affects the T-stage, with higher mean T-stage in cases where more tumour blocks are taken (Quirke et al., 1986).

Inadequate sampling of lymph nodes can also result in under staging. Fat clearance techniques have been shown to identify an average of ten additional lymph nodes per specimen compared to conventional histological assessment, resulting in an increase in N-stage in 6% of patients (Hernanz et al., 2009). Patients with three or less lymph nodes identified on histopathological examination have a 5% worse disease specific survival than patients of the same stage with twelve or more lymph nodes identified (Namm et al., 2008), possibly suggesting that lymph node sampling is inadequate in some cases although surgical and patient factors may also contribute.

These problems can also prevent adequate identification of other key prognostic factors. In a study by Stewart 32% of patients had extramural venous invasion or serosal invasion identified on review of histology which had been missed on initial routine histological examination (Stewart et al., 2007).

1.10 Radiological staging of colorectal cancer

Although histological assessment of colorectal cancer allows accurate staging of colorectal cancer, it can't be completed until the primary cancer has been excised. Even at this stage it does not allow the assessment of systemic disease. To fulfil these roles, radiological staging is required. As discussed previously (page 57), radiotherapy reduces the rate of local recurrence in rectal cancer (Gastrointestinal Tumor Study Group, 1985), but adds significant morbidity and is best given preoperatively. Neoadjuvant chemotherapy (page 63) further reduces local recurrence rates in rectal cancer but adds more morbidity. The FOXTROT trial (page 64) is investigating the benefit of neoadjuvant chemotherapy in colon cancer. Local excision (page 54) may benefit selected patients with early stage rectal cancer, whereas more radical resection may benefit colorectal cancer patients

with advanced disease through high ligation (page 50), CME (page 51), extended pelvic lymph node dissection (page 52) or ELAPE (page 53).

For those patients with systemic disease, early detection is also becoming increasingly important. Patients who are able to undergo radical resection of colorectal liver metastases may achieve a 5-year survival of up to 58%. However, many patients will not have resectable disease at the time of diagnosis, and 5 year survival is lower for those with more than 3 liver metastases (Smith and McCall, 2009). Similarly, patients with resectable lung metastases may achieve a five year survival of 55%, but those with more than one lung metastasis have significantly worse survival (Borasio et al., 2011).

Selection of the right treatment for each patient therefore relies more than ever on accurate radiological as well as histological assessment of colorectal cancer.

There are a number of different modalities currently available for the preoperative assessment of colorectal cancer. These include Computed Tomography (CT), Magnetic Resonance Imaging (MRI), Ultrasound (US), Endoscopic or Endorectal Ultrasound (EUS), 18F-Fluorodeoxyglucose Positron Emission Tomography (FDG-PET), 18F-Fluorodeoxyglucose Positron Emission Tomography/Computed Tomography (FDG-PET/CT).

Current recommendations are that patients undergoing potentially curative resection for rectal carcinoma should undergo local staging by endoluminal ultrasound or MRI, and computed tomography of the thorax, abdomen and pelvis to identify distant metastases(Scholefield, 2007, Valentini et al., 2009). For colon cancer, both local and distant staging are performed with CT.

1.10.1 Computed Tomography (CT)

Basic principles

X-ray computed tomography (CT) passes a beam of x-rays through the subject, and measures the x-rays which haven't been absorbed by the subject on the other side in a similar manor to conventional x-ray. However, in CT the beam and detection are rotated round the subject to acquire

data from multiple projections (Figure 1.1). The data from these projections in reconstructed by computer into a matrix of voxels, and the x-ray absorption for each voxel is calculated and displayed as a grayscale image.

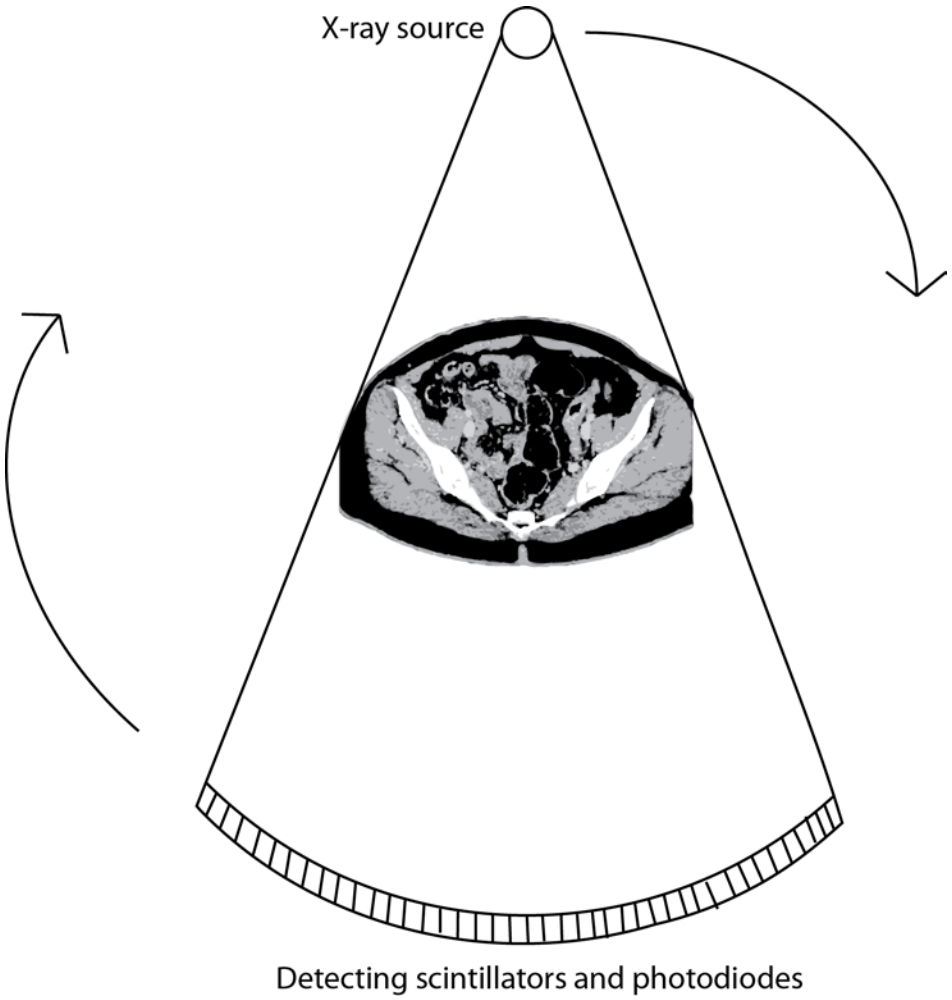


Figure 1.1: CT image acquisition

This is most easily conceptualized as a series of parallel beams passed through a two dimensional image slice (although the x-ray beam is a cone beam and diverges from the source onto the row of scintillators and photodiodes which detect it). A sinogram is produced by the series of projections which are recorded from the slice as the source and detector rotate around it. The projection of an image can be described by an equation called the Radon transform. In order to produce an image of the slice from the projections, a reverse Radon transform is performed on the projection data or sinogram. This image is blurred, and to remove this blurring a high pass filter is applied to the

sinogram before it is transformed. This process is called filtered back projection (FBP), and has been used since the inception of CT. An alternative, but more computationally intensive, process is iterative reconstruction which takes into account more complex statistical modelling of the noise in the raw data and the scanner geometry. This is employed in some modern scanners to reduce noise levels in low dose CT scanning.

The image produced is calibrated to represent x-ray absorption in Hounsfield units (HU), where air is -1000 HU and water is 0 HU.

Early CT scanners acquired images one slice of tissue at a time, but the early 1990's saw the development of spiral CT, where the x-ray source and detector rotate continuously around the subject and the subject is moved through the rotating gantry. This allows continuous acquisition of volumetric data. In most systems, this is reconstructed into axial slices with isotropic voxels, and coronal and sagittal slices are subsequently reconstructed from the thin axial slices if required, although it is technically possible to reconstruct other planes from the volumetric data.

The 2000's saw rapid development of multidetector CT systems. These use multiple rows of detectors to simultaneously acquire data about multiple axial slices in one rotation of the detector gantry. Sixty-four slice systems are now common, and 128 and 320 slice systems are available. However, the clinical benefit of systems over sixty-four slice has been debated. Dual source systems are now available. These use two perpendicular x-ray beams from two sources, allowing full data collection from 180 degree rotation.

In order to increase the contrast range, contrast agents are used in CT. These increase x-ray absorption in the tissue in which they have been distributed. Soft tissue imaging is facilitated by the administration of intravenous contrast agents, which are iodine based and water soluble. Early contrast agents were ionically bonded to iodine. Modern contrast agents are made from organic compounds covalently bonded to iodine which have a better safety profile such as iohexol (Omnipaque) and iodixanol (Visipaque).

The effect of intravenous contrast agents on tissues is dependent on the delay between administration and CT imaging, which determines whether the contrast is predominantly in the arterial compartment (arterial phase imaging), venous compartment (venous phase imaging), or other compartment (for example urine in delayed phase imaging with renally excreted contrast).

Contrast agents can also be administered directly into the gastrointestinal tract for gastrointestinal imaging, either orally or rectally. Oral contrast agents may be negative (such as water and mannitol, which primarily distend the GI tract), or positive (iodine or barium based, which increase x-ray absorption within the gastrointestinal lumen).

Dual energy CT (DECT) has recently become available on some scanners. This simultaneously performs CT with higher and lower energy level x-rays, which allows the calculation of iodine concentration within lesions following the administration of iodinated contrast agents during a single phase scan. This may be of benefit in characterising lesions, for example in differentiating liver cysts form metastases (Agrawal et al., 2014).

Local staging of colon cancer

One of the principle current uses for CT in colorectal cancer is in the local preoperative staging of colon cancer. Accuracy of CT in the assessment of T-stage has been widely reported, although the outcome measure reported varies between studies which can make comparison more challenging.

Two studies report the stage-for stage accuracy of CT for the prediction of T-stage; Smith et al report an accuracy of 60% and 61% for two observers in 126 patients (Smith et al., 2007), and Burton et al report and accuracy of 35% and 51% for two observers in 33 patients (Burton et al., 2008). Although reporting stage-for-stage accuracy results in lower values than reporting dichotomous outcomes due to the higher number of categories, this suggests that CT is only moderately accurate.

The most commonly reported endpoint for the assessment of T-stage accuracy is the distinction of T3 or greater disease from T2 or less disease. This was subject to a meta-analysis by Dighe in 2010, which included 19 studies from 1986 to 2008. The overall sensitivity in this meta-analysis was 86%

(95% CI 78-92%), the overall specificity was 78% (95% CI 71-84%), and the diagnostic odds ratio (DOR) was 22.4 (95% CI 11.9-42.4%) (Dighe et al., 2010b). The pooled sensitivity, specificity and DOR were higher for modern studies using MDCT at 93%, 86% and 83.5 respectively. This suggests that at least for the distinction between T2- and T3+ disease modern CT is very accurate. Some of these studies were performed as CT virtual colonoscopy assessments, and so utilised bowel cleansing and rectal insufflation.

Some studies have reported the accuracy of CT in the identification of locally advanced disease, which includes T4 tumours and T3 tumours with more than 5mm extramural invasion (T3c and T3d disease). This end point is more prognostically significant than the distinction between T2 and T3 disease (Merkel et al., 2001), and was the initial entry criteria for the FOXTROT study although this was subsequently extended in included all T3 tumours for medically fit younger patients. Two studies report this endpoint for T-staging accuracy on CT; Dighe reported and accuracy of 70% in 94 patients (Dighe et al., 2012), and Rollven reported an accuracy of 79% and 76% for two observers in twenty-eight patients. These studies suggest that CT has a moderate to good accuracy for identifying this clinically important endpoint.

Another important endpoint in the local assessment of colon cancer is the assessment of nodal involvement. Histopathological nodal involvement is the most important prognostic factor for deciding whether patients with colon cancer will be offered adjuvant chemotherapy, as there is a clear benefit in node positive patients. Accuracy of CT in identification of nodal involvement (N1+ disease) was investigated by Dighe in the same meta-analysis in 2010. Overall sensitivity was 70% (95% CI 59-80%), specificity was 78% (95% CI 66-86%) and DOR was 8.1 (95% CI 4.7-14.1) (Dighe et al., 2010b). This suggests that CT is moderately accurate in the identification of nodal disease, but less accurate at nodal staging than T-staging. This is unsurprising as the identification of nodal involvement on CT is largely restricted to size criteria, and there is a substantial overlap in size between benign reactive lymph nodes and small lymph nodes with metastatic deposits.

EMVI is another prognostically important tumour feature which can be identified on preoperative imaging. Accuracy of CT in identifying EMVI is less commonly reported than T-staging and N-staging. Burton reported an accuracy of 55% and 61% for two readers in thirty-three patients (Burton et al., 2008), Dighe reported an accuracy of 70% in ninety-four patients (Dighe et al., 2012), and Rollven reported an accuracy of 78% and 69% for two readers in twenty-eight patients (Rollven et al., 2013). The accuracy of CT for the identification of EMVI in colon cancer would therefore appear to be moderate to good.

Local staging of rectal cancer

CT is not usually recommended for the local staging of rectal cancer, as T-staging accuracy is generally considered superior on EUS and MRI, and assessment of mesorectal fascia involvement is considered better on MRI. However, there are situations where neither of these other imaging modalities can be used, in which case contrast enhanced CT is a reasonable alternative. In a recent single centre study of fifty patients, CT achieved a T-staging accuracy of 58-64% and an accuracy for the identification of nodal disease of 76% (Kocaman et al., 2014). The mesorectal fascia is not as well seen on CT as on MRI making accurate prediction of CRM involvement difficult.

Systemic staging of colorectal cancer

Contrast enhanced CT is the modality most commonly used for primary staging of systemic disease in colorectal cancer. It is the recommended for the systemic staging of primary rectal cancer in ten national and international guidelines (Nielsen and Wille-Jorgensen, 2014).

CT thorax is probably the best modality currently available for the detection of colorectal lung metastases. Lung metastases develop in 10 to 20% of colorectal cancer patients, with a higher incidence in low rectal cancer. CT is significantly more sensitive than chest x-ray, which will only identify around one third of these metastases. CT is also more sensitive than PET/CT for identifying small lung nodules. Unfortunately, it is not very specific and will identify indeterminate nodules in around 25% of colorectal cancer patients. Around 10% of these will be confirmed as metastases on

follow up imaging, and interval CT is the best way to distinguish benign from malignant sub-centimetre nodules which are below the resolution of PET/CT (Baek et al., 2012).

CT in the portal venous phase has a reasonable sensitivity for detecting liver metastases. In meta-analysis, per-patient sensitivity of CT for detecting liver metastases was 83.6% (Niekel et al., 2010b). CT sensitivity was significantly less than FDG-PET (94.1%), and non-significantly lower than MRI (88.2%). Despite this, the widespread availability, low cost and speed of CT make it the first line investigation for systemic staging in primary colorectal cancer in most institutions and guidelines. If there is diagnostic uncertainty, or if treatment for metastatic disease is planned, it is supplemented by liver MRI and whole body PET/CT. CT is relatively limited in its ability to identify distant lymph node metastases, and also has limited ability to identify small volume peritoneal disease.

1.10.2 Magnetic Resonance Imaging (MRI) – Primary rectal cancer

Basic principles and pulse sequences

The protons and neutrons which make up the nuclei of atoms have a quantum property called spin. In atoms with an even number of protons and an even number of neutrons, the spins of the nucleons cancel each other out and the atom has a net zero spin. However, all atoms with an uneven number of protons or nucleons have a net spin. As they also have an electrical charge, and this produces a very small magnetic field perpendicular to the spin of the nucleus. The most abundant atom with non-zero spin in the human body is hydrogen in water and fat (which is made up of a single proton). Hydrogen is therefore the element which is most commonly imaged in MRI. Although it is possible to study other atoms such as phosphorus, sodium and carbon, they are found at much lower concentrations than hydrogen and so are more difficult to image.

The orientation of the spin and magnetic field is usually randomly distributed, but when the nuclei are placed in a strong magnetic field some of the nuclei align with the external magnetic field and some align against the external magnetic field. Alignment with the external magnetic field is a lower

energy state, so a slight excess of nuclei align with the external magnetic field (nine per 2 million hydrogen atoms at 1.5 Tesla).

The spinning protons in hydrogen precess around their magnetic axis. This is analogous to a spinning top moving around its gravitational axis as it spins. The frequency of this precession is proportional to the field strength of the external magnetic field and is known as the Larmor or resonance frequency. The Larmor frequency for hydrogen nuclei (H-1) is 63.87 MHz at 1.5 Tesla (1.5T) and 127.74 MHz at 3 Tesla (3T).

If the precessing protons are exposed to an electromagnetic pulse at the Larmor frequency, then they can absorb this electromagnetic pulse and jump to a higher energy state. For hydrogen at MRI field strengths this frequency falls within the radiofrequency range of the electromagnetic spectrum. This results in their spin axis "flipping" away from alignment with the external magnetic field. The angle to which the protons flip away from the external magnetic field is dependent on the strength and duration of the radiofrequency (RF) pulse. During this excitation period, the protons are precessing together or in phase.

When the RF pulse stops, the spin axis of the protons then gradually spirals down back to alignment with the external magnetic field. This is called spin-lattice relaxation and is the exponential recovery of magnetisation in line with the external magnetic field. The time taken for this to happen is unique to each tissue at a given magnetic field strength, and is denoted T1. During this process, the protons have transverse magnetisation precessing at the Larmor frequency, and so produce an electrical current in the receiver coil. This signal disperses very rapidly, primarily due to the proton spins moving out of phase with each other, and is called free induction decay (FID). It is not measured directly in MRI. Instead, proton spins are brought back into phase by subsequent RF pulses and a signal is measured from this RF echo (McRobbie et al., 2007).

The movement of proton spins out of phase with each other is called spin-spin relaxation and is denoted T2. T2 relaxation is unique for each tissue, but is determined mainly by the chemical

environment of the protons and is less influenced by the external magnetic field strength. In addition to the T2 signal decay (caused by the interaction between spinning protons), there is decay due to inhomogeneity of the magnetic field within the tissues. This is caused by imperfections in the MRI magnet, but also by magnetic susceptibility of the tissues. This distorts the magnetic field at interfaces between different tissues, and is particularly pronounced at air/fluid interfaces or around any metal implants. This signal decay is denoted T2* (T2 decay + decay due to field inhomogeneity). The portion of T2* decay caused by field inhomogeneity can be reversed by a second RF pulse with a 180 degree flip angle given after a delay (echo time, TE) which brings the precessing protons which came out of phase due to T2* decay back into phase (but not the protons which came out of phase due to T2 decay). This results in a larger RF signal after a delay (TE), and this larger signal is called a spin echo (SE). This forms the basis of some MRI pulse sequences.

MRI images are generated by delivering an RF pulse to the protons within a tissue, and measuring the RF signal emitted as the precessing protons return to alignment with the external magnetic field. In order to generate spatial information to convert this signal into an image, a supplemental magnetic gradient is exerted on the tissues in addition to the main magnetic field. This changes the Larmor frequency of the protons in along the axis of this supplemental gradient, so that the emitted RF signal is of a difference frequency for each part of the tissue along one axis.

In order to differentiate the signal from tissue along the complementary plane, phase encoding is employed. This uses a second magnetic gradient in a complementary plane, which is switched on briefly after the excitation pulse. This causes the protons away from the centre of the gradient to precess faster or slower than the central protons. The spins are from each line of tissue in the complementary plane are successively brought back into phase to produce an RF echo, filling a line of data in k-space with each echo. The RF signal generated by the protons in the imaged tissue is recorded by the receiver coils, and this signal is sampled to produce a digital recording in k-space. K-space is the name given to the digitally sampled raw data from the received coils, which is coded by

frequency in one axis and time (from the phase encoding steps) in the second axis. A Fourier transform is then performed to convert this frequency/time data into a two dimensional image.

MRI images are usually acquired in slices, whereby a block of tissue is imaged at a time. The slice is isolated by the slice selection gradient, which is applied during the excitation RF pulse. This isolates the chosen slice of tissue by changing the Larmor frequency of the protons in the adjacent slices so that they are not excited by the RF pulse. In 3D volume acquisition MRI, phase encoding is used in 2 planes so that an entire block of tissue is imaged simultaneously rather than being divided into slices.

Different types of MRI scan can be acquired using different pulse sequences. These are combinations of RF and magnetic gradient pulses delivered by the MRI scanner to acquire the images.

Spin echo (SE) sequences use a 90 degree RF pulse, followed by one or more 180 degree RF pulses to rephase the protons which have moved out of phase due to T2* relaxation. The spin echo is produced when the protons rephase and is recorded by the receiver coils. Spin echo sequences are more resistant to susceptibility artefacts at air/fluid and tissue interfaces as they do not rely on T2* relaxation.

Fast spin echo (FSE) or turbos spin echo (TSE) sequences are similar to spin echo sequences, but multiple refocussing 180 degree RF pulses are used, and the phase encoding gradient is changed for each echo. This means that multiple phase encoding steps are recorded for each pulse sequence repetition, reducing the overall acquisition time. The reduction in acquisition time is proportional to the echo train length. This technique is of most benefit in T2 weighted imaging where longer echo train lengths can be utilised.

Single-shot fast spin echo (SS-FSE) sequences are an extension of this technique, which use a very long echo train and the phase encoding is changed for each echo, acquiring all the data for one slice from a single excitation pulse. This is called single-shot turbo spin echo (SS-TSE) on Philips MRI scanners and Half Fourier acquisition single shot turbo spin echo (HASTE) on Siemens MRI scanners.

HASTE sequences also employ half Fourier acquisition, where symmetry in k-space is used to interpolate this information and only half of the k-space data is acquired. This reduces scan acquisition time, although this may be at the expense of signal to noise ratio. The combination of these techniques means that a single HASTE sequence slice can be acquired in around 1 second, allowing breath hold abdominal imaging.

In gradient echo (GE) sequences, repeated low energy RF pulses are delivered. These result in less than 90 degree flip angle for the protons, but they are repeated before relaxation has occurred so that after a few repetitions the tissue achieves a steady state, where the amount of relaxation between each RF pulse is matched with the degree of excitation from the next pulse. If the repeated pulses are delivered before T2* relaxation is complete, then the repeated RF pulse generate echos from the residual transverse magnetisation (Hahn echos). The signal at a given time after a repeated pulse is due to free induction decay (FID) plus Hahn echos.

The flip angle induced by the initial RF pulse can be varied, and is usually between 10 and 80 degrees. Larger flip angles give more T1 weighting, whereas lower flip angles give more T2 (actually T2*) weighting. As lower flip angles are used, recovery of longitudinal magnetisation is shorter allowing for faster imaging acquisition than in SE imaging. However, GE sequences are more vulnerable to susceptibility artefacts as T2* decay is not eliminated by refocusing RF pulses.

In spoiled gradient echo sequences, only the signal from FID is measured. Gradients are used to spoil the coherence of the Hahn echos so that these to not interfere with the received signal. One line of k-space is filled per repetition. In rewound gradient echo sequences, the phase encoding gradient is reversed to bring the Hahn echos back into phase for the line of k-space being filled.

True fast imaging with steady precession (True FISP) and balanced turbo field echo (BTFE) sequences are rewound gradient echo sequences which use balanced frequency and phase encoding gradients, and maintain residual transverse magnetisation between pulse sequences by keeping the repetition

time (TR) shorter than the T1 and T2 of the tissues. This results in an image with a mixture of T1 and T2* weighting. It is prone to susceptibility artefacts.

The fast low angle shot (FLASH) and enhanced T1 high resolution isotropic volume excitation (eTHRIVE) sequences are spoiled gradient echo sequences. It is possible to use very short repetition times in the order of 20-30ms and therefore images can be acquired rapidly. The degree of T1 weighting depends on the TR and flip angle, with a large flip angle combined with a short TR giving good T1 weighting. As with other GE sequences it is prone to susceptibility artefacts, although this can be reduced by keeping the TE time short.

Diffusion weighted imaging (DWI) investigates the degree of water diffusion within tissues. Using the pulsed gradient spin echo (PGSE) method, a 90 degree RF pulse is delivered to the tissues, followed by a large gradient, followed by a 180 degree RF pulse, followed by an equal large gradient. This gives a large echo from static water molecules when the proton spins come back into phase after the second RF pulse. However, protons in water molecules which have been moving through the gradients due to diffusion will have experienced varying magnetic field strengths and will therefore have moved out of phase and not give a significant echo. The degree of diffusion weighting can be controlled by the strength of the gradients and the time between the two RF pulses, and is referred to as the b-value in seconds per millimetre squared (s/mm^2) (Stejskal and Tanner, 1965). Although this technique has been available since the late 1980's (Moseley et al., 1990), initial interest focussed on the assessment of acute cerebral ischaemia (Warach et al., 1992). However, there is now significant interest in the use of DWI to identify neoplastic lesions. Diffusion tends to be more restricted in neoplastic lesions than in normal tissue, which may be due to increased cellular density (Jacobs et al., 2009). This allows DWI to differentiate neoplastic from benign lesions, and to identify metastatic disease.

Low molecular weight paramagnetic contrast agents, such as gadolinium compounds gadopentetate dimeglumine (Magnevist) and gadobutrol (Gadovist), diffuse from the circulation to the

extravascular-extracellular space through the capillary bed. The increase in gadolinium concentration in the tissues reduces the T1 relaxation time. Following a bolus of contrast media, repeated measurement of the T1 weighting of tissues over time allows calculation of the transfer constant (K^{trans}) which describes the diffusion of the contrast medium across the capillary endothelium. Other parameters which can be measured include the fractional volumes of the extravascular-extracellular space (v_e) and plasma space (v_p), and the rate constant(k_{ep}) which is equal to the transfer constant divided by the extravascular-extracellular space (Essig et al., 2013).

Parallel imaging techniques make use of multi-channel receiver coils to reduce scan time. They make use of the differential signal received in each geometric location by the different receivers in a multichannel coil. The phase encoding steps are undersampled, which reduces the image acquisition time but would normally result in aliasing where elements of the image are wrapped. Reconstruction of the image from the different coil elements is performed in either k-space (generalized autocalibrating partially parallel acquisistions – GRAPPA) or image space (sensitivity encoding – SENSE). The resultant reduction in scan time is at the expense of the reduction in signal (and hence signal to noise ratio) which would normally be seen using a multi-channel coil.

Circumferential resection margin (CRM)

MRI is currently the principle modality for the local staging of rectal cancer, and is recommended by most national guidelines (Nielsen and Wille-Jorgensen, 2014). The main strength of MRI staging is that is allows the mesorectal fascia to be precisely visualized, and so the relationship of the tumour to the mesorectal fascia and involvement of the CRM can be assessed for patients undergoing TME surgery. This was demonstrated in two papers by Brown and Beets-Tan in 1999 and 2001 (Brown et al., 1999, Beets-Tan et al., 2001). This was subsequently confirmed in a large multicentre trial by the MERCURY study group; 408 patients underwent rectal MRI prior to resection of their primary rectal cancer. MRI had a specificity of 92% for the prediction of a clear CRM in this study (MERCURY study group, 2006).

A recent meta-analysis of fourteen studies with a total of over 1,600 patients assessed the accuracy of MRI in predicting CRM involvement. This demonstrated a sensitivity of 76% and a specificity of 88% for MRI in predicting CRM involvement.

Long term follow up is now available from the MERCURY study, and this has confirmed the prognostic significance of MRI CRM involvement. Patients with an involved CRM on MRI have a significantly worse five year overall survival (OS) and (DFS); 5-year OS was 62.2% in patients with a clear CRM compared to 42.2% for MRI CRM positive patients (Taylor et al., 2014).

In the MERCURY study, CRM involvement was less accurately predicted in low rectal cancer than in upper and mid rectal cancer. Patients with low rectal cancer undergoing APER are also more likely to have tumour perforation and CRM involvement than patients undergoing anterior resection. A sub-set analysis performed on patients in the MERCURY study with low rectal cancer demonstrated that in involved intersphincteric plane, and anterior tumour and a poor response to neoadjuvant chemoradiotherapy were significantly associated with CRM involvement (Salerno et al., 2009).

The MERCURY II low rectal cancer study was set up to investigate whether MRI directed treatment of low rectal cancer could reduce the rate of CRM involvement in low rectal cancer. In this study, patients with an MRI predicted safe surgical plane achieved a pathological CRM involvement rate of 1.6% following sphincter preserving surgery without neoadjuvant chemoradiotherapy. Patients who were MRI CRM positive pre-treatment underwent neoadjuvant chemoradiotherapy. Those who had a good response to chemoradiotherapy and who were MRI CRM negative post neoadjuvant treatment had a pathological CRM (ypCRM) involvement rate of 0%. Those with a persistently involved CRM on MRI post neoadjuvant therapy had a ypCRM positive rate of 17.5% (Battersby et al., 2015).

T-stage

MRI is also useful in the assessment of T-stage, although it is not as accurate as in the assessment of CRM involvement. In a meta-analysis of twenty-one studies MRI had a sensitivity of 87% and a

specificity of 75% for identifying T3/4 disease (Al-Sukhni et al., 2012). Specificity was significantly higher in studies using 3 Tesla MRI compared to those using 1 or 1.5T MRI.

MRI accuracy in staging early rectal cancers is lower; Waage reported that MRI had a sensitivity of 99% but a specificity of only 7% for differentiating T1-4 tumours from adenomas (Waage et al., 2014). In a meta-analysis investigating the sensitivity of MRI for identifying muscularis propria involvement (T2-4 disease) was again high at 94%, but that specificity was only moderate at 69% (Bipat et al., 2004). There is a tendency for MRI to overstage early rectal lesions (De Vargas Macciucca et al., 2010).

N-stage

Assessment of nodal stage is difficult for all imaging modalities. In a meta-analysis of twenty-one studies Al-Sukhni reported that MRI has a sensitivity of 77% and a specificity of 71% for the identification of nodal involvement (Al-Sukhni et al., 2012). However, many of these studies only used size criteria for the identification of nodal metastases. The use of morphological criteria (inhomogenous signal intensity and an irregular border) to identify lymph node involvement increases the specificity of MRI (Brown et al., 2003, Kim et al., 2004). Even allowing for this, MRI is only able to characterise lymph nodes which are at least 3mm in diameter, and 15% of nodes less than 3mm in diameter contain metastases (Park et al., 2014). MRI assessment of lymph node metastases on purely morphological characteristics is therefore likely to remain limited.

Diffusion weighted imaging (DWI) and two specific contrast agents have been investigated in an attempt to overcome this limitation. DWI does identify more lymph nodes than T2 weighted imaging alone. However, diffusion is restricted in both benign and malignant lymph nodes and so DWI is of limited benefit in distinguishing benign from malignant nodes (Lambrecht et al., 2011). Ultra-small superparamagnetic iron oxide (USPIO) has been used as a contrast agent to help identify nodal metastases, and in one study improved specificity to 93% compared to 75% with T2 weighted imaging alone. In a study of seventy-one patients investigating the accuracy of Gadofosveset

enhanced MRI in identifying nodal metastases Heijnen found that MRI had a sensitivity of 94% and a specificity of 79% for the experienced reader (Heijnen et al., 2014). Whether these results can be reproduced in larger multi-centre studies remains to be seen.

Extra-mural vascular invasion (EMVI)

MRI can also identify EMVI which as discussed in section 1.9.3 is prognostically important. In a retrospective study of 142 patients, MRI had a sensitivity of 62% and a specificity of 88% for the identification of EMVI (Smith et al., 2008a). In a larger study of 447 patients, Sohn found that MRI had a lower sensitivity of 28.2% but a very high specificity of 94% (Sohn et al., 2015). When assessing the accuracy of imaging for the detection of EMVI, it should be noted that there is substantial variation in the pathological reporting of EMVI. Betge found that the incidence of EMVI increased from 9% to 23% of expert review, and from 12% when less than 3 tumour blocks were taken to 48% when more than 7 tumour blocks were taken (Betge et al., 2012).

MRI detected EMVI has also been demonstrated to be an independent risk factor for disease recurrence and metastasis. Smith demonstrated that the 3-year recurrence free survival (RFS) was 35% for MRI EMVI positive patients compared to 74.1% for negative patients. This difference in prognosis was very similar to the difference demonstrated by pathology EMVI positive (34%) and negative (73.8%) patients (Smith et al., 2008a). Sohn noted that MRI EMVI positive patients had an odds ratio of 3.02 for distant metastases, which rose to 5.27 for large vessel EMVI identified on MRI (Sohn et al., 2015).

Locally advanced rectal cancer

MRI is the imaging modality recommended by expert consensus for the assessment of locally advanced rectal cancer for surgical planning (The Beyond TME Collaborative, 2013). There are relatively few studies which have specifically addressed this issue. Messiou investigated the accuracy of MRI for recurrent rectal cancer by organ. Sensitivity ranged from 70% for pelvic side wall involvement to 100% for prostate involvement, and specificity ranged from 33% to 100% (Messiou

et al., 2008). The number of patients with some organs involved was small (three patients had female reproductive organ involvement), limiting the precision of these estimates. Georgiou investigated the accuracy of MRI in assessing patients undergoing exenterative surgery for locally advanced and recurrent rectal cancer in sixty-four patients. Accuracy was described in terms of assessment of 7 compartments. Sensitivity for predicting each compartment involvement varied from 89.3% to 100%, and specificity form 76.9% to 100% (Georgiou et al., 2013).

MRI technique

Rectal MRI is performed in the supine position with a pelvic phased array surface coil, which have superseded endorectal coils in the majority of studies (Al-Sukhni et al., 2012). This allows visualisation of the whole pelvis, and in particular the relationship of the tumour to the mesorectal fascia. Some early studies used an endorectal coil and reported improved T-staging accuracy due to better visualisation of the layers of the bowel wall. However, this was at the expense of limited field of view which impeded visualisation of the relationship between the tumour and the mesorectal fascia. Endorectal coils were also expensive, reduced patient acceptance and could not be used with stenosing tumours. They have therefore been replaced by pelvic phased array surface coils in most units.

Some authors recommend distension of the rectum with positive or negative contrast material after purging the rectum. This allows the contour of the rectum and any lesions to be visualised clearly. However, this distension may compress the minimum distance from the tumour to the mesorectal fascia and so compromise assessment of CRM involvement (Slater et al., 2006).

Hyoscine butylbromide or glucagon is sometimes used as aperistaltic agents to reduce motion artefacts in pelvic MRI. Hyoscine butyl bromide has been shown to improve image quality in pelvic MRI (Johnson et al., 2007). Glucagon may be more effective than hyoscine butylbromide; in the small bowel glucagon more reliably introduced aperistalsis then hyoscine, and had a longer mean duration of aperistalsis (Froehlich et al., 2009).

The mainstay of rectal cancer MRI is high resolution T2 weighted imaged through the tumour. This is achieved using T2 weighted Fast Spin Echo (FSE) or Turbo Spin Echo (TSE) sequence. The rectum and tumour are first localised with wide field of view images in the sagittal plane from one pelvic side wall to the other with a 3mm slice thickness. Axial imaes are then obtained through the pelvis with a wide field of view and a 5mm slice thickness. These images are used to plane the subsequent sequences. High resolution, small field of view (160mm) images are then acquired perpendicular to the long axis of the tumour, with a slice thickness of 1-3mm (Taylor et al., 2008).

Low rectal cancers require two additional sequences. These are high resolution small field of view T2 weighted FSE sequences, acquired axial perpendicular to the long axis of the anal canal and coronal parallel to the long axis of the anal canal (Shihab et al., 2009). These additional sequences allow assessment of the relationship of the tumour and the levator ani muscles and sphincters.

1.10.3 MRI – restaging after chemoradiotherapy

The advent of effective neoadjuvant chemoradiotherapy in rectal cancer means that imaging needs to be accurate in reassessment of tumours following treatment. There is considerable variation in response to patients undergoing neoadjuvant treatment, with around 20% failing to respond or progressing, and up to 50% of patients demonstrating a complete clinical response (Habr-Gama et al., 2013). MRI plays an important role in making this reassessment following treatment.

T-stage and N-stage

Memon performed a meta-analysis in 2015 to assess the accuracy of MRI in restaging rectal cancer following neoadjuvant chemo-radiotherapy. Accuracy of MRI in reassessing stage-for -stage T-stage was addressed in twelve studies, with an overall accuracy of 52% (95% CI 44-59%) (Memon et al., 2015). This is lower than the accuracy expected in the pre-treatment staging of rectal cancer. There was a tendency for MRI to overstage rectal cancer post neoadjuvant treatment. This may partly reflect difficulty in differentiating fibrosis from residual tumour, and identifying small tumour

deposits or isolated tumour cells in pools of mucin. There was a wide range of MRI techniques employed in the studies which make up this meta-analysis together with a wide range in accuracy from 34% to 82%. Five of these studies used rectal contrast or gadolinium enhanced T1 weighted imaging, which may reduce staging accuracy.

The same study assessed the re-staging accuracy of MRI in the assessment of nodal disease. The mean accuracy was 72%, with values ranging from 60% to 88% in individual studies. This is similar to the accuracy achieved by MRI in pre-treatment nodal staging. The involution of benign reactive lymph nodes following radiotherapy may make size criteria more helpful for the identification of involved lymph nodes.

Two studies have investigated USPIO and Gadofosveset contrast agents in nodal restaging. Gadofosveset enhanced MRI was reported to have a sensitivity of 80% and a specificity of 95% in identifying lymph node metastases for the experienced reader (Lambregts et al., 2011). USPIO was reported to have a high area under the curve (AUC) on receiver operator curve (ROC) analysis of 0.97 to 0.99 ((Lahaye et al., 2009). However, these are both small studies single centre studies, and these promising results for these agents have yet to be repeated in larger studies.

CRM involvement

The accuracy of MRI in the reassessment of circumferential margin involvement following neoadjuvant chemoradiotherapy remains high. This has been assessed in six large trials involving more than 50 patients, with accuracy for prediction of CRM involvement of 83-92% (MERCURY study group, 2006, Barbaro et al., 2009, Kim et al., 2009, Pomerri et al., 2009, Simpson et al., 2014, Kim et al., 2015). Inaccuracies where present tend to be due to over staging by MRI, which means that the negative predictive value is high (around 95%), although positive predictive value is lower (43-53%) (Simpson et al., 2014, Kim et al., 2015). Patients who have an involved CRM on restaging MRI following neoadjuvant chemoradiotherapy have significantly worse three-year local recurrence free

survival and overall survival (76.9% and 73.8%) compared to patients in whom CRM has become clear on restaging MRI (100% and 96%) following surgery (Lee et al., 2014).

EMVI

There is little published data on the accuracy of MRI in the identification of EMVI after neoadjuvant chemotherapy. However, a recent study has investigated the prognostic importance of persistent EMVI on imaging following chemoradiotherapy. In patients who were MRI EMVI positive on pre-treatment MRI, but negative on MRI after neoadjuvant chemotherapy, had a 87.8% 3 year DFS compared to 45.8% in those with persistent MRI EMVI (Chand et al., 2015).

1.10.4 MRI – predicting and assessing response to neoadjuvant chemoradiotherapy

There has been considerable research into the ability of MRI features to predict and assess response to neoadjuvant chemoradiotherapy. This is important for both poor responders, who may benefit from a change in treatment strategy, and complete responders, who may avoid surgery and pursue organ preservation. Some authors have suggested that pathological complete response by definition is a lost opportunity to avoid the morbidity associated with radical surgery, in which case complete responders need to be identified by radiological and clinical means.

Morphological change on MRI following chemoradiotherapy can be used to predict response. Wu identified fourteen studies which investigated this in a meta-analysis. Morphological change on T2 weighted imaging alone was assessed in five studies, and had a relatively low sensitivity of 64% but a high specificity of 88% for predicting pathological complete response. Nine studies which incorporated DWI had a high sensitivity of 92%, although a lower specificity of 75%. A magnetic resonance imaging based tumour regression grading system (mrTRG) has been developed to help classify morphological changes seen on T2 weighted TSE imaging (Battersby et al., 2014). This has been validated in the large multicentre MERCURY study group dataset, and demonstrates a highly

significant difference in overall five-year survival between mrTRG poor responders (27%) and good responders (72%) (Patel et al., 2011).

Various quantitative analyses have been applied to both pre-and post-treatment MRIs to help differentiate pathological responders and complete responders (pCR). Cai et al investigated maximum tumour signal intensity on DWI at b800, signal intensity ratio (tumour:muscle), tumour ADC, and ADC ratio (tumour:muscle) and found that the signal intensity ratio had an area under the curve (AUC) of 0.94 with a sensitivity of 100% and a specificity of 80.9% for the prediction of pCR (Cai et al., 2014). Birlik et al investigated percentage change in tumour volume, pre and post treatment ADC values at b600 and b1000, percentage change in ADC values at b600 and b100. They reported the highest AUC for percentage change in tumour volume (0.91) and percentage of ADC increase at b600 (0.90) for predicting T-stage regression (Birlik et al., 2015). There is substantial heterogeneity between studies in terms of the parameters used to assess tumour response. However, some trends are emerging. Percentage increase in ADC value pre-and post-treatment and appears to be a better predictor of pathological response than absolute ADC value at any time point, and percentage decrease in tumour volume appears to be a better predictor of response than decrease in maximum tumour dimension or T-stage.

Several recent studies have examined the ability of tumour perfusion parameters on dynamic contrast enhanced MRI to predict response to neoadjuvant therapy. Again there is heterogeneity in the parameters studied, but small studies show promise in predicting response both on pre-treatment scans (Martens et al., 2015), and using change in parameters between pre and post-treatment scans (Petrillo et al., 2015).

Kluza et al examined the change in signal intensity variation within the tumour volume using T2 weighted imaging and found that change in the 95th centile descriptor on pre-and post-treatment MRI had an AUC of .90 with a sensitivity of 94% and a specificity of 94% for the prediction of pCR (Kluza et al., 2013).

All of these quantitative studies have derived their cut off values in small datasets, and have not been validated in large multicentre datasets, so their reported accuracies must be viewed with some caution. At present, morphological changes remain the only validated predictor of outcome.

1.10.5 MRI – local staging of colon cancer

Prior to commencing the colon MRI study reported in this thesis (Chapter 4), only two studies had investigated the accuracy of MRI in staging colon cancers; a pilot study of 7 patients reported and accuracy of 57% in identifying T3 or greater disease, and a trial of colorectal cancer patients including 27 colon cancer patients reported an accuracy of 88% for identifying T3 or greater disease (Low et al., 2003, Lomas et al., 2001). However, in 2013 Rollven reported on the accuracy of 1.5T MRI in the pre-operative local staging of colon cancer in a small prospective study. Forty-two patients were recruited, of whom twenty-eight were included in the final analysis. Rollven reported results for two observers. For the identification of T3c or greater diease, sensitivity was 77% and 92%, specificity was 100% and 94%. For the identification of nodal disease (N1 or greater), sensitivity was 86% for bother readers, specificity was 68% and 64%. For the identification of EMVI, sensitivity was 75% for both readers, specificity was 84% and 79%.

These results suggest that MRI might be very accurate for the pre-operative local staging of colon cancer, and in this study MRI was more accurate than CT although the numbers were too small for these differences in accuracy to be significant.

1.10.6 MRI – assessment of systemic disease in colorectal cancer

MRI is useful for the assessment of liver lesions. Niekel performed a meta-analysis of eighteen studies investigating the accuracy of MRI in the identification of colorectal liver metastases. In this study, MRI had an overall per-patient sensitivity of 88.2% and specificity of 92.5%. In this analysis, there was significant improvement in the sensitivity of MRI over time, with studies performed after 2004 demonstrating significantly greater per lesion sensitivity (85% post 2004 compared to 70% pre

2004). There was also a non-significant trend towards greater per lesion sensitivity with liver specific contrast (mangofodipir trisodium) (Niekel et al., 2010a).

FDG-PET/CT (section 1.10.8) is also very sensitive for the identification of colorectal liver metastases. However, the sensitivity of FDG-PET/CT is reduced following chemotherapy. In this situation, MRI is the most sensitive modality for the identification of liver metastases (van Kessel et al., 2011).

A recent study investigated the impact of combining DWI and a liver specific contrast agent for the identification of colorectal liver metastases. This found that the combination improved the sensitivity and specificity of MRI (Koh et al., 2012).

MRI has also been investigated for the whole body assessment of patients for colorectal liver metastases. In a small pilot study of twenty-four patients, using FDG-PET/CT as the reference standard, whole-body MRI was comparable in the detection of solid organ disease although inferior in the identification of nodal disease (Schmidt et al., 2009).

1.10.7 ^{18}F-Fleurodeoxyglucose Positron Emission Tomography (FDG-PET)

Positron emission tomography (PET) is an imaging technique which detects the uptake of radiolabelled tracers in tissues. Certain radioisotopes, including ^{18}Fluorine (^{18}F) and ^{11}Carbon (^{11}C), undergo radioactive decay by beta decay. This results in a proton in the nucleus emitting a positron to become a neutron, changing the atomic number of the nucleus (hence ^{18}F decays to oxygen ^{18}O and ^{11}C decays to boron ^{11}B). The emitted proton is the anti-matter equivalent to an electron. Once it has slowed adequately to combine with an electron (over the course of around 1mm), it undergoes annihilation, which results in the simultaneous emission of two photons at 180 degrees to each other in the gamma frequency range.

Positron emission tomography detects the emitted gamma rays and uses them to localise the positron emission. The patient is surrounded by a detector ring, made up of a series of detectors (a scintillator converts the gamma radiation to visible light which is in turn detected by a photodiode).

The detector only records events where two simultaneous gamma rays are detected, and is therefore able to determine a line of response (LOR) along which the positron was annihilated (Figure 1.2).

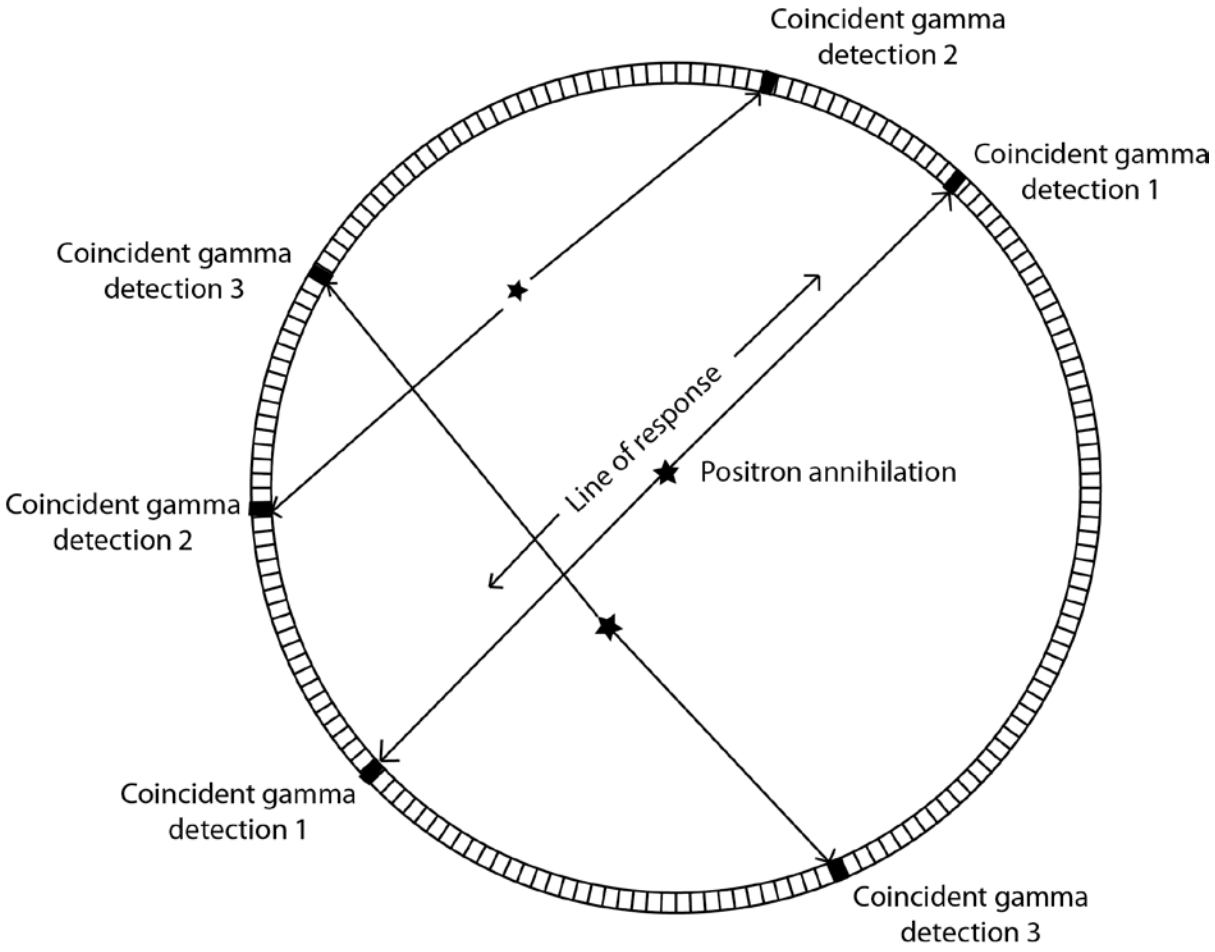


Figure 1.2: Positron detection in positron emission tomography

Very high timing resolution (around 500 picoseconds) in modern PET scanners allows time of flight assessment in addition to LOR assessment, so that the positron annihilation can be isolated to a segment of the line of response. This can be used to increase the contrast to noise ratio in PET scanning (Karp et al., 2008).

The PET scan is acquired by moving the patient through the detector ring and collecting information from thousands of annihilation events through their corresponding coincident gamma ray detections. This information produces a projection of the number of positrons emitted along each line of response, used to produce a sinogram in a similar way to the data from transmitted gamma rays in

CT. This information is reconstructed by a computer by filtered back projection or more recently by iterative reconstruction (section 1.10.1). A standardised uptake value (SUV) can also be calculated by dividing the voxel intensity of a calibrated PET image by the concentration of the injected radioactivity. This calculation is complicated as it needs to take into account injected dose, patient body weight, radioactive decay over time since injection, attenuation and scatter. It is therefore considered a semi-quantitative measurement.

The most common radiolabelled compound used in PET imaging is ^{18}F-fluorodeoxyglucose (^{18}F-FDG), in which one of the hydroxyl groups in glucose is substituted for an ^{18}F fluoride ion. This is taken up as glucose by metabolically active cells. It then accumulates in these cells as it cannot undergo glycolysis until the fluoride ion has undergone conversion to oxygen by radioactive decay. Once the fluoride ion has been converted to $^{18}O^-$, it picks up a proton from the aqueous environment and becomes a normal glucose molecule, albeit with on heavy oxygen atom (^{18}O). Other radiolabelled compounds can be used in oncological imaging, such as ^{18}F-fluoro-3-deoxy-3-L-fluorothymidine (FLT) and ^{60}Cu-diacetyl-bis(N4-methylthisemicarbazone) (^{60}Cu-ATSM), but are not currently in wide spread clinical use.

FDG-PET is useful in oncological imaging as cancer cells tend to have a high metabolic rate and abnormal glucose uptake. This form of functional imaging potentially allows the identification of metastatic disease where no anatomical abnormality is evident. A meta-analysis of 61 eligible articles suggested that on a per patient basis FDG-PET was more sensitive than CT or MRI in detecting liver metastases, with a sensitivity of 94.6%, although on a per lesion basis SPIO enhanced MRI was more sensitive (Bipat et al., 2005). A number of studies have also demonstrated FDG-PET to be accurate in the identification of extrahepatic disease. A meta-analysis found that FDG-PET had a sensitivity of 91.2% and a specificity of 95.4% in identifying extrahepatic metastases (Wiering et al., 2005).

1.10.8 FDG-PET/Computed Tomography (FDG-PET/CT)

FDG-PET/CT fuses the functional imaging of FDG-PET with the anatomical imaging of CT in one scan. This allows localisation of increased FDG uptake to a particular anatomical structure. The attenuation data from the CT also allows attenuation correction of the PET data, increasing the accuracy of the PET part of the scan. PET/CT has therefore superseded PET in most oncological applications.

Primary local staging of colorectal cancer

FDG-PET/CT is not usually used for the primary staging of colorectal cancer as it is expensive, involves an additional radiation dose to CT, and does not provide additional anatomical information over standard CT. It has been investigated for accuracy of local lymph node staging in rectal cancer, where Kim et al. found that FDG-PET/CT had a higher specificity than MRI for nodal involvement (83% compared to 67%), although sensitivity was lower in this study (61% compared to 94%) (Kim et al., 2011a). This is consistent with other studies which have suggested that FDG-PET/CT has a relatively high specificity but lower sensitivity for nodal metastases (Tsunoda et al., 2008), and is likely to be related to the resolution of which struggles to identify lesion less than around 1cm in diameter, and the fact that not all metastases are metabolically active.

Systemic staging in colorectal cancer

FDG-PET/CT is useful in the accurate systemic staging of colorectal cancer. In a recent meta-analysis, FDG-PET/CT had a pooled per patient sensitivity of 93% and a specificity of 86% for the detection of colorectal liver metastases (Maffione et al., 2015), which was similar to MRI and superior to CT. For the detection of lung metastases, FDG-PET/CT is has a very high specificity but only moderate sensitivity. In a large study of 256 patients by Bamba et al FDG-PET/CT has a sensitivity of 57% and a a specificity of 99% (Bamba et al., 2011). CT is more sensitive in the detection of lesions under 10mm, although it is only able to characterise these by serial imaging. The principle use of FDG-PET/CT in pulmonary staging is therefore characterisation of lesions over 10mm.

The area where FDG-PET/CT is superior to any other imaging modality is in the identification of extra-hepatic abdominal disease, especially peritoneal disease and retroperitoneal lymph node metastases. It is therefore recommended for patients with liver metastases who are being considered for metastasectomy, where it identifies extra-hepatic metastases not identified on imaging in approximately 32% of patients (Maffione et al., 2015). It is also recommended in most guidelines for investigation of a rising CEA post treatment for patients in whom the site of metastases or recurrence is not evident on CT and MRI.

As the cost of FDG-PET/CT comes down and it's availability becomes more widespread, it may be recommended for the primary systemic staging of colorectal cancer; in this context it identifies synchronous metastatic disease in an additional 10% of patients compared to contrast enhanced CT (Ozis et al., 2014).

Prediction and assessment of response to neoadjuvant therapy in rectal cancer

There have been a large number of published studies examining prediction of response to chemotherapy on the basis of FDG-PET/CT. Li et al performed a meta-analysis of these studies in 2014, in which FDG-PET/CT has s sensitivity of 89% and a specificity of 80% for predicting pathological complete response in rectal cancer (Li et al., 2014). This was similar to MRI using DWI, which has a sensitivity of 85% and a specificity of 73%. There was considerable heterogeneity in the studies included in this meta-analysis, with variation in the parameter used to predict response, the timing of scans in relation to neoadjuvant therapy, and the rate of pathological complete response in the trial patients. However, it would appear that FDG-PET/CT has a useful role in predicting and monitoring response after neoadjuvant treatment.

1.10.9 Ultrasound (US)

Ultrasound uses sound waves at frequencies above the range of human hearing (20 KHz), and in medical imaging the reflexion of these sound waves is used to form an image of the tissue being

scanned. A row of transducers made from piezoelectric crystals are used to create a sound wave from an electrical signal. The same transducers can also be used to convert the reflected sound waves into an electrical signal for detection and processing. Medical imaging applications usually use a pulse echo approach, where a sound wave is transmitted for a short period, and then the sound wave is switched off to listen for the echo.

Sound waves travel at a constant velocity in a given material (and hence tissue), which is determined by the acoustic density of that material. In human soft tissues, the velocity of a sound wave is between around 1450 m/s in fat and 1585 m/s in muscle (compared to 331 m/s in air). Using knowledge of this speed and the distance (depth) being scanned, the approximate timing of the echoes can be estimated which determines the timing of sequential sound pulses (eg scanning to 10cm depth in average soft tissues with a sound wave velocity of 1500 m/s, the echo will return to the transceiver in 0.1*2/1500= 0.12 ms). In 2D ultrasound scanning with a linear probe, each transducer in the row will transmit a sound pulse and listen for the echo in turn, and a 2D picture is built up from the time delay (represented by depth) and intensity (represented by grayscale pixel intensity) of the echoes (Figure 1.3). Echogenic tissues and reflective tissue interfaces appear bright, conductive tissues (such as fluid) appear dark.

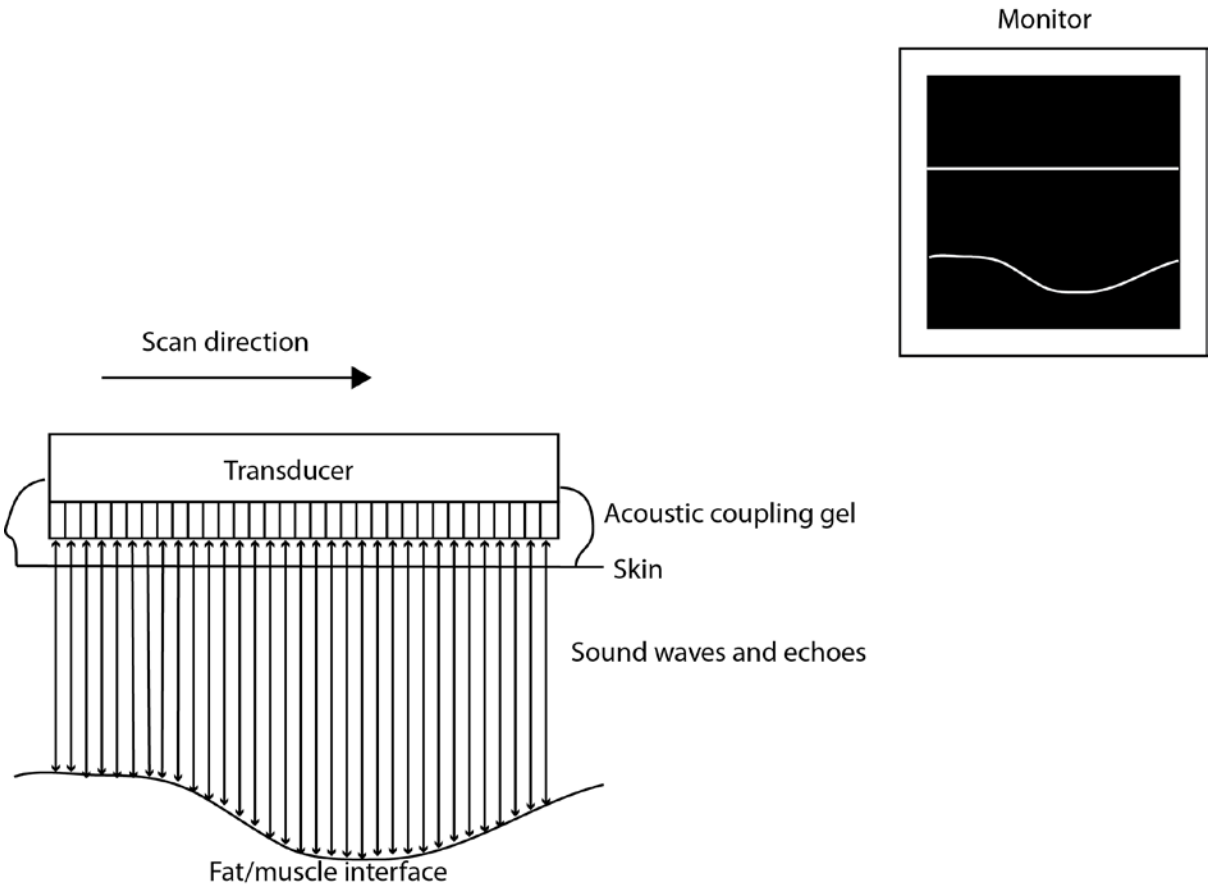


Figure 1.3: Ultrasound imaging

When a sound wave meets an interface between two materials with different acoustic densities, a proportion of the sound wave will be reflected, a proportion will be transmitted, and some will be scattered or absorbed. The proportion of sound reflected or transmitted depends on the difference in acoustic impedance of the two tissues, and is in the order of 1% for most soft tissue interfaces in humans. This allows useful visualisation of these interfaces, while allowing sound to be transmitted to visualise deeper structures. The proportion of sound reflected at air-soft tissue interfaces is around 99%, which necessitates the use of a coupling gel between the transducer and the tissue being imaged. It also means that air containing tissues (such as the lung and bowel) appear very reflective and cannot be penetrated by ultrasound.

In addition to acoustic imaging (sometimes referred to as B-Mode scanning), Doppler scanning uses the frequency shift in sound waves moving towards or away from the probe to detect movement

within the scanning area. This is most commonly used to detect blood flow, and can be overlaid on B-Mode imaging in colour to represent flow towards or away from the probe.

Three dimensional images can also be produced by ultrasound by building up rows of 2D images. These can be acquired by a specialised probe which sweeps a linear transducer array across a volume of tissue, or which rotates the row of transducers within an inserted probe. These images can be vulnerable to movement artefact if there is motion in the scanned tissues as the process is relatively slow. Phased array transducers are also available which are able to focus and scan the ultrasound beam electronically by controlling the timing of the pulse-echo sequences within the probe.

Contrast enhanced ultrasound makes use of microbubbles to increase contrast on ultrasound imaging. The microbubbles are highly echogenic, as they have multiple gas-fluid interfaces. The size of the microbubbles restricts them to the vascular system, as they are too large to diffuse across the capillary basement membrane. Contrast enhanced ultrasound therefore increases the echogenicity of highly vascular structures, and this property can be used to identify certain types of metastatic tumour. It is also possible to make quantitative measurements of tissue perfusion on contrast enhanced ultrasound through microbubble destruction and measurement of microbubble replenishment (Kern et al., 2011).

Ultrasound elastography is a relatively new technique which allows the assessment of the stiffness of tissues on ultrasound scanning. The stiffness of a material is described by Young's E modulus. This property varies significantly between different human soft tissues, and in particular is altered in pathological compared to normal tissues. It is analogous to the hardness felt on clinical palpation, and is particularly increased in some malignancies. This can be estimated using quasi-static methods, where a constant stress applied to the tissues, and the displacement of tissues and therefore generated strain is measured. The limitation of this technique is that it is not possible to quantify Young's modulus of the tissues. Dynamic methods generate shear waves in tissues by compression

(at much lower frequencies than the ultrasound waves). The propagation of the shear waves can be used map Young's modulus in tissues. The advantage of this technique is that it allows higher resolution mapping of Young's modulus than quasi-static methods, and that a quantitative analysis can be made. The disadvantages are that a more complex ultrasound probe is required to generate the shear waves, ultrafast ultrasound imaging in required to measure the shear wave displacements, and that the shear waves can deflect at tissue interfaces (Gennisson et al., 2013).

A wide variety of probes are available for ultrasound assessment which allows it to be utilised in a number of different clinical settings. Linear and phased array probes allow trans-abdominal imaging. Intraluminal probes allow trans-vaginal and trans-anal ultrasound imaging. Sterile probe covers allow direct intra-operative ultrasound imaging of organs, in particular the liver is often imaged in this way during liver metastasectomy. Finally, miniaturised probes can be passed down the channel of endoscopes allowing endoscopic ultrasound.

Assessment of primary rectal cancer

Endorectal or endoscopic ultrasonography (EUS) has been widely applied in the assessment of T-stage in rectal cancer. This was subject to a meta-analysis by Puli et al in 2009 which included forty-two studies and over five thousand patients. The pooled sensitivity and specificity for T-stage assessment were; 88% and 98% for T1 disease, 80% and 91% for T2 disease, 96% and 98% for T3 disease, and 95% and 98% for T4 disease. This analysis suggests that EUS has excellent accuracy for the T-staging of rectal cancer, with lowest accuracy for the identification of T2 disease (Puli et al., 2009a).

The accuracy of EUS is operator dependent, and some authors have questioned whether the very high accuracy reported in these clinical trials are reproduced in clinical practice. Marusch subsequently performed a nationwide study in Germany involving over seven thousand patients in the final analysis. This demonstrated a stage-for stage T-staging accuracy of 65%, with the lowest

accuracy for identifying T2 and T4 tumours. Accuracy was significantly worse in small volume centres than large volume centres (Marusch et al., 2011).

More recently, Waage et al. have investigated the addition of elastography to EUS for the detection of T1+ adenocarcinomas. In a study of 120 patients, they achieved a sensitivity of 93% and a specificity of 96% in the differentiation of T1 or greater tumours from adenomas (T0) (Waage et al., 2014). This study validated the strain ratio cut off value which had been derived in a previous study. EUS with elastography was much more specific than MRI in this study, which tended to over stage early lesions.

Puli also addressed the accuracy of nodal staging with EUS in a separate meta-analysis, which included thirty-five patients and 2732 patients. The pooled sensitivity for EUS in detecting nodal metastases in this study was 73%, with a specificity of 76% (Puli et al., 2009b). This is similar to the pooled sensitivity and specificity for MRI (section 1.10.2).

The principle weakness of EUS in the assessment of rectal cancer is that it is unable to accurately predict CRM involvement. It is therefore largely limited to T-stage assessment of early tumour being considered for local resection in current practice.

Local staging of colon cancer

Endoscopic ultrasound local staging of colon cancers is possible using a mini ultrasound probe which can be passed down an endoscope channel. Gall performed a meta-analysis of the accuracy of endoscopic ultrasound in the assessment of colon cancer, which included six studies and 261 patients for whom separate data was available on accuracy in colon cancer. Pooled sensitivity and specificity for T-staging were; 87% and 98% for T1 disease, 71% and 95% for T2 disease, 98% and 89% for combined T3/4 disease. Sensitivity for the detection of nodal disease was 54%, with a specificity of 88% (Gall et al., 2014). This is higher than the sensitivity and specificity reported for CT in the T-staging colon cancer. Despite this, endoscopic ultrasound is not in widespread use for the preoperative local staging of colon cancer.

Restaging after neo-adjuvant chemoradiotherapy

EUS can also be used to restage rectal cancer following neoadjuvant chemoradiotherapy. In meta-analysis, the pooled T-staging accuracy from eighteen studies was 65%. The range of values in the individual studies was wide, ranging from 36 to 93%. The accuracy on EUS in this study was higher than the pooled accuracy on MRI from twelve studies (52%). Pooled N-restaging with EUS was 73%, very similar to pooled N-restaging accuracy using MRI in the same study (72%) (Memon et al., 2015).

Despite the superior accuracy of EUS in restaging rectal cancer after neoadjuvant therapy, it's use is still limited by inability to accurate assess CRM involvement, and difficulty in assessing stenosing tumours; 19% of tumours could not be assessed on EUS due to stenosis in a recent study comparing EUS and MRI (Swartling et al., 2013).

Predicting and assessing response to chemoradiotherapy

In addition to morphological assessment of response following chemoradiotherapy, a couple of additional techniques have been investigated for assessment of response. Rafaelsen measured elastography before and after neoadjuvant therapy and noted a significant difference in tissue elasticity (Rafaelsen et al., 2013). Tankova investigated vascularisation reduction in tumours using power Doppler at EUS; vascularisation reduction on ES was associated with better overall survival (Tankova et al., 2012). Whether the differences seen in these small studies can provide a useful means for predicting pathological complete response needs further investigation.

Systemic staging with US

Contrast enhanced ultrasound can be used for the assessment of focal liver lesions identified on CT or unenhanced US, and in this setting has similar sensitivity and specificity to contrast enhanced CT for determining whether these lesions represent metastatic disease and is cheaper (Westwood et al., 2013). However, CT has been shown to be inferior to liver MRI and FDG-PET/CT, and it is therefore likely that contrast enhanced US is also inferior to contrast enhanced MRI and FDG-PET/CT.

Intraoperative US is used in some units during liver resection to identify additional metastases. It is reported to identify additional metastases over preoperative MRI and FDG-PET/CT and change surgical strategy in between 1.4% and 27.2% of patients (Torzilli et al., 2014, Ferrero et al., 2013).

1.11 Summary

Colorectal cancer is a major health burden, with an increasing incidence worldwide. Despite improvements in survival it remains the 8th most common cause of death in both men and women in the UK.

The number of treatment options, both surgical and non-surgical, has increased dramatically over the past few decades. Short course radiotherapy, induction chemotherapy, long course chemoradiotherapy, and adjuvant chemotherapy may all be of benefit to some patients, but carry significant morbidity and mortality. A number of more and less radical surgical options are also available. Total mesorectal excision has become standard practice. However, complete mesocolic excision, ELAPE and extended lymph node dissection may also benefit some patients but may cause unnecessary morbidity and mortality in others. Conversely, local excision of early tumours may allow some patients to escape the morbidity and mortality of radical surgery including a permanent stoma. A proportion of patients with liver or lung metastases may also be cured if their metastatic disease is resectable when identified.

This multiplicity of therapeutic options means that it is becoming ever more important to target treatments towards patients who are likely to benefit. While our understanding of the genetic basis of colorectal cancer and the cellular signalling pathways affected is improving, and is already starting to allow targeted therapeutics, the mainstay of prognostication remains accurate histological and radiological staging of colorectal cancer. It is therefore more important than ever to accurately stage colorectal cancer locally and systemically, both histologically and radiologically.

1.12 Hypotheses and aims

1.12.1 Hypotheses

I hypothesise that:

1. Patients with high risk features on local staging with rectal MRI will have a higher rate of synchronous distant metastases than patients without high risk features.
2. Adapting the techniques developed for MRI imaging of the small bowel in Crohn's disease, including oral contrast agents and breath hold images, will allow accurate imaging of the colon wall. 3D volume acquisition sequences will allow more accurate assessment of the colon wall and adjacent structures than 2D sequences.
3. Preoperative 1.5T MRI will be more accurate than CT in staging colon cancer, and 3.0T MRI will be more accurate than both these imaging modalities.
4. Reports from MRI scans which obtained good quality images will be more accurate than those with poor quality images. Reports from MRI scans with T2 weighted imaging in two or more planes through the tumour will be more accurate than those with T2 weighted imaging in less than two planes
5. Using a high resolution MRI of the specimen to help select tumour blocks will identify more adverse features than conventional histological assessment, resulting in upstaging of tumours.

1.12.2 Aims

1. To investigate whether high risk features identified on local staging in rectal MRI are associated with a greater incidence of synchronous metastatic disease.

2. To optimize MRI technique in healthy volunteers for imaging the colon at 1.5T and 3T.
3. To compare the accuracy of 1.5T MRI, 3T MRI and CT in the local staging of colon cancer, using histology as the gold standard.
4. To compare the accuracy of 1.5T MRI, 3T MRI and CT in subgroups with optimal images, using histology as the gold standard.
5. To determine whether using high resolution ex-vivo MRI of the colorectal cancer specimen to help select tumour blocks during histological assessment results in upstaging compared to conventional histological assessment.

CHAPTER 2

Investigation of whether high risk features on rectal cancer MRI are associated with an increased incidence of metastatic disease

2.1 My role in this chapter

The data for this chapter was provided by Té Vuong, Division of Radiation Oncology, Segal Cancer Centre, Montreal. With the support of my supervisor, I performed the data analysis and wrote this chapter. I was the first author for the publication arising from this chapter (Hunter et al., 2011a).

2.2 Introduction and rationale

As discussed in section 1.8.2, the introduction of radiotherapy for rectal cancer has resulted in a significant reduction in local recurrence rates from around 22% to 12.5%, and ultimately on meta-analysis a benefit in overall survival was demonstrated (Colorectal Cancer Collaborative Group, 2001). Subsequently, preoperative radiotherapy was demonstrated to be associated with lower rates of local recurrence and toxicity (Sebag-Montefiore et al., 2009, Sauer et al., 2004). The reduction in local recurrence rates is maintained with TME surgery, although the absolute benefit is low in stage I tumours due to a low rate of local recurrence with TME surgery alone (Sauer et al., 2004). The addition of preoperative 5-FU or capecitabine chemotherapy to preoperative radiotherapy increases the rate of pCR and reduces the rate of local recurrence (although these trials had high rates of local recurrence in the control arms which may limit generalisability to patients in the TME era) (Ceelen et al., 2009).

Adjuvant chemotherapy is widely offered for stage III and high risk stage II rectal cancer, despite the fact that the majority of these studies suggesting benefit have been performed in colon cancer. In 2012 a meta-analysis of twenty-one trials did ultimately show a significant benefit in OS in patients receiving adjuvant 5-FU based chemotherapy, with a hazard ratio of 0.83 for OS and 0.75 for DFS (Petersen et al., 2012). Some controversy remains however, as these studies were largely performed in patients who had not received neoadjuvant chemoradiotherapy. EORTC 22921 investigated the benefit of adjuvant 5-FU and folinic acid chemotherapy in rectal cancer patients who had received neoadjuvant radiotherapy or chemoradiotherapy. There was no significant

difference in 10-year DFS between the groups who had and had not received postoperative chemotherapy (Bosset et al., 2014).

The benefit of adjuvant chemotherapy is therefore modest, and not proven in patients who have received neoadjuvant chemoradiotherapy. Despite improvements in local recurrence rates for rectal cancer, systemic failure remains a major problem, occurring in 30% to 40% of patients after apparently curative resection of their primary rectal cancer (Dewdney et al., 2012). If the primary tumour has been effectively removed, then metachronous metastatic disease presumably occurs due to micrometastatic disease present at the time of surgery not evident on imaging. This has led some authors to investigate the addition of further chemotherapeutic agents in the preoperative treatment of rectal cancer, either as induction chemotherapy prior to chemoradiotherapy, or as an additional agent during chemoradiotherapy. This has a number of potential advantages. It moves treatment of systemic disease (which is what ultimately kills patients) forward in the treatment pathway. It improves compliance with chemotherapy; in the Grupo Cancer de Recto 3 phase II trial comparing induction neoadjuvant chemotherapy with adjuvant chemotherapy, 91% of patients completed induction chemotherapy but only 54% successfully completed adjuvant chemotherapy (Fernandez-Martos et al., 2010). It also avoids the delay to chemotherapy often seen after surgery which reduces the effectiveness of adjuvant chemotherapy; a four week increase in time to adjuvant chemotherapy is associated with a significant decrease in OS and DFS (HR 1.14) (Biagi et al., 2011). Finally, upfront systemic chemotherapy has the potential to increase the proportion of patients undergoing clinical complete response (cCR) to neoadjuvant chemoradiotherapy, who may be eligible for organ preservation.

These potential benefits led to a number of phase II trials which investigated the either the introduction of additional chemotherapy agents to the neoadjuvant long course chemoradiotherapy (CRT) regimes, or an additional course of chemotherapy before CRT (induction chemotherapy); the EXPERT trial demonstrated a promising pCR rate of 20% following the addition of 12 weeks oxaliplatin and capecitabine (CAPOX) before CRT (Chua et al., 2010), the Grupo Cancer de Recto 3

study failed to show improved pCR with induction CAPOX but did show improved compliance (Fernandez-Martos et al., 2010), and the EXPERT-C trial failed to demonstrate improved pCR with the addition of cetuximab to CAPOX long course CRT but did significantly improve OS (secondary end point) (Dewdney et al., 2012)

However, phase III trials which have investigated the impact of additional neoadjuvant chemotherapy on OS, DFS and OS have generally been disappointing; ACCORD 12/0405-Prodige 2 did not demonstrate any significant difference in LR, OS or DFS with the addition of oxaliplatin to CRT (Gerard et al., 2010, Gerard et al., 2012). The German CAO/ARO/AIO-04 trial did demonstrate a significant improvement in 3-year DFS, although this trial added oxaliplatin to neoadjuvant CRT as well as adding oxaliplatin and leucovorin to adjuvant chemotherapy in the investigation arm, compared to 5-FU based neoadjuvant CRT and adjuvant chemotherapy in the control arm (Rodel et al., 2015).

Experience with adjuvant chemotherapy in colon cancer suggests that the greatest benefit from chemotherapy is seen in those with high risk of disease recurrence; there is a proportional reduction in the risk of recurrence and death, but the absolute reduction is less in stage II disease (Gill et al., 2003). Pooled analyses have been required to demonstrate a significant benefit in stage II disease in contrast to stage III disease.

Identifying this high risk group for investigation of neoadjuvant therapy must be achieved on imaging, as histological staging is not available point in the treatment pathway. The radiological entry criteria for trials of neoadjuvant chemotherapy have been heterogeneous (Table 2.1)

(Fernandez-Martos et al., 2010, Gerard et al., 2010, Gerard et al., 2012, Aschele et al., 2011, O'Connell et al., 2014, Rodel et al., 2015, Dewdney et al., 2012).

Trial	Imaging modalities	Entry criteria
Grupo Cancer de Recto 3	MRI	Tumours within 2mm of MRF
		T3 tumours in lower 1/3rd rectum
		Resectable T4
		T3 or greater, N positive
ACCORD 12/0405-Prodige 2	EUS or MRI	Any T3 and resectable T4
		T2 anterior or low tumours
STAR-01	CT or EUS	T3 or greater tumours
		Any N positive tumours
NSABBP R04	CT and EUS, or MRI	T3 or greater tumours
		Any N positive tumours
German CAO/ARO/AIO-04	CT or EUS or MRI	T3 or greater tumours
		Any N positive tumours
EXPERT	MRI	Within 1mm MRF
		T3 at or below levators
		T3 extending >5mm (T3c+) or T4
		N2 tumours
EXPERT-C	MRI	Within 1mm MRF
		T3 at or below levators
		T3 extending >5mm (T3c+) or T4
		EMVI positive

MRF - mesorectal fascia

Table 2.1: Entry criteria on imaging for trials of additional neoadjuvant chemotherapy

However, some of the preoperative staging in these trials would not meet current recommendations for the preoperative staging of rectal cancer, and even if the preoperative staging is accurate some

of the included patients would have low risk stage II disease. Inclusion of these patients makes it less likely that neoadjuvant chemotherapy will demonstrate a significant survival benefit.

Trials of preoperative chemotherapy are more likely to demonstrate a benefit if they employ imaging modalities and selection criteria which identify patients at high risk of micrometastatic disease. It is intuitive to replicate histopathological selection criteria on imaging, which have been shown to select a group of patients who benefit from adjuvant chemotherapy in colon cancer. However, this may not be the best strategy. Some features which are reproducibly identified on histopathological examination are relatively poorly identified on imaging; nodal involvement is identified with sensitivity of around 73% and a specificity of around 76% on EUS (Puli et al., 2009b), and a sensitivity of 77% and a specificity of 71% on MRI (Al-Sukhni et al., 2012). Other prognostically important features are more reliably identified on imaging; on MRI, accuracy for the prediction of CRM involvement is 88% (MERCURY study group, 2006), and depth of extramural tumour spread is accurate to within 5mm 92.5% of the time (MERCURY study group, 2007). Some prognostically important features are not as reliably identified on conventional histopathology; in one study, the use of orcein elastic stain on histopathology increased the rate of EMVI detection from 18% to 71%, and using orcein stain all cases of distant metastases within 17 months of surgery demonstrated venous invasion. In this study venous invasion correlated more closely with distant metastases than nodal involvement (Sejben et al., 2010)

On the basis of risk factors which are known to be associated with a high risk of local or distant recurrence, and which can be reasonably reliably identified on preoperative MRI, a clinical set of criteria have been developed to differentiate “high risk” and “low risk” rectal cancer patients on preoperative MRI (Table 2.2). CRM involvement is included because it is accurately assessed on MRI (MERCURY study group, 2006), and involvement is associated with increased distant as well as local recurrence, and worse survival (Hermanek and Junginger, 2005). Intersphincteric plane involvement is included for low rectal cancers, as this has been demonstrated to be significantly associated with pCRM involvement for low rectal cancers (Salerno et al., 2009). Depth of extramural spread of more

than 5mm for T3 tumours (T3c disease) is included as it is accurately assessed on MRI (MERCURY study group, 2007), is associated with lower 5-year survival and a greater difference in survival than the distinction between T2 and T3 tumours (Merkel et al., 2001, Willett et al., 1999). EMVI is included as MRI detected EMVI is associated with significantly worse 3-year DFS (Smith et al., 2008a, Battersby et al., 2015). Nodal involvement is not included, as it is not reliably identified on MRI (Al-Sukhni et al., 2012), and T1-2 node positive patients have a better 5-year OS than T3-4 node negative patients (Kim et al., 2011b).

MRI feature	Low risk	High risk
CRM	Clear (>1mm)	Involved (<=1mm)
Intersphincteric plane (low rectal tumours <5cm)	Clear intersphincteric plane	Involved intersphincteric plane
T stage	T1-2, T3a-b (<=5mm extramural spread)	T3c-d (>5mm extramural spread), T4
EMVI	Negative	Positive
N stage	Any	Any

Table 2.2: MRI definition of "low risk" and "high risk" rectal cancer patients

This definition of MRI “low risk” patients was used in the MERCURY study to identify a group of rectal cancer patients who could be managed without neoadjuvant long course chemoradiotherapy, who were treated with TME surgery (with or without short course radiotherapy depending on local policy, and with or without adjuvant 5-FU chemotherapy on the basis of histological nodal status). In follow up, 5-year overall survival in this MRI “low risk” group was 85% (Taylor et al., 2011). This definition of MRI “high risk” rectal cancer patients is very similar to the entry criteria for the EXPERT-C trial; the only variation is that in EXPERT-C low rectal cancer patients were included as high risk if they had T3 disease, rather than intersphincteric plane involvement.

The aim of the first part of this study was to validate in an independent dataset whether these MRI criteria identify a group of patients at high risk of synchronous metastatic disease. If so, then patients without overt synchronous metastases demonstrating these tumour characteristics on preoperative MRI are likely to be at high risk of occult micrometastases. This would support the use of these entry criteria to select patients for trials of neoadjuvant chemotherapy. Patients exhibiting these high risk features might also benefit from more exhaustive investigation for synchronous metastatic disease.

The aim of the second part of this study was to use this dataset to investigate which of the rectal cancer features identified on MRI is most associated with synchronous metastatic disease. These features were then developed into a model for predicting synchronous metastatic disease. The new model was then compared to the existing clinical model previously examined in the MERCURY dataset.

2.3 Materials and Methods

2.3.1 Subjects

The dataset used in this study was taken from a Canadian trial examining the efficacy of FDG-PET/CT. Between August 2004 and June 2008 patients referred to the Montreal General Hospital for cancer staging were prospectively recruited into a trial into the efficacy of FDG-PET/CT. Institutional Review Board ethical approval was granted for this project, and informed consent was obtained from all participants. Two hundred and thirty six rectal cancer patients were retrospectively identified from this FDG-PET/CT study group. All rectal cancer patients had high resolution rectal MRI performed as part of their standard pre-operative staging. Patients were referred to the Montreal General Hospital from five Canadian institutions (Pierre Boucher Hospital, St Luc Hospital, Lakeshore General Hospital, St Mary Hospital and Valleyfield Hospital). Contrast enhanced multiple-row detector

computed tomography (CT) of the thorax, abdomen, pelvis was performed concurrently or in the immediate follow up period. Of these, 230 patients (97.5%) had FDG-PET/CT, CT and rectal MRI available for review and were included for further analysis.

2.3.2 Procedures

FDG-PET/CT studies were obtained on a hybrid PET/CT scanner (Discovery ST, General Electric Medical Systems, Waukesha, WI, USA), which combined a dedicated, full-ring PET scanner with a 16-slice spiral CT scanner. Patients were required to fast for at least 6 hours before the time of their appointment. Blood glucose levels were recorded just prior to FDG administration. If the serum glucose level was greater than 11.1 mmol/l (200mg/dl), then the study was rescheduled. A volume of 400ml of barium sulfate oral contrast was administered and between 370 and 500 MBq (10 and 13.5mCi) of FDG was injected intravenously. This is in line with the Society of Nuclear Medicine and Molecular Imaging guidelines (Delbeke et al., 2006). Sixty minutes following FDG injection, CT and FDG-PET images were consecutively acquired from the base of the skull to the upper thighs.

For the CT scan portion of the study, the settings were: 140kVp, 90-110mA (depending on body weight), a rotation time of 0.8s, a table speed of 17mm per gantry rotation, a pitch of 1.75:1, and a detector row configuration of 16 x 0.625mm. For the FDG-PET portion of the study, a 2-D acquisition was performed and images were acquired using 4-5min per bed position (depending on body weight) and 5 to 6 bed positions were used (depending on the patients height). PET attenuation-corrected, PET non-attenuation-corrected, CT, and fused images were reconstructed in the transaxial, coronal and sagittal planes with an ordered subset expectation maximization (OSEM) iterative algorithm.

Rectal MRI scans were performed on a 1.5 Tesla GE EXCITE Twinspeed HD scanner with a Torsocoil phased array coil (GE, Milwaukee). Patients received a Fleet enema, followed by 120 to 200mls of rectal contrast (ultrasound gel mixed with water), and 20mg of intramuscular hyoscine butylbromide (Buscopan, Boehringer Ingelheim) prior to the examination. T2 weighted FRFSE sequences were acquired in 3 planes through the rectal tumour (TR 3-5000, TE 102, Bandwidth 31.25kHz, ETL 17,

slice thickness 4mm, interslice gap 1mm, matrix 512x256). T1 weighted FSGR sequences were acquired in the axial plane (TR 130-155, TE 4.2 in phase, bandwidth 31.25kHz, matrix 256x160, slice thickness 5mm, interslice gap 2mm).

This rectal MRI technique differs from that used in the MERCURY study in the use of rectal contrast. Although this helps with the delineation of the contour of the rectal lumen, and can therefore help visualize polypoid rectal lesions, it can cause compression of the mesorectal fat and therefore affect measurement of the distance from the tumour to the mesorectal fascia (Slater et al., 2006). T1 weighted FSGR sequences were also acquired which were not felt to be helpful, and were not used in the study reporting. However, the high resolution T2 weighted images used for assessment of the rectal tumours in this study were of good quality.

CT scans were performed on one of two scanners. 1st CT scanner: GE 64 slice VCT scanner (120kV, Smart mAs 100-600, collimation 1.25mm, reconstructed every 0.9mm), 2nd CT scanner: GE 4 slice QXT scanner (120kV, Smart mAs 100-550, collimation 5x5mm), both GE, Milwaukee. Prior to CT scanning patients imbibed 25mls of Gastrografin, diluted in 1L of water. 80-100mls of intravenous contrast were administered at 2ml/sec, and images were acquired in the venous phase. These are the standard CT protocols used for preoperative staging of rectal cancer at the participating institutions.

2.3.3 Evaluation

Lesions were reported as metastatic disease on FDG-PET/CT and CT prospectively by consultant radiologists at the participating institutions. Reporting radiologists were blind to rectal MRI results, but had access to all other imaging and clinical information at the time of reporting, as is normal in clinical practice. Lesions were considered positive on FDG-PET/CT if abnormal FDG uptake was demonstrated in an anatomical structure which would not be expected to have physiologically increased FDG uptake. Specific SUV criteria were not employed.

For lesions to be considered distant metastases for the purposes of the study, lesions had to be confirmed on both imaging modalities. In cases where the FDG-PET/CT suggested a metastatic lesion and no abnormality had been reported on CT, a third expert reviewed the CT images and the lesions were considered metastatic if a consistent anatomical abnormality was identified.

Pre-operative pelvic MRI scans were reviewed by one consultant gastrointestinal radiologist, with more than ten years' experience, blinded to the results of FDG-PET/CT and CT. Rectal cancer features were reported using a standardised case report form. The following data were recorded:

1. Age
2. Gender
3. Tumour location (Upper, middle or lower third)
4. T stage (T1, T2, T3, T4)
5. Depth of extramural invasion (mm)
6. CRM involvement (involved = tumour within 1mm of mesorectal fascia/levators)
7. EMVI (positive or negative)
8. N stage (N0, N1, N2)
9. Intersphincteric plane involvement (for low rectal tumours)

T stage and depth of extramural invasion were also combined to provide T stage with T3 substage:

- T3a ≤ 1mm extramural invasion
- T3b > 1mm, ≤ 5mm extramural invasion
- T3c > 5mm, ≤ 15mm extramural invasion
- T3d > 15mm extramural invasion

Patients were then stratified into high risk and low risk groups according to features identified on rectal MRI. The high risk patient group included patients with any of:

1. EMVI

2. T3c or greater (more than 5mm extramural invasion or T4)
3. Involved circumferential resection margin (CRM) (tumour within 1mm)
4. Involved intersphincteric plane in low rectal tumours (<5cm from the anal verge).

This risk grouping was based on factors which have previously been identified as conferring high risk of metastases from the MERCURY study group data (Taylor et al., 2011).

The incidence of lesions considered to be metastases was then compared between high and low risks groups. Distant metastases were considered to be those outside the normal plane of surgical excision; that is inguinal, iliac or para-aortic lymph nodes were considered distant metastases, but mesorectal lymph nodes were not.

2.3.4 Statistical analysis

Statistical analysis was performed using R 3.0.1 statistical software (R Core Team, 2015), including pROC (Robin et al., 2011) and rpart (Therneau et al., 2015) packages.

For the assessment of the model derived from the MERCURY data, a two sided Fisher's exact test was used to determine whether the difference in the incidence of metastases in the high and low risk groups was significant. Means and one standard deviation are reported for normally distributed variables. Medians and interquartile ranges are reported for non-normally distributed variables. Ninety-five percent confidence intervals for proportions are calculated using the Wilson method for single proportions, as this has previously been demonstrated to be reliable (Newcombe, 1998). A p-value of <0.05 was considered statistically significant.

In order to investigate the MRI risk factors in this dataset, each risk factor was compared in the group with metastatic disease and the groups without. Normally distributed variables were compared using the student T-test, non-parametric continuous variables were compared using the Mann-Whitney U test, and categorical variables were compared using the Chi-squared test or Fisher's exact test if the any predicted count was 5 or less. The statistical significance of variation

across groups for ordered categorical variables was assessed using the Chi-squared test for trend in proportions. Univariate logistic regression analysis was also used to identify risk factors significantly associated with synchronous metastatic disease and to calculate the odds ratio for each variable. Variables which demonstrated a significant difference between the metastatic disease and control groups were taken forward for multivariate analysis ($p < 0.10$). Ordered categorical variables were partitioned using a recursive partitioning and regression tree (Breiman, 1984). Continuous variables were partitioned using the conditional inference tree method (Hothorn et al., 2006). These are automated processes which use regression identify the optimal partitioning point for an explanatory variable using by comparing the reduction in variance at different partitioning points . A multivariate regression analysis was then performed with stepwise forwards, backwards and bidirectional variable selection. Models were compared using the Akaike information criterion (AIC), and the model with the lowest AIC was selected for further evaluation (Akaike, 1974). Goodness-of-fit testing was performed using the Hosmer-Lemeshow test, with a p-value < 0.1 considered an inadequate model. Multi-collinearity was assessed using variance inflation factors. If the square root of the variance inflation factor was more than 2 this was considered to represent significant collinearity.

The predictive value of the model was assessed using the area under the curve (AUC) statistic calculated from the receiver operator curve (ROC) for model. The model derived using multivariate analysis in this dataset was compared to the clinical model previously investigated in the MERCURY dataset using AUC values. The threshold for the model was set with a relatively low specificity and high sensitivity (around 50% and 90%), as this was felt to be a clinically useful cut off for future inclusion in trials of neoadjuvant therapy or intensive surveillance.

2.4 Results

2.4.1 Patients

A total of 230 of 236 eligible patients (97.5%) had all imaging modalities available for review and were include for further analysis. The demographic characteristics of the included patients are summarised in Table 2.3: Demographic details. The mean age of patients was 64.5 years (S.D. 13.0). There were 161 male patients (70.0%) and 69 female patients (30.0%).

Demographic detail	Number of patients (%)
Gender	
Male	161 (70.0)
Female	69 (30.0)
Height of tumour	
Low rectal (<5cm)	100 (43.5)
Mid rectal (5-10cm)	54 (23.5)
Upper rectal (10-15cm)	76 (33.0)
Imaging TNM stage	
Stage I	44 (19.1)
Stage II	97 (42.2)
Stage III	57 (24.8)
Stage IV	32 (13.9)

Table 2.3: Demographic details

2.4.2 Identification of distant metastases in high and low risk groups

In the whole group, there were 32/230 (13.9%, 95%CI 10.0-19.0%) confirmed distant metastases. In the high risk group, there were 28/135 (20.7%, 95%CI 14.8-28.3%) confirmed distant metastases compared to 4/95 (4.2%, 95%CI 1.7-10.3%) in the low risk group. The odds ratio for having distant metastases in the high risk group compared to the low risk group was 5.9 (95%CI 2.0-24.0), and the difference in rates of distant metastases between the high risk group and the low risk group was highly significant p<0.001.

A flow diagram illustrating the rates of synchronous metastases in the high and low risk groups is illustrated in Figure 2.1

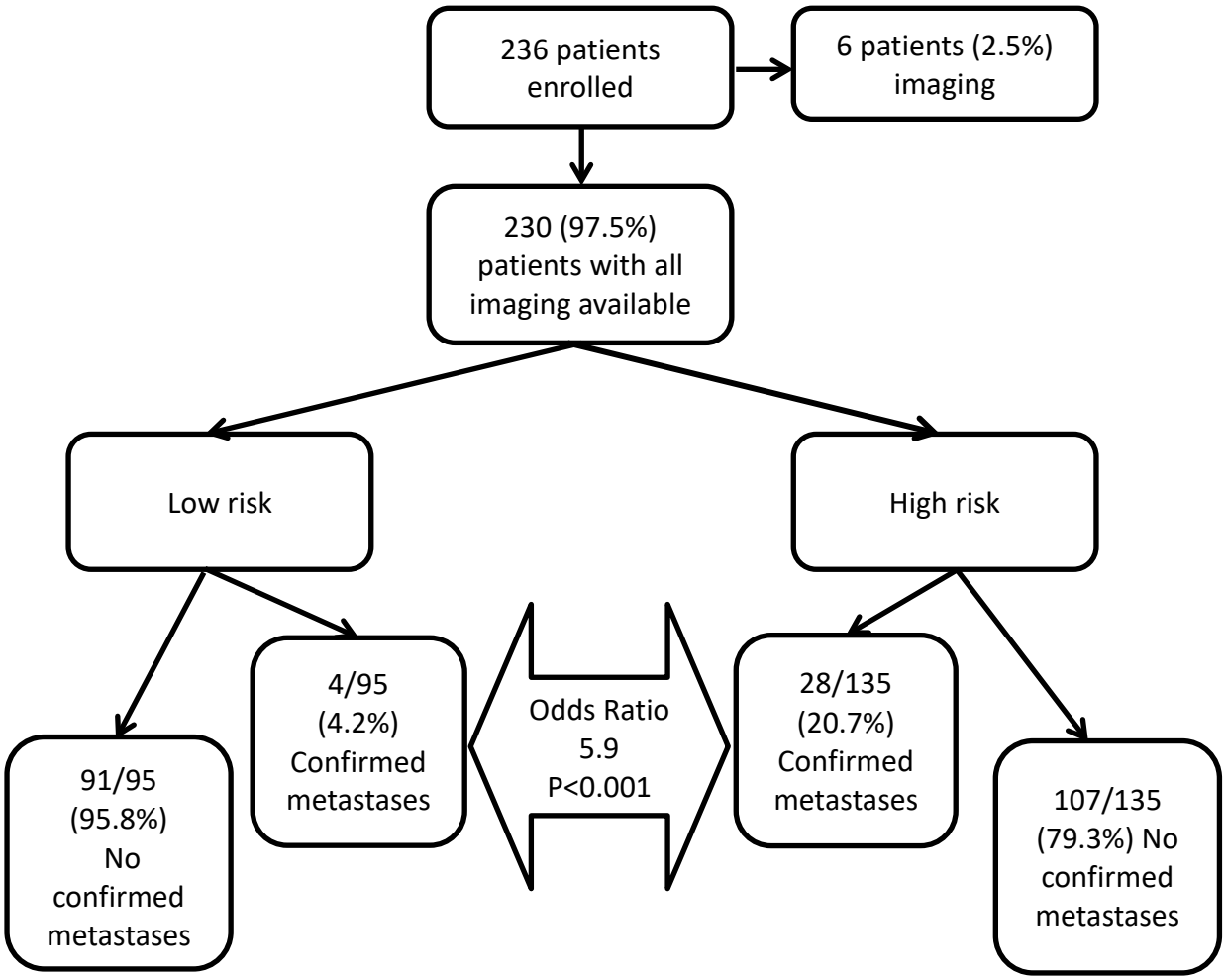


Figure 2.1: Incidence of metastatic disease in high and low risk rectal cancer

The univariate analysis for each MRI risk factor is presented in Table 2.4, together with the odds ratio for risk of metastatic disease and p-value for the significance of any difference between the metastatic disease and control groups. T-stage and depth of extramural invasion were assessed separately, and also assessed when combined into T-substage. Age and gender did not vary significantly between the two groups and were not investigated further. Tumour location, N-stage, T-stage, T-substage, depth of extra-mural invasion, circumferential margin involvement, EMVI positivity and intersphincteric plane involvement all showed significant variation between the synchronous metastatic disease and control groups on univariate analysis.

2.4.3 Univariate analysis

Parameter	No mets (n = 198)	Mets (n = 32)	Odds ratio (95% CI)	p-value	p-value (logistic regression)
Age (year)	64.3 (mean)	67.8 (mean)	1.01 (0.98-1.04)	0.45†	0.55
Gender (male)	140	21	0.79 (0.36-1.8)	0.71‡	0.56
Location					
Upper	79	21	0.42 (0.15-1.01)	0.10‡	0.07
Middle	49	5	0.56 (0.18-1.43)	0.37‡	0.26
Lower	79	21	2.9 (1.3-6.5)	0.01‡	0.008
T stage				<0.001Ŧ	
T1	19	0		0.08*	
T2	27	0		0.02*	
T3	111	16	0.78 (0.37-1.7)	0.65‡	0.52
T4	41	16	3.8 (1.8-8.4)	<0.001‡	<0.001
EMD (mm)	3 (median)	9 (median)	1.04 (1.01-1.08)	<0.001**	0.006
CRM (involved)	68	23	4.9 (2.2-11.7)	<0.001‡	<0.001
EMVI (positive)	65	22	4.5 (2.1-10.5)	<0.001‡	<0.001
N stage				<0.001Ŧ	
N0	141	14	0.31 (0.14-0.67)	0.004‡	0.003
N1	35	8	1.6 (0.61-3.6)	0.46‡	0.33
N2	22	10	3.6 (1.5-8.6)	0.006‡	0.004
IS plane (involved)	43	19	5.3 (2.4-11.8)	<0.001‡	<0.001

T substages				<0.001∓	
T1	19	0		0.08*	
T2	27	0		0.02*	
T3a	22	1	0.25 (0.01-1.3)	0.21*	0.19
T3b	47	5	0.60 (0.19-1.5)	0.37*	0.31
T3c	32	8	1.72 (0.68-4.1)	0.33‡	0.23
T3d	10	2	1.3 (0.19-5.1)	0.68*	0.78
T4	41	16	3.8 (1.8-8.4)	<0.001‡	<0.001

Table 2.4: Univariate analysis of MRI risk factors for synchronous metastases; separate variables

† Student T-test, ‡Chi-squared test, * Fisher's exact test, ** Mann-Whitney U test, ∓ Chi-squared test for trend. EMD extra-mural depth of invasion. IS intersphincteric plane

Ordered categorical variables (tumour location, T-stage, T-substage and N-stage) and the continuous variable (extra-mural depth of invasion) were partitioned using conditional inference and regression. This resulted in the following divisions;

1) Tumour location was divided into Low, and Mid/Upper rectal tumours
2) T-stage was divided into T4, and T3 or less.
3) T-substage was divided into T3b or greater, and T3a or less
4) N-stage was divided into N1 or 2, and N0
5) Depth of extramural invasion was divided into greater than 7mm, and 7mm or less.

Parameter	No mets (n = 198)	Mets (n = 32)	Odds ratio (95% CI)	p-value*	p-value (logistic regression)
Location (Low)	79	21	2.9 (1.3-6.5)	0.01	0.008
T stage (T4)	41	16	3.8 (1.8-8.4)	<0.001‡	<0.001
EMD (>7mm)	64	23	5.4 (2.4-12.8)	<0.001	<0.001
N stage (N1+)	57	18	3.2 (1.5-6.9)	0.004	0.003
T-substage (T3b+)	130	31	16.2 (3.4-292)	<0.001	0.007

Table 2.5: Univariate analysis of MRI risk factors for synchronous metastases; dichotomous variables

*Chi-squared test. EMD extra-mural depth of invasion.

2.4.4 Multivariate analysis

Multivariate logistic regression was then performed using stepwise backwards, forwards, and bidirectional variable selection. In cases where the backwards, forwards and bidirectional procedures derived different models, the models were compared using AIC values and the model with the lowest AIC value selected. A model was initially derived using separate ordered and continuous variables, and using separate T-stage and depth of extramural invasion (EMD). T-stages T1-3 had to be combined in this model due to zero cases of metastatic disease in the T1 and T2 categories. The procedure was then repeated with T-stage and EMD combined into T-substage, and with ordered and continuous variables partitioned as described previously. This was done in order to reduce collinearity and to simplify the model. The models derived with the separate variables and the partitioned variables were the same. The models derived from regression with T-stage and EMD, and the models derived regression with T-substage, included T-stage and T-substage respectively in the final model. However, the AIC value for the model including T-stage was lower (157 compared to 159), and so this model was chosen for further evaluation. The Hosmer and Lemeshow goodness

Parameter	Odds ratio (95% CI)	p-value (logistic regression)
T4 tumour	2.7 (1.2-6.2)	0.02
EMVI positive	4.8 (2.1-11.9)	<0.001
Intersphincteric plane involved	4.8 (2.1-11.3)	<0.001

Table 2.6: Multivariate analysis of MRI risk factors for synchronous metastases

of fit test for this model indicated a p-value of 0.78, suggesting adequate goodness of fit. Goodness of fit was adequate with p>0.1 for all the models tested. The variance inflation factors for the full model indicated significant collinearity for tumour location, intersphincteric plane involvement and CRM involvement. This is not unexpected as the distance from the rectal wall to the mesorectal fascia is reduced in low rectal cancers, and in very low tumours the intersphincteric plane forms the CRM. There was no significant collinearity as assessed by variance inflation factors between the predictor variables chosen for the final model.

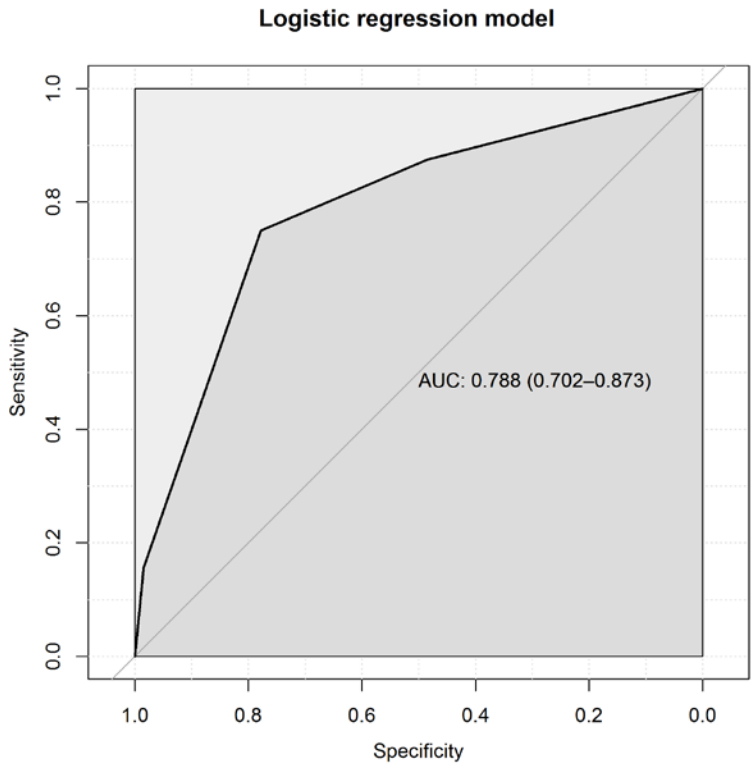
The multivariate logistic regression analysis for the final model is shown in Table 2.6. Multivariate analysis for the full model is not shown as there were an inadequate number of metastatic cases for the number of variables in the full model (seven variables and thirty-two cases, the minimum recommended number cases for logistic regression is ten per explanatory variable). The model derived from the multivariate logistic regression is similar to the previous clinical model, including T4 tumours rather than T3c or greater tumours, and dropping CRM positivity as a predictive variable.

2.4.5 Model testing

The model derived from the multivariate logistic regression (T4 disease, EMVI positive, and intersphincteric plane involvement) was then compared to the clinical model derived from the MERCURY dataset (T3c or greater, EMVI positive, CRM positive and intersphincteric plane involvement). Receiver operator curves (ROC) for both models are shown in Figure 2.2. Area under the curve (AUC) values for both models are very similar; 0.788 (95%CI 0.702-0.873) for the logistic

regression model and 0.778 (95%CI 0.690-0.867) for the clinical model from the MERCURY data, with a wide overlap in the 95% confidence intervals.

Including all cases with a score of 1 or greater in both models (i.e. any of the risk factors included in the model), the new logistic regression derived model would identify metastases in 28/130 patients in the high risk group and 4/100 patients in the low risk group. This gives an odds ratio of 6.6 (95% CI 2.5-22.9), and the difference in incidence of metastatic disease between the groups is significant ($p<0.001$ Chi-squared test). The previous clinical model would identify metastases in 28/135 patients in the high risk group compared to 4/95 in the low risk group, OR 5.9 (95%CI 2.2-20.6), $p<0.001$. The sensitivity of both models is 0.88 (95%CI 0.72-0.95), the specificity of the new model is marginally greater at 0.48 (95%CI 0.42-0.55) compared to 0.46 (95%CI 0.39-0.53).



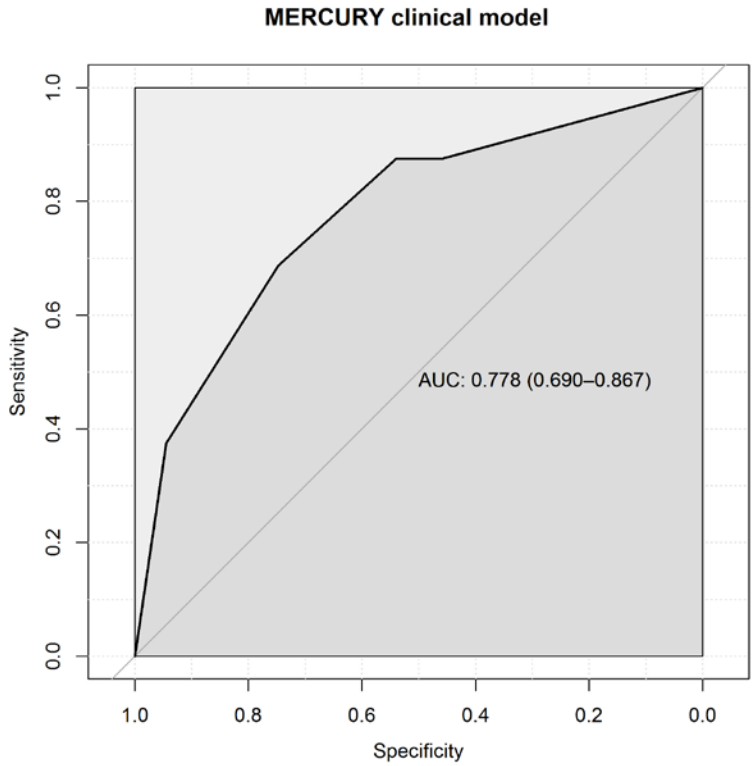


Figure 2.2: ROC curves for logistic regression and clinical models

2.5 Discussion

In this study we stratified patients into high and low risk groups on the basis of a set of MRI prognostic features which have previously been demonstrated to identify a low risk group of patients; these patients had good overall survival and disease free survival when treated with TME surgery without neoadjuvant chemoradiotherapy in follow up from the MERCURY study (Taylor et al., 2011). Based on this risk stratification, the MRI identified high risk group had a significantly higher rate of synchronous metastatic disease confirmed on two imaging modalities; 20.7% in high risk versus 4.2% in the low risk group, odds ratio 5.9 (95%CI 2.0-24.0). This is supportive evidence that this risk stratification is valid for predicting risk of systemic disease, and is generalizable to other rectal cancer patients having been validated in a separate dataset.

On univariate analysis in this dataset, tumour location, T-stage, extra-mural depth of invasion, CRM involvement, EMVI positivity, N-stage, intersphincteric plane involvement and T-substage were all significantly associated with synchronous metastatic disease. These tumour features are associated with more advanced disease, and so it unsurprising that they are also associated with synchronous metastatic disease. Low tumours have also previously been shown to be associated not only with an increased risk of local recurrence due to more frequent CRM involvement, but also with an increased risk of systemic disease (den Dulk et al., 2007). This may be related to anatomical differences in the low rectum, with lymphatic drainage to the pelvic side wall and iliac lymph nodes and vascular anastomoses with the systemic circulation. Age and gender were not significantly associated with synchronous metastases; although they have been shown to be associated with survival in previous studies, this may relate more to comorbidity and variation in treatment than to incidence of metastatic disease.

When multivariate logistic regression was performed on this dataset, a slightly different model was derived to the prior clinical model. In the assessment of individual risk factors, the optimum cut off for depth of extramural invasion was 7mm rather than 5mm in the previous model and the optimum

cut off for T-substage was T3b rather than T3c. These slight differences are probably related to random variation in a relatively small dataset. There were also some differences in the overall model derived from this dataset; the model which included T-stage (T4 cut off) and omitted CRM positivity was optimal in terms of AIC values in this dataset. Both the prior clinical model and the new model included intersphincteric plane involvement and EMVI positivity.

However, when both models were assessed in this dataset using AUC values, they were almost identical; 0.788 (95%CI 0.702-0.873) for the new model and 0.778 (95%CI 0.690-0.867) for the previous model. Including patients with a score of one or more to maximise sensitivity (i.e. patients with any risk factor), both models would identify 28/32 patients with metastatic disease (sensitivity 88%) and the new model would identify 96/198 patients without metastatic disease (specificity 48%) compared to 91/198 (specificity 46%) with the previous model. This suggests that the prior clinical model performs well in this dataset, although it is slightly more complicated as it includes four risk factors (EMVI, intersphincteric plane involvement, T3c or greater and CRM positivity) rather than three risk factors in the new model (EMVI, intersphincteric plane involvement and T4). Whether it could be simplified to three rather than four risk factors would need to be validated in an independent dataset.

On multivariate logistic regression, there was significant collinearity between CRM positivity, tumour height, and intersphincteric plane involvement. This is probably due to the fact that the intersphincteric plane forms the CRM for very low rectal cancers, and the tapering of the mesorectum in the low rectum increases the rate of CRM positivity. Therefore, although CRM positivity and low tumour location were all significant risk factors and had a high odds ratio on univariate analysis, they were not included in this model as many of these cases will have had an involved intersphincteric plane.

The risk factors included in the new model (T4 tumours, EMVI positivity and intersphincteric plane involvement) remained significant independent risk factors for synchronous metastatic disease on multivariate analysis.

EMVI was a consistent risk factor for synchronous metastatic disease on both the previously validated model and the model derived from this dataset. This is consistent with previous studies which have demonstrated MRI EMVI to be an independent risk factor for synchronous metastases (Sohn et al., 2015) and worse recurrence free survival (Smith et al., 2008a).

T-stage was also a consistent risk factor on both models, with T4 disease on the new model and T3c or greater disease on the prior model predicting synchronous metastatic disease. This is again consistent previous studies which have found T3c or greater disease (Sohn et al., 2015) and T4 disease (Smith et al., 2008a) to be significantly associated with metastatic disease.

MRI lymph node positivity was not included in the prior clinical model, and was not included in new model derived from the multivariate logistic regression in this dataset. MRI lymph node positivity was significantly associated with synchronous metastatic disease on univariate analysis. This is perhaps surprising considering that histopathological lymph node status is a strong predictor of metastatic disease, and lymph node positive patients derive the greatest benefit from adjuvant chemotherapy colorectal trials. Previous studies which have examined the association between MRI nodal status and metastatic disease have demonstrated conflicting results, with some studies suggesting that it is an independent risk factor for synchronous metastases (Sohn et al., 2015), but other studies failing to demonstrated it to be associated with recurrence free survival (Smith et al., 2008a). MRI nodal status may be a weaker predictor of metastatic disease than histopathological nodal status due to MRI inaccuracy; MRI has a relatively low sensitivity of 77% and specificity of 71% for the identification of nodal involvement (Al-Sukhni et al., 2012). The prognostic significance of histopathological lymph node status may also have been previously overestimated; the 7th edition of the AJCC staging manual recognises that T1-2 node positive patients have better 5 year survival than

T3-4 node negative patients. It also recognises that peritumoural deposits previously categorised as lymph node metastases (if they were over 3mm in size in the 5the edition of the AJCC staging manual) may represent discontinuous tumour extension, EMVI, or totally replaced lymph nodes, and these are now counted in the N1c category (Edge et al., 2010). It is therefore likely that in trials of adjuvant chemotherapy based on previous versions of TNM staging, EMVI and discontinuous tumour extension were in some cases misclassified as lymph node positivity.

The ability of rectal MRI to stratify patients into high and low risk groups preoperatively demonstrated in this study is clinical important. Patients with synchronous metastatic disease increasingly undergo different treatment pathways, that include neoadjuvant systemic chemotherapy (Aloia and Fahy, 2008), synchronous metastasectomy (Slupski et al., 2009, Hillingso and Wille-Jorgensen, 2009), and even metastasectomy prior to resection of the primary (Mentha et al., 2006, Brouquet et al., 2010). More intensive investigation for synchronous metastatic disease in high risk patients may therefore improve outcome by identifying metastatic disease at an operable stage. This is currently being investigated in the SERENADE trial (Cancer Research UK, 2016).

However, even with optimal systemic staging, micrometastatic disease will lead to late distant failure in a proportion of patients without metastases evident on initial staging investigations. Since the work by Dukes and Bussey more than fifty years ago (Dukes and Bussey, 1958, Dukes and Bussey, 1941), the importance of histopathological features in determining the risk of distant failure has been widely recognised. However, this information is only available to the clinician postoperatively. This is problematic for two reasons.

Firstly, many rectal cancer patients currently receive treatment before surgery. Long course chemoradiotherapy may significantly alter the pathological stage, with pathological complete response seen in 15-27% of patients (Maas et al., 2010). For this reason, the American National Clinical Cancer Network (NCCN) guidelines for rectal cancer recommend that adjuvant

chemotherapy is given on the basis of the pretreatment MRI stage for patients that receive long course chemoradiotherapy (Benson et al., 2012).

Secondly, there are a number of trials which are currently investigating systemic treatment dose chemotherapy in the neoadjuvant setting, on the basis that in the TME era it is largely systemic disease that kills rectal cancer patients and that compliance with adjuvant chemotherapy is poor (Boland and Fakih, 2014). Some phase II trials have shown promising results with improved rates of pathological complete response, although phase III trials have yet to show benefit in OS or DFS.

It is therefore very important to be able to stratify rectal cancer patients for risk of metastatic disease at the start of their treatment, both for suitable entry criteria for trials of induction neoadjuvant chemotherapy, and also to select the correct patients for treatment with adjuvant chemotherapy under current guidelines. This study would support the use of the MRI risk factors validated in the MERCURY dataset for the selection of patients to received induction neoadjuvant chemotherapy, and indeed these are very similar to the entry criteria for the EXPERT-C trial (EMVI positive, T3c or greater tumour, involved CRM, or T3 low rectal cancer) (Dewdney et al., 2012).

There are a number of limitations to this study. This was a retrospective analysis performed in a subgroup of patients with rectal cancer who had been recruited to a trial investigating the benefits of FDG-PET/CT. All rectal MRI's were re-reported by an expert in rectal MRI, which ensured high quality reporting for the purposes of this study. However, the MRI scans were not performed prospectively for this study. Although the scans were performed with an adequate high resolution T2 weighed protocol, rectal contrast was administered. This can cause compression of the mesorectum and so reduce the accuracy of CRM assessment (Slater et al., 2006). This may have led to underestimation of the importance of CRM involvement as a risk factor for synchronous metastatic disease, particularly in mid and upper rectal tumours.

Data collection was also limited to that which was collected in the original study or which was available from the study scans. I had hoped to assess the added value of FDG-PET/CT in identifying

metastatic disease in high and low risk rectal cancer patients, but data on clinical follow up and adjuvant therapy was insufficient for this. For the purposes of this study we therefore required lesions to be described as metastases on both FDG-PET/CT and contrast enhanced CT. While this increases the specificity, some true metastases identified on FDG-PET/CT or CT which could not be verified on complementary imaging will have been discounted.

Forty-six patients in this study were T1 or T2 on MRI imaging, and only two of these patients were MRI node positive. This means that forty-four patients in this study were very low risk on the basis of their MRI staging (Stage I disease), and indeed none of these patients had synchronous metastatic disease. This does limit the added value of this MRI risk stratification, as we would expect these very low risk patients to do well with surgery alone. However, these results suggest that MRI is accurately identifying these very low risk patients and that other MRI risk factors identify a group at increased risk within the T3+ tumours.

The number of patients with metastatic disease in this dataset was quite small (32/230 patients). This limited the power of this study to identify risk factors for synchronous metastatic disease. It is generally recommended that there are at least ten events for each risk factor investigated in multivariate logistic regression, although some authors have suggested that this could be relaxed to five events per variable (Vittinghoff and McCulloch, 2007). This means that the significance of variables in the full model with nine variables would be likely to be underestimated in this dataset. Multivariate logistic regression is therefore only presented for the three variables selected by the stepwise regression for the optimal model in this dataset (intersphincteric plane involvement, T4 disease and EMVI positivity) which remain significant. However, other important covariates in the full model may have been omitted.

In the next section of my thesis I aim to optimise abdominal MRI techniques with a view to obtaining high quality MRI scans of tumours in patients with colon cancer in the following section. I hope that

this will ultimately allow the accurate risk stratification of colon cancer patients using MRI, which will be important for trials of neoadjuvant chemotherapy such as the FOXTROT trial.

CHAPTER 3

Optimising MRI protocols for imaging colon cancer

3.1 My role in this chapter

Ethical approval and funding was already in place before these volunteer scans were performed. With the support of my supervisor, I oversaw the scans, performed the data collection and wrote this chapter. I was first author for the published abstract arising from this chapter (Hunter et al., 2011b).

3.2 Introduction and rationale

Magnetic resonance imaging (MRI) is the primary imaging modality for the local staging of rectal cancer (Nielsen and Wille-Jorgensen, 2014). MRI offers accurate assessment of circumferential resection margin (CMR) involvement. MRI also offers fairly accurate assessment of T-stage, although endorectal ultrasound (EUS) provides more accurate assessment of early tumours. In chapter 2, we demonstrated that patients with high risk features on rectal MRI are associated with an increased risk of synchronous metastatic disease.

Computed Tomography (CT) is the primary imaging modality for the local staging of colon cancer (Scottish Intercollegiate Guidelines Network (SIGN), 2015). Magnetic Resonance Imaging (MRI) has a number of potential advantages. MRI offers cross-sectional imaging in any plane, three dimensional (3D) volume acquisition, does not pose any risk in terms of radiation dose, and has excellent tissue contrast resolution in soft tissues. In chapter 4, I plan to investigate whether it is possible to perform more accurate preoperative local staging of colon cancer with MRI than with CT. In this chapter, I describe how I optimised the MRI technique at 1.5T and 3T field strength for imaging the colon on a number of healthy volunteers.

A number of technical problems complicate MRI imaging of the abdomen, and can degrade image quality. The most important of these is motion artefact, which manifests as blurring between the limits of displacement of a moving object, and as ghosting in the phase encoding direction (Wood and Henkelman, 1985). In the abdomen, these motion artefacts occur due to peristalsis of the

stomach or bowel, respiratory movement of the diaphragm, cardiac motion, and pulsatile flow of blood within large vessels. There are also a number of gas/tissue and gas/fluid interfaces in the abdomen, which occur at the lung bases and in the stomach and bowel. These can cause off-resonance or susceptibility artefacts and also degrade image quality (Lomas, 2003), causing geometric distortion, alteration of tissue intensity on T2 weighted imaging, and bands of increased signal intensity and signal void at the gas interface. The interface between fat and water containing tissues, which are again common in the abdomen, can produce chemical shift artefacts. This can cause light and dark bands on either side of a structure, ghost images in the frequency encoding direction, or a black line around structure due to phase cancellation. These technical problems have previously degraded image quality to the point that CT has been felt to be superior to MRI for imaging the colon, despite inferior contrast resolution.

The development of Magnetic Resonance Colonography (MRC) and Magnetic Resonance Enterography (MRE), have demonstrated that it is possible to overcome some of these technical problems to obtain high quality images of the bowel using MRI. The exact protocols for MRC and MRE vary between studies, but typical techniques are as follows:

MRC is performed after bowel preparation with a laxative such as polyethylene glycol solution. The colon is instilled with around 2L of warmed tap water (CO_2 insufflation is used alternatively). Hyoscine butylbromide is administered intravenously or intramuscularly. High resolution T1-weighted 3-dimensional fat-saturated volumetric interpolated breath-hold examination (VIBE, a form of T1 weighted spoiled gradient echo) images are then acquired through the abdomen and pelvis following administration of IV gadolinium (Graser et al., 2013). Images are often acquired in both the prone and supine positions.

MRE is performed following small bowel distension with water, dilute polyethylene glycol, or barium sorbitol solution. Some institutions also perform per rectal distension of the colon with water. An antiperistaltic agent is administered (glucagon or hyoscine butylbromide). T2-weighted single shot

fast spin echo (SS-FSE) and steady-state free precession (SSFP) images are usually acquired in the axial and coronal planes, and coronal T1 weighted spoiled gradient echo sequences are obtained after gadolinium administration (Pola et al., 2014).

Over the last few years, 3.0 Tesla (T) MRI scanners have become increasingly available for routine clinical use. 3.0T MRI offers a theoretical doubling of signal to noise ratio (SNR) over previous 1.5T systems, although this is more likely to represent an increase by a factor of 1.6-1.8 (Erturk et al., 2009). This can potentially be traded for a shorter acquisition time or higher spatial resolution, maintaining SNR at the same level. However, increasing magnetic field strength is not without potential problems. Magnetic field homogeneity tends to be lower, existing artefacts such as chemical shift and magnetic susceptibility artefacts may be higher, and new artefacts such as the "standing wave effect" may degrade image quality.

The focus of these techniques, however, is to obtain detailed images of the contour of the bowel lumen and for the detection of intraluminal lesions (Saar et al., 2007). In this section of my thesis I tried a number of the techniques which have been adopted in other abdominal MRI in an attempt to optimise the protocol for the MRI assessment of colon cancer before starting a trial investigating the local staging accuracy of MRI in colon cancer. This section of my thesis has a number of limitations; the scans were performed in a small number of healthy volunteers, the average age of the volunteers was younger than that of typical colon cancer patients, and only seventy-three test sequences were performed. However, useful improvements were made to the imaging protocol and the procedures and findings are described below.

3.3 Materials and Methods

3.3.1 Subjects

Ethical approval for MRI protocol development was granted by our local Research Ethics Committee, and informed consent was obtained from all volunteers. Four healthy volunteers with no past history of gastrointestinal disease or abdominal surgery were included in this study. The average age of subjects was 32 (range 29 to 37). There were two male and two female volunteers.

3.3.2 Procedures

MRI scans were initially performed on a Siemens 1.5T MRI scanner (Magnetom Avanto 1.5T, Siemens Medical Solutions, Erlangen, Germany). Optimal sequences were then converted to their equivalent sequences and tested on a Philips 3.0T MRI scanner (Achieva 3.0T, Philips Healthcare, Best, Netherlands). All imaging was performed using a multichannel abdominal phased array radiofrequency coil.

Parallel imaging techniques were employed for all scans. These use the differential signals from the channels of the phased array coils to interpolate some of the MRI data, reducing scan time while maintaining signal to noise ratio (Deshmane et al., 2012). All 1.5T sequences utilised Generalised Auto calibrating Partially Parallel Acquisitions (GRAPPA), a k-space based parallel imaging technique. All 3.0T sequences used Sensitivity Encoding (SENSE); an image space based parallel imaging technique.

Hyoscine butylbromide 20mg (Buscopan, Boehringer Ingelheim UK limited, Bracknell, UK) administered intra-muscularly was used for all imaging. Hyoscine butylbromide has been demonstrated to improve the quality of abdominal MRI imaging by reducing motion artefact due to peristalsis (Wagner et al., 2008).

The names of the MRI sequences used in this study and their acronyms for Siemens and Philips MRI scanners are summarised in Table 3.1.

Generic name	Siemens	Philips
Balanced steady-state gradient echo (BSGE)	True fast imaging with steady-state free precession (TrueFISP)	Balanced turbo field echo (BTFE)
Rapid acquisition with relaxation enhancement (RARE)	Sampling perfection with application optimized contrasts using different flip angle evolution (SPACE) and Turbo spin echo (TSE)	Volume isotropic turbo spin echo acquisition (VISTA) and fast spin echo (FSE)
Single-shot fast spin echo (SS-FSE)	Half-fourier acquisition single-shot turbo spin echo (HASTE)	Single-shot turbo spin echo (SS-TSE)
T1 weighted spoiled gradient echo (T1-SGE)	Fast low angle shot (FLASH)	T1 fast field echo (T1-FFE)

Table 3.1: MRI sequence names and acronyms

3.4 Results

3.4.1 MRI Sequences

Balanced Steady-State Gradient Echo

True fast imaging with steady-state free precession (TrueFISP) and balanced turbo field echo (BTFE) are both balanced steady-state gradient echo (BSSGE) sequences. These are ultra-fast gradient echo sequences which can be acquired in a single breath hold. They are widely used in magnetic resonance enterography (Leyendecker et al., 2009) as breath hold acquisition makes them resistant to motion artefact. Images were acquired in the coronal plane, with a field of view (FOV) of 350x350mm to 450x450mm, a slice thickness of 1.5mm to 3mm, and echo time (TE) of 1.5ms to 1.8ms and a repitition time (TR) of 3.5ms to 4ms. An example is shown in Figure 3.1.

These sequences did allow us to obtain clear images of the abdomen which were resistant to motion arterfact. However, they are vulnerable to susceptibility artefacts at tissue interfaces, and frequently created a black line around the bowel wall. We were concerned that this would limit our ability to assess the relationship between the tumour, the bowel wall and adjacent structures. Contrast is also governed by tissue T2/T1 ratio rather than true T2 weighting. We therefore decided to use these sequences to localise the tumour at the start of MRI scanning, but not as the primary sequence for the assessment of tumour T-stage.

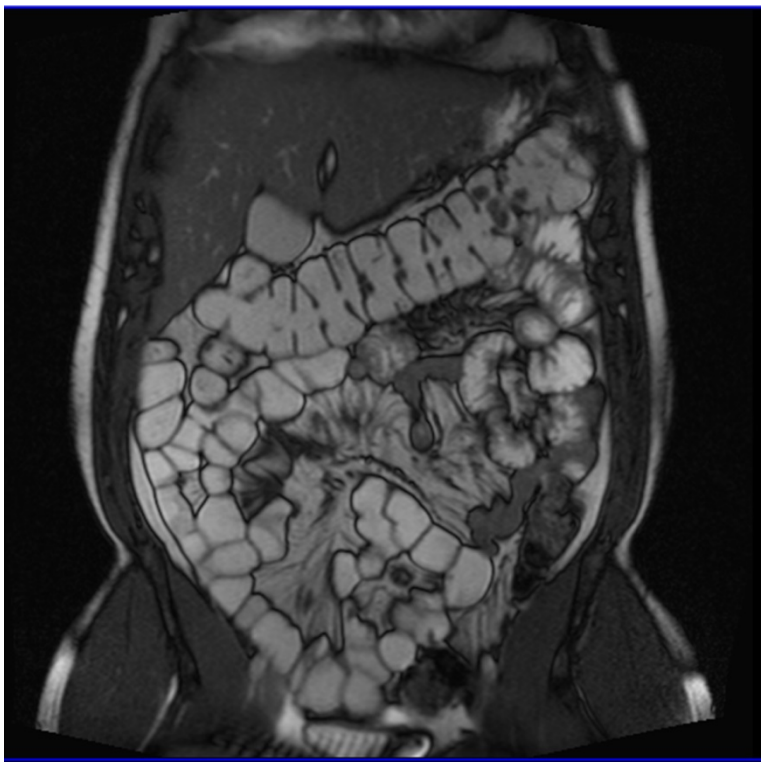


Figure 3.1: Balanced steady-state gradient echo sequence

Fast Spin Echo

Sampling perfection with application optimized contrasts using different flip angle evolution (SPACE), volume isotropic turbo spin echo acquisition (VISTA), turbo spin echo (TSE) and fast spin echo (FSE) are rapid acquisition with relaxation enhancement (RARE) sequences. These are spin echo sequences which use a refocussing 180 degree RF pulse after the initial 90 degree RF pulse to re-phase protons which have moved out of phase due to T2* relaxation, producing the echo which is detected by the received coils. RARE sequences use multiple rephasing RF pulses and collect multiple phase encoding steps for each pulse sequence repetition, reducing the scan times. These sequences give true T2 weighting, and are resistant to susceptibility artefacts. We acquired images in the coronal plane with a FOV of 250x250mm to 350x350mm, a slice thickness of 1mm to 3mm, a TE of 100ms to 150ms, and a TE of 1500ms to 4000ms. An example is shown in Figure 3.2.

However, RARE sequences are relatively slow to acquire, taking 5-10 minutes depending on the resolution and volume size. This makes them vulnerable to motion artefact, and necessitated

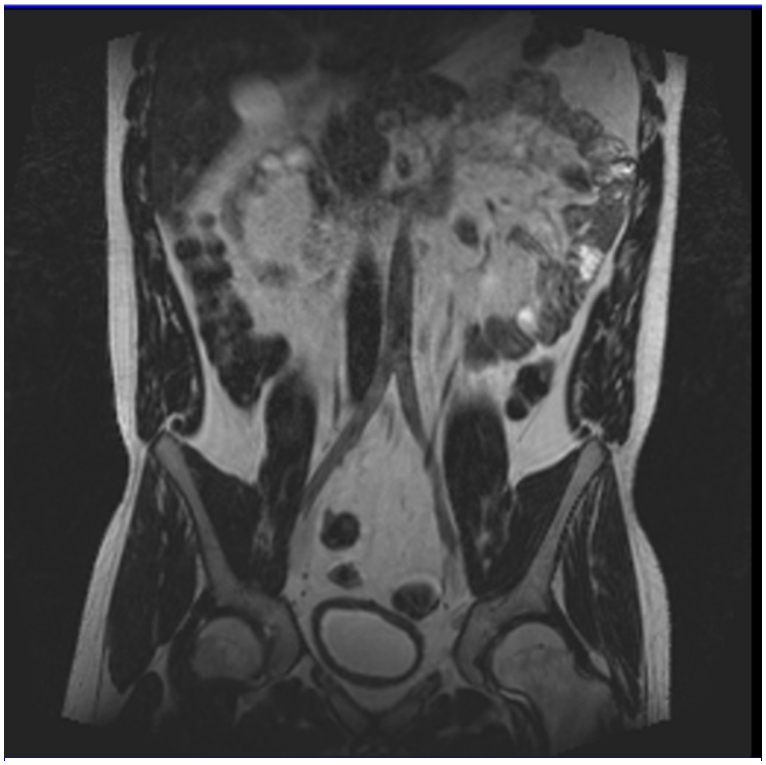


Figure 3.2: Fast spin echo sequence

respiratory triggering to reduce the effect of respiratory motion artefact. When not compromised by motion artefact, these sequences provided the best visualization of the colon wall and adjacent structures with a good signal and contrast to noise ratio. We therefore decided to use these sequences as the principle sequence in our subsequent study of colon cancer staging, except in situations respiratory triggering could not be adequately achieved.

Single-shot fast spin echo

Half-fourier acquisition single-shot turbo spin echo (HASTE) and single-shot turbo spin echo (SS-TSE) sequences are both single shot fast spin echo (SS-FSE) sequences where the whole volume is acquired following a single RF pulse with a long echo train due to multiple refocusing RF pulses. These are rapid sequences which can be acquired in a single breath hold, but give true T2 weighting. As they are spin echo sequences they are more resistant to magnetic susceptibility artefacts than the gradient echo based sequences. We obtained images in the coronal plane, with a FOV of 320x320mm, a slice thickness of 4mm, a TE of 100ms and a TR of 8000ms. An example is shown in Figure 3.3.

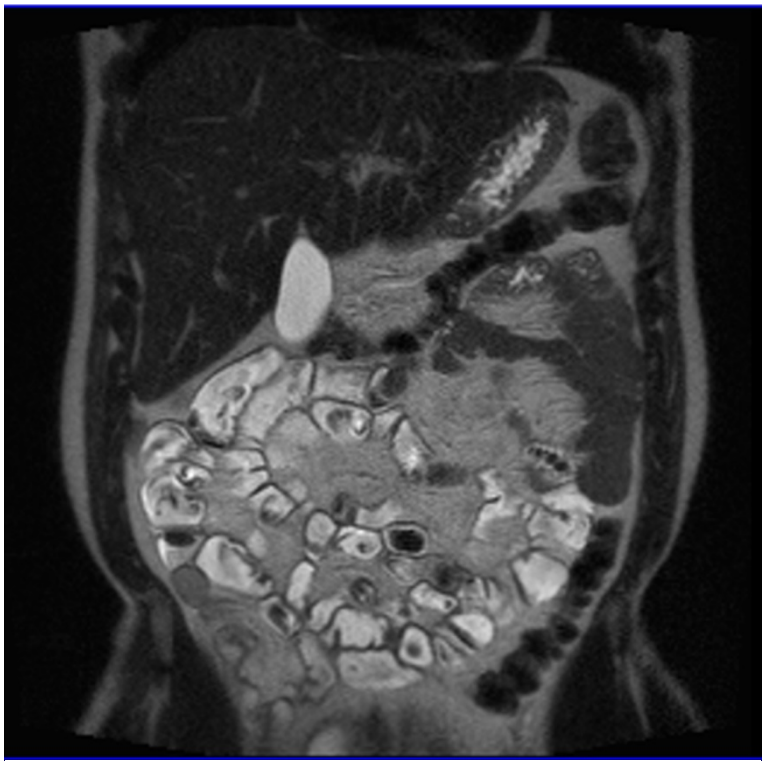


Figure 3.3: Single-shot fast spin echo sequence

These sequences were more resistant to motion artefact than the RARE sequences, particularly in cases where respiratory triggering was difficult to achieve, as they could be acquired in a single breath hold. However, the signal and contrast to noise ratio was lower than the optimum RARE sequences. We therefore decided to use SS-FSE sequences in cases where adequate RARE sequences could not be acquired due to difficulties with motion artefact or respiratory triggering.

T1 weighted spoiled gradient echo

Fast low angle shot (FLASH) and T1 fast field echo (T1-FFE) are spoiled gradient echo sequences (SGE). These use low energy RF pulses which produce a low flip angle of 20 to 80 degrees, reducing the time taken for return to longitudinal magnetization and hence reduce the repetition time between RF pulses. RF spoiling is used to spoil transverse magnetisation, so that the echo signal is produced from T1 weighting without waiting for the transverse magnetisation to decay. This combination allows the repetition time to be kept very low (3-4ms), allowing rapid image acquisition in a single breath hold. We acquired images in the coronal plane with a FOV of 350x350mm to

400x400mm, a slice thickness of 2mm, a TE of 1.1ms to 1.4ms and a TR of 3.25ms. An example is shown in Figure 3.4.

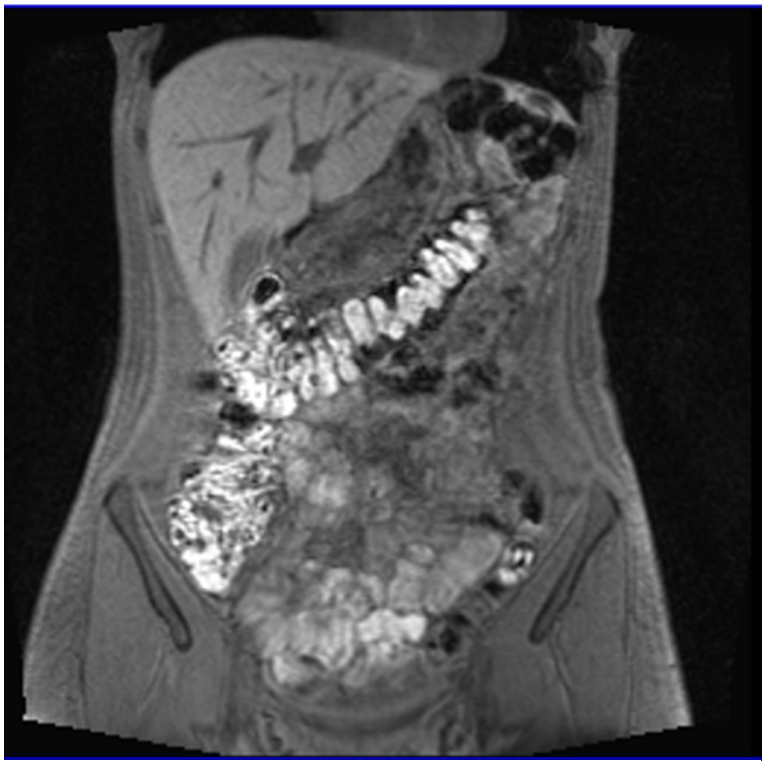


Figure 3.4: T1 weighted spoiled gradient echo sequence

These images were fairly resistant to motion artefact due to their very rapid acquisition, and were less prone to susceptibility artefacts than BSSGE sequences. However, the contrast in images derived from these sequences is dependent on T1 weighting. There is less inherent contrast in T1 weighted images of the abdominal soft tissues than in T2 weighted images. To overcome this limitation, we elected to use gadolinium enhanced SGE sequences in the colon cancer staging study. Examples of pre and post contrast images are shown in Figure 3.5. Acquisition of pre-contrast images and images after multiple time intervals following contrast administration also will also allow us to obtain dynamic contrast enhanced images.

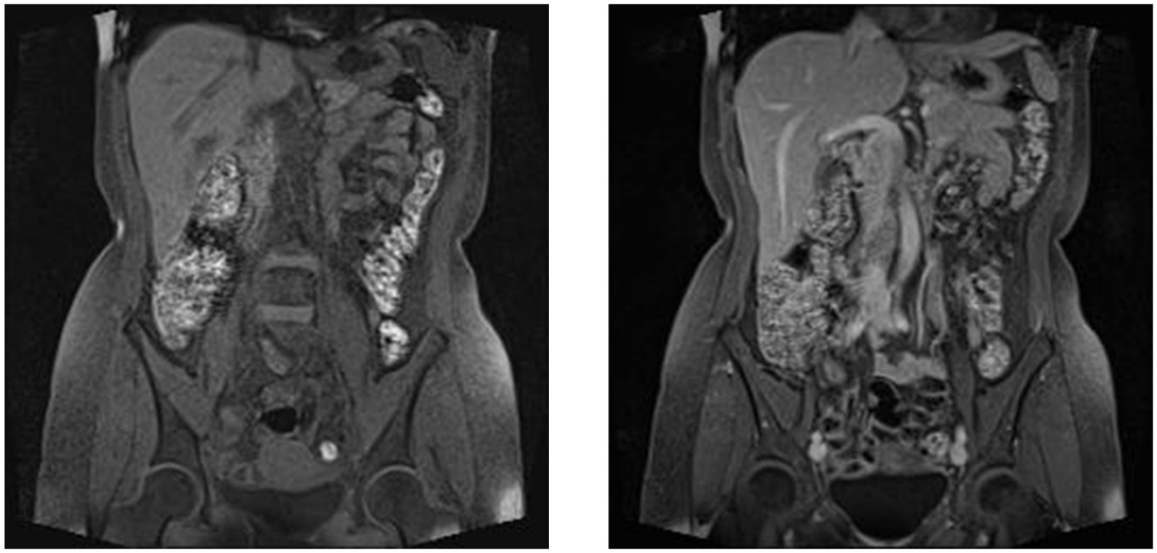


Figure 3.5: T1 weighted spoiled gradient echo images pre (left) and post (right) contrast

3.4.2 Two dimensional and three dimensional acquisition

MRI sequences can be acquired in 2-dimensional (2D) slices or as a 3-dimensional (3D) volume. When acquired as a 2D slice, a gradient is used to select a slice of tissue, the thickness of which is determined by the operator. Each pixel in the slice is encoded using frequency encoding in one axis and phase encoding in the second axis. A separate echo is required for each phase encoding step, but all the frequency encoded steps are acquired simultaneously. The time taken to acquire each slice is therefore dependent on the number of phase encoding steps. When all the information has been obtained from one slice, the next slice is selected by the slice selection gradient leaving a small gap between each slice.

For 3D acquisition, a complete volume of tissue is imaged. Voxels can be kept isotropic, so that they are the same size in each dimension, and no gaps need to be left in the imaged volume. This means that the volume can subsequently be reconstructed with slices in any plane without loss of image quality. In order to acquire information about the tissue volume, each voxel is encoded by frequency encoding in one plane and phase encoding in two further planes. This means that the

time taken to acquire data from a volume of tissue is dependent on the phase encoding steps for two planes.

Initially, we had anticipated that it would be preferable to obtain 3D scans, which would allow us to obtain a single scan of the tumour volume for each sequence and then reconstruct it in all the desired planes. However, 3D volume acquisitions were considerably more degraded by motion artefact than 2D sequences. Examples are shown in Figure 3.6 and Figure 3.7.

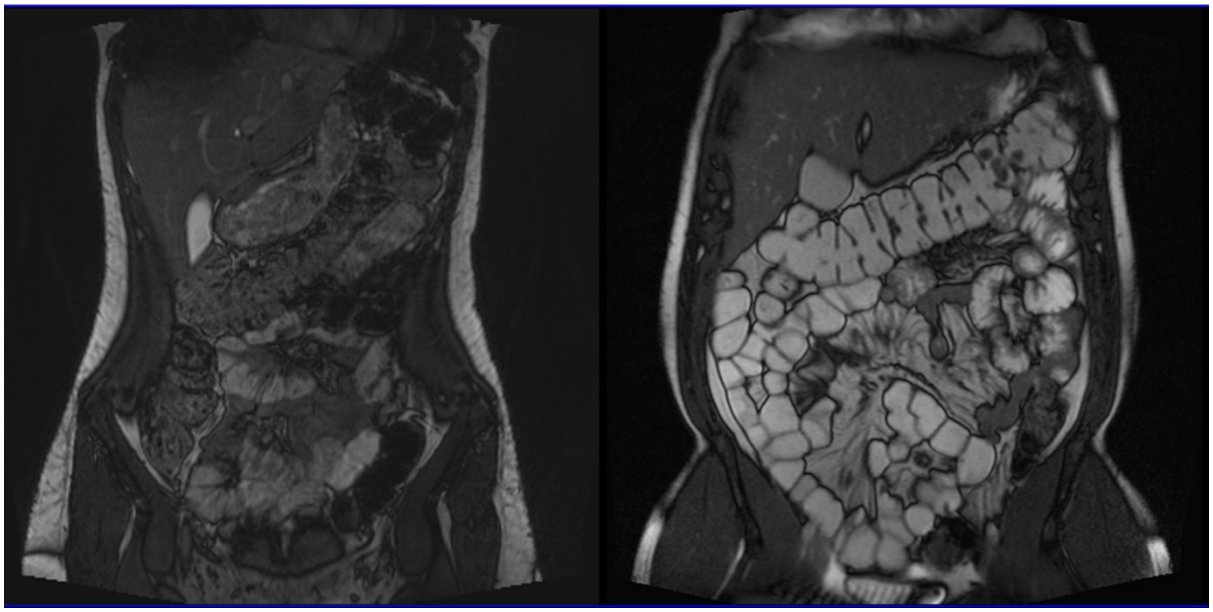


Figure 3.6: 3D (left) and 2D (right) balanced steady state gradient echo sequences

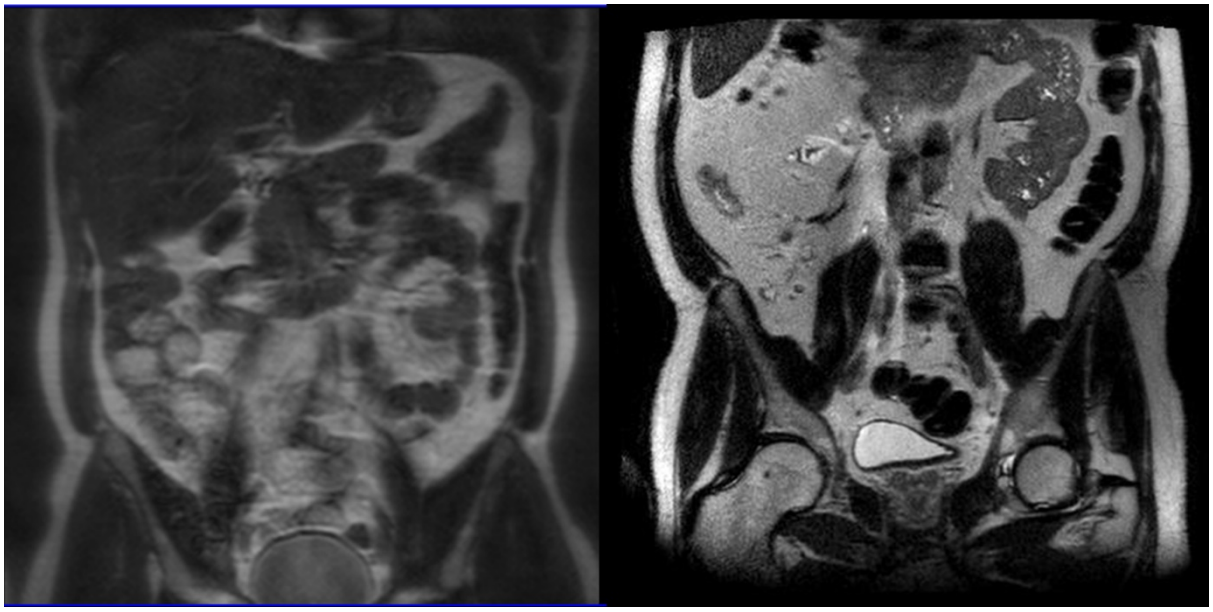


Figure 3.7: 3D (left) and 2D (right) fast spin echo sequence

We therefore elected to use 2D imaging for all sequences except the T1 weighted spoiled gradient echo sequence, where we felt that the very rapid image acquisition was sufficiently resistant to motion artefact to tolerate 3D imaging.

3.4.3 Patient positioning

Prone positioning in MR enterography may improve small bowel separation and limit motion artefact by providing abdominal compression (Cronin et al., 2008). The incidence of scan termination due to claustrophobia is also lower if patients are imaged in the prone position (Eshed et al., 2007). We therefore compared MRI imaging of the colon in the prone and supine positions. Example images are shown in Figure 3.8. We felt that there might be a small improvement in the degree of motion artefact when volunteers were imaged in the prone position. We therefore elected to image patients in the prone position in the colon cancer MRI study, unless they found this position uncomfortable and preferred to be imaged supine.

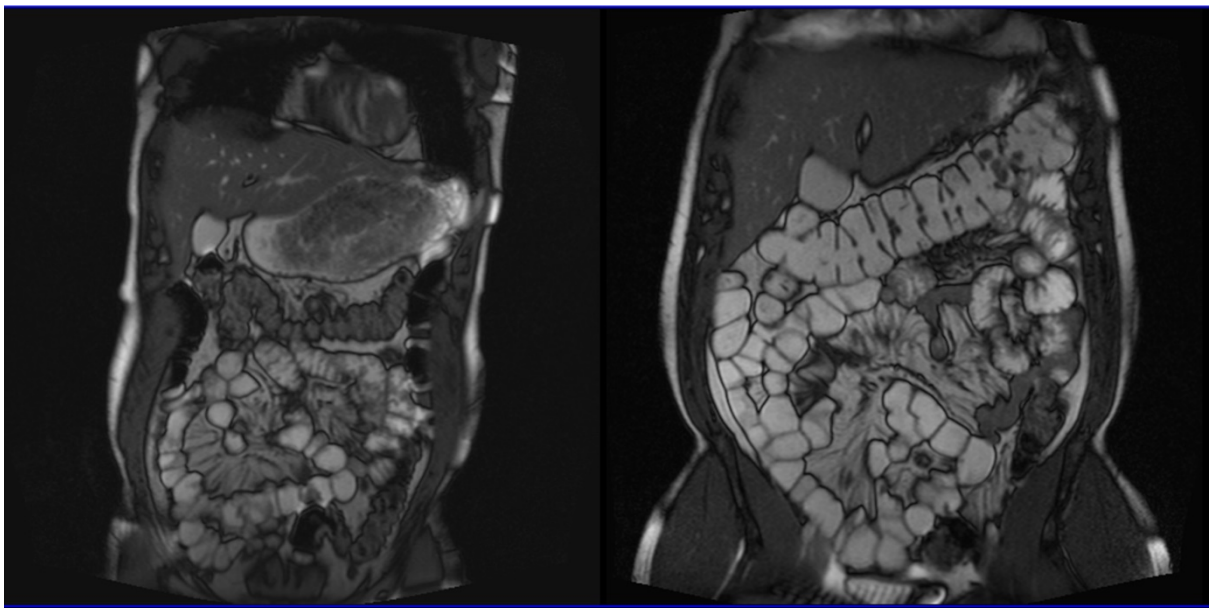


Figure 3.8: Balanced steady-state gradient echo images obtained in the supine (left) and prone (right) positions

3.4.4 Small bowel distension

The principle problems which we experienced in obtaining high quality MRI images of the colon were due to either motion artefacts or off resonance artefacts at interfaces between air, tissue, fluid, and fat. Gourtsoyiannis has suggested that distension of the small bowel with an iso-osmotic fluid which is not absorbed from the bowel lumen can reduce small bowel peristalsis (Gourtsoyiannis et al., 2002). We therefore hypothesised that filling the small bowel with fluid might help to reduce that portion of motion artefact related to small bowel peristalsis, reduce off resonance artefacts, and therefore increase the quality of abdominal MR images.

To investigate this, we performed a number of scans in volunteers with no oral preparations, following 1L of water, following 1L of Poly-Ethylene Glycol 3350 solution (PEG solution, available commercially as Klean Prep, Helsinn Healthcare S.A., Lugano, Switzerland), or 1L of 2.1% w/v barium sulphate and 3.2% w/v sorbitol (available commercially as E-Z-CAT, Bracco UK Ltd, High Wycombe, United Kingdom). Example images are shown in Figure 3.9.

Oral preparation with 1L of E-Z-CAT demonstrated the best small bowel distension, and we felt that this was associated with a small reduction in the amount of image degradation due to motion artefact. It did not have any noticeable effect on the off resonance artefacts. We therefore decided to use 1L of oral E-Z-CAT, imbibed 45 minutes before the MRI scan, for patients in the colon cancer MRI study.

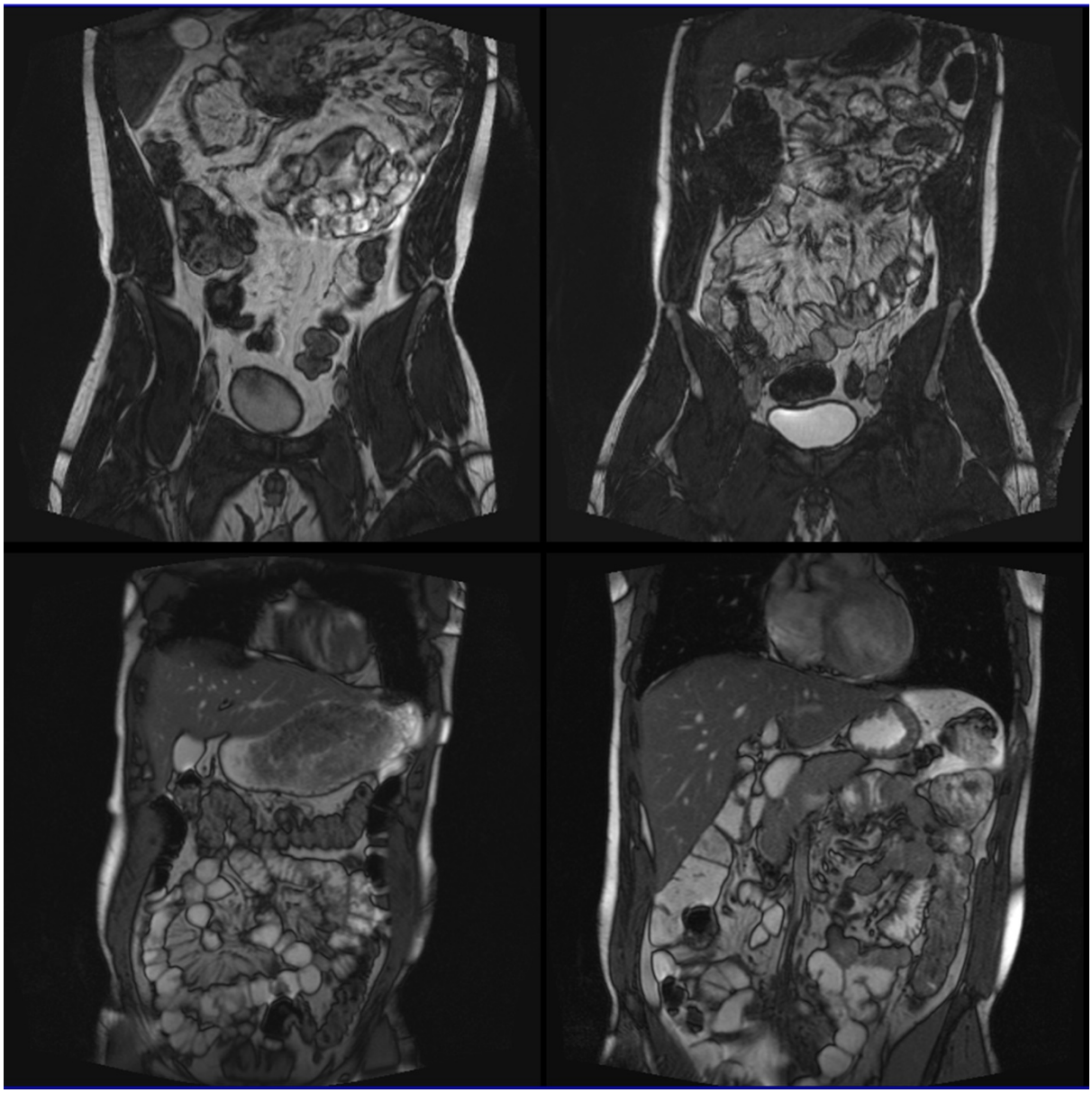


Figure 3.9: Balanced steady-state gradient echo images with no oral prep (top left), 1L of water (top left), 1L of Klean-prep (bottom left) and 1L of E-Z-CAT (bottom right)

3.4.5 Respiratory triggering

MRI sequences which can be acquired in less than around thirty seconds can be achieved comfortably in a single breath hold for most subjects. These include the BSSE, SS-FSE and T1-SGE sequences. However, RARE sequences take several minutes to acquire and so need an alternative strategy to overcome respiratory motion artefacts. This is usually achieved using respiratory

triggering; each pulse sequence for a phase encoding step is started at the same point in the respiratory cycle, so that the repetition time becomes the interval between successive breaths (around 4 seconds). Other strategies include multiple breath holds, continuous acquisition with a high number of averages, and respiratory ordered phase encoding (ROPE). Each of these strategies was tested. Multiple breath holds tended to cause problems with miss-registration of adjacent slices between breath holds, due to breath holding at different points in the respiratory cycle for different parts of the scan. Taking multiple averages for each pixel tended to lead to excessive blurring in parts of the image with a large amount of motion due to respiration. ROPE is a technique where the data from the phase encoding steps (the slow part of image acquisition vulnerable to motion artefact), rather than being taken sequentially from each slice, are taken from the same slice at the same time in the respiratory cycle on successive breaths, but in the intervening period taken from different slices at different parts of the respiratory cycle, and reconstructed at the end (Bailes et al., 1985). Unfortunately this technique still produced significant motion artefacts and was not helpful in our test scans.

Respiratory triggering can be achieved mechanically (where a bellows placed around the chest measures the respiratory cycle) or using a navigator echo trigger. The navigator echo is a continuous

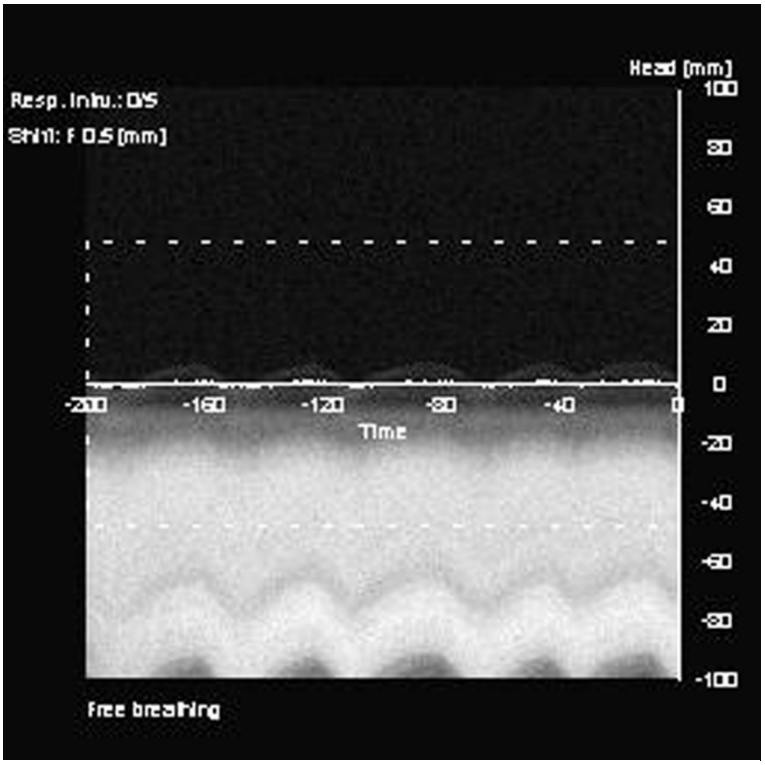


Figure 3.10: Navigator echo

real time 2D MRI which measures the movement of the diaphragm. The MRI scanner is set to trigger at a set point in the respiratory cycle. An example of a navigator echo is shown in Figure 3.10. We found navigator echo triggering to be more reliable than mechanical triggering, and so this was used in the colon cancer MRI study.

3.5 Summary

During this MRI protocol development phase, we performed seventy-three scans in four healthy volunteers. There was considerable improvement in the quality of the abdominal MRI images over the course of the protocol development. The intervention which made the greatest difference was reverting to 2D sequences for the T2 weighted images from the more recently introduced 3D sequences. This resulted in a definite reduction in motion artefact.

A number of other interventions, including parallel imaging, the use buscopan, prone subject positioning, and small bowel distension with oral E-Z-CAT, appeared to result in a small improvement in scan quality. These were carried through to the colon cancer MRI study if they were adequately tolerated by patients.

It remained difficult to be certain of the optimal pulse sequence for imaging colon cancer based on these scans performed in healthy volunteers. BSGE sequences were very resistant to motion artefact and provided good tissue contrast, but were limited by susceptibility artefacts producing a black line around the bowel. T1-SGE sequences were also resistant to motion artefact but had lower soft tissue contrast. RARE sequences had excellent soft tissue contrast and signal to noise ratio, but were vulnerable to motion artefact particularly if there were problems with respiratory triggering. SS-FSE sequences had good soft tissue contrast and were more resistant to motion artefact but had a lower signal to noise ratio.

We therefore planned to use a combination of pulse sequences in the colon cancer MRI study to try and combine the benefits of each. A breath hold BSGE sequence was taken through the whole

abdomen initially to locate the tumour. This was used to plan high resolution RARE sequences perpendicular to the long axis of the tumour. If tolerated we obtained these images in complimentary planes. SS-FSE sequences were used in place of the RARE sequences if respiratory triggering was inadequate or motion artefact degraded image quality too severely. Finally, gadolinium enhanced 3D T1-FFE sequences were taken through the abdomen which allowed multiplanar reconstruction of the abdomen.

Diffusion weighted imaging was also acquired in the colon cancer MRI study. This was not tested in the volunteer section, as the volunteers did not have any areas of restricted diffusion to image. It was instead adopted from an established protocol for imaging liver metastases.

CHAPTER 4

Comparison of the diagnostic accuracy of MRI with CT in staging colonic cancer

4.1 My role in this chapter

With the support of my supervisor, I designed and wrote the protocol for this study, obtained funding and ethical approval, recruited all the patients for the study, performed the data collection and data analysis, and wrote this chapter. I was the first author for the publication arising from it (Hunter et al., 2016). Suzanne St Rose provided statistical support during the trial design and Tom Fanshawe reviewed the statistical analysis following the write up of the trial.

4.2 Introduction and rationale

The principle aim of pre-operative staging in colon cancer has historically been to identify patients with extensive metastatic disease who would not benefit form primary surgery. Developments in the treatment pathways for patients with colon cancer have made it increasingly important to provide patients with accurate pre-operative local staging. The FOXTROT trial is currently recruiting patients with the aim of investigating whether neoadjuvant chemotherapy improves patient outcome in operable colon cancer. Encouraging results were obtained in the pilot phase of the trial (Foxtrot Collaborative, 2012b) and similarly encouraging results have been obtained in other small studies of neoadjuvant chemotherapy (Arredondo et al., 2013). This requires patients to be accurately stratified into high and low-risk groups on the basis of their local staging prior to commencing treatment, to identify patients who might benefit from neoadjuvant therapy.

The range of surgical treatment options has also increased over time, particularly following the introduction of minimally invasive techniques. These may not be suitable for patients with locally advanced tumours who may need more radical surgery. Patients with T4 disease have a high incidence of conversion from laparoscopic to open surgery, which led the Colon carcinoma laparoscopic or open resection (COLOR) trial report to recommend that patients considered for a minimally invasive approach undergo pre-operative assessment with CT to identify patients wih locally advanced disease who are not suitable for a laparoscopic approach (Buunen et al., 2009).

Although CT is currently used to assess the local stage of colon cancers, the accuracy of local staging in colon cancer falls short of that achieved using MRI in rectal cancer. Although small trials of endoscopic ultrasound have suggested that it may be more accurate than CT in the local staging of colon cancer (Gall et al., 2014), it has not been widely adopted possibly due to a paucity of expertise in performing the procedure or possible due to the invasive nature of the test. MRI offers cross-sectional imaging in any plane, does not pose any risk in terms of radiation dose, and has excellent tissue contrast resolution in soft tissues, is widely available and is non-invasive. In chapter 2 I have also demonstrated that MRI can identify patients with a six fold increased risk of synchronous metastatic disease by identifying adverse features on local staging in rectal cancer.

As discussed in chapter 3, a number of technical problems complicate MRI imaging of the abdomen, and have previously degraded image quality. As a result of these problems, studies investigating MRI staging of colon cancer prior to 2003 demonstrated only moderate accuracy in T and N staging(Low et al., 2003, Lomas et al., 2001).

The development of Magnetic Resonance Colonography (MRC) and Magnetic Resonance Enterography (MRE), have demonstrated that it is possible to overcome some of these technical problems to obtain high quality images of the bowel using MRI. Saar identified 100% of polyps over 5mm with excellent diagnostic quality in 94% with a 3D- FLASH sequence and 92% with a 3D-VIBE sequence(Saar et al., 2008). Wong used half-Fourier single shot turbo spin echo (HASTE) axial, coronal, and three dimensional fat suppressed gradient echo sequence (VIBE) coronal images to identify 100% of obstructing tumours(Wong et al., 2007). In chapter 3, we used some of these techniques in healthy volunteers to develop an MRI protocol for imaging bowel cancer which we hope will allow us to obtain high quality images for the local staging of colon cancer using MRI.

Over the last few years, 3.0 Tesla (T) MRI scanners have increasingly become available for routine clinical use. 3.0T MRI offers a theoretical doubling of signal to noise ratio (SNR) over previous 1.5T systems, which can be traded for a shorter acquisition time or higher spatial resolution, maintaining

SNR at the same level. This means that it may be possible to obtain higher quality abdominal MRI scans using 3T MRI scanners than is possible using 1.5T MRI scanners.

The aim of this study is therefore to perform preoperative staging 1.5T MRI scans and 3T MRI scans on patients undergoing resection of their primary colon cancer, and to compare the accuracy of staging on these scans and routine preoperative CT scans using histology as the gold standard.

4.3 Materials and Methods

4.3.1 Subjects

This was a prospective study of diagnostic accuracy, comparing the 1.5T MRI, 3T MRI and CT using histological assessment as the gold standard. Data was collected prospectively. The study was designed according to the Standards for the Reporting of Diagnostic accuracy studies (STARD) guidelines (Bossuyt et al., 2003).

I applied for and obtained ethical approval from the National Research Ethics Service, The Royal Marsden Research Ethics Committee, before commencing recruitment (REC reference number 10/H0801/21). The study was conducted in accordance with the conditions of ethical approval. Local R&D approval was obtained at each site (The Royal Marsden Hospital, Croydon University Hospital and Epsom and St Heliers University Hospitals). All patients provided written informed consent prior to recruitment.

I also applied for and obtained two research bursaries to support this research; from the Bowel Disease Research Foundation and from the Mayday University Hospital research fund. Funding for the 3T MRI scans was also provided by the National Institute for Health Research Biomedical Research Centre at the Royal Marsden National Health Service Foundation Trust, which I did not apply for.

Consecutive patients presenting with adenocarcinoma of the colon to Croydon University Hospital, The Royal Marsden Hospital or Epsom and St Helier Hospitals who were undergoing primary surgery to excise their colon cancer, were included in the study. Patients were considered eligible if they had a biopsy-confirmed adenocarcinoma of the colon (arising 15 cm or more from the anal verge on colonoscopy), were over the age of 18 years and were planned for resection of their primary tumour. Patients were excluded if they withheld or withdrew consent, were under the age of 18, were scheduled to receive neoadjuvant therapy for their colon cancer, or were not fit to undergo a potentially curative resection of their tumour. They were also excluded if they had a contraindication to MRI scanning, the or to the administration of gadolinium or small bowel contrast agent.

Patients were withdrawn from the study if metastatic disease was identified on their preoperative MRI scan which required neoadjuvant treatment, were unable to tolerate MRI scanning or were unable to undergo resection of their primary tumour. This included patients in whom MRI identified metastatic disease resulting in a change of treatment plan to include neoadjuvant chemotherapy.

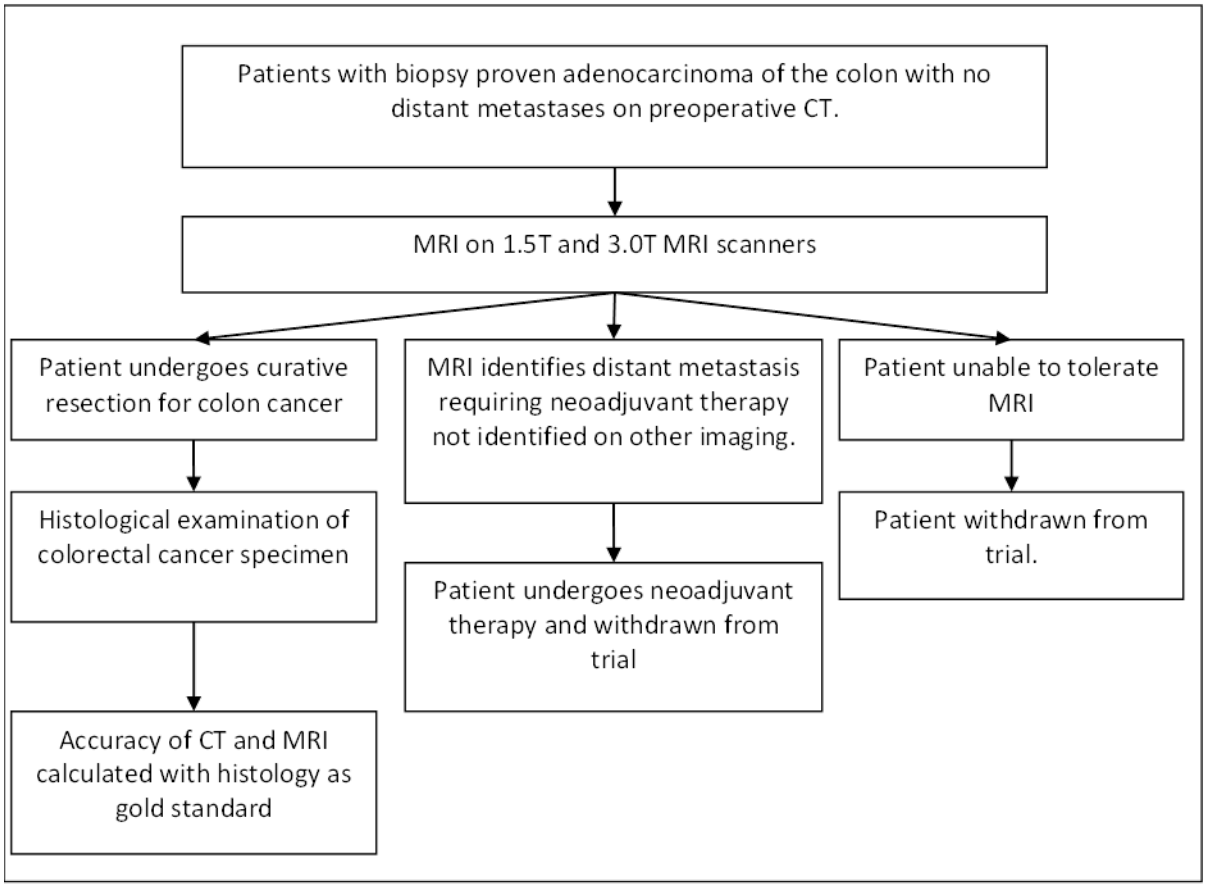


Figure 4.1: Colon MRI study flow diagram

4.3.2 Procedures

Patients enrolled in the study underwent two preoperative MRI scans of their abdomen and pelvis, in addition to their standard preoperative CT scan. One of these was performed on a 1.5T MRI scanner (Magnetom Avanto 1.5T, Siemens Medical Solutions, Erlangen, Germany). Patients recruited from the Royal Marsden Hospital site or the Epsom and St Helier Hospitals site had their 1.5T MRI scan performed at the Royal Marsden Hospital, Sutton. Patients recruited at Croydon University Hospital had their 1.5T MRI scan performed at Croydon University Hospital, Croydon. The 1.5T MRI scanners were the same at both sites (Magnetom Avanto 1.5T, Siemens Medical Solutions, Erlangen, Germany). The second MRI scan was performed on a 3.0T MRI scanner (Achieva 3.0T,

Philips Healthcare, Best, Netherlands). 3T MRI scans were performed on the same scanner at the Royal Marsden Hospital, Sutton, for all patients.

Patients were scanned in the prone position where tolerated, using a phased-array body coil. The prone position exerts a mild uniform pressure on the abdominal wall, which reduces intra-abdominal volume (Cronin et al., 2008). Scanning in the prone position is also associated with fewer scan terminations due to claustrophobia (Eshed et al., 2007).

Bowel-cleansing preparation was not performed and rectal contrast were not administered as we felt that these procedures would limit patient acceptance. Patients fasted for 4 hours prior to MRI scanning. Thirty to forty-five minutes prior to the MRI scans, patients imbibed one litre of oral contrast media for small bowel distension; 225 ml 4.9% weight/volume barium sulfate diluted in water to 1 litre (E-Z-CAT, Bracco UK Ltd, High Wycombe, United Kingdom). Intraluminal contrast helps to separate small bowel loops, and has been demonstrated to be helpful in imaging other extrahepatic abdominal malignancies (Low, 2005, Low, 2007). Twenty milligrams of intramuscular hyoscine butylbromide (Buscopan Ingelheim Limited, Bracknell, UK) was administered just before commencement of imaging, to reduce bowel motility.

A breath hold Fully Rewound Gradient Echo sequence (FRGE) coronal scout scan was taken to identify the tumour and select the target volume. This was a True Fast Imaging with Steady-state Precession (True-FISP) sequence on the Magnetom Avanto 1.5T and a Balanced Turbo Field Echo (BTFE) sequence on the Achieva 3.0T. A respiratory triggered Rapid Acquisition with Relaxation Enhancement (RARE) sequence was then acquired perpendicular to the bowel wall through the tumour. This was a Turbo Spin Echo (TSE) sequence on the Magnetom Avanto 1.5T and a Fast Spin Echo (FSE) sequence on the Achieva 3.0T. This sequence was usually acquired in the transaxial plane for ascending and descending colon tumours and in the sagittal plane for transverse colon tumours.

Where scan time and patient comfort permitted, further TSE sequences were acquired in one or two complimentary planes. In cases where adequate respiratory triggering could not be achieved, which

only occurred on the 1.5T MRI scans, breath-hold half-Fourier acquisition single-shot turbo spin-echo (HASTE) sequences were acquired instead of the TSE sequences.

Following the administration of IV gadolinium, dynamically enhanced fat suppressed T1 weighted spoiled gradient echo (SGE) sequences were acquired. These were Fast Low-Angle Shot (FLASH) sequences on the Magnetom Avanto 1.5T and enhanced T1 High-Resolution Isotropic Volume Excitation (eTHRIVE) sequences on the Achieva 3.0T. Where possible due to tumour location, the liver was also be imaged at this time to look for liver metastases. Transaxial diffusion-weighted imaging (DWI) sequences were obtained through the tumour volume.

For the 1.5T FRGE scans the field of view was 400x400mm, the in plane resolution was 0.78x0.78mm with a matrix size of 512x512 pixels. Slice thickness was 4mm. TR was 3.57ms to 4.09ms, and TE was 1.51 to 1.77ms.

For the 3T FRGE scans the field of view was 400x400mm, the in plane resolution was 1.39x1.39mm, and the matrix size was 288x288 pixels. Slice thickness was 3mm. TR was 4.57ms to 4.86ms, and TE was 2.29ms to 2.40ms.

For the 1.5T TSE sequences, the field of view ranged from 170x170mm to 420x420mm. This was dependent on tumour location, imaging plane and patient size. The voxel size was maintained with an in-plane resolution of between 0.66x0.66mm to 1.3x1.3mm by varying the matrix size from 256x256 pixels to 320x320 pixels. Slice thickness was 3mm. TR ranged from 3750ms to 5469ms due to respiratory triggering, and TE was 100ms.

For the 3T FSE sequences, the field of view ranged from 250x250mm to 420x420mm. Voxel size (in-plane) was 0.47x0.47mm 1.01x1.01mm, with the matrix size varying from 256x256 pixels to 640x640 pixels. Slice thickness was 2mm. TR ranged from 818ms to 2049ms, and TE was 80ms.

For the 1.5T HASTE sequences (where acquired), the field of view ranged from 275x309mm to 380x400mm. Voxel size (in-plane) was 1.25x1.25mm to 1.56x1.56mm, with a matrix size of 220x256

pixels to 240x256 pixels. Slice thickness was 3mm. TR ranged from 1000ms to 1500ms, with a TE of 89ms to 94ms.

For the 1.5T gadolinium enhanced T1 weighted SGE sequences, spectral attenuated inversion recovery (SPAIR) fat suppression was employed. The field of view was 400x400mm, with an in-plane resolution of 1.56x1.56mm and a matrix size of 256x256 pixels. Slice thickness was 2mm. TR was 3.25 to 3.92ms and TE was 1.16 to 1.65ms, with a flip angle of 12 degrees.

For the 3T gadolinium enhanced T1 weighted SGE sequences, SPAIR fat suppression was also used. The field of view was 397x397mm, with an in-plane resolution of 1.38x1.38mm and a matrix size of 288x288 pixels. Slice thickness was 3mm. TR was 2.95ms to 3.03ms and TE was 1.34ms to 1.43ms. The flip angle was 10 degrees.

For both 1.5T and 3T gadolinium enhanced scans, images were acquired 0, 30, 60, 90 and 120 seconds after the administration of intravenous gadolinium contrast.

DWI on the 1.5T MRI scans was acquired using a single shot spin echo sequence with echo-planar imaging (EPI) and SPAIR fat suppression. Repetition time was 4800 ms and echo time was 68 ms. Four b-values were used: 0, 100, 500 and 750 s mm^{-2}.

DWI on the 3T MRI scans was also acquired with single shot spin echo sequence with EPI, and with combined SPAIR and slice selective gradient reversal (SSGR) fat suppression. TR was 3798ms and TE was 51ms. The same b-values were used (0, 100, 500 and 750 s mm^{-2}).

The imaging time for each sequence was 4 to 8 minutes, with a total imaging time of 30 to 45 minutes. Sequence parameters are summarised in Table 4.1.

The preoperative CT scans used in the trial were the standard staging CT scans obtained for clinical assessment for each patient at each of the participating institutions. There was therefore some variation in the CT scanner and the exact scan sequence utilised between patients. The CT scans were performed on one of two scanners: Siemens SOMATON Sensation 16 (Siemens Healthcare,

Erlangen, Germany) or GE LightSpeed VCT (GE Healthcare, Buckinghamshire, UK). Imaging was performed with intravenous contrast in the portal venous phase. Images were reconstructed with a slice thickness of 2mm or 5mm and an in plane voxel size of 0.61x0.61mm to 0.85x0.85mm. Multiplanar reformatting was available.

Scan sequence	FOV (mm)	Resolution (mm^2)	Matrix (pixels)	ST (mm)	TR (ms)	TE (ms)	FA (degrees)
1.5T FRGE	400x400	0.78	512x512	4	3.57-4.09	1.51-1.77	
3T FRGE	400x400	1.39	288x288	3	4.57-4.86	2.29-2.40	
1.5T TSE	170x170 to 420x420	0.66-1.3	256x256 to 320x320	3	3750-5469	100	
3T FSE	250x250 to 420x420	0.47-1.01	256x256 to 640x640	2	818-2049	80	
1.5T HASTE	275x309 to 380x400	1.25-1.56	220x256 to 240x256	3	1000 to 1500	89-94	
1.5T T1 SGE	400x400	1.56	256x256	2	3.25-3.92	1.16-1.65	12
3T T1 SGE	397x397	1.38	288x288	3	2.95-3.03	1.34-1.43	10
1.5T DWI	308x378	1.48	208x256	6	4800	68	
3T DWI	375x375	1.46	256x256	5	3798	51	

FOV – Field of view, ST – slice thickness, TR – repetition time, TE – Echo time, FA – flip angle, FRGE – Fully rewound gradient echo, TSE – Turbo spin echo, FSE – Fast spin echo, HASTE – Half-Fourier acquisition single-shot turbo spin-echo, SGE – spoiled gradient echo, DWI – diffusion weighted imaging

Table 4.1: MRI sequence parameters

4.3.3 Evaluation

Each CT, 1.5T MRI scan and 3.0T MRI scan was reported independently by each of two consultant gastrointestinal radiologists, with 10 - 15 years' experience of reporting GI cancers on CT and MRI. Scans were reported using a standard case record form. Reporting radiologists were informed of the tumour location on colonoscopy, but were blind to the results of other investigations. For the assessment of CT, 1.5T MRI and 3.0T MRI, the reporting radiologist had access to all sequences acquired in that scanning session (as is normal clinical practice). All imaging studies were reported using a standard form. Each observer reported each imaging study on a separate occasion more than 4 weeks apart. The order in which the studies were reported (CT, 1.5T MRI and 3T MRI) was randomised for each patient. Histological assessment was performed by a consultant histopathologist with 15-20 years' experience of reporting colon cancer. The histopathologist was blind to the results of the imaging investigations.

The following clinical features were reported: T-stage, depth of extramural tumour invasion, N-stage, presence of EMVI, and any distant metastases.

T1 tumours were classified as invasive tumours limited to the submucosa. These tumours were identified on MRI by replacement of the normally high signal in the submucosal layer by an abnormal intermediate signal which did not extend into the circular muscle layer. These tumours were identified on CT by projection of a colonic lesion without any visible distortion of the bowel wall layers. T2 tumours extend through the submucosa but are limited to the muscularis propria. These tumours were identified on MRI by abnormal intermediate signal intensity (higher than normal muscle signal, lower than normal submucosal signal) extending into the muscularis propria or replacing the muscularis propria but not extending into the peri-colonic fat. These tumours were identified on CT by asymmetrical thickening of the colon wall projecting intraluminally with preservation of smooth muscle coat and clear adjacent pericolonic fat. T3 tumours invade through the muscularis propria into the subserosa or peri-colonic fat but do not invade the serosa or

adjacent organs. These tumours were identified on MRI by a broad based bulge or nodular projection of intermediate tumour intensity projecting beyond the outer muscle coat, and on CT by smooth or nodular extension of a discrete mass of tumour tissue beyond the contour of the bowel wall with extension into pericolic fat. T3 tumours were further classified depending on the depth of extramural tumour invasion measured in millimetres; T3a - 1mm or less extramural invasion, T3b – more than 1mm to 5mm extramural invasion, T3c – more than 5mm to 15mm extramural invasion, T3d more than 15mm extramural invasion. T4 tumours include those that invade the serosa or adjacent organs. These were identified on MRI by extension of the intermediate tumour signal into adjacent organs or through the peritoneal surface, and on CT by presence of nodular penetration of the tumour through the peritonealised areas of the muscle coat or an advancing edge of the tumour penetrating adjacent organs. The MRI criteria were adapted from those used in the evaluation of rectal cancer (Taylor et al., 2008), and the CT criteria were adopted from established criteria for the interpretation of CT images of colon cancer (Dighe et al., 2008).

Lymph nodes were assessed on MRI based on their border and homogeneity of signal intensity, which has been shown to have greater specificity for the identification of metastatic lymph nodes in rectal cancer than the use of size criteria alone. (Kim et al., 2004, Brown et al., 2003). Lymph nodes were considered to be involved if they had an irregular border or inhomogeneous signal intensity. This was assessed on the T2 weighted TSE imaging, or the T2 weighted HASTE images where the TSE images were inadequate. On CT, any nodal mass larger than 1 cm or a group of three or more nodes were considered metastatic, as these are the established criteria for assessing lymph node involvement on CT and signal inhomogeneity is not applicable (Dighe et al., 2008). Tumours with no involved nodes were recorded as N0, tumours with 1-3 involved nodes were registered as N1 and tumours with 4 or more involved lymph nodes were recorded as N2.

Extramural vascular invasion (EMVI) was identified on MRI by the intermediate signal intensity of the tumour growing into or along a vessel. Blood vessels were identified on T2-weigted MRI imaging by a linear signal void in continuity on adjacent slices (Smith et al., 2008b). EMVI was identified on CT

irregular expansion of peritumoral veins (Dighe et al., 2010a). EMVI was reported as small, medium, or large vessel EMVI on MRI. Any size of EMVI identified on MRI was considered positive for comparison with histopathology, as EMVI is reported as positive or negative on histopathology.

4.3.4 Statistical analysis

Sample size:

The sample size calculation was performed by Suzanne St.Rose, statistician, The Royal Marsden Hospital NHS Foundation Trust. Sample size was based on the primary end point, which was comparison of the accuracy of 1.5T MRI and CT in identifying T3 or greater disease using histology as the gold standard. Here, we anticipated an accuracy of 0.70 and 0.90 for CT and MRI, respectively. Since MRI and CT will be performed for each patient, a paired design was used for determining sample size, with a two-tailed alternative hypothesis. Given a significance level, α, of 5% and a power of 80%, the minimum number of patients required was 62 patients.

I have subsequently repeated the power calculation myself, and this would appear be a power calculation for a Pearson's Chi-squared test (suitable for an unpaired design). The power calculation for a McNemar test (paired design) requires approximately 65 patients.

This power calculation also fails to take into account the proportion of patients withdrawing from the trial, which is typically around 10% in clinical trials. This trial should therefore have aimed to recruit approximately 72 patients.

End points:

The primary end point was the accuracy of 1.5T MRI, 3T MRI and CT in differentiating T1/T2 tumours from T3/T4 tumours, using histology as the gold standard, on a per patient basis. This distinction between T2 or less and T3 or greater tumours is the entry criteria for recruitment into the FOXTROT study of neoadjuvant chemotherapy in colon cancer for younger patients in good general health

(FOXTROT Collaborative, 2012a), and is the most commonly reported endpoint for the assessment of T-staging accuracy.

The following secondary end points were also recorded:

Nodal involvement, reported as not involved (N0) or involved (N1 or N2). This is a clinically significant endpoint, as patients with pathological nodal involvement (stage III disease) demonstrate the most benefit from adjuvant chemotherapy in clinical trials (Andre et al., 2009, Gill et al., 2003).

EMVI, reported none, small, medium or large. This feature is increasing recognised as being prognostically significant; patients with MRI-detected EMVI in rectosigmoid cancer have similarly poor 3-year recurrence free survival to those with pathologically detected EMVI (Smith et al., 2008a).

T-substage, with T-stage and depth of extramural invasion were grouped into good prognosis tumours (T1, T2, T3a tumours <=1mm extramural invsion or T3b <=5mm extramural invasion) and poor prognosis tumours (T3c <=15mm extramural invasion, T3d >15mm extramural spread or T4 tumours). Diagnosis with a poor prognosis tumour defined in this way is the entry criteria for the FOXTROT trial for older and less fit patients (FOXTROT Collaborative, 2012a). This distinction has been demonstrated to have greater prognostic significance than the distinction between T2 and T3 tumours both on pathology (Merkel et al., 2001) and to have comparable prognostic significance on CT evaluation of colon cancer as on histopathological examination (Smith et al., 2007).

The accuracy of stage-for-stage T-stage assessment is also reported. Sensitivity, specifity, PPV and NPV are not applicable for this end point. Description of T-stage and N-stage was based on the TNM (version 5) classification. Essential patient demographics were also recorded, including age, gender, tumour location and operative procedure.

Descriptive statistics:

Patient and tumour characteristics are reported using means and standard deviation (SD) for normally distributed variables, and medians with interquartile ranges for other continuous variables. Categorical variables are reported as a number of patients and percentage.

Measures of validity:

The accuracy (percentage of test results that are correct), sensitivity (percentage of true positives detected), specificity (percentage of true negatives detected), positive predictive value (percentage of positives which are true positives), negative predictive value (percentage of negatives which are true negatives) and associated 95% confidence intervals of MRI and CT were compared. Histology was used as the gold standard. Results for MRI performed on a 1.5 Tesla or 3.0 Tesla MRI scanners in assessing these end points were recorded separately. 95% confidence intervals for proportions were calculated using the Wilson method (Wilson, 1927). The statistical significance of the difference in accuracy between CT and 1.5T MRI, and between CT and 3T MRI, was assessed using McNemar's test.

Stage-for-stage accuracy is reported for each imaging modality and a comparison of the accuracy of CT, 1.5T MRI and 3.0T MRI was done as a matched analysis comparing the degree of discrepancy in individual patients, using the Wilcoxon signed rank test.

Extra-mural vascular invasion was reported on histopathology as either present or absent, but was reported for each imaging modality as an ordered categorical variable depending on the size of EMVI identified by the radiologist (None, Small, Medium and Large). Area Under the Curve (AUC) values and 95% confidence intervals (DeLong et al., 1988) are presented for each imaging modality and radiologist. Accuracy, sensitivity, specificity, PPV and NPV are reported for each imaging modality and radiologist with any size of EMVI reported on imaging considered positive.

Interobserver agreement for the two radiologists reporting CT and MRI is determined using Cohen's kappa (Cohen, 1960). The magnitude of the agreement is quantified as described by Landis and

Koch (Landis and Koch, 1977); a kappa of <0.2 denotes a slight agreement; 0.2 to 0.4, a fair agreement; 0.4 to 0.6, a moderate agreement; 0.6 to 0.8, a substantial agreement, and >0.8, an almost perfect agreement. Before assessing kappa, a McNemar's test is performed to assess whether there is test bias, as indicated by the proportion positive to each test differing.

The level of significance is set at $p < 0.05$. Analyses were performed using R 3.0.1 statistical software (R Core Team, 2015), including psych (Revelle, 2013), pROC (Robin et al., 2011) and epade (Schulz, 2013) packages.

All evaluable subjects are included in the analyses and note has been made of the number eligible patients not enrolled into the study from the lower GI MDT agenda lists.

4.4 Results

4.4.1 Recruitment

Recruitment commenced November 2010 and finished in November 2012. A total of 60 patients were recruited, from a total of 158 eligible patients (38%). Reasons for patients not being recruited are listed in Table 4.2.

Reason patient not recruited	Number of patients (%)
Did not consent	40 (40.8)
Withdrew consent	1 (1.0)
Unable to contact in time	35 (35.7)
Unable to arrange MRI scans	16 (16.3)
Other	6 (6.1)
Total	98 (100)

Table 4.2: Patient recruitment

There are a relatively high proportion of patients who could not be contacted in time to discuss the study or who for whom we were not able to arrange MRI scans. This is because, due to ethical concerns, patients had to have been discussed in the MDT, be planned for surgery and then told of their diagnosis and management plan before discussing the colon MRI study. Patients were then contacted by a member of the clinical team (usually a Colorectal Nurse Specialist) to ask them whether they were willing to be contacted about the colon MRI study. Patients were then contacted about the colon MRI study by the research fellow to explain the trial and given a patient information sheet. Patients wishing to proceed with the trial then had to have two MRI scans on separate days prior to their surgery date. The time taken for this process, and the short delay between MDT discussion and surgery, meant that for many patients it was either not possible for the research fellow to contact them in time to discuss the study and arrange the additional MRI scans prior to surgery.

Of the 60 patients recruited into the study, 5 patients (8.3%) were withdrawn from the study before the MRI scans and histopathological assessment of their colon cancer specimen could be made. The reasons for this are listed in Table 4.3.

Trial ID	Reason for withdrawal
2175	Failed to attend MRI appointments
4130	No tumour identified on histopathological assessment
5260	Did not undergo surgery – liver metastases on MRI requiring neoadjuvant treatment
5695	Did not undergo surgery – ovarian tumour on MRI imaging
8958	Did not undergo surgery – liver metastases on MRI requiring neoadjuvant treatment

Table 4.3: Reasons for withdrawal from trial

One patient (1.7%) had an unresectable tumour due to duodenal invasion identified at surgery (T4). This patient is included for analysis for T assessment of T-stage, but not for other endpoints. Two

patients (3.3%) only underwent 1.5T MRI scans, and did not complete the 3.0T MRI scan. These patients are included for analysis in the assessment of accuracy of 1.5T MRI.

Figure 4.2 summarises patients recruited to the colon MRI study.

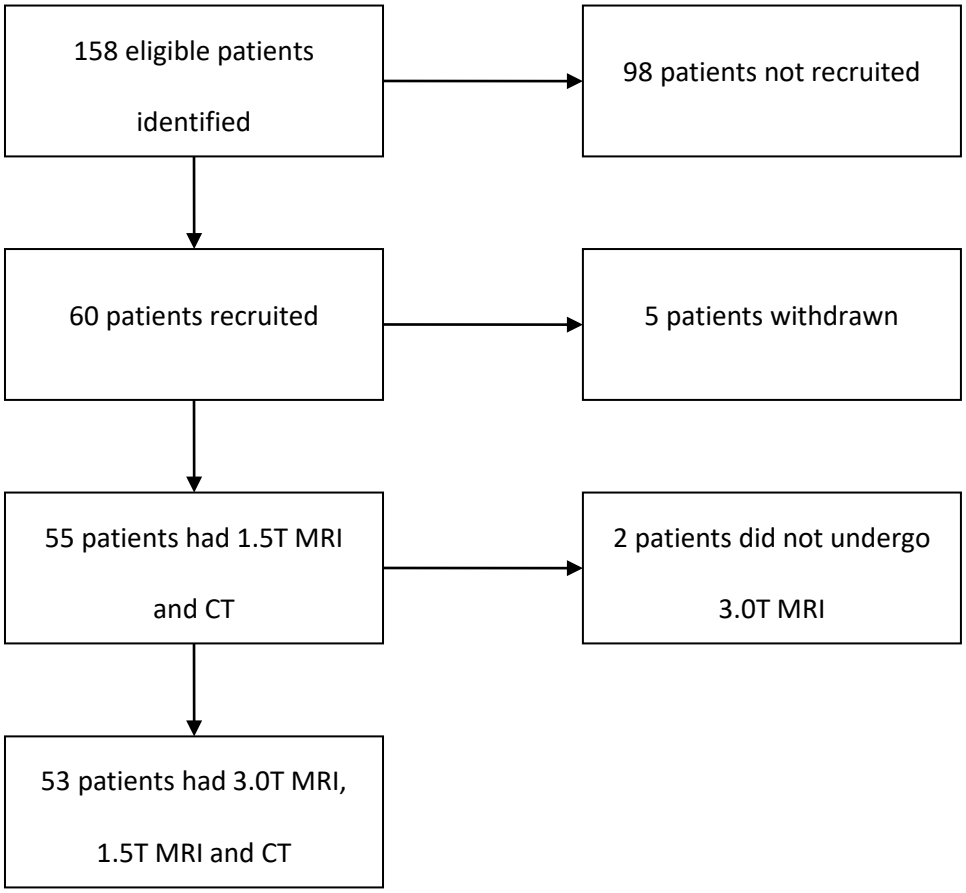


Figure 4.2: Patient recruitment flow diagram

Fifty-five patients are therefore included in the final analysis, with fity-three patients having 3.0T MRI available for analysis.

4.4.2 Patient demographics

Age:

The mean age of patients included for analysis in the colon MRI trial is shown in Table 4.4, together with suitable patients for the colon MRI trial who were either not recruited or withdrawn. There is no significant difference in the mean age of patients recruited into the trail compared to those not recruited into the trial (p=0.22, Welch two sample t-test), and this is a fairly typical age distribution for patients undergoing treatment for colon cancer in our population.

Gender:

65.5% of patients recruited to the study were male, compared to 48.5% of patients not recruited to the study or withdrawn from the study. These results are shown in Table 4.4. Although rectal cancer is more common in male patients, the sex distribution for colon cancer is fairly even (Ponz de Leon and Roncucci, 2000), and one would have expected proportion of male patients recruited to the trial to be approximately 50% as it is in non-recruited/withdrawn group. The difference in proportion of male patients between the recruited patient and the non-recruited patients just statistically significant using Fisher's exact test for count data (p=0.046). All eligible patients were invited to take part in the study if they could be contacted, so this may represent random variation, or there may have been a slight selection bias in those agreeing to take part in the study. All participants in the trial received the control test (staging CT) and so we would not expect any selection bias to have affected the outcome of the study. However, it is possible that this could affect generalizability of the study.

	Recruited patients	Not recruited/withdrawn patients	p-value
Mean age, years (SD)	69.7 (13.6)	72.36 (11.7)	0.22†
Gender			0.046‡
Male	36 (65.5%)	50 (48.5%)	
Female	19 (34.5%)	53 (51.5%)	
Tumour location			
Caecum	8 (14.5%)		
Ascending colon	14 (25.5%)		
Hepatic flexure	5 (9.1%)		
Transverse colon	6 (10.9%)		
Splenic flexure	0 (0%)		
Descending colon	4 (7.3%)		
Sigmoid colon	18 (32.7%)		
Procedure			
Right hemicolectomy	32 (58.2%)		
Subtotal colectomy	1 (1.8%)		
Left hemicolectomy	3 (5.5%)		
Sigmoid colectomy	4 (7.3%)		
Anterior resection	14 (25.5%)		
End stoma only	1 (1.8%)		
Pathological T-stage			
T1	2 (3.6%)		
T2	10 (18.2%)		
T3	28 (50.9%)		
T4	15 (27.3%)		
Pathological N-stage			
N0	31 (56.4%)		
N1	19 (34.5%)		
N2	4 (7.3%)		
Unknown	1 (1.8%)		

†Welch two sample t-test, ‡Fisher's exact test

Table 4.4: Patient demographic details

Tumour Location:

The majority of patients recruited to the trial had right colon cancer (caecal, ascending or hepatic flexure, 49.1% of patients) or sigmoid colon cancer (32.7% of patients). This is in keeping with large series which report approximately 50% of cancers occurring in the right colon and approximately 30% of colon cancers occurring in the sigmoid colon (Wray et al., 2009). The location of tumours for patients recruited to the study is shown in Table 4.4.

Operative procedure:

The operative procedure performed for patients recruited to the trial is listed in Table 4.4.

This reflects the tumour location for the patients recruited to the study. The eighteen sigmoid colon cancers were resected with either a high anterior resection (14) or sigmoid colectomy (4). The right colonic tumours and transverse colon tumours were treated by a right hemicolectomy or extended right hemicolectomy (32), except for one patient with extensive polyps who underwent a subtotal colectomy. The patients with descending colon tumours had a left hemi-colectomy performed, except in the case of one patient who had an unresectable tumour who had an end stoma formed.

Pathological T-stage:

The majority (50.9%) of patients included in the trial had T3 colonic tumours on their final pathological T-stage. The final pathological T-stage is summarised in Table 4.4

These results are broadly in keeping with the T-stage at presentation for colon cancer patients in large series; around half of patients presenting with T3 disease, around a quarter with T4 disease and the remainder with T1 or T2 disease (Jullumstro et al., 2009).

Pathological N-stage:

The majority of patients recruited to the trial (56.4) had N0 disease for their final pathological N-stage, followed by N1 disease (34.5). These results are summarised in Table 4.4. These results are again in keeping with the N-stage of colon cancers at presentation in large series (Jullumstro et al.,

2009). This data is not recorded for one patient (1.8%), who had an unresectable tumour at operation.

Delay from imaging to surgery:

The median delay from CT scan to surgery was 40 (IQR 29-49.5) days, compared to 9 (IQR 5.5-13.5) days for 1.5T MRI, and 9 (IQR 6-14) days for 3T MRI. The difference in delay from imaging to surgery between CT and 1.5T MRI is significant ($p<0.001$, Wilcoxon signed rank test), as is the difference in delay from imaging to surgery between CT and 3T MRI ($p<0.001$, Wilcoxon signed rank test). The difference in delay from imaging to surgery between 1.5T MRI and 3T MRI was not significant ($p=0.38$ Wilcoxon signed rank test). These results are illustrated in Figure 4.5.

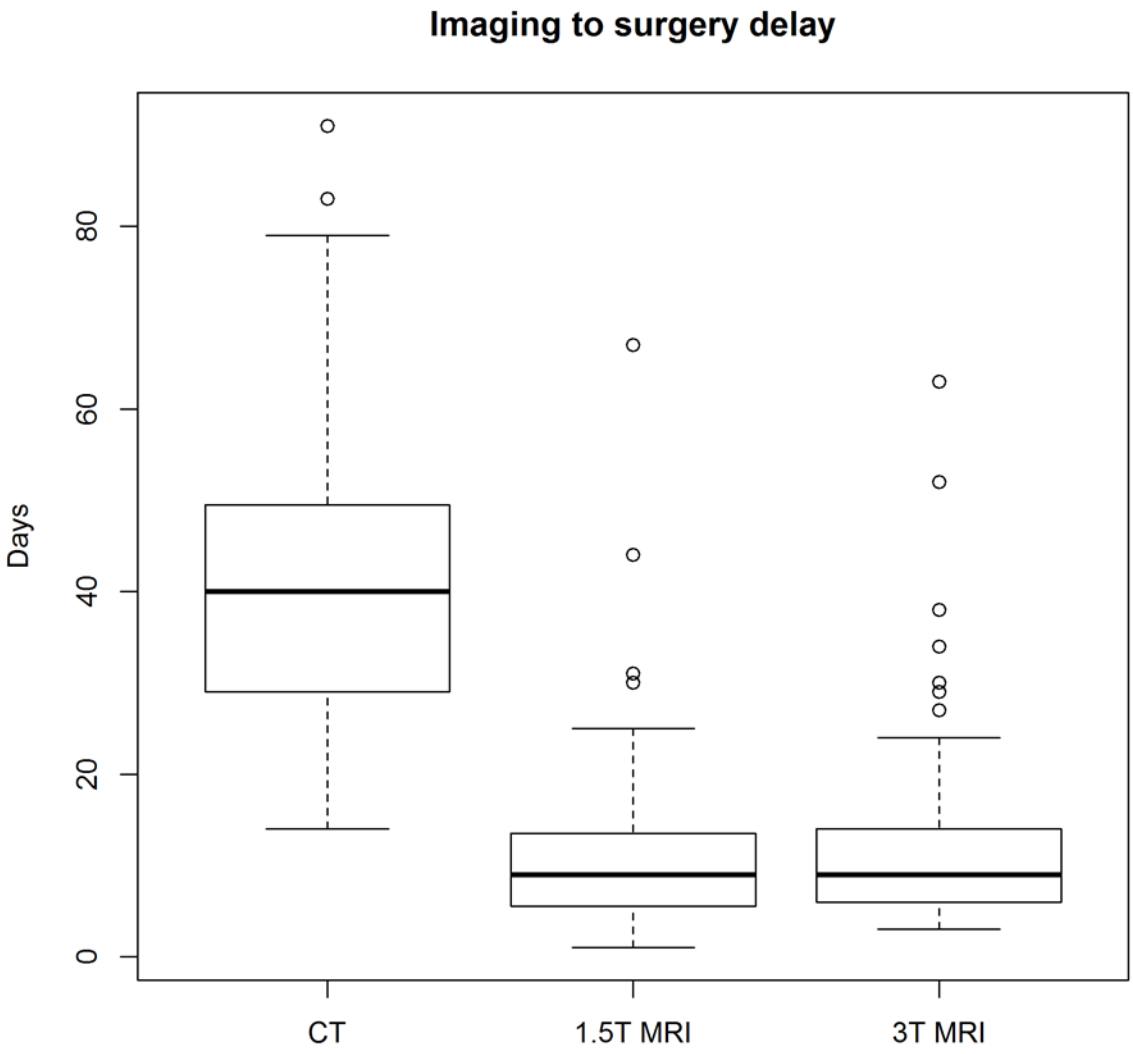


Figure 4.3: Imaging delay to surgery

The reason for this difference in delay between imaging and surgery for CT and MRI lies in ethical constraints on the trial design. To be eligible for inclusion in the trial, patients had to have a confirmed diagnosis of colon cancer and to have been discussed in the colorectal MDT and considered suitable for resection of their primary tumour before they could be recruited into the colon MRI study. This meant that all patients had to have received a staging CT before recruitment into the colon MRI study. This could not then be repeated for the purposes of the trial as this would

have exposed patients to an additional radiation dose without any benefit. All patients therefore had their CT scans performed prior to their MRI scans.

To assess whether this may have exerted any systematic bias due to tumour progression we therefore compared the overall tumour staging for all patients by both radiologists using CT, 1.5T MRI and 3T MRI. The proportion of patients assessed as positive for T3/T4 disease, N1/N2 disease and EMVI are shown in Table 4.6 for CT and 1.5T MRI and Table 4.7 for CT and 3T MRI.

	CT (%) n=110	**1.5T MRI (%)** n=110	**p-value (Fisher's exact test)**
T3/4	71.8	51.8	0.004
N1/2	59.1	26.4	<0.001
EMVI positive	38.2	26.4	0.08

Table 4.5: Overall staging on CT and 1.5T MRI

	CT (%) n=110	**3T MRI (%)** n=106	**p-value (Fisher's exact test)**
T3/4	71.8	56.6	0.02
N1/2	59.1	33.0	<0.001
EMVI positive	38.2	30.2	0.25

Table 4.6: Overall staging on CT and 3T MRI

Although the differences in T-stage an N-stage between CT and both 1.5T MRI and 3T MRI were significant, the stage was greater when assessed on CT than when assessed on MRI. As the CT scans were performed before the MRI scans, these differences were not due to disease progression in the

delay between imaging and surgery. There is however some relative understaging on MRI compared to CT.

4.4.3 Outcome measures

Primary outcome measure – Accuracy in identifying T3 disease

The primary aim was to determine whether there was a significant difference in the accuracy of MRI and CT in identifying T3 or greater disease. As the scans were performed in the same patients, this is a paired design and so McNemar's test was used to compare the accuracy of the CT and MRI scans. The accuracy (true positives and true negatives/all results) of each scan for each radiologist, and the p values calculated using McNemar's test, are shown in Table 4.12. Radiologist 1 achieved the same accuracy in identifying T3 disease with CT and 1.5T MRI (70.9%), but achieved greater accuracy reporting 3T MRI than CT (75.5% compared to 71.7%). Radiologist 2 was more accurate reporting T-stage using CT (65.5% and 66%) than reporting 1.5T and 3T MRI (50.9% and 56.6% respectively). There is a slight difference in the accuracy of CT for the same radiologist when evaluating 1.5T MRI and 3T MRI because 2 additional patients were included when evaluating 1.5T MRI. There was no significant difference in accuracy between 1.5T MRI and CT, or between 3T MRI and CT, for either radiologist.

	CT accuracy % (95% CI)	**MRI accuracy % (95% CI)**	**p-value (McNemar's test)**	**n**
1.5T MRI, radiologist 1	70.9 (57.9-81.2)	70.9 (57.9-81.2)	1	55
1.5T MRI, radiologist 2	65.5 (52.3-76.6)	50.9 (38.1-63.6)	0.7518	55
3T MRI, radiologist 1	71.7 (58.4-82.0)	75.5 (62.4-85.1)	0.1356	53
3T MRI, radiologist 2	66.0 (52.6-77.3)	56.6 (43.3-69.0)	0.332	53

Table 4.7: Comparison of scan accuracy in identifying T3/4 disease

T3 or greater disease

The accuracy of each modality in identifying T3 or greater disease has already been reported as the primary outcome measure. The sensitivity, specificity, positive predictive value and negative predictive value are shown in Table 4.8

There was a wide range in the sensitivity for identifying T3 disease, from 41.9% to 81.4%. Sensitivity was consistently lower for radiologist 2 (41.9% to 69.8%) compared to radiologist 1 (74.4% to 81.4%), due in part to a trend towards reporting a lower T-stage across all imaging modalities (reflected in a greater specificity). CT was consistently the most sensitive in identifying T3 or greater disease (69.8% and 81.4%), followed by 3T MRI (50% and 78.6%), then 1.5T MRI (41.9% and 74.4%).

Specificity for identifying T3 or greater disease was better for MRI (58.3% to 81.8%) compared to CT (33.3% and 50%). This is the opposite of the trend seen in terms of sensitivity and suggests some bias towards under reporting T3 disease on MRI compared to CT. Radiologist 2 also tended to have a higher specificity across all modalities (50% to 83.3%) compared to radiologist 1 (33.3% to 63.6%), also the inverse of the sensitivity suggesting some relative under reporting of T3 disease for radiologist 1.

The positive predictive value for both radiologists and all three modalities is high for T3 or greater disease (81.4% to 83.3%). This is important as it is one of the key entry criteria for the FOXTROT study, and suggests that a low proportion of patients recruited to the study on any of these imaging modalities would in fact be ineligible on the basis of their pathological T-stage. Positive predictive value is highest for 3T MRI (89.2% to 91.3%), then 1.5T MRI (86.5 to 90%), and lowest for CT (81.4% to 83.3%).

The negative predictive value for the identification of T3 or greater disease is fairly low for both radiologists for all imaging modalities, ranging from 28.6% to 43.8

	Accuracy % (95% CI)	Sensitivity % (95% CI)	Specificity % (95% CI)	PPV % (95% CI)	NPV % (95% CI)
CT, Reader 1	70.9 (57.9-81.2)	81.4 (67.4-90.3)	33.3 (13.8-60.9)	81.4 (67.4-90.3)	33.3 (13.8-60.9)
CT, Reader 2	65.5 (52.3-76.6)	69.8 (54.9-81.4)	50.0 (25.4-74.6)	83.3 (68.1-92.1)	31.6 (15.4-54.0)
1.5T MRI, Reader 1	70.9 (57.9-81.2)	74.4 (59.8-85.1)	58.3 (32.0-80.7)	86.5 (72.0-94.1)	38.9 (20.3-61.4)
1.5T MRI, Reader 2	50.9 (38.1-63.6)	41.9 (28.4-56.7)	83.3 (55.2-95.3)	90.0 (69.9-97.2)	28.6 (16.3-45.1)
3T MRI, Reader 1	75.5 (62.4-85.1)	78.6 (64.1-88.3)	63.6 (35.4-84.8)	89.2 (75.3-95.7)	43.8 (23.1-66.8)
3T MRI, Reader 2	56.6 (43.3-69.0)	50.0 (35.5-64.5)	81.8 (52.3-94.9)	91.3 (73.2-97.6)	30.0 (16.7-47.9)

PPV positive predictive value, NPV negative predictive value, R1 reader 1, R2 reader 2

Table 4.8: T3 or greater disease

Table 4.9 compares the proportion of patients reported as having T3 or greater disease by both radiologists for each imaging modality, with the proportion of patients positive for each of these end points on final pathology. P-values are reported for the difference in these proportions, assessed using Fisher's exact test.

Both radiologists report a similar proportion of patient as having T3 or greater disease on CT as is identified on histopathology (0.78 and 0.65 compared to 0.78 on histopathology). However, radiologist 2 reported a significantly smaller proportion of tumours as being T3 or greater on MRI (0.36 on 1.5T MRI and 0.43 on 3T MRI) than the proportion found to be T3 or greater on pathology (0.78 and 0.79). This bias towards under reporting on MRI will tend to increase specificity at the cost of sensitivity, and may reduce overall accuracy.

Inter-observer agreement for the two radiologists in assessing T3 or greater disease is shown in Table 4.15. There was substantial inter-observer agreement for CT, with moderate inter-observer agreement for both 1.5T and 3T MRI.

	CT, Reader 1		CT, Reader 2		1.5T MRI, Reader 1		1.5T MRI, Reader 2		3T MRI, Reader 1		3T MRI, Reader 2	
	Path	Rad	Path	Rad	Path	Rad	Path	Rad	Path	Rad	Path	Rad
Proportion >=T3	0.78	0.78	0.78	0.65	0.78	0.67	0.78	0.36*	0.79	0.70	0.79	0.43*
p-value	1		0.20		0.28		<0.01*		0.37		<0.01*	

p-value Fisher's exact test, * significant p<0.05

Table 4.9: Test bias: proportion positive for T3+ disease on pathology and radiology,

Modality	Cohen's kappa (95% CI)	Magnitude
CT	0.61 (0.41 to 0.80)	Substantial
1.5T MRI	0.43 (0.23 to 0.62)	Moderate
3T MRI	0.44 (0.27 to 0.61)	Moderate

Table 4.10: Inter-observer agreement for reporting T3+ disease

Stage-for-stage T-stage accuracy

The stage-for-stage accuracy of CT and MRI are presented in Table 4.16. The significance of the difference in accuracy between CT and MRI are assessed with the Wilcoxon signed rank test, using the degree of discrepancy between imaging and pathology.

Radiologist 1 achieved similar accuracy on CT (46%) and 1.5T MRI (47%), and slightly greater accuracy on 3T MRI (55%). Radiologist 2 was less accurate in reporting 1.5T MRI (38%) and 3T MRI (40%) than CT (47%). None of these differences achieved statistical significance.

	CT accuracy % (95% CI)	**MRI accuracy % (95% CI)**	**p-value (Wilcoxon signed rank test)**	**n**
1.5T MRI, radiologist 1	45.5 (33.0-58.5)	47.3 (34.7-60.2)	0.75	55
1.5T MRI, radiologist 2	47.3 (34.7-60.2)	38.2 (26.5-51.4)	0.62	55
3T MRI, radiologist 1	45.3 (32.7-58.5)	54.7 (41.5-67.3)	0.19	53
3T MRI, radiologist 2	47.2 (34.4-60.3)	39.6 (27.6-53.1)	0.53	53

Table 4.11: Stage-for-stage T-stage accuracy,

N1 or greater disease

The accuracy, sensitivity, specificity, positive predictive value and negative predictive value for both radiologists in identifying N1 or greater disease using each imaging modality is reported in Table 4.12. Accuracy in identifying N1 or greater disease was generally poor for both radiologists on all modalities, with accuracy varying from 55.6% to 63.5%. Accuracy was marginally higher on 3T MRI than 1.5T MRI (61.5% and 63.5% compared to 57.4%). Accuracy on 3T MRI was slightly higher than CT for radiologist 2 (63.5% compared to 55.6%), and similar for radiologist 1 (61.5% compared to 61.1%). There is substantial overlap in the 95% confidence intervals for all these values.

CT is the most sensitive in identifying N1 disease for both radiologists (65.2% and 73.9%), followed by 3T MRI (40.9% and 45.5%), followed by 1.5T MRI which has poor sensitivity (26.1% and 34.8%).

This is due in part to relative under calling of nodal disease on MRI compared to CT, illustrated by the relatively higher specificity.

The specificity for the identification of N1 disease was higher for both radiologists on 1.5T MRI (80.6% and 74.2%) and 3T MRI (76.7%) than on CT 58.1% and 41.9%). This is due in part to the trend towards under reporting nodal disease on MRI compared to CT leading to a higher specificity but lower sensitivity.

The positive predictive value for CT and 1.5T MRI in identifying N1 disease is similar for both radiologists (53.6% and 48.6% for CT and 50% for 1.5T MRI). The positive predictive value for 3T MRI is slightly higher (56.2% and 58.8%), although there is substantial overlap in the 95% confidence intervals.

The negative predictive value for identifying N1 disease is greatest for CT (69.2% and 68.4%) followed by 3T MRI (63.9% and 65.7%) then 1.5T MRI (59.5% and 60.5%).

Table 4.13 compares the overall proportion of patients reported as having N1 or greater disease by both radiologists for each imaging modality, with the overall proportion of patients reported as positive for each of these end points on final pathology to look for any systematic bias. The significance of the difference in these proportions is assessed using Fisher's exact test.

There is a trend towards over calling N1 or greater disease on CT for both radiologists, but this is only significant for radiologist 2 (rate of N1 disease 0.65 on CT compared to 0.43 on pathology, p=0.02). There is also a trend towards under calling N1 disease for both radiologists on both 1.5T and 3T MRI, but this is only significant for radiologist 1 on 1.5T MRI (rate of N1 disease 0.24 on 1.5T MRI compared to 0.43 on pathology, p=0.05).

Inter-observer agreement between the two radiologists for reporting N1 or greater disease on each modality is shown in Table 4.19. Inter-observer agreement was moderate for CT and substantial for 1.5T MRI, but only fair for 3T MRI although there is substantial overlap in the 95% confidence intervals for the Cohen's kappa values.

	Accuracy % (95% CI)	Sensitivity % (95% CI)	Specificity % (95% CI)	PPV % (95% CI)	NPV % (95% CI)
CT, Reader 1	61.1 (47.8-73.0)	65.2 (44.9-81.2)	58.1 (40.8-73.6)	53.6 (35.8-70.5)	69.2 (50.0-83.5)
CT, Reader 2	55.6 (42.4-68.0)	73.9 (53.5-87.5)	41.9 (26.4-59.2)	48.6 (33.0-64.4)	68.4 (46.0-84.6)
1.5T MRI, Reader 1	57.4 (44.2-69.7)	26.1 (12.5-46.5)	80.6 (63.7-90.8)	50.0 (25.4-74.6)	59.5 (44.5-73.0)
1.5T MRI, Reader 2	57.4 (44.2-69.7)	34.8 (18.8-55.1)	74.2 (56.8-86.3)	50.0 (28.0-72.0)	60.5 (44.7-74.4)
3T MRI, Reader 1	61.5 (48-73.5)	40.9 (23.3-61.3)	76.7 (59.1-88.2)	56.2 (33.2-76.9)	63.9 (47.6-77.5)
3T MRI, Reader 2	63.5 (49.9-75.2)	45.5 (26.9-65.3)	76.7 (59.1-88.2)	58.8 (36.0-78.4)	65.7 (49.2-79.2)

PPV positive predictive value, NPV negative predictive value

Table 4.12: N1 or greater disease

	CT, Reader 1		CT, Reader 2		1.5T MRI, Reader 1		1.5T MRI, Reader 2		3T MRI, Reader 1		3T MRI, Reader 2	
	Path	Rad	Path	Rad	Path	Rad	Path	Rad	Path	Rad	Path	Rad
Proportion >=N1	0.43	0.52	0.43	0.65*	0.43	0.24*	0.43	0.29	0.42	0.32	0.42	0.34
p-value	0.34		0.02*		0.04*		0.17		0.32		0.43	

p-value Fisher's exact test, *significant at p<0.05

Table 4.13: Test bias in reporting N1 or greater disease compared to pathology

Modality	Cohen's kappa (95% CI)	Magnitude
CT	0.55 (0.33 to 0.77)	Moderate
1.5T MRI	0.63 (0.38 to 0.89)	Substantial
3T MRI	0.35 (0.08 to 0.62)	Fair

Table 4.14: Inter-observer agreement for reporting N1 or greater disease

Extra Mural Vascular Invasion

A further aim of this project was to examine the utility of CT, 1.5T MRI and 3T MRI in identifying extra mural vascular invasion (EMVI). EMVI was reported by the radiologists as none, small, medium or large, although it was just reported as a binary outcome (positive or negative) on the final pathology report. Area under the curve (AUC) results are therefore reported for each imaging modality and radiologist, and the accuracy, sensitivity and specificity are reported at the optimum cut off value for each modality and radiologist.

Table 4.15 lists the area under the curve (AUC) calculated from a Receiver Operator Curve (ROC) for each imaging modality and each radiologist for the identification of EMVI. Radiologist 1 achieved a high AUC value on all three imaging modalities, (0.73, 0.77 and 0.78 on 1.5T MRI, 3T MRI and CT respectively). Radiologist 2 achieved a slightly lower value on CT and 1.5T MRI (0.56 and 0.59 respectively), but a similar value reporting 3T MRI (0.67). The most consistently accurate reporting was therefore achieved using 3T MRI. There is substantial overlap in the 95% confidence intervals for all of these values.

Table 4.15 shows the accuracy, sensitivity, specificity, PPV and NPV of each imaging modality for each radiologist in detecting EMVI. Imaging is considered positive for EMVI if it is reported as present (small, medium, or large) and negative if it is reported as absent (none).

Accuracy for reporting EMVI was similar for both radiologists across all imaging modalities, ranging from 53.7% (CT, radiologist 2) to 79.6%(CT, radiologist 1). There are no clear trends in the accuracy between the imaging modalities or radiologists, and there is substantial overlap in the 95% confidence intervals.

The sensitivity for identifying EMVI was lower for radiologist 2 than radiologist 1 (26.3% to 36.8% compared to 57.9% to 73.7%). This is due in part to a significant bias towards under-reporting EMVI compared to the pathological rate of EMVI by radiologist 2 across all imaging modalities. Sensitivity

for radiologist 1 in identifying EMVI was highest on 3T MRI (73.7%) followed by 1.5T MRI (63.2%) then CT (57.9%).

Specificity for identifying EMVI was high for radiologist 2 on all imaging modalities (91.4% to 97%), due in part to the bias towards under reporting mentioned previously. Radiologist 1 had a higher specificity on CT (94.3%) than MRI (75.8% and 80%).

Positive predictive value ranged from 62.5% to 87.5%, and was highest for radiologist 1 on CT (84.6%) and radiologist 2 on 3T MRI (87.5%). Negative predictive value ranged from 69.6% to 83.3%, and was highest for radiologist both radiologists on 3T MRI (83.3% and 72.7% for radiologist 1 and radiologist 2, respectively).

The proportion of patients reported as having EMVI on each test by each radiologist is compared to the proportion positive on final pathology in Table 4.16. There is a trend towards under reporting EMVI for both radiologists on CT, and for radiologist 2 on all imaging modalities. Fisher's exact test has been used to assess whether this difference in proportions is significant. These differences are significant for radiologist 2 for all imaging modalities.

Inter-observer agreement for reporting EMVI positivity for each modality is shown in Table 4.22. Inter-observer agreement was only slight for CT and 1.5T MRI, and fair for 3T MRI, although there is substantial overlap in the 95% confidence intervals for the Cohen's kappa values.

	Area under the curve (95% CI)	Accuracy % (95% CI)	Sensitivity % (95%CI)	Specificity % (95%CI)	PPV % (95% CI)	NPV % (95% CI)
CT, Reader 1	0.78 (0.66-0.91)	79.6 (67.1-88.2)	63.2 (41.0-80.9)	88.6 (74.0-95.5)	75.0 (50.5-89.8)	81.6 (66.6-90.8)
CT, Reader 2	0.56 (0.41-0.72)	53.7 (40.6-66.3)	47.4 (27.3-68.3)	57.1 (40.9-72.0)	37.5 (21.2-57.3)	66.7 (48.8-80.8)
1.5T MRI, Reader 1	0.73 (0.60-0.86)	74.1 (61.1-83.9)	63.2 (41.0-80.9)	80.0 (64.1-90.0)	63.2 (41.0-80.9)	80.0 (64.1-90.0)
1.5T MRI, Reader 2	0.59 (0.48-0.71)	68.5 (55.3-79.3)	26.3 (11.8-48.8)	91.4 (77.6-97.0)	62.5 (30.6-86.3)	69.6 (55.2-80.9)
3T MRI, Reader 1	0.77 (0.64-0.90)	75.0 (61.8-84.8)	73.7 (51.2-88.2)	75.8 (59.0-87.2)	63.6 (43.0-80.3)	83.3 (66.4-92.7)
3T MRI, Reader 2	0.67(0.56-0.79)	75.0 (61.8-84.8)	36.8 (19.1-59.0)	97.0 (84.7-99.5)	87.5 (52.9-97.8)	72.7 (58.2-83.7)

PPV positive predictive value, NPV negative predictive value

Table 4.15: Extra mural vascular invasion

	CT, Reader 1		CT, Reader 2		1.5T MRI, Reader 1		1.5T MRI, Reader 2		3T MRI, Reader 1		3T MRI, Reader 2	
	Path	Rad	Path	Rad	Path	Rad	Path	Rad	Path	Rad	Path	Rad
Proportion EMVI+	0.35	0.25	0.35	0.15*	0.35	0.36	0.35	0.16*	0.37	0.43	0.37	0.17*
p-value	0.30		0.02*		1		0.03*		0.55		0.03*	

p-value Fisher's exact test, *significant at p<0.05

Table 4.16: Test bias in reporting EMVI compared to pathology

Modality	Cohen's kappa (95% CI)	Magnitude
CT	0.17 (-0.08 to 0.42)	Slight
1.5T MRI	0.07 (-0.17 to 0.30)	Slight
3T MRI	0.34 (0.12 to 0.56)	Fair

Table 4.17: Inter-observer agreement for reporting EMVI positivity

T3c or greater disease

T-stage can be sub-categorised according to the depth of extramural tumour invasion; T3a (<= 1mm), T3b (>1mm, <= 5mm), T3c (>5mm, <=15mm) and T3d (>15mm). The distinction between tumours which are T3c or greater, compared to those which are T3b or less, has been demonstrated to have greater prognostic significance than the distinction between T2 and T3 tumours. Here I examine the accuracy, sensitivity, specificity, positive predictive value and negative predictive value of CT, 1.5T MRI and 3T MRI in identifying sub-categories of T3c or greater disease.

The accuracy, sensitivity, specificity, positive predictive value and negative predictive value for both radiologists in identifying T3c or greater disease using each imaging modality is reported in Table 4.18.

Accuracy is generally good for both radiologists on all three imaging modalities, ranging from 70.9% to 79.2%, with substantial overlap for the 95% confidence intervals.

There is more variation in the sensitivity between the radiologists and modalities. Sensitivity for reader 1 varies from 66.7% using 1.5T MRI to 75% using 3T MRI. Sensitivity is lower for reader 2, varying from 42.9% using 1.5T MRI to 61.9% using CT.

The opposite trend is seen for specificity, with reader 1 achieving specificity ranging from 70.6% on CT to 79.4% on 1.5T MRI, but reader 2 achieving very high specificity ranging from 88.2% on CT to 94.1% on 1.5T MRI. This suggests a tendency for relative under-reporting of T3c disease for reader 2.

Positive predictive value was moderate for reader 1 on all three modalities, ranging from 60% using CT to 66.7% using 1.5T MRI. Positive predictive value was good for reader 2 on all modalities, ranging from 76.5% on Ct to 84.6% on 3T MRI.

Negative predictive value was similar for both radiologist on all modalities, ranging from 72.7 to 83.3%.

	Accuracy % (95% CI)	Sensitivity % (95% CI)	Specificity % (95% CI)	PPV % (95% CI)	NPV % (95% CI)
CT, Reader 1	70.9 (57.9-81.2)	71.4 (50.0-86.2)	70.6 (53.8-83.2)	60.0 (40.7-76.6)	80.0 (62.7-90.5)
CT, Reader 2	78.2 (65.6-87.1)	61.9 (40.9-79.2)	88.2 (73.4-95.3)	76.5 (52.7-90.4)	78.9 (63.7-88.9)
1.5T MRI, Reader 1	74.5 (61.7-84.2)	66.7 (45.4-82.8)	79.4 (63.2-89.7)	66.7 (45.4-82.8)	79.4 (63.2-89.7)
1.5T MRI, Reader 2	74.5 (61.7-84.2)	42.9 (24.5-63.5)	94.1 (80.9-98.4)	81.8 (52.3-94.9)	72.7 (58.2-83.7)
3T MRI, Reader 1	75.5 (62.4-85.1)	75.0 (53.1-88.8)	75.8 (59.0-87.2)	65.2 (44.9-81.2)	83.3 (66.4-92.7)
3T MRI, Reader 2	79.2 (66.5-88.0)	55.0 (34.2-74.2)	93.9 (80.4-98.3)	84.6 (57.8-95.7)	77.5 (62.5-87.7)

PPV positive predictive value, NPV negative predictive value

Table 4.18: T3c or greater disease

Table 4.19 compares the overall proportion of patients reported as having T3c or greater disease by both radiologists for each imaging modality, with the overall proportion of patients reported as positive for each of these end points on final pathology, to look for any systematic bias. The significance of the difference in these proportions is assessed using Fisher's exact test.

There is a trend towards radiologist 1 over reporting T3c disease on all modalities compared to pathology, and radiologist 2 under reporting T3c disease on all modalities compared to pathology. However, neither of these trends achieves statistical significance on any imaging modality.

The inter-observer agreement for the two radiologists reporting T3c or greater disease for each modality is shown in Table 4.25. Moderate inter-observer agreement was demonstrated on all three imaging modalities.

	CT, Reader 1		CT, Reader 2		1.5T MRI, Reader 1		1.5T MRI, Reader 2		3T MRI, Reader 1		3T MRI, Reader 2	
	Path	Rad	Path	Rad	Path	Rad	Path	Rad	Path	Rad	Path	Rad
Proportion >=T3c	0.21	0.46	0.21	0.14	0.21	0.32	0.21	0.11	0.21	0.43	0.21	0.07
p-value	0.09		0.73		0.54		0.47		0.15		0.25	

p-value Fisher's exact test

Table 4.19: Test bias in reporting T3c or greater disease compared to pathology

Modality	Cohen's kappa (95% CI)	Magnitude
CT	0.47 (0.25 to 0.7)	Moderate
1.5T MRI	0.41 (0.17 to 0.64)	Moderate
3T MRI	0.51 (0.29 to 0.73)	Moderate

Table 4.20: Inter-observer agreement for reporting T3c or greater disease

4.5 Discussion

The primary aim of this project was to determine, on a per patient basis, whether the identification of T3 or greater disease is more accurate using 1.5T MRI or 3T MRI than using CT. There was no significant difference between the accuracy using CT and 1.5T MRI, or using CT and 3T MRI for either radiologist.

The accuracy of CT in identifying T3 or greater disease was assessed in a meta-analysis by Dighe et al. in 2010 which included 19 studies from 1986 to 2008, 17 of which had sufficient data to be included in a meta-analysis (Dighe et al., 2010b). The overall sensitivity for CT in this meta-analysis was 86% (95% CI 78-92%), with a specificity of 78% (95% CI 71-84%) and a DOR of 22.4 (95% CI 11.9-42.4). The diagnostic odds ratio is a measure of effectiveness of a diagnostic test, defined by the ratio of the odds of a test being positive if a patient has the disease compared to the odds of the test being positive if the patient does not have the disease. It is a single measure of the performance of a test, like accuracy, but is not depended on the prevalence of the disease (Glas et al., 2003).

Presenting the results of our study in this way for comparison, using CT radiologist 1 has a DOR of 2.2 (95% CI 0.5-9.1) and radiologist 2 has a DOR of 2.3 (95% CI 0.6-8.5). Using 1.5T MRI, radiologist 1 has a DOR of 4.1 (95% CI 1.1-15.5) and radiologist 2 has a DOR of 3.6 (95% CI 0.7-18.5). Using 3T MRI, radiologist 1 has a DOR of 6.4 (1.5-26.9) and radiologist 2 has a DOR of 4.5 (0.9-23.4). There is therefore a trend in this study towards all three modalities to being less effective diagnostic test for the identification of T3 or greater disease than CT in a recent meta-analysis. The performance of CT is this study is particularly poor, with the 95% CI for the DOR for both radiologists falling below the 95% CI for the DOR for CT in the meta-analysis. It is difficult to explain why the diagnostic effectiveness of CT in this study would be significantly lower than that reported in the literature; both radiologists are experienced consultant GI radiologists and core MDT members. Although the CT scans used in this study were not repeated with a specific trial protocol, they are the standard

clinical scans used for pre-operative staging at the participating institutions and were not felt to be poor quality by the trial radiologists.

Stage-for-stage accuracy in reporting T-stage was 45.5% and 47.3% for the two radiologists on CT, 47.3% and 38.2% for the two radiologists on 1.5T MRI, and 54.7% and 39.6% for the two radiologists on 3T MRI. Two papers report stage-for-stage accuracy for the prediction of T-stage on CT; Smith et all report 60% and 61% accuracy for two observers (Smith et al., 2007), and Burton et al. report 35% and 51% accuracy for two observers (Burton et al., 2008). The accuracy of CT, 1.5T MRI and 3T MRI in this study for the assessment of stage-for-stage T-stage is, therefore, comparable with CT in the Burton study, but slightly lower than the accuracy reported for CT in the Smith study.

Inter-observer agreement for the reporting of T3 or greater disease was substantial on CT (Cohen's kappa 0.61), and moderate on 1.5T and 3T MRI (Cohen's kappa 0.43 and 0.44 respectively). Although there was a defined criteria for reporting T-stage which was based on rectal MRI T-staging criteria (Taylor et al., 2008) and which was agreed before reporting of the trial scans, there was a significant under-reporting of T3 or greater disease by radiologist 2 on both 1.5T MRI and 3T MRI compared to the pathological rate of T3 or greater disease (36-43% compared to a pathological rate of 78%). This will have had a negative impact on inter-observer reliability and to some extent on reporting accuracy. This may be related to a learning curve in using a new modality for staging colon cancer, or lack of confidence in reporting T3 or greater disease when scan quality was suboptimal.

Another commonly reported endpoint in the assessment of local staging accuracy is the identification of nodal metastases (N1 and N2 disease). There was no significant difference in the accuracy of the three modalities in identifying lymph node positive disease for either radiologist. This endpoint was also assessed by Dighe et all in his meta-analysis and fifteen studies were included for this end point (Dighe et al., 2010b). The overall sensitivity for nodal detection in this meta-analysis was 70% (95% CI 59-80%), specificity was 78% (95% CI 66-86%) and DOR was 8.1 (95% CI 4.7-14.1).

Using CT in this study, radiologist 1 had a DOR of 2.6 (95%CI .09-7.9) and radiologist 2 had a DOR of 2.0 (0.6-6.6). Using 1.5T MRI, radiologist 1 had a DOR of 1.5 (0.4-5.3) and radiologist 2 had a DOR of 1.5 (0.5-5.0). Using 3T MRI, reader 1 had a DOR of 2.3 (0.7-7.6) and reader 2 had a DOR of 2.7 (0.8-9.0). These results suggest that in this study all three imaging modalities tended to be less effective diagnostic tests than CT in recent meta-analysis, although there is an overlap in the 95% confidence intervals.

Inter-observer agreement was moderate for CT (Cohen's kappa 0.55), substantial for 1.5T MRI (0.63), and fair for 3T MRI (0.35). The more reproducible results demonstrated for 1.5T MRI were not match by more accurate N-staging, as 1.5T MRI actually had the worst DOR of the three modalities.

Another imaging feature, which has been demonstrated to be prognostically important in colorectal cancer on rectal MRI, is EMVI (Smith et al., 2008a, Sohn et al., 2015, Chand et al., 2014). The accuracy of CT for the identification of EMVI is reported in three previous studies; Burton et al. reported an accuracy of 55% for observer 1 and 61% for reader 2 (Burton et al., 2008), Dighe et al. reported an accuracy of 70% (Dighe et al., 2010a), and Rollven et al. reported an accuracy of 78% for reader 1 and 69% for reader 2. Rollven also reported the accuracy of 1.5T MRI of 78% and 82%.

In the current study, the accuracy of CT for the identification of EMVI was 80% for radiologist 1 and 54% for radiologist 2, the accuracy for 1.5T MRI was 74% for radiologist 1 and 69% for radiologist 2, and the accuracy for 3T MRI was 75% for both radiologists. The accuracy of all three modalities in this study is therefore comparable with the reported accuracy of CT and slightly less than the reported accuracy in the only other study of MRI.

Inter-observer agreement was therefore surprisingly poor for all three modalities, with slight agreement for CT and 1.5T MRI (Cohen's kappa 0.17 and 0.07 respectively), and fair for 3T MRI (Cohen's kappa 0.34). There was again significant under reporting of EMVI by radiologist 2 on all modalities (15-17%) compared to pathology (35%), but not by radiologist 1.

The accuracy of MRI in the identification of poor prognosis disease by T-substage (T4 tumours and tumours which have invaded more than 5mm outside the bowel wall) has been demonstrated to be of greater prognostic significance than the distinction between T2 and T3 tumours both on histopathology (Merkel et al., 2001). Identification of T3c or greater tumours on CT has been also demonstrated to be as prognostically relevant as this distinction on histopathology (Smith et al., 2007). This was the initial entry criteria for the FOXTROT study and remains the entry criteria for older and frailer patients. This has previously been reported for CT by Dighe et al. at 70% (Dighe et al., 2012), and by Rollven et al. is 79% for observer 1 and 76% for observer 2 (Rollven et al., 2013), and. The Rollven study also reports the accuracy of 1.5T MRI and reports very high accuracy of 90% (95% CI 74-96%) for observer 1 and 93% (95% CI 78-98%) for observer 2 in a study of 28 patients.

In this study, the accuracy of CT was 71% for radiologist 1 and 78% for radiologist 2, the accuracy of 1.5T MRI was 75% for both radiologists, and the accuracy of 3T MRI was 76% for radiologist 1 and 79% for radiologist 2.

The accuracy of all three imaging modalities in this study in identifying T3c or greater disease is, therefore, comparable with the reported accuracy of CT, but with a trend towards being less accurate than the only other study to report the accuracy of MRI in the assessment of this outcome measure.

There are a number of reasons why this study may have failed to show the level of accuracy for T-stage illustrated in the Rollven study. Firstly, this may simply be the effect of random variation in small studies. Our study recruited 60 patients, with 55 patients with sufficient data available to be included in the final analysis. The Rollven study recruited 49 patients, but only 28 patients were included in the final analysis. This small number of cases results in wide confidence intervals for the accuracy in both studies, and as mentioned previously there is substantial overlap in the confidence intervals. Given the paucity of published trials on MRI staging of colon cancer over the last ten years

it is also possible that the excellent T-staging accuracy demonstrated in the Rollven study are subject to a publication bias.

Secondly, our study is presented on an intention to treat basis for all recruited patients with evaluable results. Five patients out of sixty recruited patients (8.8%) were withdrawn as they did not have evaluable results, and two of sixty five patients only had 1.5T MRI performed and therefore are not included in the 3T MRI results. Therefore over 90% of recruited patients were included for final evaluation. In the Rollven study, of forty-nine recruited patients, seven were withdrawn before MRI and a further fourteen were excluded from final evaluation after undergoing MRI including six in whom "MRI was not performed with the high resolution protocol". Therefore just fewer than 60% of recruited patients were included for final analysis, and 12% were withdrawn due to inadequate quality MRI. It is therefore possible that the Rollven study that the represents more optimal results in patients who are able to tolerate a relatively lengthy MRI scan, and that our study represents results which are more likely to be seen if MRI is used for staging in the whole population with colorectal cancer. Our results for subgroups of patients within the trial including the subgroup with high quality scans are presented in chapter 5 (page 213). It is worth noting that our study also only successfully recruited 38% of eligible patients, who had a non-significant trend towards younger age and a significant trend towards male gender.

Thirdly, there is a difference in the MRI equipment and protocol used in our study and the Rollven study. Different MRI scanners were used in both studies (Siemens Magnetom Avanto and Phillips Achieva in our study, Philips Intera in the Rollven study). Different anti-motility agents were used in both studies (20mg of IM Buscopan in our study, 1 IE IM Glucagon in the Rollven study). Different MRI sequences were also used in both studies. In our study, patients received a high resolution TSE sequence perpendicular to the long axis of the tumour, and where possible TSE imaging in complimentary planes, similar to the Rollven study. However, patients also received contrast enhanced T1 weighted sequences and DWI sequences. In the Rollven study, only respiratory triggered T2 weighted TSE sequences were acquired in at least 3 planes and perpendicular to the

long axis of the tumour. Both studies limited total scan time to 40 to 60 minutes for patient comfort, but the addition of T1 weighted sequences and DWI sequences limited the number T2 weighted sequences and planes which could be acquired in our study. Although we have yet to analyse in detail which sequences were most important for T-staging in our study, the reporting radiologists thought that the T2 weighted TSE sequences were the most useful during reporting. It is therefore possible that the MRI methods used for MRI acquisition in the Rollven study allowed superior T-staging to the methods used in our own study. The impact of the number of imaged planes and image quality on staging accuracy in our own study is examined in more detail in Chapter 5.

An interesting finding in this study which was not one of our planned endpoints is that two of sixty recruited patients were withdrawn from the study because liver metastases requiring neoadjuvant chemotherapy were identified on MRI which had not been identified on pre-operative CT when discussed in the colorectal MDT. When the CT scans were reviewed by both radiologists, one of these patients had liver metastases which were identified on CT by both radiologists. However, for the other patient neither radiologist identified metastatic disease on the staging CT scan. This suggests that there are a small proportion of patients who would have liver metastases identified on MRI which are not identified on CT, even without the use of a liver specific contrast agent (1/60 patients, 1.6%, 95% CI 0.3% to 8.9%). This proportion may be an underestimate of the true proportion of patients who would have liver metastases identified on liver MRI, as the liver was not imaged in its entirety on MRI for a number of patients in this study as this was not the aim of MRI imaging.

Overall, we have achieved a broadly similar accuracy in staging colon cancer using MRI and CT. MRI may therefore be a useful adjunct to current CT staging in situations where CT staging is inadequate, for example where patients are unable to receive IV contrast. MRI may also be useful in situation where CT is contra-indicated, such as pregnancy. However, it would not be possible to recommend replacing CT staging with MRI staging on the basis of this study. Of note, there was considerable

variation in the quality of MRI scans obtained in this study. We will therefore examine the accuracy of MRI where optimal images are obtained in chapter 5.

CHAPTER 5

Diagnostic accuracy of MRI and CT in subgroups

5.1 My role in this chapter

With the support of my supervisor, I wrote the trial protocol, obtained the funding and ethical approval, and performed the data collection for this chapter, which also formed the data for chapter 4. I performed the data analysis and wrote this chapter.

5.2 Introduction and rationale

In chapter 4, I compared the overall accuracy of CT, 1.5T MRI and 3T MRI. Although we attempted to keep the scan acquisition technique as consistent as possible for all modalities, there were some unavoidable variations in the scan technique and quality between patients. The effect of this variation in scan quality on the staging accuracy is investigated further in this chapter. The scans performed as part of the study in chapter 4 were therefore divided into subgroups according to tumour location, image quality and number of imaged planes and the accuracy of each modality assessed in these subgroups.

5.2.1 1.5T MRI

The 1.5T MRI scans were all acquired on a Magnetom Avanto 1.5T (Siemens Medical Solutions, Erlangen, Germany) using a phased array body coil. A coronal breath-hold T2 weighted balanced gradient echo (TrueFISP) sequence was acquired through the whole abdomen to identify the tumour. These images were then used to plan navigator echo respiratory triggered T2 weighted fast spin echo sequences (TSE) through the tumour, first perpendicular to the long axis of the tumour, and then in two complimentary planes along the long axis of the tumour. Free breathing diffusion weighted images (DWI) were then obtained through the tumour volume, perpendicular to the long axis of the tumour. Finally, breath-hold T1 weighted ultrafast gradient echo sequences (FLASH) were obtained in a coronal plane through the whole abdomen immediately, one minute and 2 minutes following the administration of intravenous gadolinium contrast.

However, the navigator echo could not always reliably identify respiratory movement in all patients, leading to severe degradation in the image quality of the TSE images in some patients. In this case, breath-hold ultra-fast spin echo (HASTE) images were obtained in place of the TSE images. The maximum total scan time available for each patient was forty minutes, and not all patients were able to tolerate a full forty minutes scan time. The TSE sequences took between five and ten minutes to acquire depending on the size of the volume being imaged, the respiratory rate of the patient and the effectiveness of the navigator echo triggering. It was therefore not possible to obtain TSE images in both long axis planes in most patients, and in either long axis planes in some patients. These limitations led to some heterogeneity between patients in the number and type of sequences obtained for 1.5T MRI scans. In addition to these limitations, tumour location and the patient's ability to breath-hold had a notable impact on motion artefact, the principle limitation in the quality of the MRI scans.

5.2.2 3T MRI

The 3T MRI scans were all obtained on an Achieva 3.0T MRI scanner (Philips Healthcare, Best, Netherlands), using a phased array body coil. A coronal breath-hold T2 weighted balanced gradient echo (BTFE) sequence was obtained through the whole abdomen, and was used to identify the tumour and plan subsequent sequences. T2 weighted navigator echo respiratory triggered fast spin echo (TSE) sequences were then obtained, first in a plane perpendicular to the long axis of the tumour, then in two complimentary planes in the long axis of the tumour. Free breathing diffusion weighted images (DWI) were then obtained through the tumour volume, perpendicular to the long axis of the tumour. Finally, breath-hold T1 weighted ultrafast gradient echo sequences (FLASH) were obtained in a coronal plane through the whole abdomen immediately, 30 seconds, one minute and 2 minutes following the administration of intravenous gadolinium contrast.

There was no severe image degradation in the T2 weighted TSE images obtained for the 3T MRI scans, so it was not necessary substitute these for breath-hold ultrafast spin echo sequences for any

of the patients. Although the TSE images were acquired more rapidly at 3T, the same scan time constraint of forty minutes, and a relatively long sequence acquisition of time for TSE images limited TSE imaging to two planes for some patients. In addition, tumour location and patient's ability to remain still and breathe quietly and regularly again noticeably impacted on motion artefacts, which had an important impact on scan quality.

5.3 Materials and Methods

5.3.1 Subjects

The scans used for this part of the study are the same scans used in Comparison of the diagnostic accuracy of MRI with CT in staging colonic cancer, and the subjects have already been described in the subjects section of that chapter (page 167).

5.3.2 Procedures

Scan acquisition and reporting has been described in the Procedures section of chapter 4 (page 169).

For each patient enrolled in the trial, the tumour plane and tumour location were prospectively recorded in an Access database. For each MRI sequence at both 1.5T and 3T, the sequence plane and sequence details were also prospectively recorded in the same database.

Following completion of the trial, all MRI scans were reviewed by one research fellow blinded to the pathology, CT and MRI results for each patient. The overall quality of each MRI scan was graded as non-diagnostic, poor, adequate or good.

5.3.3 Evaluation

The MRI scans were divided into subgroups based on the following criteria:

1. Tumour location. This has been divided into lower abdominal tumours (Caecal and sigmoid colon) and upper abdominal tumours (ascending, transverse and descending colon) to allow reasonable a reasonable number of patients to be included in each subgroup
2. Overall scan quality. Scans were grouped into adequate or worse and good for 3T MRI, as the number of non-diagnostic or poor scans was low for 3T MRI. Scans were grouped into poor or worse and adequate or better for 1.5T MRI, as the number of non-diagnostic and good scans were low at 1.5T MRI.
3. Number of planes imaged with T2 weighted sequences. Patients were grouped into those imaged in only 1 plane, and those imaged 2 or 3 planes for 1.5T MRI, due to the low number of patients imaged in 3 planes at 1.5T. For 3T MRI patients were grouped into those imaged in 1 or 2 planes, and those imaged in 3 planes, due to the low number of patients imaged in only 1 plane on 3T MRI.

5.3.4 Statistical analysis

The accuracy (percentage of test results that are correct) and associated 95% confidence intervals in assessing T-stage (T3 or greater disease), N-stage (N1 or greater disease), presence of EMVI and T3c or greater disease was compared for each of the CT and MRI subgroups, using histology as the gold standard. 95% confidence intervals for proportions are calculated using the Wilson method (Wilson, 1927). Fisher's exact test was used to determine whether the difference in accuracy between scans was statistically significant.

The level of significance is set at $p < 0.05$. Analyses were performed using R 3.0.1 statistical software (R Core Team, 2015), including psych (Revelle, 2013), pROC (Robin et al., 2011) and epade (Schulz, 2013) packages.

5.4 Results

5.4.1 Tumour location

The location of tumours for each scanning modality is listed in Table 5.1. The tumour location is the same for CT and 1.5T MRI, as all trial patients received both 1.5T MRI and CT, but is slightly different for 3T MRI as 2 patients did not receive a 3T MRI. This is a fairly typical distribution of colon cancers, with the majority being right colon cancers (caecal or ascending), followed by sigmoid tumours, with a minority being in the transverse or descending colon.

Tumour location	**CT (%)**	**1.5T MRI (%)**	**3T MRI (%)**
Caecum	9 (16.4)	9 (16.4)	9 (17.0)
Ascending colon	18 (32.7)	18 (32.7)	17 (32.1)
Transverse colon	7 (12.7)	7 (12.7)	7 (13.2)
Descending colon	3 (5.5)	3 (5.5)	3 (5.7)
Sigmoid colon	18 (32.7)	18 (32.7)	17 (32.1)
Total	**55 (100)**	**55 (100)**	**53 (100)**

Table 5.1: Tumour location

T3 or greater disease

The accuracy of the three imaging modalities identifying T3 or greater disease for tumours located in the upper abdomen (ascending, transverse or descending colon) and lower abdomen (caecum and sigmoid colon) are shown for radiologist 1 in Table 5.2 and for radiologist 2 in Table 5.3. Radiologist 1 was slightly more accurate for in reporting tumours in the upper abdomen on all imaging modalities (75% to 77.8%) compared to tumours in the lower abdomen (66.7% to 73.1%), and most accurate reporting 3T MRI. There is substantial overlap in the 95% confidence intervals.

A different trend was seen for radiologist 2. Radiologist 2 was also more accurate reporting T3 or greater disease in the upper abdomen than the lower abdomen on CT (67.9% and 63% respectively). However, radiologist 2 was much less accurate reporting T3 or greater disease in the upper abdomen on both 1.5T and 3T MRI (35.7% and 40.7% respectively) than on CT (67.9%). In the lower abdomen, radiologist 2 was more accurate in reporting T-stage on MRI (66.7% and 71.1% on 1.5T MRI and 3T MRI respectively) than on CT (63%).

		Accuracy (95% CI)	
Tumour location	CT	1.5T MRI	3T MRI
Upper abdomen (n=28)	75 (56.6-87.3)	75 (56.6-87.3)	77.8 (59.2-89.4)
Lower abdomen (n=27)	66.7 (47.8-81.4)	66.7 (47.8-81.4)	73.1 (53.9-86.3)

Table 5.2: Imaging accuracy for T3 or greater disease, radiologist 1, according to tumour location

		Accuracy (95% CI)	
Tumour location	CT	1.5T MRI	3T MRI
Upper abdomen (n=28)	67.9 (49.3-82.1)	35.7 (20.7-54.2)	40.7 (24.5-59.3)
Lower abdomen (n=27)	63 (44.2-78.5)	66.7 (47.8-81.4)	73.1 (53.9-86.3)

Table 5.3: Imaging accuracy for T3 or greater disease, radiologist 2, according to tumour location

N1 or greater disease

The accuracy of the three imaging modalities identifying N1 or greater disease for tumours located in the upper abdomen and lower abdomen are shown for radiologist 1 in Table 5.4 and for radiologist 2 in Table 5.5. The accuracy for radiologist 1 in identifying N1 or greater disease is better in the lower abdomen (65.4% to 76%) than in the upper abdomen (48.1% to 57%.1%) on all imaging modalities. The difference in accuracy is more marked on MRI and most marked on 3T MRI (76% in the lower abdomen compared with 48.1% in the upper abdomen).

Radiologist 2 was slightly more accurate in identifying N1 or greater disease in the upper abdomen on CT (64.3% in the upper abdomen compared to 46.2% in the lower abdomen), but slightly more accurate in the lower abdomen on 1.5T MRI (65.4% in the lower abdomen compared to 50% in the upper abdomen). There was no difference in accuracy between the upper and lower abdomen on 3T MRI (66.7% on both imaging modalities).

	Accuracy (95% CI)		
Tumour location	CT	1.5T MRI	3T MRI
Upper abdomen (n=28)	57.1 (39.1-73.5)	50 (32.6-67.4)	48.1 (30.7-66)
Lower abdomen (n=27)	65.4 (46.2-80.6)	65.4 (46.2-80.6)	76 (56.6-88.5)

Table 5.4: Imaging accuracy for N1 or greater disease, radiologist 1, according to tumour location

	Accuracy (95% CI)		
Tumour location	CT	1.5T MRI	3T MRI
Upper abdomen (n=28)	64.3 (45.8-79.3)	50 (32.6-67.4)	66.7 (47.8-81.4)
Lower abdomen (n=27)	46.2 (28.8-64.5)	65.4 (46.2-80.6)	66.7 (47.8-81.4)

Table 5.5: Imaging accuracy for N1 or greater disease, radiologist 2, according to tumour location

EMVI

The accuracy of the three imaging modalities identifying EMVI for tumours located in the upper abdomen and lower abdomen are shown for radiologist 1 in Table 5.6 and for radiologist 2 in Table 5.7. Radiologist 1 was slightly more accurate in identifying EMVI in the lower abdomen than the lower abdomen on CT and 1.5T MRI, and slightly more accurate in identifying EMVI in the upper abdomen than the lower abdomen on 3T MRI. However, the accuracies are close (within 6%) with substantial overlap in the 95% confidence intervals.

Radiologist 2 is more accurate in identifying EMVI in the lower abdomen than the upper abdomen on all imaging modalities, but the difference most marked on CT (80.8% lower abdomen compared to 60.7% upper abdomen). However, there is still considerable overlap in the 95% confidence intervals.

		Accuracy (95% CI)	
Tumour location	CT	1.5T MRI	3T MRI
Upper abdomen (n=28)	75 (56.6-87.3)	71.4 (52.9-84.7)	77.8 (59.2-89.4)
Lower abdomen (n=27)	80.8 (62.1-91.5)	76.9 (57.9-89)	72 (52.4-85.7)

Table 5.6: Imaging accuracy for EMVI, radiologist 1, according to tumour location

		Accuracy (95% CI)	
Tumour location	CT	1.5T MRI	3T MRI
Upper abdomen (n=28)	60.7 (42.4-76.4)	60.7 (42.4-76.4)	74.1 (55.3-86.8)
Lower abdomen (n=27)	80.8 (62.1-91.5)	76.9 (57.9-89)	76 (56.6-88.5)

Table 5.7: Imaging accuracy for EMVI, radiologist 2, according to tumour location

T3c or greater disease

The accuracy of the three imaging modalities for identifying T3c or greater disease in the upper and lower abdomen are shown in Table 5.8 for radiologist 1 and in Table 5.9 for radiologist 2.

Radiologist 1 is more accurate in identifying T3c or greater disease on all 3 imaging modalities in the lower abdomen than in the upper abdomen. The difference in accuracy is small on CT, but greater on 3T MRI and greatest on 1.5T MRI which achieves the highest accuracy for identifying T3c or greater disease in the lower abdomen (92.6%). The difference in accuracy between the upper abdomen (57.1%) and the lower abdomen (92.6%) on 1.5T MRI is significant (p=0.004 Fisher's exact test).

These findings were not repeated for radiologist 2, for whom accuracy in the identification of T3c or greater disease was similar in the upper and lower abdomen on all three imaging modalities.

	Accuracy (95% CI)		
Tumour location	CT	1.5T MRI	3T MRI
Upper abdomen (n=28)	67.9 (49.3-82.1)	57.1 (39.1-73.5)	66.7 (47.8-81.4)
Lower abdomen (n=27)	74.1 (55.3-86.8)	92.6 (76.6-97.9)	84.6 (66.5-93.8)

Table 5.8: Imaging accuracy for T3c or greater disease, radiologist 1, according to tumour location

	Accuracy (95% CI)		
Tumour location	CT	1.5T MRI	3T MRI
Upper abdomen (n=28)	75.0 (56.6-87.3)	75.0 (56.6-87.3)	77.8 (59.2-89.4)
Lower abdomen (n=27)	81.5 (63.3-91.8)	74.1 (55.3-86.8)	80.8 (62.1-91.5)

Table 5.9: Imaging accuracy for T3c or greater disease, radiologist 2, according to tumour location

5.4.2 Scan quality

Table 5.10 shows the quality of images obtained on 1.5T MRI scanning and 3T MRI scanning. The majority of 1.5T MRI scans were scored as either poor (40%) or adequate (41.8%). A minority of scans were scored as either non-diagnostic (7.3%) or good (10.9%). In contrast, on 3T MRI the majority of scans were scored as good (58.5%), with a smaller proportion scored as adequate (32.1%). A minority of scans were scored as either non-diagnostic (1.9%) or poor (7.5%).

For further analysis, 1.5T MRI scans were divided two groups including poor and non-diagnostic scans in one group and adequate or good scans in the other group. 3T MRI scans were divided into good scans, and adequate or worse scans. This was done in order to allow reasonable numbers of MRI scans in each subgroup.

Scan quality	1.5T MRI (%)	3T MRI (%)
Non-diagnostic	4 (7.3)	1 (1.9)
Poor	22 (40.0)	4 (7.5)
Adequate	23 (41.8)	17 (32.1)
Good	6 (10.9)	31 (58.5)
Total	**55 (100)**	**53 (100)**

Table 5.10: 1.5T MRI and 3T MRI scan quality – number of scans

T3 or greater disease

Table 5.11 compares the accuracy of poor/non-diagnostic scans and adequate/good scans on 1.5T MRI in identifying T3 or greater disease for radiologist 1 and radiologist 2. The accuracy was marginally better for radiologist 1 reporting adequate/good scans compared to poor/non-diagnostic scans (72.4% compared to 69.2%). The accuracy was also better for radiologist 2 reporting adequate/good scans compared to poor/non-diagnostic scans, with a greater difference in accuracy although a lower accuracy overall (58.6% compared to 42.3%).

	Accuracy (95% CI)		
Scan Quality	Radiologist 1	Radiologist 2	N
Poor or non-diagnostic	69.2 (50.0-83.5)	42.3 (25.5-61.1)	26
Adequate or good	72.4 (54.3-85.3)	58.6 (40.7-74.5)	29

Table 5.11: 1.5T MRI accuracy in identifying T3 or greater disease, according to scan quality

Table 5.12 compares the accuracy of good scans with the accuracy of adequate or worse scans on 3T MRI for radiologist 1 and radiologist 2. The accuracy was better when reporting good 3T MRI scans than when reporting adequate or worse 3T MRI scans for both radiologists (77.2% and 61.3% compared to 72.7% and 50%). The accuracy for radiologist 1 reporting good quality 3T MRI scans

(77.4%) was higher than CT (70.9%). Radiologist 2 was more accurate reporting CT (65.5%) than reporting good quality 3T MRI scans (61.3%).

	Accuracy (95% CI)		
Scan Quality	Radiologist 1	Radiologist 2	N
Adequate or worse	72.7 (51.8-86.8)	50.0 (30.7-69.3)	22
Good	77.4 (60.2-88.6)	61.3 (43.8-76.3)	31

Table 5.12: 3T MRI accuracy in identifying T3 or greater disease, according to scan quality

N1 or greater disease

Table 5.13 compares the accuracy of adequate/good scans 1.5T MRI scans with the accuracy of poor/non-diagnostic 1.5T MRI scans for identifying N1 or greater disease for both radiologists. The accuracy is exactly the same for both radiologists. The accuracy is better for adequate/good scans (60.7%) than for poor/non-diagnostic scans (53.8%) for both radiologists.

	Accuracy (95% CI)		
Scan Quality	Radiologist 1	Radiologist 2	N
Poor or non-diagnostic	53.8 (35.5-71.2)	53.8 (35.5-71.2)	26
Adequate or good	60.7 (42.4-76.4)	60.7 (42.4-76.4)	28

Table 5.13: 1.5T MRI accuracy in identifying N1 or greater disease, according to scan quality

Table 5.14 compares the accuracy of good 3T MRI scans with the accuracy of adequate or worse 3T MRI scans in identifying N1 or greater disease. Accuracy is greater for radiologist 1 reporting good 3T MRI scans than reporting adequate or worse 3T MRI scans (67.7% compared to 52.4%), although not radiologist 2 (61.3% compared to 66.7%). Accuracy reporting good 3T MRI scans is greater than the accuracy reporting CT for both radiologists (61.1% for radiologist 1 and 55.6% for radiologist 2).

	Accuracy (95% CI)		
Scan Quality	Radiologist 1	Radiologist 2	N
Adequate or worse	52.4 (32.4-71.7)	66.7 (45.4-82.8)	21
Good	67.7 (50.1-81.4)	61.3 (43.8-76.3)	31

Table 5.14: 3T MRI accuracy in identifying N1 or greater disease, according to scan quality

EMVI

Table 5.15 compares the accuracy of good/adequate 1.5T MRI scans with poor/non-diagnostic 1.5T MRI scans in identifying EMVI for both radiologists. The accuracy achieved by radiologist 1 was surprisingly very high reporting poor/non-diagnostic 1.5T MRI scans and greater than reporting adequate/good scans (80.8% compared to 67.9%), although this was not the case for radiologist 2 (61.5% poor/non-diagnostic compared to 75% good).

	Accuracy (95% CI)		
Scan Quality	Radiologist 1	Radiologist 2	N
Poor or non-diagnostic	80.8 (62.1-91.5)	61.5 (42.5-77.6)	26
Adequate or good	67.9 (49.3-82.1)	75 (56.6-87.3)	28

Table 5.15: 1.5T MRI accuracy in identifying EMVI, according to scan quality

Table 5.16 compares the accuracy of good 3T MRI scans with adequate or worse 3T MRI scans in identifying EMVI for both radiologists. Surprisingly, the accuracy on adequate or worse 3T MRI scans for both radiologists is very high and greater than that achieved with good 3T MRI scans (81% and 87.5% adequate/worse compared to 71% and 63.6% good). Accuracy on adequate or worse 3T MRI scans was equivalent to or better than that achieved on CT (81.5% and 70.4%)

	Accuracy (95% CI)		
Scan Quality	Radiologist 1	Radiologist 2	N
Adequate or worse	81 (60-92.3)	87.5 (52.9-97.8)	21
Good	71 (53.4-83.9)	63.6 (35.4-84.8)	31

Table 5.16: 3T MRI accuracy in identifying EMVI, according to scan quality

T3c or greater disease

The accuracy for each radiologist in identifying T3c or greater disease on poor/non-diagnostic scans and on adequate/good scans on 1.5T MRI is shown in Table 5.17. As might be expected, the accuracy was higher for both radiologist on the scans which were rated as adequate or good than those rated as poor or non-diagnostic, with the highest accuracy achieved by radiologist 2 with adequate or good scans (88%). These differences are not statistically significant.

	Accuracy (95% CI)		
Scan Quality	Radiologist 1	Radiologist 2	N
Poor or non-diagnostic	65.4 (46.2-80.6)	68.2 (47.3-83.6)	26
Adequate or good	82.8 (65.5-92.4)	87.8 (57.9-87.8)	28

Table 5.17: 1.5T MRI accuracy in identifying T3c or greater disease, according to scan quality

The accuracy for each radiologist in identifying T3c or greater disease on good quality scans compared to adequate or worse scans using 3T MRI is shown in Table 5.18. There wasn't a clear trend in the accuracy, with radiologist slightly more accurate using the MRI scans rated good, but radiologist 2 marginally more accurate using the lower quality 3T MRI scans.

	Accuracy % (95% CI)		
Scan Quality	Radiologist 1	Radiologist 2	N
Adequate or worse	68.2 (47.3-83.6)	81.8 (61.5-92.7)	21
Good	80.6 (63.7-90.8)	77.4 (60.2-88.6)	31

Table 5.18: 3T MRI accuracy in identifying T3c or greater disease, according to scan quality

5.4.3 Number of imaged planes

Table 5.19 shows the number of imaged planes obtained on 1.5T MRI scanning and 3T MRI scanning. The majority of 1.5T MRI scans achieved imaging in either 1 plane (41.8%) or 2 planes (52.7%), with a minority of scans (5.5%) achieving imaging in 3 planes. In contrast, on 3T MRI the majority of scans achieved imaging in 2 planes (52.8%) or 3 planes (45.3%), with a minority achieving imaging in only 1 plane (1.9%).

For further analysis, 1.5T MRI scans were divided two groups; those imaged in only 1 plane in one group and those imaged in 2 or 3 planes in the other group. 3T MRI scans were divided into those imaged in 1 or 2 planes, and those imaged in 3 planes. This was done in order to allow reasonable numbers of MRI scans in each subgroup.

Number of planes	**1.5T MRI (%)**	**3T MRI (%)**
1	23 (41.8)	1 (1.9)
2	29 (52.7)	28 (52.8)
3	3 (5.5)	24 (45.3)
Total	**55 (100)**	**53 (100)**

Table 5.19: 1.5T MRI and 3T MRI number of imaged planes

T3 or greater disease

Table 5.20 compares the accuracy of 1.5T MRI acquired in 2 or 3 planes with the accuracy of 1.5T MRI acquired in only 1 plane for the identification of T3 or greater disease for both radiologists. The accuracy for both radiologists is greater on 1.5T MRI where imaging was achieved in 2 or 3 planes (71.9% and 56.2%) compared to where imaging was achieved in only 1 planes (69.6% and 43.5%).

	Accuracy (95% CI)		
Number of planes	Radiologist 1	Radiologist 2	N
1	69.6 (49.1-84.4)	43.5 (25.6-63.2)	23
2 or 3	71.9 (54.6-84.4)	56.2 (39.3-71.8)	32

Table 5.20: 1.5T MRI accuracy in identifying T3 or greater disease, according to number of imaged planes

Table 5.21 compares the accuracy of 3T MRI acquired in 3 planes with the accuracy of 3T MRI acquired in 1 or 2 planes for the identification of T3 or greater disease for both radiologists. The accuracy for both radiologists was greater where 3T MRI was acquired in 3 planes (79.2% and 66.7%) compared to where 3T MRI was acquired in 1 on 2 planes (72.4% and 48.3%). The accuracy for radiologist 1 reporting 3T MRI scans acquired in 3 planes (79.2%) was higher than CT (70.9%), and this was the highest accuracy of any modality in identifying T3 disease in this study. Radiologist 2 was also slightly more accurate reporting 3T MRI scans acquired in 3 planes (66.7%) than reporting CT (65.5%).

	Accuracy (95% CI)		
Number of planes	Radiologist 1	Radiologist 2	N
1 or 2	72.4 (54.3-85.3)	48.3 (31.4-65.6)	29
3	79.2 (59.5-90.8)	66.7 (46.7-82)	24

Table 5.21: 3T MRI accuracy in identifying T3 or greater disease, according to number of imaged planes

N1 or greater disease

Table 5.22 compares the accuracy of 1.5T MRI acquired in 2 or 3 planes with the accuracy of 1.5T MRI acquired in only 1 plane for the identification of N1 or greater disease for both radiologists. The accuracy for 1.5T MRI acquired in 2 or 3 planes (58.1% for both radiologists) is slightly higher than the accuracy achieved on 1.5T MRI acquired in only 1 plane (56.5% for both radiologists).

	Accuracy (95% CI)		
Number of planes	Radiologist 1	Radiologist 2	N
1	56.5 (36.8-74.4)	56.5 (36.8-74.4)	23
2 or 3	58.1 (40.8-73.6)	58.1 (40.8-73.6)	32

Table 5.22: 1.5T MRI accuracy in identifying N1 or greater disease, according to number of imaged planes

Table 5.23 compares the accuracy of 3T MRI acquired in 3 planes with the accuracy of 3T MRI acquired in 1 or 2 planes for the identification of N1 or greater disease for both radiologists. The accuracy is higher for radiologist 1 reporting 3T MRI acquired in 3 planes (65.2%) compared to 3T MRI acquired in 1 or 2 planes (58.6%). However, the opposite is true for radiologist 2 who achieved greater accuracy reporting 3T MRI acquired in 1 or 2 planes (65.5%) than 3T MRI acquired in 3 planes (60.9%). Accuracy reporting N stage on MRI acquired in 3 planes for both radiologists (65.2%

radiologist 1 and 60.9% radiologist 2) is more accurate accuracy reporting CT for both radiologists (61.1% for radiologist 1 and 55.6% for radiologist 2).

	Accuracy (95% CI)		
Number of planes	Radiologist 1	Radiologist 2	N
1 or 2	58.6 (40.7-74.5)	65.5 (47.3-80.1)	29
3	65.2 (44.9-81.2)	60.9 (40.8-77.8)	24

Table 5.23: 3T MRI accuracy in identifying N1 or greater disease, according to number of imaged planes

EMVI

Table 5.24 compares the accuracy of 1.5T MRI acquired in 2 or 3 planes with the accuracy of 1.5T MRI acquired in only 1 plane for the identification of EMVI for both radiologists. Accuracy was greater for radiologist 1 when reporting 1.5T MRI acquired in 2 or 3 planes (83.9%) than when reporting 1.5T MRI acquired in 1 plane. Accuracy for radiologist 2 was similar when reporting 1.5T MRI acquired in 2 or 3 planes (67.7%) and 1 plane (69.6%).

	Accuracy (95% CI)		
Number of planes	Radiologist 1	Radiologist 2	N
1	60.9 (40.8-77.8)	69.6 (49.1-84.4)	23
2 or 3	83.9 (67.4-92.9)	67.7 (50.1-81.4)	31

Table 5.24: 1.5T MRI accuracy in identifying EMVI, according to number of imaged planes

Table 5.25 compares the accuracy of 3T MRI acquired in 3 planes with the accuracy of 3T MRI acquired in 1 or 2 planes for the identification of EMVI for both radiologists. For radiologist 1, accuracy was similar when reporting 3T MRI acquired in 3 planes (73.9%) and 1 or 2 planes (75.9%).

For radiologist 2, accuracy was better when reporting 3T MRI acquired in 1 or 2 planes (86.2%) than reporting 3T MRI acquired in 3 planes (60.9%).

	Accuracy (95% CI)		
Number of planes	Radiologist 1	Radiologist 2	N
1 or 2	75.9 (57.9-87.8)	86.2 (69.4-94.5)	29
3	73.9 (53.5-87.5)	60.9 (40.8-77.8)	23

Table 5.25: 3T MRI accuracy in identifying EMVI, according to number of imaged planes

T3c or greater disease

The accuracy for each radiologist in identifying T3c or greater disease on 1.5T MRI scans with the tumour imaged in 1 plane, and on 1.5T MRI scans imaged in 2 or 3 planes, is shown in Table 5.26. There was no difference in accuracy for radiologist 1, with radiologist 2 demonstrating slightly greater accuracy when tumours were imaged in only one plane. There is wide overlap in the 95% confidence intervals.

	Accuracy (95% CI)		
Number of planes	Radiologist 1	Radiologist 2	N
1	73.9 (53.5-87.5)	82.6 (62.9-93.0)	23
2 or 3	75 (57.9-86.7)	68.8 (51.4-82.0)	31

Table 5.26: 1.5T MRI accuracy in identifying T3c or greater disease, according to number of imaged planes

The accuracy for each radiologist in identifying T3c or greater disease on 3T MRI with the tumour imaged in 1 or 2 planes, and on 3T MRI with the tumour imaged in 3 planes, is shown in Table 5.27. There was no difference in accuracy according to the number of imaged planes for radiologist 1, but

a slightly higher accuracy for radiologist 2 when the tumour was imaged in 3 planes. There is again wide overlap in the 95% confidence intervals.

	Accuracy (95% CI)		
Number of planes	Radiologist 1	Radiologist 2	N
1 or 2	75.9 (57.9-87.8)	72.4 (54.3-85.3)	29
3	75.0 (55.1-88.0)	87.5 (69.0-95.7)	23

Table 5.27: 3T MRI accuracy in identifying T3c or greater disease, according to number of imaged plane

5.4.4 Discussion

There are some significant limitations to this study, which necessitate some caution in the interpretation of the results. This was a secondary analysis of the colon MRI trial reported in chapter 4, performed as a result of the observed variation in scan quality particularly with in upper abdominal tumours on 1.5T MRI. This secondary analysis was not part of the original trial protocol. Subdividing of the scans into smaller groups means that the number of patients in each group is small (20-30 patients), making the 95% CI for the accuracy values broad. I have also performed multiple hypothesis testing in this chapter, increasing the risk of a type I error. The results reported in this chapter can therefore only be used as an indication of the direction for possible further research.

When examining the local staging accuracy of CT and MRI in subgroups divided on the tumour location, we had anticipated that there would be little difference in CT staging between the upper and lower abdomen, but that staging on MRI would be more accurate in the lower abdomen than in the upper abdomen, and that this difference would be most pronounced for 1.5T MRI. The rationale for this is based on the amount of movement in the upper and lower abdomen. We already know from rectal cancer studies that MRI is fairly accurate for local staging of the rectum in the pelvis,

where the bowel is fixed and there is relatively little motion artefact. However, in the abdomen, small bowel peristalsis creates motion artefact which degrades MRI image quality. In the upper abdomen, this is compounded further by movement of the diaphragm from respiration. 1.5T MRI is more susceptible to image degradation from motion artefact than 3T MRI due to longer acquisition time.

We did observe this trend in the identification of T3 or greater disease for radiologist 2 at both field strengths, the identification of N1 or greater disease for both radiologists and both field strengths, the identification of EMVI for radiologist 1 at 1.5T MRI and radiologist 2 at both field strengths, and for the identification of T3c disease for radiologist 1 at both field strengths and radiologist 2 on 3T MRI. However, T-staging for radiologist 1 at both field strengths and the identification of EMVI at 3T was more accurate in the upper abdomen. The number of patients in each subgroup is quite small, so there is substantial overlap in the 95% confidence intervals and so no definite conclusions can be drawn from these results, but overall the trends do suggest that MRI may be more accurate in the lower abdomen than the upper abdomen.

The number of poor quality scans was high, particularly on 1.5T MRI with almost half being graded as less than adequate. This is despite the steps taken to optimise the MRI protocol in a series of volunteer scans (chapter 3), and the majority of scans being performed by one of 3 research radiographers at the Royal Marsden Hospital site. The principle limiting factor was motion artefact for the T2 weighted imaging, particularly from diaphragmatic movement in the upper abdomen. Although a number of ultrafast sequences have been introduced to abdominal MRI in recent years, they all have some compromise in terms of susceptibility artefacts, loss of true T2 weighting or reduction in signal to noise ratio. It therefore remains difficult to obtain high quality T2 weighted imaging in the presence of motion. It may be this limitation which has led to the paucity of published trials assessing MRI in the staging of colon cancer. It is interesting to note that in the only recent published trial investigating MRI staging of colon cancer 6 of 34 eligible patients (18%) could not have an adequate MRI scan performed with the high resolution protocol (Rollven et al., 2013).

The overall quality of MRI scans obtained at 3T MRI was better than the overall quality of scans obtained using 1.5T MRI, with 58.5% compared to 10.9% of scans being graded as good, and 9.4% of scans compared to 47.3% of scans being graded as less than adequate. This is in keeping with the anticipated benefits from 3T MRI in terms of better signal to noise ratio and shorter image acquisition time. Unfortunately, the scans were only graded by one observer who was not a radiologist which limits the clinical relevance of this finding. I was not able to obtain grading of the scans by expert radiologists, as this was not part of the original trial protocol.

For radiologist 1, accuracy in identifying T3 disease increased from 69.2% to 72.4% in the adequate or better scans compared to the poor or worse scans at 1.5T, and increased from 72.7% to 77.4% in the good compared to the adequate or worse scans at 3T. This compares favourably to 70.9% using CT.

For radiologist 2, accuracy in identifying T3 disease increased from 42.3% to 58.6% in the adequate or better scans compared to the poor or worse scans at 1.5T, and increased from 50.0% to 61.3% in the good compared to the adequate or worse scans at 3T. This is compared to an accuracy of 65.5% for CT.

For both radiologists, accuracy in identifying T3 disease increased with better quality scans, as might be expected. Radiologist 1 was able to achieve a greater accuracy in correctly identifying T3 disease using adequate or higher quality MRI scans than either radiologist were able to achieve using CT scan, although this was not the case for radiologist 2.

However, caution must be used in the interpretation of these results as the number of scans in each subgroup is quite small making the confidence intervals relatively wide, and so these differences in accuracy do not achieve statistical significance.

Similar trends were seen when assessing the accuracy of MRI in identifying N1 or greater disease, with both radiologist being more accurate on 1.5T MRI with better quality scans, and radiologist 1

also being more accurate on 3T MRI with better quality scans. Surprisingly, this trend was not continued in the assessment of EMVI, accuracy generally being lower on better quality scans.

I have also assessed the accuracy of both radiologists in the identification of T3c or greater disease. This combines assessment of T-stage with assessment of depth of extramural invasion, and as previously discussed is a clinically important end point. This end point was also presented in the study by Rollven et al which assessed the accuracy of 1.5T MRI in the assessment of colon cancer (Rollven et al., 2013). Accuracy for radiologist 1 reporting adequate or good 1.5T MRI scans is then 82.8% (95% CI 65.5% to 92.4%), and reporting good 3T MRI scans is 75.9% (95% CI 57.9% to 87.8%). Accuracy for radiologist 2 reporting adequate or good 1.5T MRI scans is 87.8 (95% CI 57.9% to 87.8%), and good 3T MRI scans 77.4% (95% CI 60.2% to 88.6%). These accuracies are still lower than those reported by Rollven et al (89.7% for observer 1 and 93.1% for observer 2), but are comparable with overlap in the 95% confidence intervals.

The final subgroup analysis involved separating patients according to the number of imaged planes using T2 weighted sequences. There was unsurprisingly substantial overlap between the number of imaged planes and the overall scan quality, as patients who were able to lie still and tolerate imaging in multiple planes generally had better quality MRI scans than those who were not.

Similar trends were therefore seen in terms of accuracy for the subgroup of patients imaged in multiple planes as the subgroup of patients who had better quality MRI scans. T stage accuracy was better for both radiologists on both 1.5T MRI and 3T MRI when the tumour was imaged in more planes. The highest accuracy in identifying T3 disease was achieved by radiologist 1 on 3T MRI with the tumour imaged in 3 planes (79.2%, 95% CI 59.5% to 90.8%).

The results were also similar in the assessment of N1 disease, with smaller improvements in accuracy for images acquired in multiple planes then seen in the T-staging, except for radiologist 2 on 3T MRI. There was again no clear trend in the accuracy of the identification of EMVI.

Higher accuracies were achieved in the identification of T3c disease with images obtained in multiple planes through the tumour. On 1.5T MRI with images in 2 or 3 planes, radiologist 1 achieved an accuracy of 75% (95% CI 58% to 87%) and radiologist 2 achieved an accuracy of 69% (95% CI 51% to 82%). On 3T MRI with images in 3 planes radiologist 1 achieved a similar accuracy of 75% (95% CI 55% to 88%), and radiologist 2 again achieved a very high accuracy of 88% (95% CI 69% to 96%). This is again comparable with the accuracy achieved by Rollven et al (90% for observer 1 and 93% for observer 2).

In summary, although these results need to be interpreted with caution due to the low number of patients in the subgroup analysis, it does appear that highly accurate local staging of colon cancer may be possible using MRI when high quality T2 weighted images can be acquired in multiple planes, and these results are consistent with the only other published recent trial which has examined the accuracy of MRI in staging colon cancer. N-staging is less accurate, but the accuracy achieved on high quality MRI again compares favourably to the accuracy achieved using CT. Staging accuracy of EMVI is more inconsistent. It is interesting to note that this is also the prognostic feature with the lowest inter-observer reliability on histopathological assessment, suggesting that histopathological assessment of EMVI may be less accurate than other prognostic factors. In chapter 6, we will examine whether the incorporation of high resolution MRI of the ex-vivo specimen can help improve the accuracy of histopathological assessment.

CHAPTER 6

Randomised comparison of conventional histological processing of colorectal cancers with MRI guided specimen dissection for histology

6.1 My role in this chapter

With the support of my supervisor, I wrote the trial protocol, obtained ethical approval, prospectively recruited the patients for this study, performed the data collection and data analysis, and wrote this chapter. I was the first author for the published abstract arising from it (Hunter et al., 2012). Suzanne St Rose provided statistical support during the trial design and Tom Fanshawe reviewed the statistical analysis following the write up of the trial.

6.2 Introduction and rationale

Prior to microscopic assessment, colorectal cancer specimens must first have histological sections prepared. This is a multi-step process.

The colorectal cancer specimen is first inspected and macroscopic features are recorded. These include the site of the tumour, the maximum tumour diameter, distance to the nearest end resection margin, evidence of tumour perforation, and for rectal tumours the relation of the tumour to the peritoneal reflection and grade of surgical excision. For abdominoperineal resections the distance of the tumour from the dentate line is also recorded. At this stage the non-peritonealised resection should be inked so that it can be identified when examining histological sections.

Next, the specimen is fixed in formalin. The Royal College of Pathology recommend that the specimen is opened except for the segment including 1 or 2 cm above and below the tumour. The specimen pinned out on a cork board and submerged in 10% neutral buffered formalin (4% formaldehyde in phosphate buffered saline), for a minimum of 48 hours (Williams et al., 2007). This allows adequate fixation of the specimen to prevent autolysis and preserve the tissues by cross linking proteins. Adequate fixation also allows thin transverse slicing through the tumour and helps in the identification of lymph nodes.

Following fixation, the colorectal cancer specimen is carefully dissected by the histopathologist, with thin transverse slicing through the tumour and attached mesentery. Tumour blocks are then selected from these slices and should aim to represent (Williams et al., 2007):

- Deepest penetration of the tumour into the bowel wall or surrounding tissue
- Any involvement of the serosal surface
- Any extramural venous invasion
- Any involvement of adjacent organs
- The closest circumferential resection margin (non-peritonealised resection margin)
- The distance of the tumour from the proximal or distal resection margins if within 30mm
- All lymph nodes within the specimen

The Royal College of Pathologist recommends that a minimum of 4 tumour blocks and any identified lymph nodes should be selected for this purpose.

Next, the selected tumour blocks are dehydrated through submersion in successive baths of increasing alcohol concentration and a clearing agent before being embedded in paraffin wax. This creates Formalin Fixed, Paraffin Embedded (FFPE) tissues, the most common type used for light microscopy.

FFPE tissues are then sectioned using a microtome to produce 4µm sections, which can be mounted on a glass slide. The sections are then stained, most commonly with hematoxylin and eosin stain, so that they can be viewed on a light microscope.

According to the Royal College of Pathologist guidelines, if 4 tumour blocks are selected and one section is taken from each tumour block, then a total of 4 x 4µm = 16µm thick sample of tissue will be examined from the tumour. In the current study, tumours ranged from 5mm to 130mm in length. This means that between 0.32% and 0.012% of the tumour would be viewed in the selected sections if whole mount sections were taken through the entire diameter of the tumour. In practice, the tumour diameter is often larger than the maximum tumour block size, so tumour slices are cut down

when producing tumour blocks. This further reduces the proportion of the tumour which is examined microscopically.

Histopathological assessment of colorectal cancer is an accurate process, with UICC/AJCC tumor node metastasis stage (TNM) considered the gold standard prognostic indicator (Zlobec and Lugli, 2008). However, there is substantial evidence that inadequate tumour sampling at the time of the specimen dissection can reduce this accuracy.

Many prognostic factors, such as peritoneal involvement, are reliably reported when different pathologists review the same hematoxylin and eosin (H&E) stained slides with a high level of interobserver agreement (Littleford et al., 2009). However, there is considerable variation in the frequency with which the same prognostic factors are reported between pathologist; this varies from 7% to 39% for peritoneal involvement, and from less than 10% to more than 30% for EMVI (Messenger et al., 2011).

Previous studies have demonstrated that the number of tumor blocks taken during cut-up impacts on the identification of adverse prognostic features; a higher number tumor blocks are associated with a greater T-stage (Quirke et al., 2007), an increased incidence of non-peritonealised resection margin involvement (Quirke et al., 1986), and increased likelyhood of identifying EMVI (Betge et al., 2012). Careful selection of representative tumor blocks by the histopathologist is paramount. Inadequate initial dissection of the colorectal cancer specimen and insufficient tumor block selection can result in under staging of tumor, and this cannot be redeemed with a sophisticated microscopic examination at a later stage (Shepherd and Quirke, 1997).

Lymph nodes may also be missed during standard specimen dissection and result in under-staging. Fat clearance techniques have been demonstrated to identify an average of 10 additional lymph nodes per specimen compared to traditional histological examination, and 4.4% of these contain tumour deposits increasing the N-stage in 6% of patients (Hernanz et al., 2010). Apparently N0

patients with <3 lymph nodes identified on histological examination have a 5% worse disease specific survival at 5 years compared to those with >12 lymph nodes identified (Namm et al., 2008).

We have demonstrated in chapters 4 and 5 that using MRI it is possible in some cases to obtain high quality MRI images of colon as well as rectal cancers (although movement artefact degraded image quality in a significant number of cases), and that when high quality images MRI images are used to stage colon cancers a high degree of staging accuracy can be achieved. Ex-vivo scanning of colorectal cancer specimens offers the potential to obtain higher quality images, as problems of motion artefact are removed.

However, there is an inherent limitation in the spatial and contrast resolution of MRI. The limit to the spatial resolution of standard optical microscopy in the visible light spectrum is around 250nm (Nienhaus and Nienhaus, 2014), whereas the lowest resolution achieved in the ex-vivo MRI scans in this study was approximately 0.5mm. Clinical MRI is therefore approximately five orders of magnitude lower than that which can be obtained using light microscopy.

MRI is capable of visualising the entire colorectal cancer specimen, but at a relatively low resolution. Optical microscopy used for histology visualises the colorectal cancer specimen with a resolution around 2×10^5 greater than MRI, but only examines approximately 0.1% of the specimen. Although the tumour slices are carefully inspected by the histopathologist at dissection, key histological features can be obscured within a tumour slice so that the correct tumour slice is not selected or sectioned deeply enough. In addition, the tumour is commonly sliced in only one plane, perpendicular to the long axis of the bowel. This can make it difficult to appreciate the nature of tumour extension or deposits running through plane, particularly EMVI (Sternberg et al., 2006).

We hypothesized that combining the benefits of MRI imaging and histopathology by using high resolution ex-vivo MRI scans of the colorectal cancer specimens to select tumour blocks for histological assessment might improve the selection of tumour blocks for histopathology. We further hyptothesised that this would increase the T-stage and N-stage of tumours where blocks

were selected with the help of MRI, in the same way that selecting additional tumour blocks is associated with a higher T-stage (Quirke et al., 2007), and that fat clearance techniques which identify more lymph nodes are associated with an increase in N-stage (Hernanz et al., 2010).

6.3 Materials and Methods

6.3.1 Subjects

This was a prospective randomised controlled study, comparing two methods of histological examination to determine whether selecting tumour blocks on the basis of a high resolution specimen MRI would result in upstaging compared to conventional histology. Patients were recruited from Croydon University, and Epsom and St Helier Hospitals.

Consecutive patients presenting with adenocarcinoma of the colon or rectum who were to undergo surgery to excise their colorectal cancer, were included in the study. Patients were excluded if they withheld or withdrew consent, were under the age of 18, or were not fit to undergo a potentially curative resection of their tumour.

Patients in the study were treated according to the plan determined by the multi-disciplinary team responsible for their care. All staging information determined as part of this study was made available to the multidisciplinary team.

Ethical approval was been obtained from the National Research Ethics Service, Kent Research Ethics Committee before commencing recruitment (REC reference number 10/H1101/25). The study was conducted in accordance with the conditions of ethical approval. Local R&D approval was obtained at each site. Informed consent was obtained from all patients prior to recruitment.

6.3.2 Randomisation

Specimens were randomised to undergo “conventional histology” (tumour blocks selected by visual inspection only) or “MRI assisted histology” (where an MRI of the specimen was performed and used to aid in the selection of tumour blocks), following informed consent and successful surgical resection of their colorectal cancer. Randomisation was performed using a telephone randomisation service run by the Institute for Cancer Research, 15 Cotswold Road, Belmont, Sutton, Surrey SM2 5NG. This service was based on a computerised block randomisation and the researcher was blind to the randomisation result until after allocation.

6.3.3 Procedures

All specimens were pinned out anatomically on a cork board, and then underwent formalin fixation in a large volume of 10% neutral buffered formalin (4% formaldehyde in phosphate buffered saline) for a minimum of 48 hours. Those specimens randomised to MRI assisted histology were taken in a sealed bag to the MRI scanner and high resolution axial and 3D imaging was performed through the entire specimen.

6.3.4 MRI technique

MR imaging was performed on a Siemens Avanto 1.5T MRI scanner. The specimen was placed in the MRI scanner in a sealed plastic bag, in a head or body coil depending on specimen size. T2 weighted 3D SPACE sequence was then performed through the whole specimen, which allows reformatting of images in any plane and visualisation of any mesenteric lymph nodes. The field of view for these images varied from 200x200mm to 360x360mm depending on tumour size. The acquisition matrix was 256x256 pixels, giving a voxel size of 0.78x0.78x0.78mm to 1.4x1.4x1.4mm. The slice thickness corresponded the voxel size to maintain isotropic voxels (0.78-1.4mm), with no inter-slice gap. TR was 1500ms and TE was 100ms.

Following acquisition of the 3D images, these were used to plan high resolution T2 weighted 2D TSE images perpendicular to the long axis of the tumour through the entire tumour and adjacent mesentery. The field of view was kept constant at 160x160mm, with a matrix size of 256x256 pixels and resulting pixel size of 0.625x0.625mm. The slice thickness was 3mm, with a 10% inter-slice gap. The number of slices varied from 22 to 47 to include the entire length of the tumour with a margin at each end. TR was 4300ms and TE was 100ms.

Finally, DWI was obtained through the same region and in the same orientation as the 2D TSE weighted sequences. DWI was acquired using a single shot spin echo sequence with echo-planar imaging (EPI) and SPAIR fat suppression. Repetition time was 4800 ms and echo time was 68 ms. Three b-values were used: 0, 350 and 750 s mm^{-2}.

6.3.5 Specimen MRI assessment

Prior to dissection of the colorectal cancer specimen, all specimen MRIs were reviewed by one consultant specialist GI radiologist with more than 10 years' experience interpreting colorectal cancer imaging. The maximum depth of invasion, closest non-peritonealised resection margin, any areas of serosal involvement, any extra mural vascular invasion and all lymph nodes were identified on the specimen MRI. These were highlighted for the research fellow who attended cut up on each with graphical markers highlighting these features in each relevant MRI slice.

6.3.6 MRI-Specimen correlation

Prior to dissection of the colorectal cancer specimen, each MRI slice was printed on to a sheet of plain A4 paper to allow annotation in the cut up room. In addition, the specimen MRI was also available on a DICOM viewer in the cut up room. The DICOM viewer allowed multi-planar reformatting to aid in correlation between the specimen MRI and the colorectal cancer specimen if the orientation of the MRI slices and the specimen slices was not exact. Colonic size and shape, tumour morphology, shape and location of the mesentery, size and location of blood vessels and any

lymph nodes were used to correlate each histological slice with the corresponding MRI slice. An example of the correlation between the specimen MRI slices and the specimen slices is shown in Figure 6.1 and Figure 6.2. In Figure 6.2 the specimen MRI slice and histological sections are taken at slightly different angles, so lymph nodes (a and b) are seen in adjacent slices on the specimen MRI

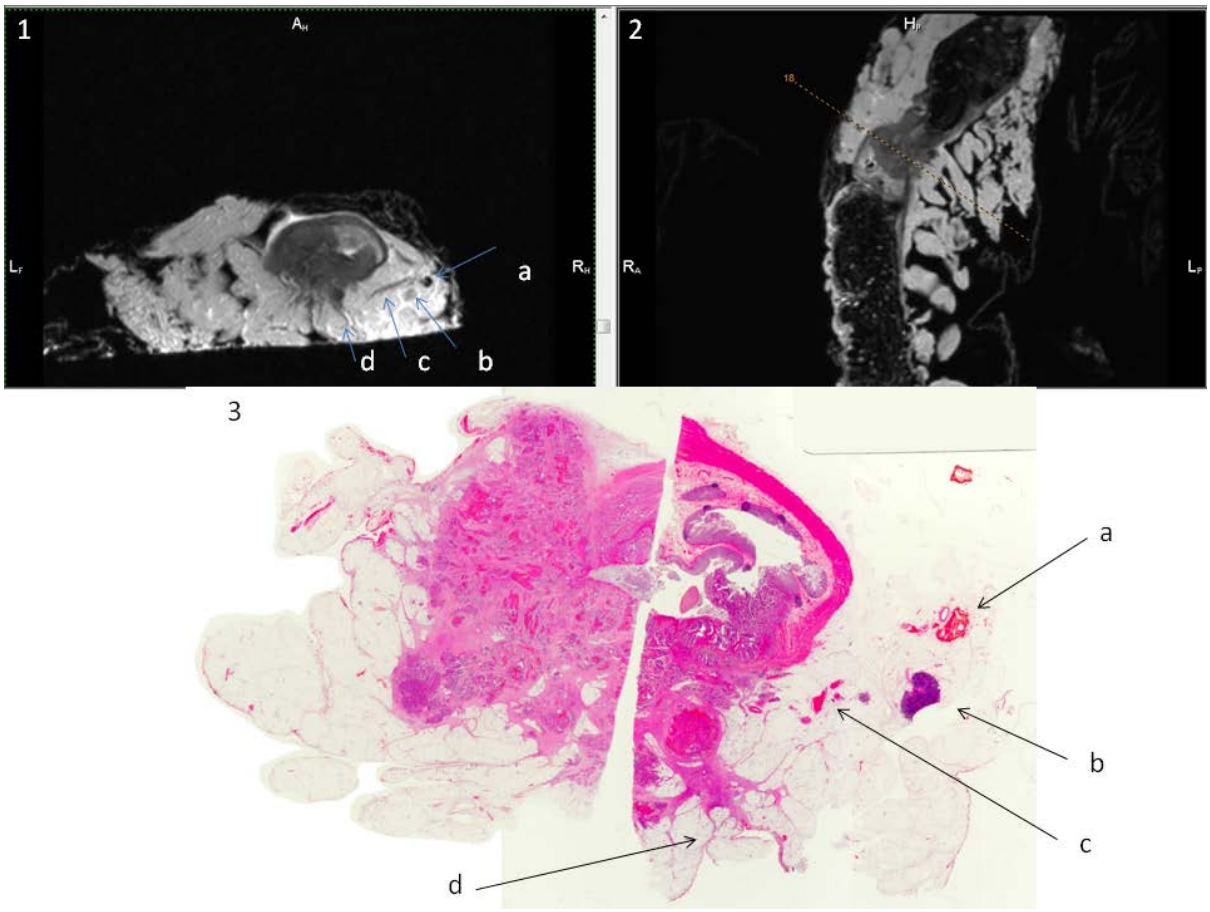


Figure 6.1: Specimen MRI and histological section correlation

a) Blood vessel in transverse section b) Lymph node c) Blood vessel in longitudinal section d) EMVI

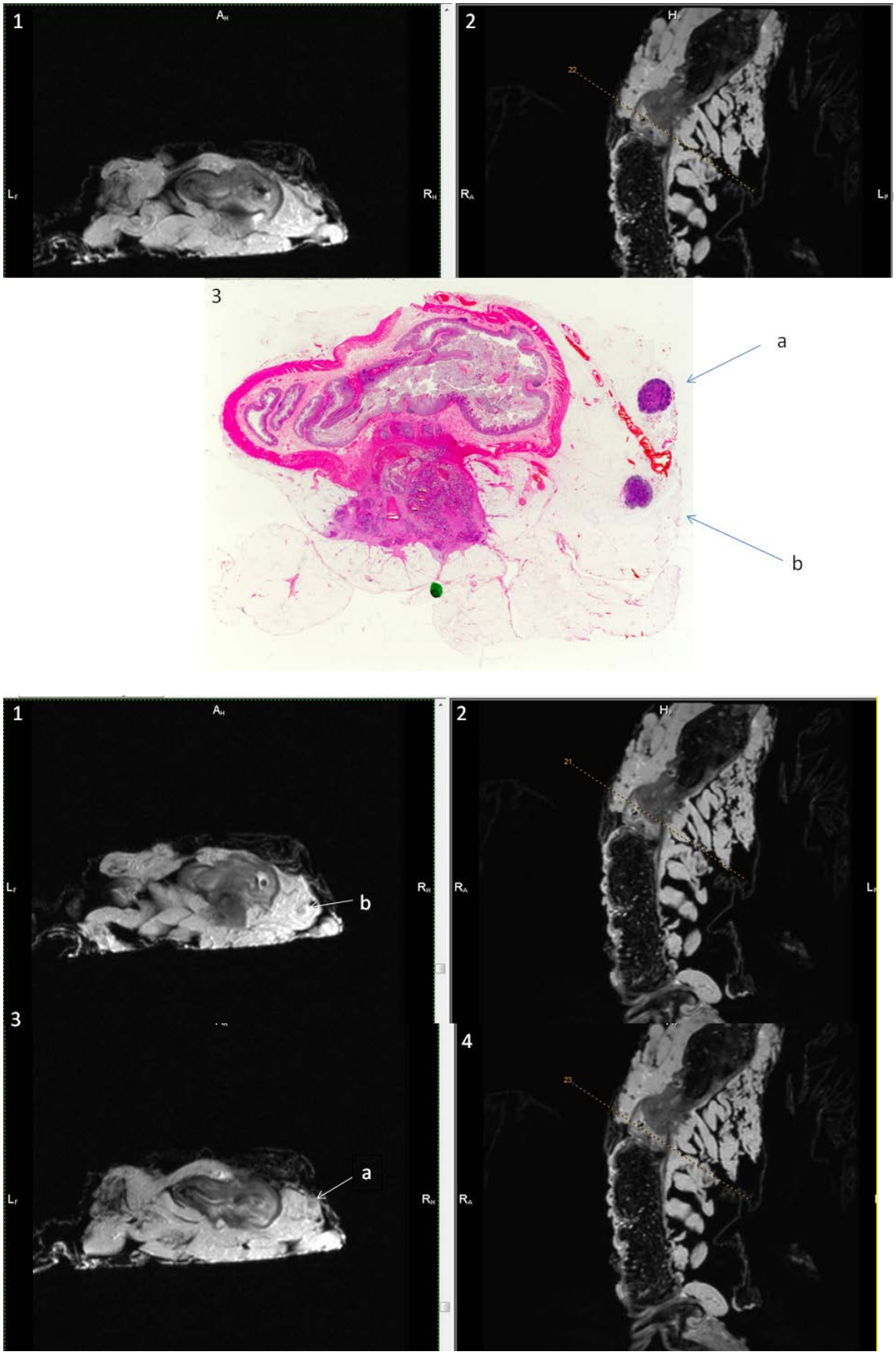


Figure 6.2: Correlation of off axis specimen MRI and histological section

6.3.7 Tumour block selection

All histopathological assessments were performed by one of four consultant histopathologists with more than 10 years' experience and a subspecialty interest in gastro-intestinal pathology. For all specimens, the histopathologist performed their usual examination of the specimen. Axial sectioning of the specimen was performed at 5mm intervals, and the tissue slices were laid out and inspected. The pathologist chose the tumour blocks from which they would normally take sections for microscopic examination. The pathologist was then asked to select four additional tumour blocks. The Royal College of Pathologists recommends that the minimum number of tumour blocks taken for the assessment of a colorectal cancer is four, with as many additional blocks taken as necessary to ensure that the tumour has been adequately sampled. The number of tumour blocks taken varies widely, with some studies routinely taking a mean of 24 tumour blocks (Sternberg et al., 2006). It was important in this study to standardise the number of additional tumour blocks taken in both arms, so that any difference between the two groups was not due to a higher number of sampled tumour blocks. Four additional tumour blocks were agreed by the two principle pathologists participating in the study (Louis Temple and Abed Arnaout), as being a good compromise with a reasonable chance of detecting additional pathological features while being attainable in the majority of tumours.

For specimens randomised to MRI assisted histology four additional tumour blocks were selected by the research fellow to include any areas which had previously been marked as significant on MRI scans by the consultant GI radiologist, and which had not been included in the initial tumour blocks selected by the consultant histopathologist.

For specimens assigned to conventional histology, the four additional tumour blocks selected by the histopathologist by visual inspection were taken for histological examination, so that the number of additional slices taken was the same in both arms.

A histology report was then prepared from the selected tumour blocks (standard blocks and additional blocks selected by visual inspection in the conventional histology arm, standard blocks and additional blocks selected by MRI in the MRI arm). In some small tumours, it was not possible to take four additional tumour blocks in addition to the standard tumour blocks, in which case all available additional blocks were taken. The T-stage, N-stage, depth of invasion and presence of EMVI, number of lymph nodes identified, and overall AJCC stage (American Joint Committee on Cancer stage which incorporates T and N-stage) was recorded.

In addition, blocks were taken to include all lymph nodes identified in by visual inspection and palpation in both groups. Any additional lymph nodes identified with the aid of the MRI in the specimen MRI group were also taken. A flow diagram illustrating the trial is shown in Figure 6.3.

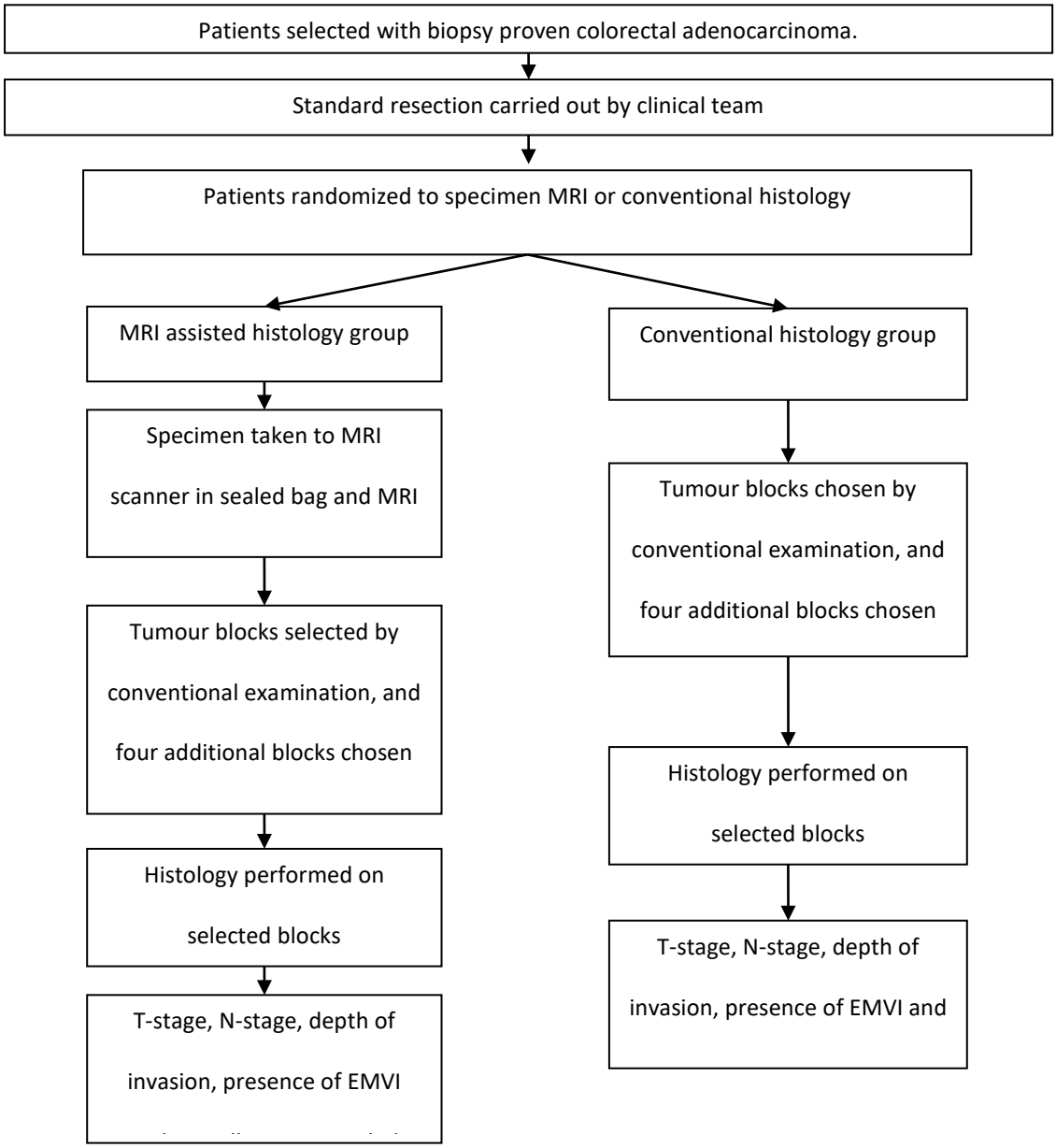


Figure 6.3: Specimen MRI trial flow diagram

6.3.8 Evaluation

The primary end point was overall stage in the MRI assisted histology and conventional histology groups.

Secondary end points were; T-stage, N-stage, number of involved lymph nodes, number of examined lymph nodes, apical lymph node involvement, depth of extramural spread, tumor perforation, CRM distance and presence of EMVI. These endpoints were also considered as dichotomous adverse features; T3 or greater disease, lymph node positive disease, less than twelve examined lymph nodes, apical node involved, more than 5mm extramural spread, tumor perforation, involved CRM (<1mm) and EMVI positive. Histological staging was based on the TNM version 5 classification.

Essential patient demographics were also recorded, including age, gender, tumour location, operation performed, method of resection (open/laparoscopic), surgeon experience, TNM stage based on pre-operative assessments, and any neoadjuvant therapy received.

6.3.9 Statistical analysis

Power calculation:

The study was designed to have 80% power to detect a 15% difference in the proportion of patients with an overall AJCC stage of IIB or greater in each group, with a significance level (or α) of 0.05. This was an unpaired design, so a Chi-squared test was used. I anticipated that 65% of patients in the control group would be AJCC stage IIB or greater, and that 80% of patients in the intervention arm would be AJCC stage IIB or greater. A Chi-square test with a one-sided significance level of 0.05 therefore required 109 tissue specimens in each arm. This required a total of 218 tissue specimens and 218 patients (109 in each arm) undergoing histological assessment.

This power calculation was initially for a two-sided significance level, but was changed at the request of the Royal Marsden committee for clinical research (CCR), as they felt that the MRI intervention could only result in upstaging. On reflexion, this was a mistake as selecting additional tumour blocks by visual selection may be superior to selecting additional tumour blocks using MRI, and we should have continued with a two-sided significance level. This would have resulted in a power calculation requiring 152 patients in each arm, or 304 in total.

I also failed to take account of drop outs following recruitment. Anticipating a dropout rate of approximately 10%, which is typical for clinical trials, the total number of patients that would have needed to be recruited was 334 patients.

Descriptive statistics:

Patients were included in the analysis if they had histology available on the basis of their intended group (evaluable patients on intended method for histological examination). Descriptive statistics were used to summarize patient baseline characteristics (including age, sex, tumour location, pre-operative staging, pre-operative chemo-radiotherapy, operation performed). Quantitative variables were expressed as means with standard deviation (SD) if normally distributed or as medians with interquartile range (IQR). Qualitative variables were expressed as frequencies and percentages.

Summary statistics:

The Welch 2 sample t-test was used to compare whether difference in the mean of normally distributed variables was significant between the conventional histology group and the MRI assisted histology groups.

The non-parametric Wilcoxon rank sum test was used for non-normally distributed continuous and ordinal variables. Chi-square or Fisher's exact test was used to test whether there was a significant difference in proportions (that is, proportion of EMVI positivity and involvement of non-peritonealised resection margins) between the two groups.

The level of significance is set at $P<0.05$. Missing data is recorded. Analysis was performed using R statistics (version 3.2.1) software (R Core Team, 2015).

6.4 Results

6.4.1 Recruitment

Recruitment commenced September 2010 and ended in August 2012. During this period, 260 potentially suitable patients were identified at two trusts (Croydon University Hospital NHS Trust and Epsom and St Helier University Hospitals NHS Trust). Of these, 145 patients were recruited into the specimen MRI study (55.8%). Reasons for patient non recruitment are listed in Table 6.1.

Reason	Number of patients	Percentage of suitable patients
Unable to contact before surgery	42	16.2
Unable to arrange specimen MRI	29	11.2
Did not consent	24	9.2
Other	20	7.7
Total	**115**	**44.3**

Table 6.1: Reasons patients not recruited to specimen MRI trial

Of the 145 patients recruited into the study, 15 (10.4%) were withdrawn from the study prior to randomisation into MRI assisted or conventional histology group. The reasons for withdrawal prior to randomisation are listed in Table 6.2.

Reason	Number of patients	Percentage of recruited patients
Trial pathologist unavailable	9	6.2
Did not undergo surgery	3	2.1
Lab error	2	1.4
Operation performed at different trust	1	0.7
Total	**15**	**10.4**

Table 6.2: Reasons for withdrawal from specimen MRI trial

Of the 130 patients randomised, 64 (49.2%) were allocated to the conventional histology group, and 66 (50.7%) were allocated to the specimen MRI group. One patient (0.8%) allocated to the specimen MRI group was incorrectly processed in the conventional histology group, due to lab error. However, the results were analysed on an intention to treat basis so this patient was analysed in the specimen MRI group.

6.4.2 Demographics

Essential demographic data for the whole group, patients randomised to the conventional group and patients randomised to the MRI group are shown in Table 6.3.

Age:

The mean age and standard deviation of patients randomised as part of the study are shown in Table 6.3. The mean age of patients randomised to the specimen MRI group is slightly lower than that of patients randomised to the conventional group, and this difference almost achieves statistical significance (p=0.05), using the Welch two sample t-test for normally distributed data. However, as the patients were blindly randomly assigned to conventional or MRI groups this is probably due to random chance. It is also unlikely to have had an impact on the outcome of the study. The normal

Q-Q plot for the age of patients in the trial indicates that the age of patient included in the trial is fairly normally distributed.

Gender:

The gender of patients included in the trial, and randomised to each group, is shown in Table 6.3. Overall, 60% of patients were male, and there is no significant difference between the conventional group and the MRI groups.

Tumour location:

The locations of tumours for patients recruited to the study, and randomised to each arm, are shown in Table 6.3. The largest number of tumours is located within the rectum, followed by the sigmoid colon and right colon. There is no significant difference in the distribution of tumours between the two groups.

Pre-operative T-stage

The T-stage, as assessed on pre-operative imaging, is listed in Table 6.3. The majority of tumours are T3 tumours (64.5%). Importantly there is no significant difference in the pre-operative T-stage of tumours in the conventional and MRI group, as it might have been expected to influence the results if there was a significant bias in pre-operative staging between the groups.

Pre-operative N-stage

The pre-operative N-stage on imaging of patients recruited to the specimen MRI trial and randomised to each group is shown in Table 6.3. Half of patients are N0, with the majority of the remainder N1 and around 10% of patients having N2 disease. There is no significant difference between the conventional group and MRI group. Again this is important, as if there was a substantial difference in the pre-operative staging between the two groups this might have been expected to influence the outcome of the study.

	All patients (n=130)	Control group (n=64)	MRI Group (n=66)	p-value
Mean age, years (SD)	71.6 (12.6)	73.8 (11.4)	69.5 (13.4)	0.05†*
Gender				0.47‡
Male	78 (60%)	36 (56.3%)	42 (63.6%)	
Female	52 (40.0%)	28 (43.8%)	24 (36.4%)	
Tumour location				0.75Ŧ
Caecum	14 (10.8%)	7 (1.1%)	7 (10.6%)	
Ascending colon	16 (12.3%)	10 (15.6%)	6 (9.1%)	
Hepatic flexure	6 (4.6%)	3 (4.7%)	3 (4.5%)	
Transverse colon	12 (9.2%)	7 (10.9%)	5 (7.6%)	
Splenic flexure	2 (1.5%)	0 (0.0%)	2 (3.0%)	
Descending colon	7 (5.4%)	2 (3.1%)	5 (7.6%)	
Sigmoid colon	33 (25.4%)	15 (23.4%)	18 (27.3%)	
Rectum	40 (30.8%)	20 (31.3%)	20 (30.3%)	
Pre-operative T-stage				0.97§
T1	6 (4.8%)	5 (8.3%)	1 (1.6%)	
T2	26 (21.0%)	9 (15.0%)	17 (26.6%)	
T3	80 (64.5%)	41 (68.3%)	39 (60.9%)	
T4	12 (9.7%)	5 (8.3%)	7 (10.9%)	
Missing	6	4	2	
Pre-operative N-stage				0.97§
N0	62 (50.0%)	30 (50.0%)	32 (50.0%)	
N1	48 (38.7%)	23 (38.3%)	25 (39.1%)	
N2	14 (11.3%)	7 (11.7%)	7 (10.9%)	
Missing	6	4	2	
Pre-operative M-stage				1.0‡
M0	118 (95.2%)	57 (95.0%)	61 (95.3%)	
M1	6 (4.8%)	3 (5.0%)	3 (4.7%)	
Missing	6	4	2	

†Welch two sample t-test, ‡Fisher's exact test, §Wilcoxon rank sum test, *Statistically significant

Table 6.3: Demographic details

Pre-operative M-stage

The pre-operative M-stage of patients recruited to the study are shown in Table 6.3. Only a small proportion (around 5%) of patients recruited to the study had metastatic disease on pre-operative imaging, as patients had to be undergoing resection of their primary tumour to be recruited into the study. Again, there was no significant difference between the conventional group and the MRI assisted histology group with significant overlap in the 95% confidence interval for the difference in proportions.

Operation performed

The operation performed for patients recruited to the study and randomised to each group is listed in Table 6.4. The most commonly performed operations were right hemicolectomy (38.4%) and anterior resection (38.4%). There was no significant difference between the two study groups.

Laparoscopic surgery

The type of surgery performed (Laparoscopic, converted to open, or open) for each group is shown in Table 6.3. There was a trend towards a higher number of cases which were converted to from laparoscopic to open in the conventional group compared to the MRI group (28% compared to 11%), and a lower number of primary open operations in the conventional group compared to the MRI group (44% compared to 52%). These trends did not reach statistical significance but did approach it ($p=0.07$ Fisher's exact test).

Surgeon experience

The grade of surgeon completing the surgery for each group is shown in Table 6.3. Over 90% of operations in both groups were completed by consultant surgeons and there was no significant difference between the two groups.

Pre-operative radiotherapy

The proportion of patients receiving pre-operative radiotherapy in the whole study group, and randomised to each arm, is shown in Table 6.4. Overall, 10.8% of patients received pre-operative radiotherapy, which is approximately 1/3rd of the rectal cancer patients. This is a relatively low proportion of patients, due in part to the small proportion of patients receiving short course radiotherapy locally. Some patients participating in other studies also had their histopathology performed centrally rather than at the participating hospitals and therefore were not eligible for recruitment. More patients in the MRI group (9, 13.6%) received radiotherapy than the conventional group (5, 7.8%). However, this difference did not achieve statistical significance.

Pre-operative chemotherapy

The number of patients recruited to the study undergoing pre-operative chemotherapy overall and in each arm of the trial is listed in Table 6.4. Overall, 11.5% of patients received pre-operative chemotherapy. There was no significant difference between the conventional histology group and the MRI group.

	All patients (n=130)	Control group (n=64)	MRI Group (n=66)	p-value (Fisher's exact test)
Operation				0.65
Right hemicolectomy	48 (38.4%)	26 (42.6%)	22 (34.4%)	
Subtotal colectomy	1 (0.8%)	1 (1.6%)	0 (0.0%)	
Transverse colectomy	1 (0.8%)	1 (1.6%)	0 (0.0%)	
Left hemicolectomy	7 (5.6%)	3 (4.9%)	4 (6.2%)	
Sigmoid colectomy	9 (7.2%)	4 (6.6%)	5 (7.8%)	
Anterior resection	48 (38.4%)	21 (34.4%)	27 (42.2%)	
APER	7 (5.6%)	2 (3.3%)	5 (7.8%)	
Hartman's procedure	4 (3.2%)	3 (4.9%)	1 (1.6%)	
Missing data	5	3	2	
Laparoscopic surgery				0.07
Laparoscopic	41 (32.8%)	16 (28.1%)	25 (36.8%)	
Converted to open	24 (19.2%)	16 (28.1%)	8 (11.8%)	
Open	60 (48.0%)	25 (43.9%)	35 (51.5%)	
Missing data	5	3	2	
Surgeon experience				0.37
Consultant	108 (91.5%)	52 (91.2%)	56 (91.8%)	
SpR	8 (6.7%)	3 (5.3%)	5 (8.2%)	
Staff Grade	2 (1.7%)	2 (3.5%)	0 (0%)	
Missing data	12	7	5	
Pre-operative radiotherapy				0.40
Received	14 (10.8%)	5 (7.8%)	9 (13.6%)	
Not received	116 (89.2%)	59 (92.2%)	57 (86.4%)	
Pre-operative chemotherapy				1.0
Received	15 (11.5%)	7 (10.9%)	8 (12.1%)	
Not received	115 (88.5%)	57 (89.1%)	58 (87.9%)	

Table 6.4: Pre-operative treatment

6.4.3 Specimen characteristics

Specimen length

The median length of colorectal cancer specimens is listed in Table 6.5. The median length of specimens in the conventional group was slightly greater (220 mm compared to 200 mm), but this difference did not achieve statistical significance.

Number of Tumour Blocks

The median number of tumour blocks taken for histological assessment in the conventional histology group and the specimen MRI groups is listed in Table 6.5. The median number of tumour blocks was the same in both arms of the trial (5 tumour blocks).

Histological type

The proportion of tumours of each histological type in the conventional histology group and the specimen MRI group is listed in Table 6.5. The large majority in both groups are adenocarcinomas (84.4% and 87.9% in the conventional and MRI groups, respectively). Approximately 10% of tumours were mucinous adenocarcinomas in both groups. There was a single neoplasm in the specimen MRI group which was an adenoma on final histological assessment, and five specimens in the control group where no residual tumour could be identified, despite the fact that adenocarcinoma had been confirmed on biopsy prior to recruitment into the trial.

Histological grade:

The histological grade of tumours in the conventional histology group and specimen MRI group are listed in Table 6.5. The histological grade was very similar in both groups with the large majority being well or moderately differentiated (95% and 93.9% in the conventional and specimen MRI groups respectively), with the remainder being poorly differentiated.

	All patients (n=130)	Control group (n=64)	MRI Group (n=66)	p-value
Specimen length, mm				0.27§
Median (IQR)	200 (155-260)	220 (168-260)	200 (144-257)	
Number of tumor blocks				0.96§
Median (IQR)	5 (4-7)	5 (4-7)	5 (3-6.25)	
Histological type				0.46‡
Adenocarcinoma	111 (85.4%)	53 (82.8%)	58 (87.9%)	
Mucinous adenocarcinoma	13 (10.0%)	6 (9.4%)	7 (10.6%)	
Adenoma	1 (0.77%)	0 (0.0%)	1 (1.5%)	
No residual tumor	5 (3.9%)	5 (7.8%)	0 (0.0%)	
Histological grade				1‡
Well/moderately differentiated	117 (94.4%)	56 (94.9%)	61 (93.8%)	
Poorly differentiated	7 (5.7%)	3 (5.1%)	4 (6.2%)	
Not applicable	6	5	1	

‡Fisher's exact test §Wilcoxon rank sum test

Table 6.5: Specimen characteristics

6.4.4 Primary outcome measure

AJCC stage

The primary outcome measure for this study was the proportion of patients in each group with an AJCC stage of IIB or greater, which formed the basis of the power calculation for this study. The proportion was similar in the two groups, with 45.3% of patients in the conventional group having an AJCC stage of IIB or greater compared to 40.9% in the MRI group. The difference between the two groups was not significant (p=0.74, Pearson's Chi-squared test). The difference in proportions was 4.4% (95% CI -14.2% to +23.0%). Although the study was underpowered due to poor recruitment, our predicted difference in AJCC stage III disease of -15% in the control group compared to the MRI group does not lie within the 95% confidence interval for the difference in proportions.

The overall AJCC stage for the whole group and both randomization groups is shown in Table 6.6. The median AJCC stage in the both groups was stage IIA, and there was no significant difference between the two groups (p=0.66, Wilcoxon rank sum test).

Pathological AJCC stage	All patients (n=130)	Control group (n=64)	MRI Group (n=66)
0	6 (4.6%)	5 (7.8%)	1 (1.5%)
I	29 (22.3%)	11 (17.2%)	18 (27.3%)
IIA	39 (30.0%)	19 (29.7%)	20 (30.3%)
IIB	13 (10.0%)	6 (9.4%)	7 (10.6%)
IIIA	3 (2.3%)	2 (3.1%)	1 (1.5%)
IIIB	30 (23.1%)	15 (23.4%)	15 (22.7%)
IIIC	10 (7.7%)	6 (9.4%)	4 (6.1%)
IV	0 (0.0%)	0 (0.0%)	0 (0.0%)
Total	**130 (100%)**	**64 (100%)**	**66 (100%)**
Median	IIA	IIA	IIA

p=0.66 (Wilcoxon rank sum test)

Table 6.6: Primary end point (AJCC stage)

6.4.5 Secondary outcome measures

A summary of the secondary outcomes measures is shown in Table 6.7. There were no significant differences in overall T-stage, N-stage, number of involved lymph nodes, number of examined lymph nodes, number of involved apical lymph nodes, depth of extramural spread, proportion of patients with tumor perforation, distance to the CRM, or proportion of patients with EMVI.

	All patients (n=130)	Control group (n=64)	MRI Group (n=66)	p-value
T-stage				0.68§
T0	6 (4.6%)	5 (7.8%)	1 (1.5%)	
T1	6 (4.6%)	3 (4.7%)	3 (4.5%)	
T2	26 (20.0%)	10 (15.6%)	16 (24.2%)	
T3	64 (49.2%)	30 (46.9%)	34 (51.5%)	
T4a	3 (2.3%)	2 (3.1%)	1 (1.5%)	
T4b	25 (19.2%)	14 (21.9%)	11 (16.7%)	
N-stage				0.46§
N0	87 (66.9%)	41 (64.1%)	46 (69.7%)	
N1	33 (25.4%)	17 (26.6%)	16 (24.2%)	
N2	10 (7.7%)	6 (9.4%)	4 (6.1%)	
Involved lymph node number				0.36§
Median (IQR)	0 (0-1)	0 (0-1.25)	0 (0-1)	
Examined lymph node number				0.44§
Median (IQR)	13 (9-19)	13 (10-19)	11 (8-18)	
Missing data	2	1	1	
Apical lymph node involvement				0.67‡
Involved	5 (3.9%)	3 (4.8%)	2 (3.0%)	
Not involved	123 (96.1%)	59 (95.2%)	64 (97.0%)	
Missing data	2	2	0	
Depth of extramural spread, mm				0.25§
Median (IQR)	1.5 (0-5)	2.75 (0-6)	1 (0-3.5)	
Missing data	33	12	11	
Tumor perforation				0.60‡
Present	16 (12.3%)	9 (14.1%)	7 (10.6%)	
Absent	114 (87.7%)	55 (85.9%)	59 (89.4%)	
CRM distance, mm				0.55§
Median (IQR)	9.5 (4-39.5)	9 (5.25-11)	10 (9-16)	
Missing data	16	9	7	
EMVI				0.28‡
Present	48 (36.9%)	27 (42.2%)	21 (31.8%)	
Absent	82 (63.1%)	37 (57.8%)	45 (68.2%)	

‡Fisher's exact test, §Wilcoxon rank sum test

Table 6.7: Secondary end points

The secondary end points are also presented as dichotomous outcomes, with the difference in proportion positive in the control and MRI groups and associated 95% confidence intervals (Table 6.8). There were non-significant trends toward a higher proportion of patients with the following adverse features in the control group; T3 or greater disease, lymph node positive disease, apical lymph node involvement, more than 5mm extramural spread, tumor perforation, CRM involvement and EMVI positivity. The only adverse feature with a trend towards greater prevalence in the MRI group than the control group is examination of less than twelve lymph nodes, which although an adverse risk factor is also a marker of lower quality histopathological assessment. All of these results therefore support a non-significant trend towards better histopathological assessment in the control group than the MRI group.

	Control group	**MRI Group**	**Difference in proportions (%/95% CI)**	**p-value (Fisher's exact test)**
T3 or greater	46 (72%)	46 (70%)	2 (-15 to +19)	0.85
N1 or greater	23 (36%)	20 (30%)	6 (-12 to +23)	0.58
<12 examined lymph nodes	24 (38%)	34 (52%)	-14 (-33 to +4)	0.11
Apical lymph node positive	3 (5%)	2 (3%)	2 (-7 to +10)	0.67
>5mm extramural spread	15 (29%)	11 (20%)	9 (-9 to +27)	0.37
Tumor perforation	9 (14%)	7 (11%)	3 (-9 to +16)	0.60
CRM involved	7 (11%)	6 (9%)	2 (-10 to +14)	0.78
EMVI positive	27 (42%)	21 (32%)	10 (-8 to +28)	0.28

Table 6.8: Secondary end points (binary outcomes)

6.5 Discussion

There were no significant differences between the "conventional histology" group and the "MRI assisted histology" group for any of the demographic measures (age, gender, tumour location, pre-operative T-stage, pre-operative N-stage, pre-operative M-stage, operation performed, mode of surgery, pre-operative radiotherapy or pre-operative chemotherapy). The difference in mean age of the patients in the two groups was the closest demographic measure to reaching significance ($p=0.05$), although the difference in mean age was only 4 years. None of the specimen characteristics (specimen length, number of tumour blocks, histological type or histological grade) approached significance. This suggests that the two groups were equivalent and that there was no systematic bias in group allocation as would be expected given the blind randomisation technique.

None of the outcome measures for this study have shown a significant difference between the "conventional histology" group and the "MRI assisted histology" group. This study has therefore failed to demonstrate any benefit in the addition of high resolution specimen MRI to help guide the dissection of the colorectal cancer specimen prior to histological assessment. This is contrary to our hypothesis, and a number of previous studies have shown that techniques which improve sampling during colorectal cancer specimen dissection result in upstaging of tumours (Betge et al., 2012, Hernanz et al., 2009). It is also contrary to one previous study which suggested that MRI-guided histological assessment resulted in the identification of more ypT4 disease following neoadjuvant treatment in locally advanced rectal cancer (Hole et al., 2013).

There are a number of reasons why the current study might have failed to demonstrate any benefit in the addition of specimen MRI to help specimen dissection. Firstly, this study under-recruited. The power calculation also failed to take account of a two-tailed alternative hypothesis and drop outs following recruitment. As a result this study was therefore under powered. However, the 95% CI for the difference in proportions for adverse features (Table 6.8) suggests that any benefit from MRI

assisted histology would be less than the 15% benefit which we felt would be sufficiently clinically significant to justify the additional cost and time associated with MRI assisted tumour block selection.

The non-significant trends for difference mean number of involved lymph nodes, mean number of lymph nodes retrieved, proportion of apical lymph nodes involved, mean depth of extra-mural spread, proportion of perforated tumours, proportion of tumours with an involved circumferential resection margin, mean distance from tumour edge to circumferential resection margin and proportion of tumours with extra mural vascular invasion all support a mild upstaging in the conventional histology group compared to the MRI assisted histology group.

These data would suggest that there is no advantage to MRI assisted dissection in histopathological assessment of colorectal cancer. This is despite anecdotal examples where both the research fellow and the histopathologist felt that the specimen MRI definitely helped to identify important features in certain colorectal cancer specimens which might otherwise have been missed, such as extra mural vascular invasion or involved lymph nodes.

One weakness of this study is that it was not possible to blind the histopathologist as to which study group the specimen belonged to. This is because histopathologist had to be present in the cut up room to perform the initial macroscopic description and dissection of the colorectal cancer specimen, to select the standard tumour blocks, and select four extra tumour blocks in the "conventional histology" group. In the MRI group, the research fellow had to show the histopathologist which additional blocks had been selected on the basis of the specimen MRI and point out any lymph nodes identified on the specimen MRI not identified by the histopathologists standard visual inspection and palpation. This process prevented blinding of the histopathologist at this stage.

It is possible that the inability to blind the histopathologist introduced some bias into the study. The histopathologist may subconsciously have felt that the specimen MRI would identify key tumour areas and lymph nodes, and therefore not performed such a thorough a visual search and palpation

of the specimen in the “MRI assisted histology” arm as they did in the “conventional histology” arm where this was not available.

A limitation of the technique of using high resolution MRI to select tumour blocks is correlating the specimen MRI with the correct area of the colorectal cancer specimen. This is particularly difficult when the MRI slices have been acquired in a different orientation to the tumour slices cut by the histopathologist during cut up. Although the MRI radiographers aim to image the specimen perpendicular to the tumour and the histopathologist aims to slice the specimen perpendicular to the long axis of the specimen, precise orientation of both slices can vary. This is a particularly the case in certain parts of the colon, when the long axis of the bowel and the tumour may curve such as in the sigmoid colon and at the flexures. Although multiplanar reformatting of 3D volume acquired images can mitigate against these difficulties to some extent by allowing the MRI scan to be reformatted in a different plane to match the specimen slices, these images are lower resolution and have a lower SNR than the 2D TSE slices which makes image interpretation more difficult.

A further limitation of this study is that the area of interest on the specimen MRI may not be included in the histological section even when the correct tumour block is selected. Each section is approximately 4µm thick, whereas each tumour block is typically 5mm thick, and may be thicker if the tumour is difficult to slice. Therefore approximately 0.1% of each tumour block is represented in each section. It is therefore possible that a key histological feature may have been correctly identified on the specimen MRI and that the correct tumour slice may have been selected on the basis of the specimen MRI without this histological feature being visible on the final histological section. It is possible to go back to the tumour block and to take multiple sections from each tumour block (taking “deeper levels”), but this is not done routinely and time and cost constraints prevented us from doing so in this study.

The histopathologists involved in this study were all consultant histopathologists with more than 10 years’ experience and with a subspecialty interest in gastrointestinal histopathology. This means

that the quality of histopathology reporting in both arms of the trial was very high. This is demonstrated by the high mean lymph node yield seen in both the "conventional histology" arm (15.1) and the "MRI assisted histology" arm (14.5), and by the high rate of EMVI pick up in both the "conventional histology" arm (42.2%) and the "MRI assisted histology" arm (31.8%). These measures are commonly used to assess the quality of colorectal cancer histopathology. Mean lymph node yields of more than 12 and EMVI pick up rates over 25% are generally considered to be indicative of high quality histopathology reporting in colorectal cancer (Williams et al., 2007). It is therefore likely that the expert selection of colorectal cancer tumour blocks in the control arm reduced the potential for improvement in the intervention arm using specimen MRI in this study. Studies which have used various techniques to increase lymph node yield and rate of EMVI detection, on which the power calculation for this study were based, have had a lower baseline consistent with non-specialist histopathology reporting (Betge et al., 2012, Crucitti et al., 1992, Scott and Grace, 1989).

In order not to perform and inadequate histological assessment for any patient included in the trial, and in view of the fact that MRI assisted tumour block selection is a previously untried technique, all tumours had four standard blocks selected as normal by the histopathologist, with additional blocks for the study selected where possible either on by the histopathologist or on the basis of the specimen MRI depending on group allocation. However, 25% of tumours in the trial were 2.5 cm or less in size. This made additional tumour block selection impossible in some cases, and a quarter of patients in the trial were only able to have the four standard blocks selected from the tumour, with additional tissue blocks taken for any additional lymph nodes. There was therefore limited opportunity for MRI assisted histology to benefit these patients.

The selection of additional tumour blocks in both the control and intervention arms of this trial may also have improved the standard of histopathological assessment in both arms of the trial. Previous studies have shown that selecting additional tumour blocks increases the T-stage (Quirke et al., 2007), rate of CRM invovlement (Quirke et al., 1986), and rate of EMVI positivity (Betge et al., 2012).

These studies have selected tumour blocks on the basis of visual inspection by an expert histopathologist, as was done in the control group in this study.

On the basis of this study, it is not possible to recommend the addition of high resolution specimen MRI to the assessment of colorectal cancer specimens.

CHAPTER 7

General discussion

7.1 Summary

I have demonstrated that it is possible to stratify patients into high and low risk groups on the basis of adverse features identified on rectal MRI, and that patients in the high risk group have a 6 fold increased risk of synchronous metastatic disease compared to patients in the low risk group. High risk patients are those with EMVI, T3 tumours with more than 5mm extramural invasion or T4 tumours, an involved circumferential resection margin or an involved intersphincteric plane for low rectal cancers. Of note, this risk stratification does not include N-stage, which is difficult to identify on imaging compared to other adverse features.

I have developed an MRI imaging protocol at 1.5T and 3T which allows high quality images to be obtain of the colon wall in healthy volunteers. The quality of images obtained colon cancer patients was more variable, but similar staging accuracy was achieved with MRI to that achieved with CT.

In the subgroup of patients where high quality MRI images were obtained in multiple planes through the tumour, accurate T-staging was achieved. This was particularly true for the identification of T3c or more advanced disease, a distinction which has previously been demonstrated to be of particular prognostic significance.

I was not able to demonstrate any benefit in the addition of high resolution ex-vivo MRI of the colorectal cancer specimen to aid selection of tumour blocks for histopathological assessment.

7.2 Further work

Despite the work undertaken with volunteers at the start of this project to optimise the MRI protocol, there was substantial variation in the quality of the acquired images, particularly on 1.5T MRI. If the T-staging accuracy achieved in subgroups in the colon MRI study is to be achieved in a representative colon cancer population, then the further work is needed to increase the overall quality of MRI imaging in the target population. The consistency of the navigator echo triggering to

acquire TSE images in eupnoea was a particular problem in this study, and resolving these technical difficulties would substantially improve the overall image quality.

If the proportion of patients with good quality MRI imaging could be improved in this way, then it may be worth repeating the colon MRI trial. The MRI protocol in such a trial should focus on obtaining high quality T2 weighted images in three planes through the tumour, as this resulted in optimum T-staging accuracy in the subgroup analysis of the our colon MRI trial and in the trial of Rollven et al which reported excellent accuracy in the assessment of T-stage with colon cancer MRI (Rollven et al., 2013).

The colon MRI trial also identified one patient with synchronous liver metastases, despite the fact the liver was incompletely imaged in a large proportion of patients in the study. This suggests that there are a small but significant proportion of patients with liver metastases who are not identified on routine pre-operative staging with CT. This is consistent with a meta-analysis of the sensitivity of CT and MRI in the identification of liver metastases which suggested that MRI was superior to CT (Bipat et al., 2005). These patients are likely to have small volume and therefore potentially resectable liver metastases, and so may benefit from early diagnosis. A prospective trial could establish whether routine pre-operative liver MRI for colorectal cancer patients identified additional patients with liver metastases who might benefit from early treatment of their metastatic disease.

Although we have established that the patients with adverse features on rectal MRI have a higher incidence on synchronous metastatic disease, we have not done so for patients with adverse features on colon MRI. It would be interesting to examine the disease free survival in patients stratified into high and low risk groups on the basis of their colon MRI to see if adverse features predict systemic disease in colon cancer.

Although accuracy of T-stage assessment on MRI, and to a lesser extent N-stage assessment, improved with improved image quality, the same trend was not observed in the assessment of EMVI. EMVI has been shown to be commonly missed in patients with disease recurrence and good

prognostic tumours on initial histopathological assessment, when histopathology is reviewed (Stewart et al., 2007). This raises the possibility that some of the "inaccuracy" observed in the identification of EMVI on imaging is actually due to under-reporting on histopathology. A large scale cohort study comparing the incidence of disease recurrence in pathological EMVI positive/negative and radiological EMVI positive/negative patients could determine which has whether pathological EMVI status or radiological EMVI status has greater prognostic significance.

7.3 Conclusion

The multiplicity of treatment options for colorectal cancer means that there is no "one size fits all" treatment. It is therefore becoming ever more important to be able to identify patients who are likely to benefit from different treatment pathways. Although there are a number of exciting developments in our genetic and molecular understanding of colorectal cancer, accurate staging remains the best way of stratifying patients to receive different treatments. Increasing emphasis on pre-operative treatment, and the increasing variety of surgical treatments, means that much of this staging must be performed radiologically.

CT is the workhorse of systemic staging in rectal cancer, and the local and systemic staging of colon cancer. However, MRI offers superior contrast resolution and therefore better differentiation between soft tissues than CT in optimum settings. This has already seen it supersede CT in the local staging of rectal cancer, and as technical advances continue it may also replace CT in the local staging of colon cancer and in the identification of liver metastases in colorectal cancer.

Accurate nodal staging remains an elusive goal for all imaging modalities. It seems unlikely that the steadily improving spatial and contrast resolution of CT and MRI will ever allow the accurate identification of solitary small nodal metastases. It is possible that functional imaging may improve this aspect of radiological staging in the future. In the interim, perhaps focussing on risk stratification based on radiologically apparent features, rather than trying to imitate histopathology

as accurately as possible, will allow selection the best pre-operative and operative treatments for our patients.

8 References

ADAM, R., AVISAR, E., ARICHE, A., GIACHETTI, S., AZOULAY, D., CASTAING, D., KUNSTLINGER, F., LEVI, F. & BISMUTH, F. 2001. Five-year survival following hepatic resection after neoadjuvant therapy for nonresectable colorectal. *Ann Surg Oncol,* 8**,** 347-53.

AGRAWAL, M. D., PINHO, D. F., KULKARNI, N. M., HAHN, P. F., GUIMARAES, A. R. & SAHANI, D. V. 2014. Oncologic applications of dual-energy CT in the abdomen. *Radiographics,* 34**,** 589-612.

AKAIKE, H. 1974. A new look at the statistical model identification. *IEEE Transactions on Automatic Control,* 19**,** 716-723.

AKASU, T., SUGIHARA, K. & MORIYA, Y. 2009. Male urinary and sexual functions after mesorectal excision alone or in combination with extended lateral pelvic lymph node dissection for rectal cancer. *Ann Surg Oncol,* 16**,** 2779-86.

AL-SUKHNI, E., MILOT, L., FRUITMAN, M., BEYENE, J., VICTOR, J. C., SCHMOCKER, S., BROWN, G., MCLEOD, R. & KENNEDY, E. 2012. Diagnostic accuracy of MRI for assessment of T category, lymph node metastases, and circumferential resection margin involvement in patients with rectal cancer: a systematic review and meta-analysis. *Ann Surg Oncol,* 19**,** 2212-23.

ALARCON, F., LASSET, C., CARAYOL, J., BONADONA, V., PERDRY, H., DESSEIGNE, F., WANG, Q. & BONAITI-PELLIE, C. 2007. Estimating cancer risk in HNPCC by the GRL method. *Eur J Hum Genet,* 15**,** 831-6.

ALEXANDER, D. D., CUSHING, C. A., LOWE, K. A., SCEURMAN, B. & ROBERTS, M. A. 2009. Meta-analysis of animal fat or animal protein intake and colorectal cancer. *Am J Clin Nutr,* 89**,** 1402-9.

ALEXANDER, D. D., WEED, D. L., CUSHING, C. A. & LOWE, K. A. 2011. Meta-analysis of prospective studies of red meat consumption and colorectal cancer. *Eur J Cancer Prev,* 20**,** 293-307.

ALOIA, T. A. & FAHY, B. N. 2008. A decision analysis model predicts the optimal treatment pathway for patients with colorectal cancer and resectable synchronous liver metastases. *Clin Colorectal Cancer,* 7**,** 197-201.

ANDRE, T., BONI, C., MOUNEDJI-BOUDIAF, L., NAVARRO, M., TABERNERO, J., HICKISH, T., TOPHAM, C., ZANINELLI, M., CLINGAN, P., BRIDGEWATER, J., TABAH-FISCH, I. & DE GRAMONT, A. 2004. Oxaliplatin, fluorouracil, and leucovorin as adjuvant treatment for colon cancer. *N Engl J Med,* 350**,** 2343-51.

ANDRE, T., BONI, C., NAVARRO, M., TABERNERO, J., HICKISH, T., TOPHAM, C., BONETTI, A., CLINGAN, P., BRIDGEWATER, J., RIVERA, F. & DE GRAMONT, A. 2009. Improved Overall Survival With Oxaliplatin, Fluorouracil, and Leucovorin As Adjuvant Treatment in Stage II or III Colon Cancer in the MOSAIC Trial. *Journal of Clinical Oncology,* 27**,** 3109-3116.

ANDRES, A., MAJNO, P. E., MOREL, P., RUBBIA-BRANDT, L., GIOSTRA, E., GERVAZ, P., TERRAZ, S., ALLAL, A. S., ROTH, A. D. & MENTHA, G. 2008. Improved long-term outcome of surgery for advanced colorectal liver metastases: reasons and implications for management on the basis of a severity score. *Ann Surg Oncol,* 15**,** 134-43.

AOKI, K. & TAKETO, M. M. 2007. Adenomatous polyposis coli (APC): a multi-functional tumor suppressor gene. *J Cell Sci,* 120**,** 3327-35.

ARREDONDO, J., PASTOR, C., BAIXAULI, J., RODRIGUEZ, J., GONZALEZ, I., VIGIL, C., CHOPITEA, A. & HERNANDEZ-LIZOAIN, J. L. 2013. Preliminary outcome of a treatment strategy based on perioperative chemotherapy and surgery in patients with locally advanced colon cancer. *Colorectal Dis,* 15**,** 552-7.

ASCHELE, C., CIONINI, L., LONARDI, S., PINTO, C., CORDIO, S., ROSATI, G., ARTALE, S., TAGLIAGAMBE, A., AMBROSINI, G., ROSETTI, P., BONETTI, A., NEGRU, M. E., TRONCONI, M. C., LUPPI, G., SILVANO, G., CORSI, D. C., BOCHICCHIO, A. M., CHIAULON, G., GALLO, M. & BONI, L. 2011. Primary tumor response to preoperative chemoradiation with or without oxaliplatin in locally advanced rectal cancer: pathologic results of the STAR-01 randomized phase III trial. *J Clin Oncol,* 29**,** 2773-80.

ASSOCIATION OF COLOPROCTOLOGY OF GREAT BRITAIN AND IRELAND (ACPGBI) 2007. Guidelines for the Management of Colorectal Cancer 3rd edition. The Association of Coloproctology of Great Britain and Ireland.

ATALLAH, S., MARTIN-PEREZ, B., ALBERT, M., DEBECHE-ADAMS, T., NASSIF, G., HUNTER, L. & LARACH, S. 2014. Transanal minimally invasive surgery for total mesorectal excision (TAMIS-TME): results and experience with the first 20 patients undergoing curative-intent rectal cancer surgery at a single institution. *Tech Coloproctol,* 18**,** 473-80.

ATKIN, W. S., MORSON, B. C. & CUZICK, J. 1992. Long-Term Risk of Colorectal-Cancer after Excision of Rectosigmoid Adenomas. *New England Journal of Medicine,* 326**,** 658-662.

AYOUB, S. F. 1978. Arterial supply to the human rectum. *Acta Anat (Basel),* 100**,** 317-27.

BAEK, S. J., KIM, S. H., KWAK, J. M., CHO, J. S., SHIN, J. W., AMAR, A. H. & KIM, J. 2012. Indeterminate pulmonary nodules in rectal cancer: a recommendation for follow-up guidelines. *J Surg Oncol,* 106**,** 481-5.

BAILES, D. R., GILDERDALE, D. J., BYDDER, G. M., COLLINS, A. G. & FIRMIN, D. N. 1985. Respiratory ordered phase encoding (ROPE): a method for reducing respiratory motion artefacts in MR imaging. *J Comput Assist Tomogr,* 9**,** 835-8.

BAKER, S. J., PREISINGER, A. C., JESSUP, J. M., PARASKEVA, C., MARKOWITZ, S., WILLSON, J. K., HAMILTON, S. & VOGELSTEIN, B. 1990. p53 gene mutations occur in combination with 17p allelic deletions as late events in colorectal tumorigenesis. *Cancer Res,* 50**,** 7717-22.

BALSLEV, I., PEDERSEN, M., TEGLBJAERG, P. S., HANBERG-SOERENSEN, F., BONE, J., JACOBSEN, N. O., OVERGAARD, J., SELL, A., BERTELSEN, K., HAGE, E. & ET AL. 1986. Postoperative radiotherapy in Dukes' B and C carcinoma of the rectum and rectosigmoid. A randomized multicenter study. *Cancer,* 58**,** 22-8.

BAMBA, Y., ITABASHI, M. & KAMEOKA, S. 2011. Value of PET/CT imaging for diagnosing pulmonary metastasis of colorectal cancer. *Hepatogastroenterology,* 58**,** 1972-4.

BARBARO, B., FIORUCCI, C., TEBALA, C., VALENTINI, V., GAMBACORTA, M. A., VECCHIO, F. M., RIZZO, G., COCO, C., CRUCITTI, A., RATTO, C. & BONOMO, L. 2009. Locally advanced rectal cancer: MR imaging in prediction of response after preoperative chemotherapy and radiation therapy. *Radiology,* 250**,** 730-9.

BATTERSBY, N. J., BALYASNIKOVA, S. & BROWN, G. 2014. Guiding post-treatment decisions in rectal cancer: mrTRG is a practical place to start. *Oncology (Williston Park),* 28**,** 677-80.

BATTERSBY, N. J., HOW, P., MORAN, B., STELZNER, S., WEST, N. P., BRANAGAN, G., STRASSBURG, J., QUIRKE, P., TEKKIS, P., PEDERSEN, B. G., GUDGEON, M., HEALD, B. & BROWN, G. 2015. Prospective Validation of a Low Rectal Cancer Magnetic Resonance Imaging Staging System and Development of a Local Recurrence Risk Stratification Model: The MERCURY II Study. *Ann Surg*.

BEETS-TAN, R. G., BEETS, G. L., VLIEGEN, R. F., KESSELS, A. G., VAN BOVEN, H., DE BRUINE, A., VON MEYENFELDT, M. F., BAETEN, C. G. & VAN ENGELSHOVEN, J. M. 2001. Accuracy of magnetic resonance imaging in prediction of tumour-free resection margin in rectal cancer surgery. *Lancet,* 357**,** 497-504.

BELT, E. J., VAN STIJN, M. F., BRIL, H., DE LANGE-DE KLERK, E. S., MEIJER, G. A., MEIJER, S. & STOCKMANN, H. B. 2010. Lymph node negative colorectal cancers with isolated tumor deposits should be classified and treated as stage III. *Ann Surg Oncol,* 17**,** 3203-11.

BEMBENEK, A., SCHNEIDER, U., GRETSCHEL, S., FISCHER, J. & SCHLAG, P. M. 2005. Detection of lymph node micrometastases and isolated tumor cells in sentinel and nonsentinel lymph nodes of colon cancer patients. *World J Surg,* 29**,** 1172-5.

BENSON, A. B., 3RD, BEKAII-SAAB, T., CHAN, E., CHEN, Y. J., CHOTI, M. A., COOPER, H. S., ENGSTROM, P. F., ENZINGER, P. C., FAKIH, M. G., FUCHS, C. S., GREM, J. L., HUNT, S., LEONG, L. A., LIN, E., MARTIN, M. G., MAY, K. S., MULCAHY, M. F., MURPHY, K., ROHREN, E., RYAN, D. P., SALTZ, L., SHARMA, S., SHIBATA, D., SKIBBER, J. M., SMALL, W., JR., SOFOCLEOUS, C. T., VENOOK, A. P., WILLETT, C. G., FREEDMAN-CASS, D. A. & GREGORY, K. M. 2012. Rectal cancer. *J Natl Compr Canc Netw,* 10**,** 1528-64.

BETGE, J., POLLHEIMER, M. J., LINDTNER, R. A., KORNPRAT, P., SCHLEMMER, A., REHAK, P., VIETH, M., HOEFLER, G. & LANGNER, C. 2012. Intramural and extramural vascular invasion in colorectal cancer: prognostic significance and quality of pathology reporting. *Cancer,* 118**,** 628-38.

BIAGI, J. J., RAPHAEL, M. J., MACKILLOP, W. J., KONG, W., KING, W. D. & BOOTH, C. M. 2011. Association between time to initiation of adjuvant chemotherapy and survival in colorectal cancer: A systematic review and meta-analysis. *JAMA,* 305**,** 2335-2342.

BIPAT, S., GLAS, A. S., SLORS, F. J., ZWINDERMAN, A. H., BOSSUYT, P. M. & STOKER, J. 2004. Rectal cancer: local staging and assessment of lymph node involvement with endoluminal US, CT, and MR imaging--a meta-analysis. *Radiology,* 232**,** 773-83.

BIPAT, S., VAN LEEUWEN, M. S., COMANS, E. F., PIJL, M. E., BOSSUYT, P. M., ZWINDERMAN, A. H. & STOKER, J. 2005. Colorectal liver metastases: CT, MR imaging, and PET for diagnosis--meta-analysis. *Radiology,* 237**,** 123-31.

BIRLIK, B., OBUZ, F., ELIBOL, F. D., CELIK, A. O., SOKMEN, S., TERZI, C., SAGOL, O., SARIOGLU, S., GORKEN, I. & OZTOP, I. 2015. Diffusion-weighted MRI and MR- volumetry--in the evaluation of tumor response after preoperative chemoradiotherapy in patients with locally advanced rectal cancer. *Magn Reson Imaging,* 33**,** 201-12.

BLACKSTOCK, W., RUSSO, S. M., SUH, W. W., COSMAN, B. C., HERMAN, J., MOHIUDDIN, M., POGGI, M. M., REGINE, W. F., SALTZ, L., SMALL, W., JR., ZOOK, J. & KONSKI, A. A. 2010. ACR Appropriateness Criteria: local excision in early-stage rectal cancer. *Curr Probl Cancer,* 34**,** 193-200.

BOLAND, P. M. & FAKIH, M. 2014. The emerging role of neoadjuvant chemotherapy for rectal cancer. *Journal of Gastrointestinal Oncology,* 5**,** 362-373.

BORASIO, P., GISABELLA, M., BILLE, A., RIGHI, L., LONGO, M., TAMPELLINI, M. & ARDISSONE, F. 2011. Role of surgical resection in colorectal lung metastases: analysis of 137 patients. *Int J Colorectal Dis,* 26**,** 183-90.

BORI, R., SEJBEN, I., SVEBIS, M., VAJDA, K., MARKO, L., PAJKOS, G. & CSERNI, G. 2009. Heterogeneity of pT3 colorectal carcinomas according to the depth of invasion. *Pathol Oncol Res,* 15**,** 527-32.

BOSSET, J. F., CALAIS, G., MINEUR, L., MAINGON, P., STOJANOVIC-RUNDIC, S., BENSADOUN, R. J., BARDET, E., BENY, A., OLLIER, J. C., BOLLA, M., MARCHAL, D., VAN LAETHEM, J. L., KLEIN, V.,

GIRALT, J., CLAVERE, P., GLANZMANN, C., CELLIER, P. & COLLETTE, L. 2014. Fluorouracil-based adjuvant chemotherapy after preoperative chemoradiotherapy in rectal cancer: long-term results of the EORTC 22921 randomised study. *Lancet Oncol,* 15**,** 184-90.

BOSSUYT, P. M., REITSMA, J. B., BRUNS, D. E., GATSONIS, C. A., GLASZIOU, P. P., IRWIG, L. M., LIJMER, J. G., MOHER, D., RENNIE, D. & DE VET, H. C. 2003. Towards complete and accurate reporting of studies of diagnostic accuracy: the STARD initiative. Standards for Reporting of Diagnostic Accuracy. *Clin Chem,* 49**,** 1-6.

BREIMAN, L. 1984. *Classification and regression trees*, Wadsworth International Group.

BROUQUET, A., MORTENSON, M. M., VAUTHEY, J. N., RODRIGUEZ-BIGAS, M. A., OVERMAN, M. J., CHANG, G. J., KOPETZ, S., GARRETT, C., CURLEY, S. A. & ABDALLA, E. K. 2010. Surgical strategies for synchronous colorectal liver metastases in 156 consecutive patients: classic, combined or reverse strategy? *J Am Coll Surg,* 210**,** 934-41.

BROWN, G., RICHARDS, C. J., BOURNE, M. W., NEWCOMBE, R. G., RADCLIFFE, A. G., DALLIMORE, N. S. & WILLIAMS, G. T. 2003. Morphologic predictors of lymph node status in rectal cancer with use of high-spatial-resolution MR imaging with histopathologic comparison. *Radiology,* 227**,** 371-7.

BROWN, G., RICHARDS, C. J., NEWCOMBE, R. G., DALLIMORE, N. S., RADCLIFFE, A. G., CAREY, D. P., BOURNE, M. W. & WILLIAMS, G. T. 1999. Rectal carcinoma: thin-section MR imaging for staging in 28 patients. *Radiology,* 211**,** 215-22.

BURKITT, H., YOUNG, B. & HEATH, W. 1993. *Wheater's Functional Histology,* New York, Churchill Livingstone.

BURTON, S., BROWN, G., BEES, N., NORMAN, A., BIEDRZYCKI, O., ARNAOUT, A., ABULAFI, A. M. & SWIFT, R. I. 2008. Accuracy of CT prediction of poor prognostic features in colonic cancer. *Br J Radiol,* 81**,** 10-9.

BUTT, H. Z., SALEM, M. K., VIJAYNAGAR, B., CHAUDHRI, S. & SINGH, B. 2013. Perineal reconstruction after extra-levator abdominoperineal excision (eLAPE): a systematic review. *Int J Colorectal Dis,* 28**,** 1459-68.

BUUNEN, M., VELDKAMP, R., HOP, W. C., KUHRY, E., JEEKEL, J., HAGLIND, E., PAHLMAN, L., CUESTA, M. A., MSIKA, S., MORINO, M., LACY, A. & BONJER, H. J. 2009. Survival after laparoscopic surgery versus open surgery for colon cancer: long-term outcome of a randomised clinical trial. *Lancet Oncol,* 10**,** 44-52.

CAI, P. Q., WU, Y. P., AN, X., QIU, X., KONG, L. H., LIU, G. C., XIE, C. M., PAN, Z. Z., WU, P. H. & DING, P. R. 2014. Simple measurements on diffusion-weighted MR imaging for assessment of complete response to neoadjuvant chemoradiotherapy in locally advanced rectal cancer. *Eur Radiol,* 24**,** 2962-70.

CAMMA, C., GIUNTA, M., FIORICA, F., PAGLIARO, L., CRAXI, A. & COTTONE, M. 2000. Preoperative radiotherapy for resectable rectal cancer: A meta-analysis. *JAMA,* 284**,** 1008-15.

CANCER RESEARCH UK. 2016. *A study looking at a diffusion weighted MRI scan to check for bowel cancer spread (SERENADE)* [Online]. Available: http://www.cancerresearchuk.org/about-cancer/find-a-clinical-trial/a-study-looking-at-a-diffusion-weighted-mri-scan-to-check-for-bowel-cancer-spread-serenade [Accessed 10/04/2016 2016].

CEDERMARK, B., JOHANSSON, H., RUTQVIST, L. E. & WILKING, N. 1995. The Stockholm I trial of preoperative short term radiotherapy in operable rectal carcinoma. A prospective randomized trial. Stockholm Colorectal Cancer Study Group. *Cancer,* 75**,** 2269-75.

CEELEN, W., FIERENS, K., VAN NIEUWENHOVE, Y. & PATTYN, P. 2009. Preoperative chemoradiation versus radiation alone for stage II and III resectable rectal cancer: A systematic review and meta-analysis. *International Journal of Cancer,* 124**,** 2966-2972.

CERVONE, A., SARDI, A. & CONAWAY, G. L. 2000. Intraoperative ultrasound (IOUS) is essential in the management of metastatic colorectal liver lesions. *American Surgeon,* 66**,** 611-5.

CHAND, M., EVANS, J., SWIFT, R. I., TEKKIS, P. P., WEST, N. P., STAMP, G., HEALD, R. J. & BROWN, G. 2015. The prognostic significance of postchemoradiotherapy high-resolution MRI and histopathology detected extramural venous invasion in rectal cancer. *Ann Surg,* 261**,** 473-9.

CHAND, M., SWIFT, R. I., TEKKIS, P. P., CHAU, I. & BROWN, G. 2014. Extramural venous invasion is a potential imaging predictive biomarker of neoadjuvant treatment in rectal cancer. *Br J Cancer,* 110**,** 19-25.

CHAO, A., THUN, M. J., CONNELL, C. J., MCCULLOUGH, M. L., JACOBS, E. J., FLANDERS, W. D., RODRIGUEZ, C., SINHA, R. & CALLE, E. E. 2005. Meat consumption and risk of colorectal cancer. *JAMA,* 293**,** 172-82.

CHETTY, R., GILL, P., GOVENDER, D., BATEMAN, A., CHANG, H. J., DESHPANDE, V., DRIMAN, D., GOMEZ, M., GREYWOODE, G., JAYNES, E., LEE, C. S., LOCKETZ, M., ROWSELL, C., RULLIER, A., SERRA, S., SHEPHERD, N., SZENTGYORGYI, E., VAJPEYI, R. & WANG, L. M. 2012. International study group on rectal cancer regression grading: interobserver variability with commonly used regression grading systems. *Hum Pathol,* 43**,** 1917-23.

CHO, E., SMITH-WARNER, S. A., RITZ, J., VAN DEN BRANDT, P. A., COLDITZ, G. A., FOLSOM, A. R., FREUDENHEIM, J. L., GIOVANNUCCI, E., GOLDBOHM, R. A., GRAHAM, S., HOLMBERG, L., KIM, D. H., MALILA, N., MILLER, A. B., PIETINEN, P., ROHAN, T. E., SELLERS, T. A., SPEIZER, F. E., WILLETT, W. C., WOLK, A. & HUNTER, D. J. 2004. Alcohol intake and colorectal cancer: a pooled analysis of 8 cohort studies. *Ann Intern Med,* 140**,** 603-13.

CHO, K. C. & GOLD, B. M. 1985. Computed tomography of Krukenberg tumors. *AJR Am J Roentgenol,* 145**,** 285-8.

CHOTI, M. A., SITZMANN, J. V., TIBURI, M. F., SUMETCHOTIMETHA, W., RANGSIN, R., SCHULICK, R. D., LILLEMOE, K. D., YEO, C. J. & CAMERON, J. L. 2002. Trends in long-term survival following liver resection for hepatic colorectal metastases. *Annals of Surgery,* 235**,** 759-66.

CHRISTOFORIDIS, D., MCNALLY, M. P., JAROSEK, S. L., MADOFF, R. D. & FINNE, C. O. 2009. Endocavitary contact radiation therapy for ultrasonographically staged T1 N0 and T2 N0 rectal cancer. *Br J Surg,* 96**,** 430-6.

CHUA, Y. J., BARBACHANO, Y., CUNNINGHAM, D., OATES, J. R., BROWN, G., WOTHERSPOON, A., TAIT, D., MASSEY, A., TEBBUTT, N. C. & CHAU, I. 2010. Neoadjuvant capecitabine and oxaliplatin before chemoradiotherapy and total mesorectal excision in MRI-defined poor-risk rectal cancer: a phase 2 trial. *Lancet Oncol,* 11**,** 241-8.

CLAVIEN, P. A., SELZNER, N., MORSE, M., SELZNER, M. & PAULSON, E. 2002. Downstaging of hepatocellular carcinoma and liver metastases from colorectal cancer by selective intra-arterial chemotherapy. *Surgery,* 131**,** 433-42.

COAKLEY, F. V. & HRICAK, H. 1999. Imaging of peritoneal and mesenteric disease: key concepts for the clinical radiologist. *Clin Radiol,* 54**,** 563-74.

COHEN, J. 1960. A Coefficient of Agreement for Nominal Scales. *Educational and Psychological Measurement,* 20**,** 37-46.

COLORECTAL CANCER COLLABORATIVE GROUP 2001. Adjuvant radiotherapy for rectal cancer: a systematic overview of 8,507 patients from 22 randomised trials. *Lancet,* 358**,** 1291-304.

CRONIN, C. G., LOHAN, D. G., MHUIRCHEARTAIGH, J. N., MCKENNA, D., ALHAJERI, N., ROCHE, C. & MURPHY, J. M. 2008. MRI small-bowel follow-through: prone versus supine patient positioning for best small-bowel distention and lesion detection. *AJR Am J Roentgenol,* 191**,** 502-6.

CRUCITTI, F., DOGLIETTO, G. B., BELLANTONE, R., SOFO, L., BOSSOLA, M., RATTO, C., NUCERA, P., SILVESTRI, E., CRUCITTI, A., VECCHIO, F. M. & ET AL. 1992. Accurate specimen preparation and examination is mandatory to detect lymph nodes and avoid understaging in colorectal cancer. *J Surg Oncol,* 51**,** 153-7; discussion 157-8.

DALTON, R. S., SMART, N. J., EDWARDS, T. J., CHANDLER, I. & DANIELS, I. R. 2012. Short-term outcomes of the prone perineal approach for extra-levator abdomino-perineal excision (elAPE). *Surgeon,* 10**,** 342-6.

DAVIES, H., BIGNELL, G. R., COX, C., STEPHENS, P., EDKINS, S., CLEGG, S., TEAGUE, J., WOFFENDIN, H., GARNETT, M. J., BOTTOMLEY, W., DAVIS, N., DICKS, E., EWING, R., FLOYD, Y., GRAY, K., HALL, S., HAWES, R., HUGHES, J., KOSMIDOU, V., MENZIES, A., MOULD, C., PARKER, A., STEVENS, C., WATT, S., HOOPER, S., WILSON, R., JAYATILAKE, H., GUSTERSON, B. A., COOPER, C., SHIPLEY, J., HARGRAVE, D., PRITCHARD-JONES, K., MAITLAND, N., CHENEVIX-TRENCH, G., RIGGINS, G. J., BIGNER, D. D., PALMIERI, G., COSSU, A., FLANAGAN, A., NICHOLSON, A., HO, J. W., LEUNG, S. Y., YUEN, S. T., WEBER, B. L., SEIGLER, H. F., DARROW, T. L., PATERSON, H., MARAIS, R., MARSHALL, C. J., WOOSTER, R., STRATTON, M. R. & FUTREAL, P. A. 2002. Mutations of the BRAF gene in human cancer. *Nature,* 417**,** 949-54.

DAY, D. W. & MORSON, B. C. 1978. The adenoma-carcinoma sequence. *Major Probl Pathol,* 10**,** 58-71.

DE LACY, A. M., RATTNER, D. W., ADELSDORFER, C., TASENDE, M. M., FERNANDEZ, M., DELGADO, S., SYLLA, P. & MARTINEZ-PALLI, G. 2013. Transanal natural orifice transluminal endoscopic surgery (NOTES) rectal resection: "down-to-up" total mesorectal excision (TME)--short-term outcomes in the first 20 cases. *Surg Endosc,* 27**,** 3165-72.

DE SMEDT, L., PALMANS, S. & SAGAERT, X. 2015. Tumour budding in colorectal cancer: what do we know and what can we do? *Virchows Arch*.

DE VARGAS MACCIUCCA, M., CASALE, A., MANGANARO, L., FLORIANI, I., FIORE, F., MARCHETTI, L. & PANZIRONI, G. 2010. Rectal villous tumours: MR features and correlation with TRUS in the preoperative evaluation. *Eur J Radiol,* 73**,** 329-33.

DELBEKE, D., COLEMAN, R. E., GUIBERTEAU, M. J., BROWN, M. L., ROYAL, H. D., SIEGEL, B. A., TOWNSEND, D. W., BERLAND, L. L., PARKER, J. A., HUBNER, K., STABIN, M. G., ZUBAL, G., KACHELRIESS, M., CRONIN, V. & HOLBROOK, S. 2006. Procedure guideline for tumor imaging with 18F-FDG PET/CT 1.0. *J Nucl Med,* 47**,** 885-95.

DELONG, E. R., DELONG, D. M. & CLARKE-PEARSON, D. L. 1988. Comparing the areas under two or more correlated receiver operating characteristic curves: a nonparametric approach. *Biometrics,* 44**,** 837-45.

DEMEO, J. H., FULCHER, A. S. & AUSTIN, R. F., JR. 1995. Anatomic CT demonstration of the peritoneal spaces, ligaments, and mesenteries: normal and pathologic processes. *Radiographics,* 15**,** 755-70.

DEN DULK, M., MARIJNEN, C. A. M., PUTTER, H., RUTTEN, H. J. T., BEETS, G. L., WIGGERS, T., NAGTEGAAL, I. D. & VAN DE VELDE, C. J. H. 2007. Risk Factors for Adverse Outcome in Patients With Rectal Cancer Treated With an Abdominoperineal Resection in the Total Mesorectal Excision Trial. *Annals of Surgery,* 246.

DENNOSUKE, J. 1983. General rules for clinical and pathological studies on cancer of the colon, rectum and anus. *The Japanese journal of surgery,* 13**,** 557-573.

DESHMANE, A., GULANI, V., GRISWOLD, M. A. & SEIBERLICH, N. 2012. Parallel MR imaging. *J Magn Reson Imaging,* 36**,** 55-72.

DEWDNEY, A., CUNNINGHAM, D., TABERNERO, J., CAPDEVILA, J., GLIMELIUS, B., CERVANTES, A., TAIT, D., BROWN, G., WOTHERSPOON, A., DE CASTRO, D. G., CHUA, Y. J., WONG, R., BARBACHANO, Y., OATES, J. & CHAU, I. 2012. Multicenter Randomized Phase II Clinical Trial Comparing Neoadjuvant Oxaliplatin, Capecitabine, and Preoperative Radiotherapy With or Without Cetuximab Followed by Total Mesorectal Excision in Patients With High-Risk Rectal Cancer (EXPERT-C). *Journal of Clinical Oncology,* 30**,** 1620-1627.

DIGHE, S., BLAKE, H., KOH, M. D., SWIFT, I., ARNAOUT, A., TEMPLE, L., BARBACHANO, Y. & BROWN, G. 2010a. Accuracy of multidetector computed tomography in identifying poor prognostic factors in colonic cancer. *Br J Surg,* 97**,** 1407-15.

DIGHE, S., PURKAYASTHA, S., SWIFT, I., TEKKIS, P. P., DARZI, A., A'HERN, R. & BROWN, G. 2010b. Diagnostic precision of CT in local staging of colon cancers: a meta-analysis. *Clin Radiol,* 65**,** 708-19.

DIGHE, S., SWIFT, I. & BROWN, G. 2008. CT staging of colon cancer. *Clin Radiol,* 63**,** 1372-9.

DIGHE, S., SWIFT, I., MAGILL, L., HANDLEY, K., GRAY, R., QUIRKE, P., MORTON, D., SEYMOUR, M., WARREN, B. & BROWN, G. 2012. Accuracy of radiological staging in identifying high-risk colon cancer patients suitable for neoadjuvant chemotherapy: a multicentre experience. *Colorectal Dis,* 14**,** 438-44.

DUKES, C. & BUSSEY, H. J. 1941. Venous spread in Rectal Cancer. *Proc R Soc Med,* 34**,** 571-73.

DUKES, C. E. & BUSSEY, H. J. 1958. The spread of rectal cancer and its effect on prognosis. *Br J Cancer,* 12**,** 309-20.

DWORAK, O., KEILHOLZ, L. & HOFFMANN, A. 1997. Pathological features of rectal cancer after preoperative radiochemotherapy. *Int J Colorectal Dis,* 12**,** 19-23.

EADEN, J. A., ABRAMS, K. R. & MAYBERRY, J. F. 2001. The risk of colorectal cancer in ulcerative colitis: a meta-analysis. *Gut,* 48**,** 526-35.

EDGE, S. B., BYRD, D. R., COMPTON, C., FRITZ, A. G., GREENE, F. L. & TROTTI, A. 2010. *AJCC Cancer Staging Manual,* Chicago, Springer.

EDGE, S. B. & COMPTON, C. C. 2010. The American Joint Committee on Cancer: the 7th edition of the AJCC cancer staging manual and the future of TNM. *Ann Surg Oncol,* 17**,** 1471-4.

ERTURK, S. M., ALBERICH-BAYARRI, A., HERRMANN, K. A., MARTI-BONMATI, L. & ROS, P. R. 2009. Use of 3.0-T MR imaging for evaluation of the abdomen. *Radiographics,* 29**,** 1547-63.

ESHED, I., ALTHOFF, C. E., HAMM, B. & HERMANN, K. G. 2007. Claustrophobia and premature termination of magnetic resonance imaging examinations. *J Magn Reson Imaging,* 26**,** 401-4.

ESSIG, M., SHIROISHI, M. S., NGUYEN, T. B., SAAKE, M., PROVENZALE, J. M., ENTERLINE, D., ANZALONE, N., DÖRFLER, A., ROVIRA, À., WINTERMARK, M. & LAW, M. 2013. Perfusion MRI: The Five Most Frequently Asked Technical Questions. *AJR. American journal of roentgenology,* 200**,** 24-34.

FERLAY, J., SOERJOMATARAM, I., ERVIK, M., DIKSHIT, R., ESER, S., MATHERS, C., REBELO, M., PARKIN, D., FORMAN, D. & BRAY, F. 2012. *GLOBOCAN 2012, Estimated Cancer Incidence, Mortality and Prevalence Worldwide* [Online]. Lyon: International Agency for Research on Cancer.

Available: http://globocan.iarc.fr/Pages/fact_sheets_cancer.aspx?cancer=colorectal [Accessed 11/05/2014 2014].

FERNANDEZ-MARTOS, C., PERICAY, C., APARICIO, J., SALUD, A., SAFONT, M., MASSUTI, B., VERA, R., ESCUDERO, P., MAUREL, J., MARCUELLO, E., MENGUAL, J. L., SAIGI, E., ESTEVAN, R., MIRA, M., POLO, S., HERNANDEZ, A., GALLEN, M., ARIAS, F., SERRA, J. & ALONSO, V. 2010. Phase II, randomized study of concomitant chemoradiotherapy followed by surgery and adjuvant capecitabine plus oxaliplatin (CAPOX) compared with induction CAPOX followed by concomitant chemoradiotherapy and surgery in magnetic resonance imaging-defined, locally advanced rectal cancer: Grupo cancer de recto 3 study. *J Clin Oncol,* 28**,** 859-65.

FERRERO, A., LANGELLA, S., GIULIANTE, F., VIGANO, L., VELLONE, M., ZIMMITTI, G., ARDITO, F., NUZZO, G. & CAPUSSOTTI, L. 2013. Intraoperative liver ultrasound still affects surgical strategy for patients with colorectal metastases in the modern era. *World J Surg,* 37**,** 2655-63.

FISHER, B., WOLMARK, N., ROCKETTE, H., REDMOND, C., DEUTSCH, M., WICKERHAM, D. L., FISHER, E. R., CAPLAN, R., JONES, J., LERNER, H. & ET AL. 1988. Postoperative adjuvant chemotherapy or radiation therapy for rectal cancer: results from NSABP protocol R-01. *J Natl Cancer Inst,* 80**,** 21-9.

FLEMING, I. D., COOPER, J. S., HENSON, D. E., HUTTER, R. V. P., KENNEDY, B. J., MURPHY, G. P., O'SULLIVAN, B., SOBIN, L. H. & YARBRO, J. W. 1997. *AJCC Cancer Staging Manual,* Chicago, Lippincott-Raven.

FONG, Y., COHEN, A. M., FORTNER, J. G., ENKER, W. E., TURNBULL, A. D., COIT, D. G., MARRERO, A. M., PRASAD, M., BLUMGART, L. H. & BRENNAN, M. F. 1997. Liver resection for colorectal metastases. *J Clin Oncol,* 15**,** 938-46.

FONG, Y., FORTNER, J., SUN, R. L., BRENNAN, M. F. & BLUMGART, L. H. 1999. Clinical score for predicting recurrence after hepatic resection for metastatic colorectal cancer: analysis of 1001 consecutive cases. *Ann Surg,* 230**,** 309-18; discussion 318-21.

FOROUTANI, A., GARLAND, A. M., BERBER, E., STRING, A., ENGLE, K., RYAN, T. L., PEARL, J. M. & SIPERSTEIN, A. E. 2000. Laparoscopic ultrasound vs triphasic computed tomography for detecting liver tumors. *Archives of Surgery,* 135**,** 933-8.

FOXTROT COLLABORATIVE. 2012a. *FOXTROT Protocol version 6.0* [Online]. Birmingham Clinical Trials Unit. [Accessed 15/12/2015 2015].

FOXTROT COLLABORATIVE, G. 2012b. Feasibility of preoperative chemotherapy for locally advanced, operable colon cancer: the pilot phase of a randomised controlled trial. *Lancet Oncol,* 13**,** 1152-60.

FREEDMAN, L. S., MACASKILL, P. & SMITH, A. N. 1984. Multivariate analysis of prognostic factors for operable rectal cancer. *Lancet,* 2**,** 733-6.

FROEHLICH, J. M., DAENZER, M., VON WEYMARN, C., ERTURK, S. M., ZOLLIKOFER, C. L. & PATAK, M. A. 2009. Aperistaltic effect of hyoscine N-butylbromide versus glucagon on the small bowel assessed by magnetic resonance imaging. *Eur Radiol,* 19**,** 1387-93.

GALL, T. M., MARKAR, S. R., JACKSON, D., HAJI, A. & FAIZ, O. 2014. Mini-probe ultrasonography for the staging of colon cancer: a systematic review and meta-analysis. *Colorectal Dis,* 16**,** O1-8.

GASH, K. J., COOPER, L., SMART, N., LONGMAN, R. & THOMAS, M. 2014. No observable difference in operative oncological outcomes between extra-levator versus standard abdominoperineal excision. *Tech Coloproctol*.

GASTROINTESTINAL TUMOR STUDY GROUP 1985. Prolongation of the disease-free interval in surgically treated rectal carcinoma. Gastrointestinal Tumor Study Group. *N Engl J Med,* 312**,** 1465-72.

GENNISSON, J. L., DEFFIEUX, T., FINK, M. & TANTER, M. 2013. Ultrasound elastography: Principles and techniques. *Diagnostic and Interventional Imaging,* 94**,** 487-495.

GEOGHEGAN, J. G. & SCHEELE, J. 1999. Treatment of colorectal liver metastases. *Br J Surg,* 86**,** 158-69.

GEORGIOU, P. A., TEKKIS, P. P., CONSTANTINIDES, V. A., PATEL, U., GOLDIN, R. D., DARZI, A. W., JOHN NICHOLLS, R. & BROWN, G. 2013. Diagnostic accuracy and value of magnetic resonance imaging (MRI) in planning exenterative pelvic surgery for advanced colorectal cancer. *Eur J Cancer,* 49**,** 72-81.

GERARD, J. P., AZRIA, D., GOURGOU-BOURGADE, S., MARTEL-LAFAY, I., HENNEQUIN, C., ETIENNE, P. L., VENDRELY, V., FRANCOIS, E., DE LA ROCHE, G., BOUCHE, O., MIRABEL, X., DENIS, B., MINEUR, L., BERDAH, J. F., MAHE, M. A., BECOUARN, Y., DUPUIS, O., LLEDO, G., SEITZ, J. F., BEDENNE, L., JUZYNA, B. & CONROY, T. 2012. Clinical outcome of the ACCORD 12/0405 PRODIGE 2 randomized trial in rectal cancer. *J Clin Oncol,* 30**,** 4558-65.

GERARD, J. P., AZRIA, D., GOURGOU-BOURGADE, S., MARTEL-LAFFAY, I., HENNEQUIN, C., ETIENNE, P. L., VENDRELY, V., FRANCOIS, E., DE LA ROCHE, G., BOUCHE, O., MIRABEL, X., DENIS, B., MINEUR, L., BERDAH, J. F., MAHE, M. A., BECOUARN, Y., DUPUIS, O., LLEDO, G., MONTOTO-GRILLOT, C. & CONROY, T. 2010. Comparison of two neoadjuvant chemoradiotherapy regimens for locally advanced rectal cancer: results of the phase III trial ACCORD 12/0405-Prodige 2. *J Clin Oncol,* 28**,** 1638-44.

GERARD, J. P., FRIN, A. C., DOYEN, J., ZHOU, F. X., GAL, J., ROMESTAING, P., BARBET, N., COQUARD, R., CHAPET, O., FRANCOIS, E., MARCIE, S. & BENEZERY, K. 2015. Organ preservation in rectal adenocarcinoma (T1) T2-T3 Nx M0. Historical overview of the Lyon Sud - nice experience using contact x-ray brachytherapy and external beam radiotherapy for 120 patients. *Acta Oncol,* 54**,** 545-51.

GIACCHETTI, S., ITZHAKI, M., GRUIA, G., ADAM, R., ZIDANI, R., KUNSTLINGER, F., BRIENZA, S., ALAFACI, E., BERTHEAULT-CVITKOVIC, F., JASMIN, C., REYNES, M., BISMUTH, H., MISSET, J. L. & LEVI, F. 1999. Long-term survival of patients with unresectable colorectal cancer liver metastases following infusional chemotherapy with 5-fluorouracil, leucovorin, oxaliplatin and surgery. *Ann Oncol,* 10**,** 663-9.

GILL, S., THOMAS, R. R. & GOLDBERG, R. M. 2003. Review article: colorectal cancer chemotherapy. *Aliment Pharmacol Ther,* 18**,** 683-92.

GLAS, A. S., LIJMER, J. G., PRINS, M. H., BONSEL, G. J. & BOSSUYT, P. M. M. 2003. The diagnostic odds ratio: a single indicator of test performance. *Journal of Clinical Epidemiology,* 56**,** 1129-1135.

GLEHEN, O., KWIATKOWSKI, F., SUGARBAKER, P. H., ELIAS, D., LEVINE, E. A., DE SIMONE, M., BARONE, R., YONEMURA, Y., CAVALIERE, F., QUENET, F., GUTMAN, M., TENTES, A. A., LORIMIER, G., BERNARD, J. L., BEREDER, J. M., PORCHERON, J., GOMEZ-PORTILLA, A., SHEN, P., DERACO, M. & RAT, P. 2004. Cytoreductive surgery combined with perioperative intraperitoneal chemotherapy for the management of peritoneal carcinomatosis from colorectal cancer: a multi-institutional study. *J Clin Oncol,* 22**,** 3284-92.

GOEL, A. & BOLAND, C. R. 2010. Recent insights into the pathogenesis of colorectal cancer. *Curr Opin Gastroenterol,* 26**,** 47-52.

GOODENBERGER, M. & LINDOR, N. M. 2011. Lynch syndrome and MYH-associated polyposis: review and testing strategy. *J Clin Gastroenterol,* 45**,** 488-500.

GORDON, T. A. & CAMERON, J. L. 2000. *Evidence-based surgery*, B.C. Decker, Inc.

GOSS, K. H. & GRODEN, J. 2000. Biology of the adenomatous polyposis coli tumor suppressor. *J Clin Oncol,* 18**,** 1967-79.

GOURTSOYIANNIS, N., PAPANIKOLAOU, N., GRAMMATIKAKIS, J. & PRASSOPOULOS, P. 2002. MR enteroclysis: technical considerations and clinical applications. *Eur Radiol,* 12**,** 2651-8.

GRADY, W. M., RAJPUT, A., MYEROFF, L., LIU, D. F., KWON, K., WILLIS, J. & MARKOWITZ, S. 1998. Mutation of the type II transforming growth factor-beta receptor is coincident with the transformation of human colon adenomas to malignant carcinomas. *Cancer Res,* 58**,** 3101-4.

GRASER, A., MELZER, A., LINDNER, E., NAGEL, D., HERRMANN, K., STIEBER, P., SCHIRRA, J., MANSMANN, U., REISER, M. F., GOKE, B. & KOLLIGS, F. T. 2013. Magnetic resonance colonography for the detection of colorectal neoplasia in asymptomatic adults. *Gastroenterology,* 144**,** 743-750 e2.

GRAY, R., BARNWELL, J., MCCONKEY, C., HILLS, R. K., WILLIAMS, N. S. & KERR, D. J. 2007a. Adjuvant chemotherapy versus observation in patients with colorectal cancer: a randomised study. *Lancet,* 370**,** 2020-9.

GRAY, R., BARNWELL, J., MCCONKEY, C., HILLS, R. K., WILLIAMS, N. S. & KERR, D. J. 2007b. Adjuvant chemotherapy versus observation in patients with colorectal cancer: a randomised study. *Lancet,* 370**,** 2020-2029.

GRINNELL, R. S. 1939. The Grading and Prognosis of Carcinoma of the Colon and Rectum. *Ann Surg,* 109**,** 500-33.

HABOUBI & SCOTT 2000. Clinicopathological management of the patient with a malignant colorectal adenoma. *Colorectal Dis,* 2**,** 2-7.

HABR-GAMA, A., SABBAGA, J., GAMA-RODRIGUES, J., SAO JULIAO, G. P., PROSCURSHIM, I., BAILAO AGUILAR, P., NADALIN, W. & PEREZ, R. O. 2013. Watch and wait approach following extended neoadjuvant chemoradiation for distal rectal cancer: are we getting closer to anal cancer management? *Dis Colon Rectum,* 56**,** 1109-17.

HAGGAR, F. A. & BOUSHEY, R. P. 2009. Colorectal cancer epidemiology: incidence, mortality, survival, and risk factors. *Clin Colon Rectal Surg,* 22**,** 191-7.

HEALD, R. J. 1988. The 'Holy Plane' of rectal surgery. *J R Soc Med,* 81**,** 503-8.

HEALD, R. J., HUSBAND, E. M. & RYALL, R. D. 1982. The mesorectum in rectal cancer surgery--the clue to pelvic recurrence? *Br J Surg,* 69**,** 613-6.

HEALD, R. J., MORAN, B. J., RYALL, R. D., SEXTON, R. & MACFARLANE, J. K. 1998. Rectal cancer: the Basingstoke experience of total mesorectal excision, 1978-1997. *Arch Surg,* 133**,** 894-9.

HEIJNEN, L. A., LAMBREGTS, D. M., MARTENS, M. H., MAAS, M., BAKERS, F. C., CAPPENDIJK, V. C., OLIVEIRA, P., LAMMERING, G., RIEDL, R. G., BEETS, G. L. & BEETS-TAN, R. G. 2014. Performance of gadofosveset-enhanced MRI for staging rectal cancer nodes: can the initial promising results be reproduced? *Eur Radiol,* 24**,** 371-9.

HERMANEK, P. & JUNGINGER, T. 2005. The circumferential resection margin in rectal carcinoma surgery. *Tech Coloproctol,* 9**,** 193-9; discussion 199-200.

HERNANZ, F., GARCIA-SOMACARRERA, E. & FERNANDEZ, F. 2009. The assessment of lymph nodes missed in mesenteric tissue after standard dissection of colorectal cancer specimens. *Colorectal Dis*.

HERNANZ, F., GARCIA-SOMACARRERA, E. & FERNANDEZ, F. 2010. The assessment of lymph nodes missed in mesenteric tissue after standard dissection of colorectal cancer specimens. *Colorectal Dis,* 12**,** e57-60.

HIDA, J. & OKUNO, K. 2013. High ligation of the inferior mesenteric artery in rectal cancer surgery. *Surg Today,* 43**,** 8-19.

HILLINGSO, J. G. & WILLE-JORGENSEN, P. 2009. Staged or simultaneous resection of synchronous liver metastases from colorectal cancer--a systematic review. *Colorectal Dis,* 11**,** 3-10.

HOHENBERGER, W., WEBER, K., MATZEL, K., PAPADOPOULOS, T. & MERKEL, S. 2009. Standardized surgery for colonic cancer: complete mesocolic excision and central ligation--technical notes and outcome. *Colorectal Dis,* 11**,** 354-64; discussion 364-5.

HOLE, K. H., LARSEN, S. G., GROHOLT, K. K., GIERCKSKY, K. E. & REE, A. H. 2013. Magnetic resonance-guided histopathology for improved accuracy of tumor response evaluation of neoadjuvant treatment in organ-infiltrating rectal cancer. *Radiother Oncol,* 107**,** 178-83.

HOLM, T., LJUNG, A., HAGGMARK, T., JURELL, G. & LAGERGREN, J. 2007. Extended abdominoperineal resection with gluteus maximus flap reconstruction of the pelvic floor for rectal cancer. *Br J Surg,* 94**,** 232-8.

HOTHORN, T., HORNIK, K. & ZEILEIS, A. 2006. Unbiased Recursive Partitioning: A Conditional Inference Framework. *Journal of Computational and Graphical Statistics,* 15**,** 651-674.

HUNTER, C., BLAKE, H., JEYADEVAN, N., ABULAFI, M., SWIFT, I., TOOMEY, P. & BROWN, G. 2016. Local staging and assessment of colon cancer with 1.5 Tesla Magnetic Resonance Imaging. *The British Journal of Radiology***,** 20160257.

HUNTER, C. & BROWN, G. 2015. MRI and CT for the Preoperative T and N Staging of Rectal Cancer. *In:* BAATRUP, G. (ed.) *Multidisciplinary Treatment of Colorectal Cancer: Staging – Treatment – Pathology – Palliation.* Cham: Springer International Publishing.

HUNTER, C., BROWN, G., TEMPLE, L., ABULAFI, M. & ARNAOUT, A. 2012. Magnetic resonance imaging assisted tumour block selection in colorectal cancer. *Virchows Archiv,* 461**,** S179-S179.

HUNTER, C. J. & BROWN, G. 2013. Radiological Staging for Systemic Disease. *Manual of Total Mesorectal Excision.* CRC Press.

HUNTER, C. J., GARANT, A., VUONG, T., ARTHO, G., LISBONA, R., TEKKIS, P., ABULAFI, M. & BROWN, G. 2011a. Adverse Features on Rectal MRI Identify a High-risk Group that May Benefit from More Intensive Preoperative Staging and Treatment. *Ann Surg Oncol*.

HUNTER, C. J., SCURR, E., JEYADEVAN, N., COLLINS, D. J., ABULAFI, M., TEKKIS, P. P., GEORGIOU, P. A., LEACH, M. O. & BROWN, G. 2011b. Optimising magnetic resonance imaging for preoperative staging and surgical planning in colon cancer at 1.5 tesla and 3.0 tesla. *Journal of Clinical Oncology,* 29.

ISSA, J. P. 2004. CpG island methylator phenotype in cancer. *Nat Rev Cancer,* 4**,** 988-93.

JACKMAN, R. J. & MAYO, C. W. 1951. The adenoma-carcinoma sequence in cancer of the colon. *Surg Gynecol Obstet,* 93**,** 327-30.

JACOBS, M. A., PAN, L. & MACURA, K. J. 2009. Whole-body diffusion-weighted and proton imaging: a review of this emerging technology for monitoring metastatic cancer. *Semin Roentgenol,* 44**,** 111-22.

JAECK, D., BACHELLIER, P., GUIGUET, M., BOUDJEMA, K., VAILLANT, J. C., BALLADUR, P. & NORDLINGER, B. 1997. Long-term survival following resection of colorectal hepatic metastases. Association Francaise de Chirurgie. *Br J Surg,* 84**,** 977-80.

JAKOBSEN, A., PLOEN, J., VUONG, T., APPELT, A., LINDEBJERG, J. & RAFAELSEN, S. R. 2012. Dose-effect relationship in chemoradiotherapy for locally advanced rectal cancer: a randomized trial comparing two radiation doses. *Int J Radiat Oncol Biol Phys,* 84**,** 949-54.

JASS, J. R. 2007. Classification of colorectal cancer based on correlation of clinical, morphological and molecular features. *Histopathology,* 50**,** 113-30.

JOHNSON, W., TAYLOR, M. B., CARRINGTON, B. M., BONINGTON, S. C. & SWINDELL, R. 2007. The value of hyoscine butylbromide in pelvic MRI. *Clin Radiol,* 62**,** 1087-93.

JONES, O. M., SMEULDERS, N., WISEMAN, O. & MILLER, R. 1999. Lateral ligaments of the rectum: an anatomical study. *Br J Surg,* 86**,** 487-9.

JULLUMSTRO, E., LYDERSEN, S., MOLLER, B., DAHL, O. & EDNA, T. H. 2009. Duration of symptoms, stage at diagnosis and relative survival in colon and rectal cancer. *Eur J Cancer,* 45**,** 2383-90.

KARAHASANOGLU, T., HAMZAOGLU, I., AYTAC, E. & BACA, B. 2011. Transvaginal assisted totally laparoscopic single-port right colectomy. *J Laparoendosc Adv Surg Tech A,* 21**,** 255-7.

KARP, J. S., SURTI, S., DAUBE-WITHERSPOON, M. E. & MUEHLLEHNER, G. 2008. The benefit of time-of-flight in PET imaging: Experimental and clinical results. *Journal of nuclear medicine : official publication, Society of Nuclear Medicine,* 49**,** 462-470.

KERN, R., DIELS, A., PETTENPOHL, J., KABLAU, M., BRADE, J., HENNERICI, M. G. & MEAIRS, S. 2011. Real-time ultrasound brain perfusion imaging with analysis of microbubble replenishment in acute MCA stroke. *J Cereb Blood Flow Metab,* 31**,** 1716-24.

KIM, D. J., KIM, J. H., RYU, Y. H., JEON, T. J., YU, J. S. & CHUNG, J. J. 2011a. Nodal staging of rectal cancer: high-resolution pelvic MRI versus (1)(8)F-FDGPET/CT. *J Comput Assist Tomogr,* 35**,** 531-4.

KIM, I. Y., CHA, S. W., AHN, J. H. & KIM, Y. W. 2015. Factors affecting the restaging accuracy of magnetic resonance imaging after preoperative chemoradiation in patients with rectal cancer. *Eur J Surg Oncol,* 41**,** 493-8.

KIM, J. H., BEETS, G. L., KIM, M. J., KESSELS, A. G. & BEETS-TAN, R. G. 2004. High-resolution MR imaging for nodal staging in rectal cancer: are there any criteria in addition to the size? *Eur J Radiol,* 52**,** 78-83.

KIM, K. H., YANG, S. S., YOON, Y. S., LIM, S.-B., YU, C. S. & KIM, J. C. 2011b. Validation of the 7th edition of the AJCC TNM staging in patients with stage II and III colorectal carcinoma: Analysis of 2511 cases from a medical centre in Korea. *Colorectal Disease,* 13**,** e220-e226.

KIM, S. H., KIM, W. H., PARK, K. J., LEE, J. K. & KIM, J. S. 1996. CT and MR findings of Krukenberg tumors: comparison with primary ovarian tumors. *J Comput Assist Tomogr,* 20**,** 393-8.

KIM, S. H., LEE, J. M., HONG, S. H., KIM, G. H., LEE, J. Y., HAN, J. K. & CHOI, B. I. 2009. Locally advanced rectal cancer: added value of diffusion-weighted MR imaging in the evaluation of tumor response to neoadjuvant chemo- and radiation therapy. *Radiology,* 253**,** 116-25.

KLUZA, E., ROZEBOOM, E. D., MAAS, M., MARTENS, M., LAMBREGTS, D. M., SLENTER, J., BEETS, G. L. & BEETS-TAN, R. G. 2013. T2 weighted signal intensity evolution may predict pathological complete response after treatment for rectal cancer. *Eur Radiol,* 23**,** 253-61.

KOBAYASHI, H., MOCHIZUKI, H., KATO, T., MORI, T., KAMEOKA, S., SHIROUZU, K. & SUGIHARA, K. 2009. Outcomes of surgery alone for lower rectal cancer with and without pelvic sidewall dissection. *Dis Colon Rectum,* 52**,** 567-76.

KOCAMAN, O., BAYSAL, B., SENTURK, H., INCE, A. T., MUSLUMANOGLU, M., KOCAKOC, E., ARICI, S., UYSAL, O., YILDIZ, K., TURKDOGAN, K. & DANALIOGLU, A. 2014. Staging of rectal carcinoma: MDCT, MRI or EUS. Single center experience. *Turk J Gastroenterol,* 25**,** 669-73.

KOH, D. M., COLLINS, D. J., WALLACE, T., CHAU, I. & RIDDELL, A. M. 2012. Combining diffusion-weighted MRI with Gd-EOB-DTPA-enhanced MRI improves the detection of colorectal liver metastases. *Br J Radiol,* 85**,** 980-9.

KOSINSKI, L., HABR-GAMA, A., LUDWIG, K. & PEREZ, R. 2012. Shifting concepts in rectal cancer management: a review of contemporary primary rectal cancer treatment strategies. *CA Cancer J Clin,* 62**,** 173-202.

KUDO, S., LAMBERT, R., ALLEN, J. I., FUJII, H., FUJII, T., KASHIDA, H., MATSUDA, T., MORI, M., SAITO, H., SHIMODA, T., TANAKA, S., WATANABE, H., SUNG, J. J., FELD, A. D., INADOMI, J. M., O'BRIEN, M. J., LIEBERMAN, D. A., RANSOHOFF, D. F., SOETIKNO, R. M., TRIADAFILOPOULOS, G., ZAUBER, A., TEIXEIRA, C. R., REY, J. F., JARAMILLO, E., RUBIO, C. A., VAN GOSSUM, A., JUNG, M., VIETH, M., JASS, J. R. & HURLSTONE, P. D. 2008. Nonpolypoid neoplastic lesions of the colorectal mucosa. *Gastrointest Endosc,* 68**,** S3-47.

KUHLMAN, J. E., HRUBAN, R. H. & FISHMAN, E. K. 1989. Krukenberg tumors: CT features and growth characteristics. *South Med J,* 82**,** 1215-9.

KYE, B. H., JUNG, J. H., KIM, H. J., KANG, S. G., CHO, H. M. & KIM, J. G. 2012. Tumor budding as a risk factor of lymph node metastasis in submucosal invasive T1 colorectal carcinoma: a retrospective study. *BMC Surg,* 12**,** 16.

LAHAYE, M. J., BEETS, G. L., ENGELEN, S. M., KESSELS, A. G., DE BRUINE, A. P., KWEE, H. W., VAN ENGELSHOVEN, J. M., VAN DE VELDE, C. J. & BEETS-TAN, R. G. 2009. Locally advanced rectal cancer: MR imaging for restaging after neoadjuvant radiation therapy with concomitant chemotherapy. Part II. What are the criteria to predict involved lymph nodes? *Radiology,* 252**,** 81-91.

LAMBRECHT, M., VANDECAVEYE, V., DE KEYZER, F., ROELS, S., PENNINCKX, F., VAN CUTSEM, E., FILIP, C. & HAUSTERMANS, K. 2011. Value of Diffusion-Weighted Magnetic Resonance Imaging for Prediction and Early Assessment of Response to Neoadjuvant Radiochemotherapy in Rectal Cancer: Preliminary Results. *Int J Radiat Oncol Biol Phys*.

LAMBREGTS, D. M., BEETS, G. L., MAAS, M., KESSELS, A. G., BAKERS, F. C., CAPPENDIJK, V. C., ENGELEN, S. M., LAHAYE, M. J., DE BRUINE, A. P., LAMMERING, G., LEINER, T., VERWOERD, J. L., WILDBERGER, J. E. & BEETS-TAN, R. G. 2011. Accuracy of Gadofosveset-enhanced MRI for Nodal Staging and Restaging in Rectal Cancer. *Ann Surg,* 253**,** 539-45.

LANDIS, J. R. & KOCH, G. G. 1977. The Measurement of Observer Agreement for Categorical Data. *Biometrics,* 33**,** 159-174.

LANGE, M. M., MARIJNEN, C. A., MAAS, C. P., PUTTER, H., RUTTEN, H. J., STIGGELBOUT, A. M., MEERSHOEK-KLEIN KRANENBARG, E. & VAN DE VELDE, C. J. 2009. Risk factors for sexual dysfunction after rectal cancer treatment. *Eur J Cancer,* 45**,** 1578-88.

LAURIE, J. A., MOERTEL, C. G., FLEMING, T. R., WIEAND, H. S., LEIGH, J. E., RUBIN, J., MCCORMACK, G. W., GERSTNER, J. B., KROOK, J. E., MALLIARD, J. & ET AL. 1989. Surgical adjuvant therapy of large-bowel carcinoma: an evaluation of levamisole and the combination of levamisole and fluorouracil. The North Central Cancer Treatment Group and the Mayo Clinic. *J Clin Oncol,* 7**,** 1447-56.

LEE, N. K., KIM, C. Y., PARK, Y. J., YANG, D. S., YOON, W. S., KIM, S. H. & KIM, J. 2014. Clinical implication of negative conversion of predicted circumferential resection margin status after preoperative chemoradiotherapy for locally advanced rectal cancer. *Eur J Radiol,* 83**,** 245-9.

LEYENDECKER, J. R., BLOOMFELD, R. S., DISANTIS, D. J., WATERS, G. S., MOTT, R. & BECHTOLD, R. E. 2009. MR enterography in the management of patients with Crohn disease. *Radiographics,* 29**,** 1827-46.

LI, C., LAN, X., YUAN, H., FENG, H., XIA, X. & ZHANG, Y. 2014. 18F-FDG PET predicts pathological response to preoperative chemoradiotherapy in patients with primary rectal cancer: a meta-analysis. *Ann Nucl Med,* 28**,** 436-46.

LIANG, J. T., HUANG, K. C., LAI, H. S., LEE, P. H. & SUN, C. T. 2007. Oncologic results of laparoscopic D3 lymphadenectomy for male sigmoid and upper rectal cancer with clinically positive lymph nodes. *Ann Surg Oncol,* 14**,** 1980-90.

LIEBIG, C., AYALA, G., WILKS, J. A., BERGER, D. H. & ALBO, D. 2009. Perineural invasion in cancer: a review of the literature. *Cancer,* 115**,** 3379-91.

LITTLEFORD, S. E., BAIRD, A., ROTIMI, O., VERBEKE, C. S. & SCOTT, N. 2009. Interobserver variation in the reporting of local peritoneal involvement and extramural venous invasion in colonic cancer. *Histopathology,* 55**,** 407-13.

LOMAS, D. J. 2003. Technical developments in bowel MRI. *Eur Radiol,* 13**,** 1058-71.

LOMAS, D. J., SOOD, R. R., GRAVES, M. J., MILLER, R., HALL, N. R. & DIXON, A. K. 2001. Colon carcinoma: MR imaging with CO2 enema--pilot study. *Radiology,* 219**,** 558-62.

LOW, R. N. 2005. Magnetic resonance imaging in the oncology patient: evaluation of the extrahepatic abdomen. *Semin Ultrasound CT MR,* 26**,** 224-36.

LOW, R. N. 2007. MR imaging of the peritoneal spread of malignancy. *Abdom Imaging,* 32**,** 267-83.

LOW, R. N., MCCUE, M., BARONE, R., SALEH, F. & SONG, T. 2003. MR staging of primary colorectal carcinoma: comparison with surgical and histopathologic findings. *Abdom Imaging,* 28**,** 784-93.

MAAS, M., NELEMANS, P. J., VALENTINI, V., DAS, P., RODEL, C., KUO, L. J., CALVO, F. A., GARCIA-AGUILAR, J., GLYNNE-JONES, R., HAUSTERMANS, K., MOHIUDDIN, M., PUCCIARELLI, S., SMALL, W., JR., SUAREZ, J., THEODOROPOULOS, G., BIONDO, S., BEETS-TAN, R. G. & BEETS, G. L. 2010. Long-term outcome in patients with a pathological complete response after chemoradiation for rectal cancer: a pooled analysis of individual patient data. *Lancet Oncol,* 11**,** 835-44.

MAFFIONE, A. M., LOPCI, E., BLUEMEL, C., GIAMMARILE, F., HERRMANN, K. & RUBELLO, D. 2015. Diagnostic accuracy and impact on management of (18)F-FDG PET and PET/CT in colorectal liver metastasis: a meta-analysis and systematic review. *Eur J Nucl Med Mol Imaging,* 42**,** 152-63.

MAGUIRE, A. & SHEAHAN, K. 2014. Controversies in the pathological assessment of colorectal cancer. *World J Gastroenterol,* 20**,** 9850-61.

MANDARD, A. M., DALIBARD, F., MANDARD, J. C., MARNAY, J., HENRY-AMAR, M., PETIOT, J. F., ROUSSEL, A., JACOB, J. H., SEGOL, P., SAMAMA, G. & ET AL. 1994. Pathologic assessment of tumor regression after preoperative chemoradiotherapy of esophageal carcinoma. Clinicopathologic correlations. *Cancer,* 73**,** 2680-6.

MARKOWITZ, S. D. & BERTAGNOLLI, M. M. 2009. Molecular origins of cancer: Molecular basis of colorectal cancer. *N Engl J Med,* 361**,** 2449-60.

MARSH, P. J., JAMES, R. D. & SCHOFIELD, P. F. 1994. Adjuvant preoperative radiotherapy for locally advanced rectal carcinoma. Results of a prospective, randomized trial. *Dis Colon Rectum,* 37**,** 1205-14.

MARTENS, M. H., SUBHANI, S., HEIJNEN, L. A., LAMBREGTS, D. M., BUIJSEN, J., MAAS, M., RIEDL, R. G., JEUKENS, C. R., BEETS, G. L., KLUZA, E. & BEETS-TAN, R. G. 2015. Can perfusion MRI predict response to preoperative treatment in rectal cancer? *Radiother Oncol,* 114**,** 218-23.

MARUSCH, F., PTOK, H., SAHM, M., SCHMIDT, U., RIDWELSKI, K., GASTINGER, I. & LIPPERT, H. 2011. Endorectal ultrasound in rectal carcinoma--do the literature results really correspond to the realities of routine clinical care? *Endoscopy,* 43**,** 425-31.

MCROBBIE, D. W., MOORE, E. A., GRAVES, M. J. & PRINCE, M. R. 2007. *MRI From Picture to Proton*, Cambridge University Press.

MEDICAL RESEARCH COUNCIL RECTAL CANCER WORKING PARTY 1996. Randomised trial of surgery alone versus radiotherapy followed by surgery for potentially operable locally advanced rectal cancer. *Lancet,* 348**,** 1605-10.

MEMON, S., LYNCH, A. C., BRESSEL, M., WISE, A. G. & HERIOT, A. G. 2015. Systematic review and meta-analysis of the accuracy of MRI and endorectal ultrasound in the restaging and response assessment of rectal cancer following neoadjuvant therapy. *Colorectal Dis,* 17**,** 748-61.

MENTHA, G., MAJNO, P. E., ANDRES, A., RUBBIA-BRANDT, L., MOREL, P. & ROTH, A. D. 2006. Neoadjuvant chemotherapy and resection of advanced synchronous liver metastases before treatment of the colorectal primary. *Br J Surg,* 93**,** 872-8.

MERCURY STUDY GROUP 2006. Diagnostic accuracy of preoperative magnetic resonance imaging in predicting curative resection of rectal cancer: prospective observational study. *Bmj,* 333**,** 779.

MERCURY STUDY GROUP 2007. Extramural depth of tumor invasion at thin-section MR in patients with rectal cancer: results of the MERCURY study. *Radiology,* 243**,** 132-9.

MERKEL, S., MANSMANN, U., SIASSI, M., PAPADOPOULOS, T., HOHENBERGER, W. & HERMANEK, P. 2001. The prognostic inhomogeneity in pT3 rectal carcinomas. *Int J Colorectal Dis,* 16**,** 298-304.

MERRIE, A. E., PHILLIPS, L. V., YUN, K. & MCCALL, J. L. 2001. Skip metastases in colon cancer: assessment by lymph node mapping using molecular detection. *Surgery,* 129**,** 684-91.

MESSENGER, D. E., DRIMAN, D. K., MCLEOD, R. S., RIDDELL, R. H. & KIRSCH, R. 2011. Current practice patterns among pathologists in the assessment of venous invasion in colorectal cancer. *Journal of Clinical Pathology,* 64**,** 983-989.

MESSIOU, C., CHALMERS, A. G., BOYLE, K., WILSON, D. & SAGAR, P. 2008. Pre-operative MR assessment of recurrent rectal cancer. *Br J Radiol,* 81**,** 468-73.

MEYERS, M. A., OLIPHANT, M., BERNE, A. S. & FELDBERG, M. A. 1987. The peritoneal ligaments and mesenteries: pathways of intraabdominal spread of disease. *Radiology,* 163**,** 593-604.

MIKE, M. & KANO, N. 2014. Laparoscopic surgery for colon cancer: a review of the fascial composition of the abdominal cavity. *Surg Today*.

MILES, W. E. 1971. A method of performing abdomino-perineal excision for carcinoma of the rectum and of the terminal portion of the pelvic colon (1908). *CA Cancer J Clin,* 21**,** 361-4.

MOERTEL, C. G., FLEMING, T. R., MACDONALD, J. S., HALLER, D. G., LAURIE, J. A., GOODMAN, P. J., UNGERLEIDER, J. S., EMERSON, W. A., TORMEY, D. C., GLICK, J. H. & ET AL. 1990. Levamisole and fluorouracil for adjuvant therapy of resected colon carcinoma. *N Engl J Med,* 322**,** 352-8.

MOERTEL, C. G., FLEMING, T. R., MACDONALD, J. S., HALLER, D. G., LAURIE, J. A., TANGEN, C. M., UNGERLEIDER, J. S., EMERSON, W. A., TORMEY, D. C., GLICK, J. H., VEEDER, M. H. & MAILLIARD, J. A. 1995. Fluorouracil plus levamisole as effective adjuvant therapy after resection of stage III colon carcinoma: a final report. *Ann Intern Med,* 122**,** 321-6.

MONGAN, J. P., FADUL, C. E., COLE, B. F., ZAKI, B. I., SURIAWINATA, A. A., RIPPLE, G. H., TOSTESON, T. D. & PIPAS, J. M. 2009. Brain metastases from colorectal cancer: risk factors, incidence, and the possible role of chemokines. *Clin Colorectal Cancer,* 8**,** 100-5.

MOORE, K. L. A. A. M. R. D. A. F. 2011. *Essential clinical anatomy,* Baltimore, MD, Lippincott Williams & Wilkins.

MORIKAWA, E., YASUTOMI, M., SHINDOU, K., MATSUDA, T., MORI, N., HIDA, J., KUBO, R., KITAOKA, M., NAKAMURA, M., FUJIMOTO, K. & ET AL. 1994. Distribution of metastatic lymph nodes in colorectal cancer by the modified clearing method. *Dis Colon Rectum,* 37**,** 219-23.

MOSELEY, M. E., COHEN, Y., KUCHARCZYK, J., MINTOROVITCH, J., ASGARI, H. S., WENDLAND, M. F., TSURUDA, J. & NORMAN, D. 1990. Diffusion-weighted MR imaging of anisotropic water diffusion in cat central nervous system. *Radiology,* 176**,** 439-45.

MOSKAL, A., NORAT, T., FERRARI, P. & RIBOLI, E. 2007. Alcohol intake and colorectal cancer risk: a dose-response meta-analysis of published cohort studies. *Int J Cancer,* 120**,** 664-71.

MOU, S., SOETIKNO, R., SHIMODA, T., ROUSE, R. & KALTENBACH, T. 2013. Pathologic predictive factors for lymph node metastasis in submucosal invasive (T1) colorectal cancer: a systematic review and meta-analysis. *Surg Endosc,* 27**,** 2692-703.

NAGTEGAAL, I. D., MARIJNEN, C. A., KRANENBARG, E. K., VAN DE VELDE, C. J. & VAN KRIEKEN, J. H. 2002a. Circumferential margin involvement is still an important predictor of local recurrence in rectal carcinoma: not one millimeter but two millimeters is the limit. *Am J Surg Pathol,* 26**,** 350-7.

NAGTEGAAL, I. D., VAN DE VELDE, C. J., MARIJNEN, C. A., VAN KRIEKEN, J. H. & QUIRKE, P. 2005. Low rectal cancer: a call for a change of approach in abdominoperineal resection. *J Clin Oncol,* 23**,** 9257-64.

NAGTEGAAL, I. D., VAN DE VELDE, C. J., VAN DER WORP, E., KAPITEIJN, E., QUIRKE, P. & VAN KRIEKEN, J. H. 2002b. Macroscopic evaluation of rectal cancer resection specimen: clinical significance of the pathologist in quality control. *J Clin Oncol,* 20**,** 1729-34.

NAMM, J., NG, M., ROY-CHOWDHURY, S., MORGAN, J. W., LUM, S. S. & WONG, J. H. 2008. Quantitating the impact of stage migration on staging accuracy in colorectal cancer. *J Am Coll Surg,* 207**,** 882-7.

NATIONAL INSTITUES OF HEALTH (NIH) 1990. NIH consensus conference. Adjuvant therapy for patients with colon and rectal cancer. *JAMA,* 264**,** 1444-50.

NATIONAL INSTITUTE FOR HEALTH AND CLINICAL EXCELLENCE. 2014. *Interventional procedure overview of preoperative high dose rate brachytherapy for rectal cancer. Clinical Guideline IP 342/2* [Online]. London. Available: http://www.nice.org.uk/guidance/ipg531/evidence/overview-544382173 [Accessed 07/03/2016 2016].

NEWCOMBE, R. G. 1998. Improved confidence intervals for the difference between binomial proportions based on paired data. *Stat Med,* 17**,** 2635-50.

NIEKEL, M. C., BIPAT, S. & STOKER, J. 2010a. Diagnostic imaging of colorectal liver metastases with CT, MR imaging, FDG PET, and/or FDG PET/CT: a meta-analysis of prospective studies including patients who have not previously undergone treatment. *Radiology,* 257**,** 674-84.

NIEKEL, M. C., BIPAT, S. & STOKER, J. 2010b. Diagnostic Imaging of Colorectal Liver Metastases with CT, MR Imaging, FDG PET, and/or FDG PET/CT: A Meta-Analysis of Prospective Studies Including Patients Who Have Not Previously Undergone Treatment. *Radiology*.

NIELSEN, L. B. & WILLE-JORGENSEN, P. 2014. National and international guidelines for rectal cancer. *Colorectal Dis,* 16**,** 854-65.

NIENHAUS, K. & NIENHAUS, G. U. 2014. Fluorescent proteins for live-cell imaging with super-resolution. *Chemical Society Reviews,* 43**,** 1088-1106.

NORDLINGER, B. & WIND, P. 1994. Repeat resections of primary hepatic malignancies. *Cancer Treat Res,* 69**,** 53-6.

O'CONNELL, M. J., COLANGELO, L. H., BEART, R. W., PETRELLI, N. J., ALLEGRA, C. J., SHARIF, S., PITOT, H. C., SHIELDS, A. F., LANDRY, J. C., RYAN, D. P., PARDA, D. S., MOHIUDDIN, M., ARORA, A., EVANS, L. S., BAHARY, N., SOORI, G. S., EAKLE, J., ROBERTSON, J. M., MOORE, D. F., JR., MULLANE, M. R., MARCHELLO, B. T., WARD, P. J., WOZNIAK, T. F., ROH, M. S., YOTHERS, G. & WOLMARK, N. 2014. Capecitabine and oxaliplatin in the preoperative multimodality treatment of rectal cancer: surgical end points from National Surgical Adjuvant Breast and Bowel Project trial R-04. *J Clin Oncol,* 32**,** 1927-34.

OGATA, Y., MATONO, K., HAYASHI, A., TAKAMOR, S., MIWA, K., SASATOMI, T., ISHIBASHI, N., SHIDA, S. & SHIROUZU, K. 2005. Repeat pulmonary resection for isolated recurrent lung metastases yields results comparable to those after first pulmonary resection in colorectal cancer. *World J Surg,* 29**,** 363-8.

ORTHOLAN, C., ROMESTAING, P., CHAPET, O. & GERARD, J. P. 2012. Correlation in rectal cancer between clinical tumor response after neoadjuvant radiotherapy and sphincter or organ preservation: 10-year results of the Lyon R 96-02 randomized trial. *Int J Radiat Oncol Biol Phys,* 83**,** e165-71.

OZIS, S. E., SOYDAL, C., AKYOL, C., CAN, N., KUCUK, O. N., YAGCI, C., ERKEK, A. B. & KUZU, M. A. 2014. The role of 18F-fluorodeoxyglucose positron emission tomography/computed tomography in the primary staging of rectal cancer. *World J Surg Oncol,* 12**,** 26.

PARK, J. S., JANG, Y. J., CHOI, G. S., PARK, S. Y., KIM, H. J., KANG, H. & CHO, S. H. 2014. Accuracy of preoperative MRI in predicting pathology stage in rectal cancers: node-for-node matched histopathology validation of MRI features. *Dis Colon Rectum,* 57**,** 32-8.

PATEL, U. B., TAYLOR, F., BLOMQVIST, L., GEORGE, C., EVANS, H., TEKKIS, P., QUIRKE, P., SEBAG-MONTEFIORE, D., MORAN, B., HEALD, R., GUTHRIE, A., BEES, N., SWIFT, I., PENNERT, K. & BROWN, G. 2011. Magnetic resonance imaging-detected tumor response for locally advanced rectal cancer predicts survival outcomes: MERCURY experience. *J Clin Oncol,* 29**,** 3753-60.

PENG, J., SHENG, W., HUANG, D., VENOOK, A. P., XU, Y., GUAN, Z. & CAI, S. 2011. Perineural invasion in pT3N0 rectal cancer: the incidence and its prognostic effect. *Cancer,* 117**,** 1415-21.

PEPPONE, L. J., MAHONEY, M. C., CUMMINGS, K. M., MICHALEK, A. M., REID, M. E., MOYSICH, K. B. & HYLAND, A. 2008. Colorectal cancer occurs earlier in those exposed to tobacco smoke: implications for screening. *J Cancer Res Clin Oncol,* 134**,** 743-51.

PETERSEN, S. H., HARLING, H., KIRKEBY, L. T., WILLE-JORGENSEN, P. & MOCELLIN, S. 2012. Postoperative adjuvant chemotherapy in rectal cancer operated for cure. *Cochrane Database Syst Rev,* 3**,** CD004078.

PETERSEN, V. C., BAXTER, K. J., LOVE, S. B. & SHEPHERD, N. A. 2002. Identification of objective pathological prognostic determinants and models of prognosis in Dukes' B colon cancer. *Gut,* 51**,** 65-9.

PETRILLO, A., FUSCO, R., PETRILLO, M., GRANATA, V., SANSONE, M., AVALLONE, A., DELRIO, P., PECORI, B., TATANGELO, F. & CILIBERTO, G. 2015. Standardized Index of Shape (SIS): a quantitative DCE-MRI parameter to discriminate responders by non-responders after neoadjuvant therapy in LARC. *Eur Radiol,* 25**,** 1935-45.

PEZIM, M. E. & NICHOLLS, R. J. 1984. Survival after high or low ligation of the inferior mesenteric artery during curative surgery for rectal cancer. *Ann Surg,* 200**,** 729-33.

POLA, S., SANTILLAN, C., LEVESQUE, B. G., FEAGAN, B. G. & SANDBORN, W. J. 2014. An overview of magnetic resonance enterography for Crohn's disease. *Dig Dis Sci,* 59**,** 2040-9.

POMERRI, F., MARETTO, I., PUCCIARELLI, S., RUGGE, M., BURZI, S., ZANDONA, M., AMBROSI, A., URSO, E., MUZZIO, P. C. & NITTI, D. 2009. Prediction of rectal lymph node metastasis by pelvic computed tomography measurement. *Eur J Surg Oncol,* 35**,** 168-73.

PONZ DE LEON, M. & RONCUCCI, L. 2000. The cause of colorectal cancer. *Dig Liver Dis,* 32**,** 426-39.

PRABHUDESAI, A. G., CORNES, P., GLEES, J. P. & KUMAR, D. 2005. Long-term morbidity following short-course, pre-operative radiotherapy and total mesorectal excision for rectal cancer. *Surgeon,* 3**,** 347-51.

PRYTZ, M., ANGENETE, E., EKELUND, J. & HAGLIND, E. 2014. Extralevator abdominoperineal excision (ELAPE) for rectal cancer-short-term results from the Swedish Colorectal Cancer Registry. Selective use of ELAPE warranted. *Int J Colorectal Dis,* 29**,** 981-7.

PULI, S. R., BECHTOLD, M. L., REDDY, J. B., CHOUDHARY, A., ANTILLON, M. R. & BRUGGE, W. R. 2009a. How good is endoscopic ultrasound in differentiating various T stages of rectal cancer? Meta-analysis and systematic review. *Ann Surg Oncol,* 16**,** 254-65.

PULI, S. R., REDDY, J. B., BECHTOLD, M. L., CHOUDHARY, A., ANTILLON, M. R. & BRUGGE, W. R. 2009b. Accuracy of endoscopic ultrasound to diagnose nodal invasion by rectal cancers: a meta-analysis and systematic review. *Ann Surg Oncol,* 16**,** 1255-65.

QUIRKE, P., DURDEY, P., DIXON, M. F. & WILLIAMS, N. S. 1986. Local recurrence of rectal adenocarcinoma due to inadequate surgical resection. Histopathological study of lateral tumour spread and surgical excision. *Lancet,* 2**,** 996-9.

QUIRKE, P., STEELE, R., MONSON, J., GRIEVE, R., KHANNA, S., COUTURE, J., O'CALLAGHAN, C., MYINT, A. S., BESSELL, E., THOMPSON, L. C., PARMAR, M., STEPHENS, R. J. & SEBAG-MONTEFIORE, D. 2009. Effect of the plane of surgery achieved on local recurrence in patients with operable rectal cancer: a prospective study using data from the MRC CR07 and NCIC-CTG CO16 randomised clinical trial. *Lancet,* 373**,** 821-8.

QUIRKE, P., WILLIAMS, G. T., ECTORS, N., ENSARI, A., PIARD, F. & NAGTEGAAL, I. 2007. The future of the TNM staging system in colorectal cancer: time for a debate? *Lancet Oncol,* 8**,** 651-7.

R CORE TEAM 2015. R: A Language and Environment for Statistical Computing. Vienna, Austria: R Foundation for Statistical Computing.

RAFAELSEN, S. R., VAGN-HANSEN, C., SORENSEN, T., LINDEBJERG, J., PLOEN, J. & JAKOBSEN, A. 2013. Ultrasound elastography in patients with rectal cancer treated with chemoradiation. *Eur J Radiol,* 82**,** 913-7.

RAMA, N., MONTEIRO, A., BERNARDO, J. E., EUGENIO, L. & ANTUNES, M. J. 2009. Lung metastases from colorectal cancer: surgical resection and prognostic factors. *Eur J Cardiothorac Surg,* 35**,** 444-9.

REINHARDT, M. J., WIETHOELTER, N., MATTHIES, A., JOE, A. Y., STRUNK, H., JAEGER, U. & BIERSACK, H. J. 2006. PET recognition of pulmonary metastases on PET/CT imaging: impact of

attenuation-corrected and non-attenuation-corrected PET images. *Eur J Nucl Med Mol Imaging,* 33**,** 134-9.

REVELLE, W. 2013. psych: Procedures for Psychological, Psychometric, and Personality Research. Evanston, Illinois: Northwestern University.

ROBIN, X., TURCK, N., HAINARD, A., TIBERTI, N., LISACEK, F., SANCHEZ, J.-C. & MÜLLER, M. 2011. pROC: an open-source package for R and S+ to analyze and compare ROC curves. *BMC Bioinformatics,* 12.

ROBSAHM, T. E., AAGNES, B., HJARTAKER, A., LANGSETH, H., BRAY, F. I. & LARSEN, I. K. 2013. Body mass index, physical activity, and colorectal cancer by anatomical subsites: a systematic review and meta-analysis of cohort studies. *Eur J Cancer Prev,* 22**,** 492-505.

RODEL, C., GRAEVEN, U., FIETKAU, R., HOHENBERGER, W., HOTHORN, T., ARNOLD, D., HOFHEINZ, R. D., GHADIMI, M., WOLFF, H. A., LANG-WELZENBACH, M., RAAB, H. R., WITTEKIND, C., STROBEL, P., STAIB, L., WILHELM, M., GRABENBAUER, G. G., HOFFMANNS, H., LINDEMANN, F., SCHLENSKA-LANGE, A., FOLPRECHT, G., SAUER, R. & LIERSCH, T. 2015. Oxaliplatin added to fluorouracil-based preoperative chemoradiotherapy and postoperative chemotherapy of locally advanced rectal cancer (the German CAO/ARO/AIO-04 study): final results of the multicentre, open-label, randomised, phase 3 trial. *Lancet Oncol,* 16**,** 979-89.

ROH, M. S., YOTHERS, G. A., O'CONNELL, M. J., BEART, R. W., PITOT, H. C., SHIELDS, A. F., PARDA, D. S., SHARIF, S., ALLEGRA, C. J., PETRELLI, N. J., LANDRY, J. C., RYAN, D. P., ARORA, A., EVANS, T. L., SOORI, G. S., CHU, L., LANDES, R. V., MOHIUDDIN, M., LOPA, S. & WOLMARK, N. 2011. The impact of capecitabine and oxaliplatin in the preoperative multimodality treatment in patients with carcinoma of the rectum: NSABP R-04. *Journal of Clinical Oncology,* 29.

ROLLVEN, E., HOLM, T., GLIMELIUS, B., LORINC, E. & BLOMQVIST, L. 2013. Potentials of high resolution magnetic resonance imaging versus computed tomography for preoperative local staging of colon cancer. *Acta Radiol*.

ROSENBLUM, J. D., BOYLE, C. M. & SCHWARTZ, L. B. 1997. The mesenteric circulation. Anatomy and physiology. *Surg Clin North Am,* 77**,** 289-306.

RUTTER, M., SAUNDERS, B., WILKINSON, K., RUMBLES, S., SCHOFIELD, G., KAMM, M., WILLIAMS, C., PRICE, A., TALBOT, I. & FORBES, A. 2004. Severity of inflammation is a risk factor for colorectal neoplasia in ulcerative colitis. *Gastroenterology,* 126**,** 451-9.

SAAR, B., GSCHOSSMANN, J. M., BONEL, H. M., KICKUTH, R., VOCK, P. & NETZER, P. 2008. Evaluation of magnetic resonance colonography at 3.0 Tesla regarding diagnostic accuracy and image quality. *Invest Radiol,* 43**,** 580-6.

SAAR, B., MEINING, A., BEER, A., SETTLES, M., HELMBERGER, H., FRIMBERGER, E., RUMMENY, E. J. & ROSCH, T. 2007. Prospective study on bright lumen magnetic resonance colonography in comparison with conventional colonoscopy. *Br J Radiol,* 80**,** 235-41.

SALERNO, G. V., DANIELS, I. R., MORAN, B. J., HEALD, R. J., THOMAS, K. & BROWN, G. 2009. Magnetic resonance imaging prediction of an involved surgical resection margin in low rectal cancer. *Dis Colon Rectum,* 52**,** 632-9.

SAUER, R., BECKER, H., HOHENBERGER, W., RODEL, C., WITTEKIND, C., FIETKAU, R., MARTUS, P., TSCHMELITSCH, J., HAGER, E., HESS, C. F., KARSTENS, J. H., LIERSCH, T., SCHMIDBERGER, H. & RAAB, R. 2004. Preoperative versus postoperative chemoradiotherapy for rectal cancer. *N Engl J Med,* 351**,** 1731-40.

SCHMIDT, G. P., BAUR-MELNYK, A., HAUG, A., UTZSCHNEIDER, S., BECKER, C. R., TILING, R., REISER, M. F. & HERMANN, K. A. 2009. Whole-body MRI at 1.5 T and 3 T compared with FDG-PET-CT

for the detection of tumour recurrence in patients with colorectal cancer. *Eur Radiol,* 19**,** 1366-78.

SCHOLEFIELD, J. H. 2007. Guidelines for the Management of Colorectal Cancer. Third ed.: The Association of Coloproctology of Great Britain and Ireland.

SCHRAG, D. 2013. Evolving role of neoadjuvant therapy in rectal cancer. *Curr Treat Options Oncol,* 14**,** 350-64.

SCHULZ, A. 2013. epade: Easy Plots.

SCOTT, K. W. & GRACE, R. H. 1989. Detection of lymph node metastases in colorectal carcinoma before and after fat clearance. *Br J Surg,* 76**,** 1165-7.

SCOTTISH INTERCOLLEGIATE GUIDELINES NETWORK (SIGN) 2015. *SIGN 126 Diagnosis and management of colorectal cancer,* Edinburgh.

SEBAG-MONTEFIORE, D., STEPHENS, R. J., STEELE, R., MONSON, J., GRIEVE, R., KHANNA, S., QUIRKE, P., COUTURE, J., DE METZ, C., MYINT, A. S., BESSELL, E., GRIFFITHS, G., THOMPSON, L. C. & PARMAR, M. 2009. Preoperative radiotherapy versus selective postoperative chemoradiotherapy in patients with rectal cancer (MRC CR07 and NCIC-CTG C016): a multicentre, randomised trial. *Lancet,* 373**,** 811-20.

SEJBEN, I., BORI, R. & CSERNI, G. 2010. Venous invasion demonstrated by orcein staining of colorectal carcinoma specimens is associated with the development of distant metastasis. *J Clin Pathol,* 63**,** 575-8.

SHANKAR, A., LEONARD, P., RENAUT, A. J., LEDERMAN, J., LEES, W. R., GILLAMS, A. R., HARRISON, E. & TAYLOR, I. 2001. Neo-adjuvant therapy improves resectability rates for colorectal liver metastases. *Ann R Coll Surg Engl,* 83**,** 85-8.

SHEPHERD, N. A. & QUIRKE, P. 1997. Colorectal cancer reporting: are we failing the patient? *J Clin Pathol,* 50**,** 266-7.

SHIHAB, O. C., MORAN, B. J., HEALD, R. J., QUIRKE, P. & BROWN, G. 2009. MRI staging of low rectal cancer. *Eur Radiol,* 19**,** 643-50.

SIMPSON, G. S., EARDLEY, N., MCNICOL, F., HEALEY, P., HUGHES, M. & ROONEY, P. S. 2014. Circumferential resection margin (CRM) positivity after MRI assessment and adjuvant treatment in 189 patients undergoing rectal cancer resection. *Int J Colorectal Dis,* 29**,** 585-90.

SLANETZ, C. A., JR. & GRIMSON, R. 1997. Effect of high and intermediate ligation on survival and recurrence rates following curative resection of colorectal cancer. *Dis Colon Rectum,* 40**,** 1205-18; discussion 1218-9.

SLATER, A., HALLIGAN, S., TAYLOR, S. A. & MARSHALL, M. 2006. Distance between the rectal wall and mesorectal fascia measured by MRI: Effect of rectal distension and implications for preoperative prediction of a tumour-free circumferential resection margin. *Clin Radiol,* 61**,** 65-70.

SLUPSKI, M., WLODARCZYK, Z., JASINSKI, M., MASZTALERZ, M. & TUJAKOWSKI, J. 2009. Outcomes of simultaneous and delayed resections of synchronous colorectal liver metastases. *Can J Surg,* 52**,** E241-4.

SMITH, M. D. & MCCALL, J. L. 2009. Systematic review of tumour number and outcome after radical treatment of colorectal liver metastases. *Br J Surg,* 96**,** 1101-13.

SMITH, N. J., BARBACHANO, Y., NORMAN, A. R., SWIFT, R. I., ABULAFI, A. M. & BROWN, G. 2008a. Prognostic significance of magnetic resonance imaging-detected extramural vascular invasion in rectal cancer. *Br J Surg,* 95**,** 229-36.

SMITH, N. J., BEES, N., BARBACHANO, Y., NORMAN, A. R., SWIFT, R. I. & BROWN, G. 2007. Preoperative computed tomography staging of nonmetastatic colon cancer predicts outcome: implications for clinical trials. *Br J Cancer,* 96**,** 1030-6.

SMITH, N. J., SHIHAB, O., ARNAOUT, A., SWIFT, R. I. & BROWN, G. 2008b. MRI for detection of extramural vascular invasion in rectal cancer. *AJR Am J Roentgenol,* 191**,** 1517-22.

SOHN, B., LIM, J. S., KIM, H., MYOUNG, S., CHOI, J., KIM, N. K. & KIM, M. J. 2015. MRI-detected extramural vascular invasion is an independent prognostic factor for synchronous metastasis in patients with rectal cancer. *Eur Radiol,* 25**,** 1347-55.

SONDENAA, K., QUIRKE, P., HOHENBERGER, W., SUGIHARA, K., KOBAYASHI, H., KESSLER, H., BROWN, G., TUDYKA, V., D'HOORE, A., KENNEDY, R. H., WEST, N. P., KIM, S. H., HEALD, R., STORLI, K. E., NESBAKKEN, A. & MORAN, B. 2014. The rationale behind complete mesocolic excision (CME) and a central vascular ligation for colon cancer in open and laparoscopic surgery : proceedings of a consensus conference. *Int J Colorectal Dis,* 29**,** 419-28.

STEELE, S. R., PARK, G. E., JOHNSON, E. K., MARTIN, M. J., STOJADINOVIC, A., MAYKEL, J. A. & CAUSEY, M. W. 2014. The impact of age on colorectal cancer incidence, treatment, and outcomes in an equal-access health care system. *Dis Colon Rectum,* 57**,** 303-10.

STEJSKAL, E. O. & TANNER, J. E. 1965. Spin Diffusion Measurements: Spin Echoes in the Presence of a Time-Dependent Field Gradient. *The Journal of Chemical Physics,* 42**,** 288-292.

STELZNER, S., HELLMICH, G., SCHUBERT, C., PUFFER, E., HAROSKE, G. & WITZIGMANN, H. 2011. Short-term outcome of extra-levator abdominoperineal excision for rectal cancer. *Int J Colorectal Dis,* 26**,** 919-25.

STERNBERG, A., MIZRAHI, A., AMAR, M. & GROISMAN, G. 2006. Detection of venous invasion in surgical specimens of colorectal carcinoma: the efficacy of various types of tissue blocks. *J Clin Pathol,* 59**,** 207-10.

STEWART, C. J., MORRIS, M., DE BOER, B. & IACOPETTA, B. 2007. Identification of serosal invasion and extramural venous invasion on review of Dukes' stage B colonic carcinomas and correlation with survival. *Histopathology,* 51**,** 372-8.

STOCKHOLM COLORECTAL CANCER STUDY GROUP 1996. Randomized study on preoperative radiotherapy in rectal carcinoma. *Ann Surg Oncol,* 3**,** 423-30.

STRASBERG, S. M., DEHDASHTI, F., SIEGEL, B. A., DREBIN, J. A. & LINEHAN, D. 2001. Survival of patients evaluated by FDG-PET before hepatic resection for metastatic colorectal carcinoma: a prospective database study. *Annals of Surgery,* 233**,** 293-9.

SUGARBAKER, P. H., SCHELLINX, M. E., CHANG, D., KOSLOWE, P. & VON MEYERFELDT, M. 1996. Peritoneal carcinomatosis from adenocarcinoma of the colon. *World J Surg,* 20**,** 585-91; discussion 592.

SUGIHARA, K., KOBAYASHI, H., KATO, T., MORI, T., MOCHIZUKI, H., KAMEOKA, S., SHIROUZU, K. & MUTO, T. 2006. Indication and benefit of pelvic sidewall dissection for rectal cancer. *Dis Colon Rectum,* 49**,** 1663-72.

SUNDERMEYER, M. L., MEROPOL, N. J., ROGATKO, A., WANG, H. & COHEN, S. J. 2005. Changing patterns of bone and brain metastases in patients with colorectal cancer. *Clin Colorectal Cancer,* 5**,** 108-13.

SURTEES, P., RITCHIE, J. K. & PHILLIPS, R. K. 1990. High versus low ligation of the inferior mesenteric artery in rectal cancer. *Br J Surg,* 77**,** 618-21.

SWARTLING, T., KALEBO, P., DERWINGER, K., GUSTAVSSON, B. & KURLBERG, G. 2013. Stage and size using magnetic resonance imaging and endosonography in neoadjuvantly-treated rectal cancer. *World J Gastroenterol,* 19**,** 3263-71.

SWEDISH RECTAL CANCER TRIAL 1997. Improved survival with preoperative radiotherapy in resectable rectal cancer. *N Engl J Med,* 336**,** 980-7.

TANKOVA, L. T., PENCHEV, P. I., KOVATCHKI, D., STOILOV, G. & HADJIEVA, T. 2012. Endosonographic assessment of rectal cancer after neoadjuvant radiotherapy. *Med Ultrason,* 14**,** 19-23.

TAYLOR, F. G., QUIRKE, P., HEALD, R. J., MORAN, B., BLOMQVIST, L., SWIFT, I., SEBAG-MONTEFIORE, D. J., TEKKIS, P. & BROWN, G. 2011. Preoperative High-resolution Magnetic Resonance Imaging Can Identify Good Prognosis Stage I, II, and III Rectal Cancer Best Managed by Surgery Alone: A Prospective, Multicenter, European Study That Recruited Consecutive Patients With Rectal Cancer. *Ann Surg,* 253**,** 711-9.

TAYLOR, F. G., QUIRKE, P., HEALD, R. J., MORAN, B. J., BLOMQVIST, L., SWIFT, I. R., SEBAG-MONTEFIORE, D., TEKKIS, P. & BROWN, G. 2014. Preoperative magnetic resonance imaging assessment of circumferential resection margin predicts disease-free survival and local recurrence: 5-year follow-up results of the MERCURY study. *J Clin Oncol,* 32**,** 34-43.

TAYLOR, F. G., SWIFT, R. I., BLOMQVIST, L. & BROWN, G. 2008. A systematic approach to the interpretation of preoperative staging MRI for rectal cancer. *AJR Am J Roentgenol,* 191**,** 1827-35.

TENESA, A. & DUNLOP, M. G. 2009. New insights into the aetiology of colorectal cancer from genome-wide association studies. *Nat Rev Genet,* 10**,** 353-8.

THE BEYOND TME COLLABORATIVE 2013. Consensus statement on the multidisciplinary management of patients with recurrent and primary rectal cancer beyond total mesorectal excision planes. *Br J Surg,* 100**,** 1009-14.

THERNEAU, T., ATKINSON, B. & RIPLEY, B. 2015. *rpart: Recursive Partitioning and Regression Trees*.

THOMAS, P. R. & LINDBLAD, A. S. 1988. Adjuvant postoperative radiotherapy and chemotherapy in rectal carcinoma: a review of the Gastrointestinal Tumor Study Group experience. *Radiother Oncol,* 13**,** 245-52.

TORRES, R. A., ORBAN, R. D., TOCAIMAZA, L., VALLEJOS PEREIRA, G. & AREVALO, J. R. 2012. Transvaginal specimen extraction after laparoscopic colectomy. *World J Surg,* 36**,** 1699-702.

TORZILLI, G., BOTEA, F., DONADON, M., CIMINO, M., PROCOPIO, F., PEDICINI, V., PORETTI, D. & MONTORSI, M. 2014. Criteria for the selective use of contrast-enhanced intra-operative ultrasound during surgery for colorectal liver metastases. *HPB (Oxford),* 16**,** 994-1001.

TOYOTA, S., OHTA, H. & ANAZAWA, S. 1995. Rationale for extent of lymph node dissection for right colon cancer. *Dis Colon Rectum,* 38**,** 705-11.

TSUNODA, Y., ITO, M., FUJII, H., KUWANO, H. & SAITO, N. 2008. Preoperative diagnosis of lymph node metastases of colorectal cancer by FDG-PET/CT. *Jpn J Clin Oncol,* 38**,** 347-53.

TWELVES, C., WONG, A., NOWACKI, M. P., ABT, M., BURRIS, H., CARRATO, A., CASSIDY, J., CERVANTES, A., FAGERBERG, J., GEORGOULIAS, V., HUSSEINI, F., JODRELL, D., KORALEWSKI, P., KRONING, H., MAROUN, J., MARSCHNER, N., MCKENDRICK, J., PAWLICKI, M., ROSSO, R., SCHULLER, J., SEITZ, J. F., STABUC, B., TUJAKOWSKI, J., VAN HAZEL, G., ZALUSKI, J. & SCHEITHAUER, W. 2005. Capecitabine as adjuvant treatment for stage III colon cancer. *New England Journal of Medicine,* 352**,** 2696-2704.

UENO, H., MURPHY, J., JASS, J. R., MOCHIZUKI, H. & TALBOT, I. C. 2002. Tumour 'budding' as an index to estimate the potential of aggressiveness in rectal cancer. *Histopathology,* 40**,** 127-32.

UNG, L., CHUA, T. C. & ENGEL, A. F. 2014. A systematic review of local excision combined with chemoradiotherapy for early rectal cancer. *Colorectal Dis,* 16**,** 502-15.

VALENTINI, V., ARISTEI, C., GLIMELIUS, B., MINSKY, B. D., BEETS-TAN, R., BORRAS, J. M., HAUSTERMANS, K., MAINGON, P., OVERGAARD, J., PAHLMAN, L., QUIRKE, P., SCHMOLL, H. J., SEBAG-MONTEFIORE, D., TAYLOR, I., VAN CUTSEM, E., VAN DE VELDE, C., CELLINI, N. & LATINI, P. 2009. Multidisciplinary Rectal Cancer Management: 2nd European Rectal Cancer Consensus Conference (EURECA-CC2). *Radiother Oncol,* 92**,** 148-63.

VAN GIJN, W., MARIJNEN, C. A., NAGTEGAAL, I. D., KRANENBARG, E. M., PUTTER, H., WIGGERS, T., RUTTEN, H. J., PAHLMAN, L., GLIMELIUS, B. & VAN DE VELDE, C. J. 2011. Preoperative radiotherapy combined with total mesorectal excision for resectable rectal cancer: 12-year follow-up of the multicentre, randomised controlled TME trial. *Lancet Oncol,* 12**,** 575-82.

VAN KESSEL, C. S., VAN LEEUWEN, M. S., VAN DEN BOSCH, M. A., BOREL RINKES, I. H., MALI, W. P., WESTERS, P. & VAN HILLEGERSBERG, R. 2011. Accuracy of Multislice Liver CT and MRI for Preoperative Assessment of Colorectal Liver Metastases after Neoadjuvant Chemotherapy. *Dig Surg,* 28**,** 36-43.

VASEN, H. F., WATSON, P., MECKLIN, J. P. & LYNCH, H. T. 1999. New clinical criteria for hereditary nonpolyposis colorectal cancer (HNPCC, Lynch syndrome) proposed by the International Collaborative group on HNPCC. *Gastroenterology,* 116**,** 1453-6.

VITTINGHOFF, E. & MCCULLOCH, C. E. 2007. Relaxing the Rule of Ten Events per Variable in Logistic and Cox Regression. *American Journal of Epidemiology,* 165**,** 710-718.

VOGELSTEIN, B., FEARON, E. R., HAMILTON, S. R., KERN, S. E., PREISINGER, A. C., LEPPERT, M., NAKAMURA, Y., WHITE, R., SMITS, A. M. & BOS, J. L. 1988. Genetic alterations during colorectal-tumor development. *N Engl J Med,* 319**,** 525-32.

VOGELSTEIN, B. & KINZLER, K. W. 2004. Cancer genes and the pathways they control. *Nat Med,* 10**,** 789-99.

VOSKUIL, D. W., VASEN, H. F., KAMPMAN, E. & VAN'T VEER, P. 1997. Colorectal cancer risk in HNPCC families: development during lifetime and in successive generations. National Collaborative Group on HNPCC. *Int J Cancer,* 72**,** 205-9.

WAAGE, J. E., LEH, S., ROSLER, C., PFEFFER, F., BACH, S. P., HAVRE, R. F., HALDORSEN, I. S., ODEGAARD, S. & BAATRUP, G. 2014. Endorectal ultrasonography, strain elastography and MRI differentiation of rectal adenomas and adenocarcinomas. *Colorectal Dis,* 17**,** 124-31.

WAGNER, M., KLESSEN, C., RIEF, M., ELGETI, T., TAUPITZ, M., HAMM, B. & ASBACH, P. 2008. High-resolution T2-weighted abdominal magnetic resonance imaging using respiratory triggering: impact of butylscopolamine on image quality. *Acta Radiol,* 49**,** 376-82.

WALLNER, C., LANGE, M. M., BONSING, B. A., MAAS, C. P., WALLACE, C. N., DABHOIWALA, N. F., RUTTEN, H. J., LAMERS, W. H., DERUITER, M. C. & VAN DE VELDE, C. J. 2008. Causes of fecal and urinary incontinence after total mesorectal excision for rectal cancer based on cadaveric surgery: a study from the Cooperative Clinical Investigators of the Dutch total mesorectal excision trial. *J Clin Oncol,* 26**,** 4466-72.

WANG, C. L., QU, G. & XU, H. W. 2014. The short- and long-term outcomes of laparoscopic versus open surgery for colorectal cancer: a meta-analysis. *Int J Colorectal Dis,* 29**,** 309-20.

WANG, L. M., KEVANS, D., MULCAHY, H., O'SULLIVAN, J., FENNELLY, D., HYLAND, J., O'DONOGHUE, D. & SHEAHAN, K. 2009. Tumor budding is a strong and reproducible prognostic marker in T3N0 colorectal cancer. *Am J Surg Pathol,* 33**,** 134-41.

WARACH, S., LI, W., RONTHAL, M. & EDELMAN, R. R. 1992. Acute cerebral ischemia: evaluation with dynamic contrast-enhanced MR imaging and MR angiography. *Radiology,* 182**,** 41-7.

WEST, N. P., HOHENBERGER, W., WEBER, K., PERRAKIS, A., FINAN, P. J. & QUIRKE, P. 2010. Complete mesocolic excision with central vascular ligation produces an oncologically superior specimen compared with standard surgery for carcinoma of the colon. *J Clin Oncol,* 28**,** 272-8.

WESTLAKE, S. 2009. Cancer incidence and mortality in the United Kingdom and constituent countries, 2004-06. *Health Stat Q***,** 56-62.

WESTWOOD, M., JOORE, M., GRUTTERS, J., REDEKOP, K., ARMSTRONG, N., LEE, K., GLOY, V., RAATZ, H., MISSO, K., SEVERENS, J. & KLEIJNEN, J. 2013. Contrast-enhanced ultrasound using SonoVue(R) (sulphur hexafluoride microbubbles) compared with contrast-enhanced computed tomography and contrast-enhanced magnetic resonance imaging for the characterisation of focal liver lesions and detection of liver metastases: a systematic review and cost-effectiveness analysis. *Health Technol Assess,* 17**,** 1-243.

WEXNER, S. D. & EDDEN, Y. 2009. NOTES/NOSE/NOSCAR/LATAS: what does it all mean? *Tech Coloproctol,* 13**,** 1-3.

WIBE, A., RENDEDAL, P. R., SVENSSON, E., NORSTEIN, J., EIDE, T. J., MYRVOLD, H. E. & SOREIDE, O. 2002. Prognostic significance of the circumferential resection margin following total mesorectal excision for rectal cancer. *Br J Surg,* 89**,** 327-34.

WIERING, B., KRABBE, P. F., JAGER, G. J., OYEN, W. J. & RUERS, T. J. 2005. The impact of fluor-18-deoxyglucose-positron emission tomography in the management of colorectal liver metastases. *Cancer,* 104**,** 2658-70.

WILLETT, C. G., BADIZADEGAN, K., ANCUKIEWICZ, M. & SHELLITO, P. C. 1999. Prognostic factors in stage T3N0 rectal cancer: do all patients require postoperative pelvic irradiation and chemotherapy? *Dis Colon Rectum,* 42**,** 167-73.

WILLIAMS, G. T., QUIRKE, P. & SHEPHERD, N. A. 2007. Dataset for colorectal cancer (2nd edition). The Royal College of Pathologists.

WILSON, E. B. 1927. Probable Inference, the Law of Succession, and Statistical Inference. *Journal of the American Statistical Association,* 22**,** 209-212.

WILTINK, L. M., CHEN, T. Y., NOUT, R. A., KRANENBARG, E. M., FIOCCO, M., LAURBERG, S., VAN DE VELDE, C. J. & MARIJNEN, C. A. 2014. Health-related quality of life 14years after preoperative short-term radiotherapy and total mesorectal excision for rectal cancer: Report of a multicenter randomised trial. *Eur J Cancer,* 50**,** 2390-8.

WINDLE, R., BELL, P. R. & SHAW, D. 1987. Five year results of a randomized trial of adjuvant 5-fluorouracil and levamisole in colorectal cancer. *Br J Surg,* 74**,** 569-72.

WONG, T. Y., LAM, W. W., SO, N. M., LEE, J. F. & LEUNG, K. L. 2007. Air-inflated magnetic resonance colonography in patients with incomplete conventional colonoscopy: Comparison with intraoperative findings, pathology specimens, and follow-up conventional colonoscopy. *Am J Gastroenterol,* 102**,** 56-63.

WOOD, M. L. & HENKELMAN, R. M. 1985. MR image artifacts from periodic motion. *Med Phys,* 12**,** 143-51.

WORLD CANCER RESEARCH FUND / AMERICAN INSTITUTE FOR CANCER RESEARCH 2007. Food, Nutrition, Physical Activity, and the Prevention of Cancer: a Global Perspective. Washington DC: AIRC.

WRAY, C. M., ZIOGAS, A., HINOJOSA, M. W., LE, H., STAMOS, M. J. & ZELL, J. A. 2009. Tumor Subsite Location Within the Colon Is Prognostic for Survival After Colon Cancer Diagnosis. *Diseases of the Colon & Rectum,* 52**,** 1359-1366.

WU, X., ZHANG, J., HE, X., WANG, C., LIAN, L., LIU, H., WANG, J. & LAN, P. 2012. Postoperative adjuvant chemotherapy for stage II colorectal cancer: a systematic review of 12 randomized controlled trials. *J Gastrointest Surg,* 16**,** 646-55.

WUNSCH, K., MULLER, J., JAHNIG, H., HERRMANN, R. A., ARNHOLDT, H. M. & MARKL, B. 2010. Shape is not associated with the origin of pericolonic tumor deposits. *Am J Clin Pathol,* 133**,** 388-94.

ZAUBER, A. G., WINAWER, S. J., O'BRIEN, M. J., LANSDORP-VOGELAAR, I., VAN BALLEGOOIJEN, M., HANKEY, B. F., SHI, W., BOND, J. H., SCHAPIRO, M., PANISH, J. F., STEWART, E. T. & WAYE, J. D. 2012. Colonoscopic polypectomy and long-term prevention of colorectal-cancer deaths. *N Engl J Med,* 366**,** 687-96.

ZHAO, J., HALFYARD, B., ROEBOTHAN, B., WEST, R., BUEHLER, S., SUN, Z., SQUIRES, J., MCLAUGHLIN, J. R., PARFREY, P. S. & WANG, P. P. 2010. Tobacco smoking and colorectal cancer: a population-based case-control study in Newfoundland and Labrador. *Can J Public Health,* 101**,** 281-9.

ZLOBEC, I. & LUGLI, A. 2008. Prognostic and predictive factors in colorectal cancer. *J Clin Pathol,* 61**,** 561-9.

9 Appendix – Publications arising from this work

Hunter, C. J., E. Scurr, et al. (2011). "Optimising magnetic resonance imaging for preoperative staging and surgical planning in colon cancer at 1.5 tesla and 3.0 tesla." Journal of Clinical Oncology 29(4). (Published abstract).

Hunter, C. J., A. Garant, et al. (2011). "Adverse Features on Rectal MRI Identify a High-risk Group that May Benefit from More Intensive Preoperative Staging and Treatment." Ann Surg Oncol.

Hunter, C., G. Brown, et al. (2012). "Magnetic resonance imaging assisted tumour block selection in colorectal cancer." Virchows Archiv 461: S179-S179. (Published abstract).

Hunter, C. J. and G. Brown (2013). Radiological Staging for Systemic Disease. Manual of Total Mesorectal Excision, CRC Press: 71-86. (Book chapter)

Hunter, C. and G. Brown (2015). MRI and CT for the Preoperative T and N Staging of Rectal Cancer. Multidisciplinary Treatment of Colorectal Cancer: Staging – Treatment – Pathology – Palliation. G. Baatrup. Cham, Springer International Publishing: 177-193. (Book chapter)

Hunter, C. and G. Brown (2016). "Preoperative staging of rectal cancer: A review of imaging techniques." Expert Rev Gastroenterol Hepatol.

Hunter, C., H. Blake, et al. (2016). "Local staging and assessment of colon cancer with 1.5 Tesla Magnetic Resonance Imaging." The British Journal of Radiology: 20160257.